ADSORPTIVE TREATMENT OF PYRIDINE AND ITS DERIVATIVES FROM WASTEWATERS

A THESIS

*Submitted in partial fulfilment of the
requirements for the award of the degree*
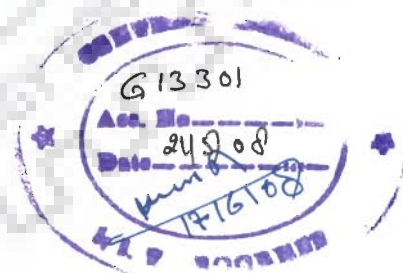
of

DOCTOR OF PHILOSOPHY

in

CHEMICAL ENGINEERING

by

DILIP HIRADRAM LATAYE

DEPARTMENT OF CHEMICAL ENGINEERING
INDIAN INSTITUTE OF TECHNOLOGY ROORKEE
ROORKEE-247 667 (INDIA)

JUNE, 2007

PUBLICATIONS FROM THE PRESENT WORK

1. International Peer Reviewed Journals:

(a) Published/In Press

1. **Lataye D. H.,** Mishra I. M., Mall I. D., Removal of pyridine from aqueous solution by adsorption on bagasse fly ash. *Ind. Eng. Chem. Res.* **2006**, 45(11), 3934-3943.
2. **Lataye D. H.,** Mishra I. M., Mall I. D., Adsorption of 2-picoline onto bagasse fly ash from aqueous solution. *Chemical Engineering Journal*, **2007**, doi:10.1016/j.cej.2007.05.043.

(b) Communicated/Under Review

1. **Lataye D. H.,** Mishra I. M., Mall I. D., Adsorption of α-picoline on granular activated carbon and rice husk ash from aqueous solution: equilibrium and thermodynamic study, Separation and Purification Technology (**Communicated 2007**).
2. **Lataye D. H.,** Mishra I. M., Mall I. D., Pyridine Sorption from Aqueous Solution by Rice Husk Ash (RHA) and Granular Activated Carbon (GAC). *Journal of Hazardous Materials* (**Under Review, 2007**).

(c) Under preparation

1. **Lataye D. H.,** Mishra I. M., Mall I. D., Adsorptive treatment of multicomponent toxics-pyridine, 2-picoline and 4-picoline in aqueous solution by bagasse fly ash using Taguchi's Design of Experimental methodology.
2. **Lataye D. H.,** Mishra I. M., Mall I. D., Treatment of binary mixture of pyridine and 2-picoline in aqueous solution using bagasse fly ash: Application of Taguchi's Design of Experimental methodology.
3. **Lataye D. H.,** Mishra I. M., Mall I. D., Removal of 4-picoline from aqueous solution by adsorption onto bagasse fly ash: Equilibrium and kinetics
4. **Lataye D. H.,** Mishra I. M., Mall I. D., Adsorption of 3-aminopyridine onto bagasse fly ash (BFA), rice husk ash (RHA) and granular activated carbon (GAC): Equilibrium and thermodynamics.

2. Paper Presented in Conferences/Seminars

1) **Lataye D. H.,** Mishra I. M., Mall I. D., Adsorptive Removal of Pyridine and its Derivatives by using Cheap Adsorbents. National seminar on *"Technology for Sustainable- Development-Perspective and Strategies"* Institute of Technology, Guru Ghasidas University, Bilaspur (Chhattisgarh). January 6-7, **2007**.
2) **Lataye D. H.,** Mishra I. M., Mall I. D., Adsorptive Removal of Pyridine from Aqueous Solution by Rice Husk Ash. All India Seminar on "Energy and Environmental Issues Related to Chemical Industry", Organised by The Institution of Engineers (India) U.P. State Centre, Lucknow in association with Harcourt Butler Technological Institute, Kanpur, U.P. on 10th and 11th March, **2007**.
3) **Lataye D. H.,** Mishra I. M., Mall I. D., Removal of Pyridine from Aqueous Solution by Adsorption on Commercial Grade Granular Activated Carbon (GAC). National Conference on "Emerging Technology and Developments in Civil Engineering" Organised by Department of Civil Engineering, Govt. College of Engineering, Amravati on 22nd-23rd March, **2007**.

INDIAN INSTITUTE OF TECHNOLOGY ROORKEE
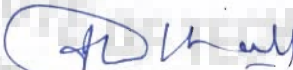# ROORKEE

CANDIDATE'S DECLARATION

I hereby certify that the work which is being presented in the thesis entitled **ADSORPTIVE TREATMENT OF PYRIDINE AND ITS DERIVATIVES FROM WASTEWATERS** in partial fulfilment of the requirements for the award of the degree of Doctor of Philosophy and submitted in the Department of Chemical Engineering, Indian Institute of Technology Roorkee, Roorkee is an authentic record of my own work carried out during a period from July 2004 to June 2007 under the supervision of Dr. I. M. Mishra, Professor, Department of Chemical Engineering and Dean, Saharanpur Campus and Dr. I. D. Mall, Professor, Department of Chemical Engineering, Indian Institute of Technology Roorkee, Roorkee.

The matter presented in this thesis has not been submitted by me for the award of any other degree of this or any other Institute.

(DILIP HIRADRAM LATAYE)

This is to certify that the above statement made by the candidate is correct to the best of our knowledge.

(Dr. I. D. MALL)　　　　　　　　　(Dr. I. M. MISHRA)
Supervisor　　　　　　　　　　　　Supervisor

Date: June 15 , 2007

The Ph.D. Viva-Voce Examination of **Mr. DILIP HIRADRAM LATAYE**, Research Scholar, has been held on ....

Signature of Supervisors　　　　　　　　　Signature of External Examiner

i

ABSTRACT

Pyridine (Py) and its derivatives, like 2-picoline (2Pi), 4-picoline (4Pi), 3-aminopyridine (AmPy), vinylpyridine, etc. are volatile, toxic and flammable with a pungent and unpleasant odour. Py is the parent of a series of chemicals, and is used as a solvent in paint and rubber preparation, as an intermediate in making insecticides and herbicides for agricultural applications and in research laboratories as extraction solvents. Py and its derivatives are also used to make different products such as medicines, vitamins, food flavorings, dyes, adhesives, and in water proofing for fabrics [Kirk, 1996; Lataye et al., 2006; 2007a-f]. When heated to decomposition, these compounds emit highly toxic vapours of NO_x in an oxidative atmosphere.

Adsorption as a wastewater treatment process has aroused considerable interest during recent years. Commercial grade granular activated carbon (GAC) is mostly used as an effective adsorbent for controlling the various organic and inorganic pollutants [Deshpande et al., 1996]. However, due to high cost of GAC and about 10-15 % loss during its regeneration, alternate adsorbents are being explored. Unconventional adsorbents like bagasse fly ash (BFA), rice husk ash (RHA), carbon slurry, kaolin, soil and clay, silica, peat, lignite, bagasse pith, wood, saw dust, molecular sieves, resins, montmorillonite, etc. have attracted the attention of several investigators. Mall et al. [1996] and Bailey et al. [1999] have presented a critical review of such low cost adsorbents for the treatment of various wastewaters. BFA and RHA have been found to be a very effective adsorbent for a number of toxics and pollutants from wastewater.

Various physico-chemical and biological treatment techniques are suggested for the treatment of wastewaters containing Py and its derivatives. These techniques include concentration followed by incineration, adsorption [Kumar et al., 1995; Bludau et al., 1998; Mall et al., 2003; Lataye et al., 2006, 2007a-f], biodegradation [Shukla, 1973; Sims et al., 1986; Sandhya et al., 2002], Ozonation [Stern et al., 1997], etc. The adsorption of these toxic materials by using low cost adsorbents like BFA and RHA has not been reported in the literature. Also, very scarce literature is available on the Taguchi's optimized design of experiments on the single and multicomponent adsorption from aqueous solutions [Srivastava et al., 2007]. In the present study, Taguchi method [Roy, 1990] has been used in the design of adsorption experiments using BFA, RHA and GAC as adsorbents for the removal of Py and its derivatives.

Objectives of the Work

The present study has been undertaken with the following objectives:

1. To characterize the agri-based waste materials like BFA, RHA and GAC for their physico-chemical and adsorption properties. These characteristics include the analysis of particle size and pore size (and area) distribution, proximate and ultimate analysis, and the surface and functional characteristics by FTIR, XRD, TGA and SEM analyses.

2. To utilize BFA, RHA and GAC as adsorbents for the treatment of Py, 2Pi, 4Pi and AmPy bearing synthetic wastewater and to compare their performance with that of available GAC.

3. To study the effect of various parameters like initial pH (pH_0), adsorbent dose (m), contact time (t), initial concentration (C_0), and temperature (T) on the removal of Py, 2Pi, 4Pi and AmPy from the aqueous solution in batch study.

4. To carry out kinetic and equilibrium adsorption studies of Py, 2Pi, 4Pi and AmPy onto various adsorbents and to analyze the experimental data using various kinetic and isotherm models.

5. To understand the thermodynamics of adsorption and to estimate the isosteric heat of adsorption for Py, 2Pi, 4Pi and AmPy using BFA, RHA and GAC as adsorbents.

6. To utilize Taguchi's optimization method for the design of experiments for estimating the effects of various adsorption parameters in single, binary, and multi-component (solute) adsorption systems in the batch adsorption mode.

7. To perform desorption study for the possible regeneration of adsorbents and to develop a method for disposing off the spent adsorbents by fixing the pyridine and picoline chemically or physically.

8. To perform the multistage treatment to reduce the residual concentration of Py, 2Pi, 4Pi and AmPy upto the maximum permissible discharge limit in the wastewaters.

To fulfill the above objectives, the adsorbents were procured, washed and sieved to the required particle size. The physico-chemical characterization of the adsorbents has been done using standard methods e.g. sieving, scanning electron microscopy (SEM),

X-ray diffraction (XRD), FTIR spectroscopy, etc. Pore size distribution and pore area/volume have also been determined. The X-ray spectra of the adsorbents reflected the presence of various types of oxides in all the adsorbents along with some characteristic components. The BFA and RHA showed a mesoporous nature. FTIR spectra of the adsorbents indicated the presence of various types of functional groups e.g. free and hydrogen bonded OH group, the silanol grous (Si-OH), CO group stretching from aldehydes and ketones on the surface of adsorbents. The FTIR of loaded adsorbents show the characteristic bands of Lewis and Bronsted sites. Thermogravimetric analysis exhibited the thermal stability of the adsorbents upto 400 °C.

All the batch experiments were carried out at 30 ± 1 °C. For each experimental run, 0.05 dm^3 of solution of known C_0, pH_0 (2 - 12) and m taken in a 0.25 dm^3 stoppered conical flasks, was agitated in a temperature-controlled orbital shaker at a constant speed of 150 ± 5 rpm. Samples were withdrawn at appropriate time intervals and centrifuged using a research centrifuge (Remi Instruments, Mumbai, India). The residual concentration (C_r) of the centrifuged supernatant was then determined using Perkin Elmer double beam spectrophotometer. The optimum dosages of BFA, RHA and GAC were found to be 8, 30 and 20 g dm^{-3}, for C_0 =100 mg dm^{-3} for Py and AmPy respectively. The optimum dosages were found to be 5, 20 and 10 g dm^{-3} for 2Pi and 4Pi, respectively, for BFA, RHA and GAC for C_0 =100 mg dm^{-3}.

Various kinetic models, viz. pseudo-first-order, pseudo-second-order, intra-particle diffusion, Elovich, Bangham and modified Freundlich models have been used to study the kinetics of adsorption of Py, 2Pi, 4Pi and AmPy onto adsorbents. The pseudo-second-order kinetic model represented the equilibrium data well for all the adsorbate-adsorbent systems. Equilibrium isotherms were analyzed by using Langmuir, Freundlich, Temkin, Redlich-Peterson, Toth and Radke-Prausnitz isotherm models. The removal efficiencies of the pyridine and its derivatives from the synthetic wastewaters were found to be in the range of 95-99%, 84-97%, and 90-98% for BFA, RHA and GAC, respectively. Redlich-Peterson, Toth and Radke-Prausnitz isotherms generally well represent the equilibrium adsorption of Py, 2Pi, 4Pi and AmPy onto BFA, RHA and GAC. The heat of adsorption (ΔH^0) and change in entropy (ΔS^0) for adsorption on BFA, RHA and GAC were found to be in the range of 23-108 kJ mol^{-1} and 0.12-0.15 kJ mol^{-1} K^{-1}; 8-21 kJ mol^{-1} and 0.1-0.13 kJ mol^{-1} K^{-1}; and 13-26 kJ mol^{-1}

and 0.1-0.15 kJ mol^{-1} K^{-1}; respectively. The values of change in Gibbs free energy (ΔG_{ads}^0) were found in the range of 18-36 kJ mol^{-1}, 14-20 kJ mol^{-1} and 15-22 kJ mol^{-1} for BFA, RHA and GAC, respectively. The negative value of change in Gibbs free energy indicated the feasibility and spontaneity of adsorption on the adsorbents.

Batch conditions for individual and simultaneous Py, 2Pi, 4Pi and AmPy removal by BFA, RHA and GAC were optimized by using Taguchi's design of experimental (DOE) methodology. Significant parameters viz. C_0, pH_0, m, T and t at three levels with orthogonal array (OA) layout of L$_9$ (3^4) for single and binary systems and L$_{27}$ (3^{13}) for ternary system were selected for the proposed experimental design. For single and binary systems, 9 sets of experiments were conducted. Whereas, 27 sets of experiments were conducted for the adsorption in ternary system. Taguchi's approach is found to be a potential design methodology for the optimization of adsorption processes.

The real wastewater discharged from a unit manufacturing Py and its derivatives was given adsorptive treatment using BFA, RHA and GAC as adsorbents. Taguchi's DOE methodology was used for the purpose. The parameter q_{tot} was considered to be optimized. The optimum q_{tot} by BFA, RHA and GAC was 9.96, 3.51 and 5.17 mg g^{-1}, respectively. The adsorbent dose was found to have the highest influence on the treatment process.

The removal efficiency in the I stage was found to be in the range of 90–95%, 86-92% and 90-95% for BFA, RHA and GAC, respectively. Whereas, at the II stage the efficiency was found to be 71-87%, 58-81% and 76-93% for BFA, RHA and GAC, respectively.

For the desorption experiments, water at various pH (2-12), acids, alcohol and soil-water solution have been used. The use of water at lower pH and diluted acids resulted in higher amount of desorption (~80%). The desorption capacity of soil-water solution is found to be very small.

The spent BFA and RHA need not be regenerated and can be used as a fuel and fired in a furnace to recover their energy value and to dispose them off.

The results from the present studies indicate that the use of BFA and RHA which are available at almost no cost could be viable alternatives to the activated carbons for the removal of toxic compounds from aqueous solutions.

ACKNOWLEDGEMENTS

CONTENTS

LIST OF TABLES

LIST OF FIGURES

Figure No.	Title	Page No.

Figure No.	Title	Page No.

Figure No.	Title	Page No.

ABBREVIATIONS AND NOTATIONS

ABBREVIATIONS

ACGIH	American Conference of Governmental Industrial Hygienists
2Pi	2-Picoline
4Pi	4-Picoline
AmPy	3-Aminopyridine
ANOVA	Analysis of Variance
BFA	Bagasse fly ash
CNS	Central nervous system
COD	Chemical oxygen demand
DOF	Degree of freedom
DTA	Differential thermal analysis
DTG	Differential thermal gravimetery
EOP	End of pipe
ETP	Effluent treatment plants
F	Variance ratio
FTIR	Fourier transform infrared spectroscopy
GAC	Granular Activated Carbon
HB	Higher-the-better
HYBRID	Hybrid fractional error function
IDLH	Immediately dangerous to life or health
LB	Lower-the-better
MPSD	Marquardt's percent standard deviation
MSD	Mean squared deviation from the target value
NB	Nominal-is-best
OA	Orthogonal array

OSHA	Occupational safety & health administration
P	% Contribution
Py	Pyridine
RHA	Rice husk ash
S	Sum of the Squares
SEM	Scanning electron micrograph
STEL	Short term exposure limit
TG	Thermal gravimetery
TGA	Thermo-gravimetric analysis
TLV	Threshold limit value
TWA	Time-weighted average
V	Variance
VOC	Volatile organic compound
XRD	X-ray diffraction spectra

<u>NOTATIONS</u>

$A(1)$	Level total due to parameter A at level L_1
b	Temkin isotherm constant
C_0	Initial concentration of adsorbate in solution, mg dm^{-3}
C_e	Equilibrium liquid phase concentration, mg dm^{-3}
C_S	Adsorbent concentration in the solution, mg dm^{-3}
CI_{POP}	Confidence interval for the entire population
$C.F$	Correction factor.
C_0	Initial concentration of adsorbate in solution, mg dm^{-3}
C_e	Unadsorbed concentration of the single-component at equilibrium, mg dm^{-3}
D_e	Effective diffusion coefficient of adsorbate in the adsorbent phase, m^2 s^{-1}
f_T	Total DOF
f_A	DOF of parameter A

h	Initial sorption rate, mg g^{-1} min^{-1}
k_{0B}	Constant in Bangham equation, g
k_A	Adsorption rate constant for the adsorption equilibrium, min^{-1}
k_D	Desorption rate constant for the adsorption equilibrium, min^{-1}
k_f	Rate constant of pseudo-first-order adsorption model, min^{-1}
k_{int}	Intra-particle diffusion rate constant, mg g^{-1} min$^{-1/2}$
k_S	Rate constant of pseudo-second-order adsorption model, g mg^{-1} min
K_F	Constant of Freundlich isotherm, (mg g^{-1}) (dm^3 mg^{-1})$^{-1/n}$
K_L	Constant of Langmuir isotherm, dm^3 mg^{-1}
K_R	Constant of Redlich-Peterson isotherm, g dm^{-3}
K_L	Constant of Langmuir isotherm, dm^3 mg^{-1}
K_T	Equilibrium binding constant corresponding to the maximum binding energy, J mol^{-1}
m	Mass of adsorbent per liter of solution, g dm^{-3}
m_T	Target value
n_m	Number of measurements
n_p	Number of parameters
N	Number of data points
pH_0	Initial pH of the solution
q_e	Equilibrium single-component solid phase concentration, mg g^{-1}
$q_{e,cal}$	Calculated value of solid phase concentration of adsorbate at equilibrium, mg g^{-1}
$q_{e,exp}$	Experimental value of solid phase concentration of adsorbate at equilibrium, mg g^{-1}
q_m	Maximum adsorption capacity of adsorbent, mg g^{-1}
q_t	Amount of adsorbate adsorbed by adsorbent at time t, mg g^{-1}
q_e^∞	Constant in Toth equation, monolayer adsorptive uptake, mg g^{-1}
R_a	Radius of the adsorbent particle assumed to be spherical, m
$\overline{T}$	Overall mean of response
t	Time, min

T	Absolute temperature, K
V	Volume of the solution, dm^3
V_A	Variance due to a parameter A
V_E	Variance due to error
w	Mass of the adsorbent, g
X_{Ae}	Fraction of the adsorbate adsorbed on the adsorbent under equilibrium
ΔH^0	Enthalpy change, kJ mol^{-1}
ΔS^0	Entropy change, kJ mol^{-1} K^{-1}
$\Delta H_{st, a}$	Isosteric heat of adsorption, kJ kg^{-1}
$1/n$	Mono-component (non-competitive) Freundlich heterogeneity factor of the single component
a_R	Constant of Redlich-Peterson isotherm, $dm^3 mg^{-1}$
B_T	Temkin isotherm constant, related to the heat of adsorption, J mol^{-1}
C_s	Adsorbent concentration in solution
I	Weber-Morris constant that gives idea about the thickness of boundary layer, mg g^{-1}
k	Constant in Taguchi loss-function
k_A	Adsorption rate constant
k_D	Desorption rate constant
K_{RP}	Constant in Radke-Prausnitz isotherm , dm^3 g^{-1}
k_{rp}	Constant in Radke-Prausnitz isotherm , $[(mg\ g^{-1})/(mg\ dm^{-3})^{1/P}]$
K_{Th}	Constant in Toth equation, dimensionless
L_N	OA designation
n	Number of units in a given sample
R	Universal gas constant, 8.314 J K^{-1} mol^{-1}
S/N	Signal-to-noise ratio
Th	Toth isotherm equation constant
X_A	Amount adsorbed
X_{AE}	Amount adsorbed at equilibrium

GREEK LETTERS

α	Constant used in Elovich equation, Bangham equation
β	Constant used in Redlich-Peterson equation
λ_{max}	wavelength, nm
χ^2	Chi-square

INTRODUCTION

1.1   GENERAL

Water is one of the most important matters responsible for life on earth. Water resources need to be conserved and their quality preserved. Wastewater discharges from domestic and industrial activities, and urban agglomerates into surface and ground water are affecting the water quality and its usage for different activities. The rapid industrialization with the use of the various types of raw materials for the production of final products is resulting in wastewater discharge with various inorganic and organic components. These components have different physico-chemical, thermal and toxic characteristics. Most of the industries use different amounts of water for their processing and discharge wastewater in the surface and ground water. Such wastewater discharges affect the quality of water resources. Chemical, petrochemical and agri-based chemical industries are the sources of various pollutants. Several of these industries are the sources of generating toxic materials and hazardous wastes. The wastewaters emanating from such industries find their way into natural water sources in various material states viz., solid, liquid, vapour or gas thereby affecting adversely the quality of water.

Toxics in wastewater often pass through effluent treatment plants (ETPs) which are not designed to remove them. They can also interfere with the operation of ETPs. Biological effluent treatment plants, are often badly hit with the presence or spillage of toxics into wastewaters being treated. It is therefore, necessary to properly reduce or minimize the pollution load at the source and then treat the wastewater either at the source or at the treatment facility (end of pipe, EOP treatment). The minimization of toxicity at source can be achieved by following the rules of the municipality and pollution regulating agencies regarding the limiting pollutant discharges to the

sewerage system. The reduction of the load at the source can be achieved by minimizing the use and/or spillage and the proper inventory control of the toxics, proper and adequate treatment prior to toxics discharge, recycling and reuse of waste by-products, changes in the manufacturing processes-both the use of raw materials and the unit operations. There are some organic compounds which when present in wastewater streams and/or air, are a cause of major emission concern as they are considered to be toxic and hazardous to various target organisms including human beings.

1.2   VOLATILE ORGANIC COMPOUNDS

Volatile organic compounds (VOCs) are organic chemical compounds which have high vapour pressures under normal conditions to vaporize and enter the atmosphere. Aldehydes, ketones and hydrocarbons are some of the carbon based VOCs. The VOCs are emitted from some household products including: paints, paint strippers, and other solvents; wood preservatives; aerosol sprays; cleansers and disinfectants; moth repellents and air fresheners; stored fuels and automotive products; dry-cleaned clothing. These are also emitted from the petroleum fuels (e.g. gasoline and natural gas). The VOCs have some health effects such as eye, nose, and throat irritation; headaches, loss of coordination, nausea; damage to liver, kidney, and central nervous system. Some organics can cause cancer in animals and some are also known to cause cancer in humans. As with other pollutants, the extent and nature of the health effect will depend upon many factors including the level of exposure and the length of time exposed. Eye and respiratory tract irritation, headaches, dizziness, visual disorders, and memory impairment are among the immediate symptoms that some people have experienced soon after exposure to some organics. Some VOCs are discharged into the air environment or into the water bodies as an effluent from various industries which use these materials as raw materials or manufacture some these compounds. The presence of the toxic materials in excess of the exposure limit in wastewater to be discharged in the environment or in water bodies is dangerous for the living matter including aquatic life forms. Therefore, the treatment of wastewater containing toxic

materials is very essential to save the live forms from health problems and the environment from being polluted.

1.3   PYRIDINE AND ITS DERIVATIVES

Pyridine (Py) are volatile, toxic and flammable with a pungent and unpleasant odour. Py is the parent of a series of chemicals, and is used as a solvent in paint and rubber preparation, as an intermediate in making insecticides and herbicides for agricultural applications and in research laboratories for functions such as extracting plant hormones. It is also used directly in the denaturation of alcohol and to make many different products such as medicines, vitamins, food flavorings, dyes, adhesives, and in water proofing for fabrics [Kirk and Othmer, 1982; Yates, 1984; Kumar et al., 1995; Mall et al., 2003; Lataye et al., 2006]. Industrial wastewater containing Py and its derivatives show toxicity to aquatic life and create nuisance because of their malodorous and pungent smell [Lataye et al., 2006, 2007a-f]. Py is a colourless liquid with penetrating, empyresmatic odour. It mixes very easily with water and is soluble in alcohol, ether, and benzene. It is a fire and explosion hazard in the form of vapour, when exposed to flame or spark. When heated to decomposition, it emits highly toxic vapours of NO_x in an oxidative atmosphere. It has very high half-life when released in the atmosphere. It is also mildly toxic by inhalation; its vapour is skin and severe eye irritant and exposure to it can cause depression, gastrointestinal upset, liver and kidney damage, headache, nervousness, dizziness, insomnia, nausea, anorexia, frequent urination and dermatitis [Lewis, 2004].

Py-bearing wastewaters emanate from Py manufacturing units, pharmaceutical units, etc. The typical concentration of Py in wastewaters produced in a multidrug intermediates-product plant manufacturing Py and its derivatives and other products is in the range of 20-300 mg dm^{-3}. During emergency spills, the concentration may be as high as 600-1000 mg dm^{-3}. At a Py concentration of 0.82 mg dm^{-3} in wastewaters, unpleasant Py odor is detectable [Baker, 1963]. However, the vapor (odor) concentration may be as low as 7 µg dm^{-3}, while the threshold odor concentration can be ~0.3 µg dm^{-3}. Py does not have any BOD or COD. Although no concentration limit

has been prescribed in the industrial wastewaters for their safe discharge into sewers or on land, it is imperative that the wastewater should not have more than 1 mg dm^{-3} of Py, so as to minimize the toxicity of wastewater and reduce the odor emanating from it. The plants related to pyridine are plagued with the problem of intense odour emanating either from the wastewater or from the handling and storage facilities. In a typical plant producing pyridine and its derivatives and other associated chemicals, wastewaters are concentrated in evaporators and then incinerated. This method of treatment is capital-intensive and requires fuel to be used to effect evaporation, concentration and incineration. Any problem arising in the incineration system forces the plant to store the concentrated wastewater, as no other alternative treatment system, generally, exists in the plant. Removal of pyridine from the wastewater stream is therefore of vital importance.

Physical Properties

The physical properties of pyridines are the consequence of a stable, cyclic, 6-π-electron, π-deficient, aromatic structure containing a ring nitrogen atom. The ring nitrogen is more electronegative than the ring carbons, making the two-, four- and six-ring carbons more electropositive than otherwise would be expected from knowledge of benzene chemistry. The aromatic π-electron system does not require the participation of the lone pair of electrons on the nitrogen atom; hence the terms weakly basic and π-deficient are used to describe pyridine compounds. Pyridine has a boiling point 35.2 °C higher than benzene (115.3 vs. 80.1 °C), and unlike benzene, it is miscible with water in all proportions at ambient temperatures. The much higher dipole moment of pyridine relative to that of benzene is responsible, in significant part, for the higher boiling point and water solubility. Benzene and pyridine are aromatic compounds having resonance energies of similar magnitude, and both are miscible with most other organic solvents. Pyridine is a weak base (pea = 5.22), being both an electron-pair donor and proton acceptor, whereas benzene has little tendency to donate electron pairs or accept protons. Pyridine is less basic than aliphatic, tertiary amines. Table 1.3.1 shows the properties of Py, 2Pi, 4Pi and amply whereas, Table 1.3.2 show the uses of Py and its derivatives.

4

Table 1.3.1: Properties of Py, 2Pi, 4Pi and AmPy [www.jubl.net/msds, Kirk and Other, 1996; Lewis, 2004]

S. No.	Property	Py	2Pi	4Pi	AmPy
1	Synonyms	Azabenzene, Azine, Piridina, etc.	α-picoline, α-methylpyridine	γ-picoline, 4-methylpyridine	3-pyridinamine, β-aminopyridine
2	Chemical Formula	C_5H_5N	C_6H_7N	C_6H_7N	$C_5H_6N_2$
3	Molecular Weight	79.11	93.14	93.14	94.13
4	Physical Properties	Colourless liquid, sharp penetrating empyeumatic odor, burning taste	Colourless liquid, strong unpleasant odor	Colourless liquid, disagreeable odour	solid yellow to brown
5	Density ($g\ cm^{-3}$)	0.98	0.94	0.95	0.75
6	Boiling Point (°C)	115.3	129	145	248
7	Freezing Point (°C)	-42'	-70	3.6	60-63
8	Flash Point (°C)	68	102	134	124
9	Soluble in	water alcohol, ether	water, alcohol, ether	water, alcohol, ether	water
10	IDLH (Immediately Dangerous to Life or Health), $mg\ dm^{-3}$	1000	Not known	Not known	Not known
11	OSHA PEL ($mg\ dm^{-3}$)	TWA 5	TWA 2 (8 h exposure)	TWA 2 (8 h exposure)	
12	ACGIH TLV ($mg\ dm^{-3}$)	TWA 5 (Proposed: TWA 1 $mg\ dm^{-3}$ Confirmed Animal Carcinogen)	5 (STEL, 15 min)	5 (STEL, 15 min)	

S. No.	Property	Pyridine	2-picoline	4-picoline	3-aminopyridine
13	UN Hazard Class	3	3	3	
14	Safety Profile	Poison by intraperitorial route, moderately toxic by ingestion, skin contact, intravenous and subcutaneous routes. Mildly toxic by inhalation, skin and severe eye irritant	Poison by intraperitorial route, moderately toxic by ingestion, skin contact, intravenous and subcutaneous routes. Mildly toxic by inhalation, skin and severe eye irritant	Poison by intraperitorial route, moderately toxic by ingestion, skin contact, intravenous and subcutaneous routes. Mildly toxic by inhalation, skin and severe eye irritant	Fatal if swallowed, fatal in contact with skin, fatal if inhaled, irritating eyes and resperatory system,
15	Health Effects	Can cause CNS depression, gastrointestinal upset, and liver and kidney damage	Can cause CNS depression, gastrointestinal upset, and liver and kidney damage	Can cause CNS depression, gastrointestinal upset, and liver and kidney damage	May be fatal if swallowed, inhaled or absorbed through skin, High concentration are extremely destructive to tissues of mucous, membranes, upper respiratory tract, eyes and skin. May cause convulsion, Damage to nervous system

Table 1.3.2: Uses of pyridines and its derivatives [Kirk and Othmer, 1996]

Compounds	Uses
Pyridine	Solvents in organic chemistry, dehydrochlorination reaction and extraction of antibiotics, starting material for agrochemicals and pharmaceuticals, pyridine is used as precursor for herbicides such as diquat and paraquat, insecticide such as chlorpyrifos and antifungal agents.
2-picolines	Used as a precursor of 2-vinylpyridine, used in agrochemicals and pharmaceuticals, such as nitrapyrin to prevent loss of ammonia from fertilizers; picloram, a herbicide; and amprolium, acoccidiostat. Used for making fungicides such as piperalin.
3-picoline	Used as a starting material for agrochemicals and pharmaceuticals. Used to make insecticides such as chlorpyrifos, food additives such as niacin and its amide, and herbicides such as fluazifop-butyl.
4-picoline	In the production of antituberculosis agent, isoniazid. It is also used to make 4-vinylpyridine, subsequently polymers.

1.4 TREATEMENT PROCESSES FOR PYRIDINE BEARING WASTEWATERS

Several investigators have used a number of in lab-scale experiments for the removal of Py and Py-derivatives: Rundle oil shale [Zhu et al., 1988], montmorillonite and kaolinites [Baker and Lu, 1971], α-Al_2O_3 and iron powders [Ardizzone et al., 1998], zeolites [Bludau and Karge, 1998], sepiolite [Sabah and Celik, 2002], activated carbon [Kumar et al., 1995, Mohan et al., 2004] and ion-exchange and porous resins [Akita and Takeuchi, 1993]. Mohan et al., [2004] have used activated carbons (AC) manufactured from agricultural waste materials for the sorptive removal of Py. Granular activated carbon (GAC) is an excellent adsorbent for the removal of dyes, organics and metals from wastewaters. Kumar et al. [1995] used GAC for the removal

7

of Py from an aqueous solution with an initial concentration (C_0) in the range of 50–250 mg dm^{-3}. They presented batch and continuous (fixed bed) adsorption studies and reported 96.4% Py removal which is equivalent to q_e=1.2 mg Py g^{-1} of carbon. The equilibrium was found to occur in ~2 h. However, they have studied the adsorption at C_0=150 and 200 mg dm^{-3} in the aqueous solution. The effect of contact time (t) and temperature on the adsorption process and the variation in the system pH during adsorption process have, however, not been reported. They have also not studied the thermodynamic and kinetic aspects of adsorption.

Various treatment processes used for the removal of pyridine and its derivatives from water/wastewater are biodegradation, adsorption and electrosorption, ozonation and ion exchange. Among these adsorption systems are rapidly gaining prominence as treatment processes, which produce good quality effluents. The adsorbents utilized for the removal of pyridine include Rundle oil shale, montmorillonite and kaolinites, α-Al_2O_3 and iron powders, zeolites, sepiolite, carbon and ion-exchange and porous resins. Granular/powdered activated carbon (GAC/PAC) is the most widely used adsorbent, as it has a good capacity for the adsorption of heavy metals. However, high cost of activated carbon and 10-15% loss during its regeneration has been a deterrent in the utilization of activated carbon in the developing countries. This has led to a search for cheaper alternative materials as adsorbents such as lignin, bagasse pith, peat, saw dust, coal fly ash, rice husk ash and bagasse fly ash. These unconventional adsorbents have been used as adsorbents for the removal of various pollutants like carbon slurry [Singh and Tiwari, 1997], kaolin [Sen et al., 2002], resins [Koul and Gupta, 2004], soil and clay [Drillia et al., 2005], silica, peat, fly ash and bentonite [Viraraghavan and Alfaro, 1998], lignite, bagasse pith, wood, saw dust [Chakraborty et al., 2006], molecular sieves [Zhao et al., 1996], bagasse fly ash (BFA) [Swamy et al., 1997; Mall et al., 2005a,b; Lataye et al., 2006, 2007d], rice husk ash (RHA) [Srivastava et al., 2006a; Lataye et al., 2007b-f].

1.5 BAGASSE FLY ASH (BFA) AND RICE HUSK ASH (RHA) AS ADSORBENTS

Large quantities of industrial by-products are produced every year by chemical and agricultural process industries in India. These materials pose problems of disposal and their management, and also health hazards. However, some of these agricultural wastes have been found to be good adsorbents for the treatment of wastewaters and industrial effluents. BFA has been used by many researchers as an adsorbent for the removal of various metals and other chemicals from the wastewaters. RHA as agri-based waste material available free of cost from the particulate removal equipment attached to the boiler furnaces using rice husk as the fuel, has been shown to have high adsorption efficiency for the removal of cadmium (Cd(II)), nickel (Ni(II)) and zinc (Zn(II)) metal ions [Srivastava et al., 2006a], lead and mercury [Feng et al. 2004] and palmytic acid [Adam and Chua, 2004].

A number of low-cost alternative adsorbents have been limited in their use. The surface area of most of the alternative adsorbents has been found to be low resulting in poor adsorptive capacity. The comparative studies on the adsorption of Py on different adsorbents have not been carried out. However, the development of low-cost adsorbents with good surface area, exhibiting good adsorption potential for the removal of toxic compounds from wastewater is an important area.

BFA is a waste material formed during the combustion of bagasse, as a fuel in the boilers of the sugar mills. BFA is also obtained from particulate collection equipment connected to bagasse-fired boilers and emission stacks on the upstream and downstream sides, respectively. About 10 million tonnes of bagasse is produced annually in India. About 90% of this bagasse is used as a fuel in bagasse fired boilers. The production of bagasse fly ash is estimated to be about 3 kg/tonne of sugar produced. With the overall bagasse fly ash collection efficiency of 80% in the dust collection equipment, it is estimated that fly ash availability from the sugar industry would be of the order of 0.5 million tonnes/year.

The adsorption properties of BFA are highly influenced with the firing practices of bagasse. Several investigators have recently shown interest in the use of bagasse fly ash as an adsorbent. It has been used for the COD removal from sugar mill [Mall et al., 1994], and paper mill effluents [Srivastava et al., 2005a]. BFA has also been used for the adsorptive removal of phenolic compounds [Srivastava et al., 2005b], dyes [Mall et al., 2005a, b], and pyridine [Lataye et al., 2006] from wastewaters.

The annual production of paddy rice (*Oryza sativa*) globally was 579,500,000 tonnes in 2002 [FAO Statistical Database, 2002]. Rice is grown on every continent except Antarctica, over an area that covers about 1% of the earth's surface. It is a primary source of food for billions of people, and ranks second to wheat in terms of area and production [FAO Statistical Database, 2002]. Most paddy is produced by China (31%) followed by India (21%). During the milling process of paddy, rice husk is dehulled and removed. Thus the rice husk is an agricultural waste, accounting for about one-fifth of the annual gross rice production about 545 million tons, in the world [Feng et al., 2005]. Rice husk is generally used for burning. Rice mills and other rural area based industries use it as a fuel in their boilers/furnaces. Some rice mills also use it as a fuel to produce producer gas. Rice husk can be used for energy production and the production of activated carbon [Usmani et al., 1993], silicon carbide [Moustafa et al., 1997] and tetra-methoxy silane [Akiyama et al., 1993] as also for the production of silica for ceramics [James and Rao, 1986a, b] and portland cement [Barkakati et al., 1994]. Rice husk ash (RHA) is generally collected from the particulate-collection equipment attached upstream of flue gas stacks. Roughly about 15-18% of the mass of the husk is collected as RHA in the particulate collection equipment.

RHA has many applications due to its attractive properties. It is an excellent insulator, so has applications in industrial processes such as steel foundries, and in the manufacture of insulation for houses and refractory bricks. RHA has also been used in the production of sodium silicate films [Kalapathy et al., 2000a, b]. It is an active pozzolan and has several applications in the cement and concrete industry [Salas, 1987;

Boateng and Skeete, 1990; Hara et al., 1992; Tuts, 1994]. Since the main components of rice husk are carbon and silica, it has the potential to be used as an adsorbent as well. For example, rice husk ash heated at 500°C has been used as an adsorbent in vegetable oil refining [Proctor and Palaniappan, 1989; Palaniappan and Proctor, 1990; Proctor et al., 1995]. RHA produced by heating rice husks at 300°C has been shown to adsorb more gold-thiourea than the conventionally used activated carbon [Nakbanpote et al., 2000]. RHA has been used for the removal of metals [Srivastava et al., 2006a] and dyes [Mane et al., 2006].

1.6   TAGUCHI'S DESIGN OF EXPERIMENTAL METHODOLOGY

Taguchi's design of experimental methodology has been used extensively in carrying out experiments and devising a strategy for quality control in the manufacturing industries. Taguchi's method to improve quality of the products depends heavily on designing and testing a system based on engineer's judgment of selected materials, parts and nominal product/process parameters based on current technology. While system design helps to identify the working levels of the design parameters, process parameter design seeks to determine the parameter levels that produce the best performance of the product/process under study. The optimum condition is selected so that the influence of uncontrollable factors (noise factors) causes minimum variation to the system performance. The orthogonal arrays, variance and signal to noise analysis are the essential tools of the parameter design.

Tolerance design is a step to fine-tune the results of parameter design by tightening the tolerance of parameters with significant influence on the product.

Taguchi's method of experimental design provides the optimal selection of parametric values, based on their intra-parametric interaction, to accomplish a process. This method minimizes the number of experiments to be conducted based on the statistical significance of parameters and the interactive influences of these parameters. It is intended to use this method in adsorption studies of Pi, 2Pi, 4Pi and AmPy using BFA, RHA and GAC as adsorbents.

1.7   OBJECTIVES OF THE PRESENT STUDY

No work has been found in the open literature on adsorption of pyridine bearing wastewater by low-cost adsorbents such as bagasse fly ash and rice husk ash. Also, no literature is available utilizing Taguchi's optimization method for designing experiments on the simultaneous adsorption of pyridine and its derivatives from aqueous solutions. The use of low-cost adsorbents for the treatment of various wastewaters generates large volumes of solid waste. These solid wastes have great potential for energy recovery. However, no study has been reported on the thermal degradation characteristics and kinetics of spent adsorbents under oxidizing environment. In view of the literature survey and the necessity of developing a treatment process for pyridine bearing aqueous solutions, the following aims and objectives have been set for the present work.

1. To characterize the agri-based waste materials like bagasse fly ash (BFA), rice husk ash (RHA) and commercial grade activated carbon (GAC) for their physico-chemical and adsorption properties. These characteristics include the analysis of particle size and pore size (and area) distribution, proximate and ultimate analysis, and the surface and functional characteristics by FTIR, XRD and SEM analyses.

2. To utilize BFA, RHA and GAC as adsorbents for the treatment of pyridine, 2-picoline, 4-picoline and 3-aminopyridine bearing synthetic wastewater and to compare their performance with that of available granular activated carbon (GAC).

3. To study the effect of various parameters like initial pH (pH_0), adsorbent dose (m), contact time (t), initial concentration (C_0), and temperature (T) on the removal of of pyridine, 2-picoline, 4-picoline and 3-aminopyridine from the aqueous solution in batch study.

4. To carry out kinetic and equilibrium adsorption and studies for the adsorption of pyridine, 2-picoline, 4-picoline and 3-aminopyridine onto

various adsorbents and to analyze the experimental data using various kinetic and isotherm models.

5. To understand the thermodynamics of adsorption and to estimate the isosteric heat of adsorption for pyridine, 2-picoline, 4-picoline and 3-aminopyridine using BFA, RHA and GAC as adsorbents.

6. To utilize Taguchi's optimization method for the design of experiments for estimating the effects of various adsorption parameters in single, binary, and multi-component (solute) adsorption systems in the batch adsorption mode.

7. To perform desorption study for the possible regeneration of adsorbents and to develop a method for disposing off the spent adsorbents by fixing the pyridine and picoline chemically or physically.

8. To perform the multistage treatment to reduce the residual concentration of pyridine, 2-picoline, 4-picoline and 3-aminopyridine upto the permissible discharge limit in the wastewaters.

LITERATURE REVIEW

2.1 GENERAL

The treatment methods used for the removal of Py and its derivatives from the wastewaters include physico-chemical, biological, and electrochemical treatment and thermal incineration. In this chapter, a critical review of the treatment methods for the removal of Py, 2Pi, 4Pi and AmPy from wastewater/aqueous solution is presented.

2.2 PHYSICOCHEMICAL TREATMENT OF PYRIDINE AND ITS DERIVATIVES

Adsorption is a simple and cost effective method for the removal of Py and its derivatives. The critical review on the physico-chemical methods used for the removal of pyridine and its derivatives has been discussed in this section.

Baker and Luh [1971] reported the sorption of pyridine onto highly purified sodium montmorillonite and sodium kaolinite in aqueous solution over a range of clay to pyridine ratios and as a function of pH and temperatures. They studied the sorption isotherms for the removal of pyridine. Pyridine sorption onto sodium kaolinite and sodium montmorillonite was found to be rapid. Significant sorption took place within 17 min and was complete within 24 h. The process was attributed to cationic exchange with the extent of pyridinium ion sorption depending upon the pH of the solution. The maximum adsorption was reported to be 46 % for sodium kaolinite at pH 5.5 and 67% for sodium montmorillonite at pH 4.0. They found that the pyridine molecules do not sorb at pH > 7.

Luh and Baker [1971] also studied the desorption of pyridine from loaded clay in aqueous solution as a function of solution pH, time, the number of stages of desorption with transfer to fixed volumes of solution and with transfer to solutions of

varying volume. For kaolinite no pyridine desorption occurred at pH 9 or 11 over 7 days after the initial pyridine release in 17 min. For the montmorillonite, maximum desorption occurs in 17 min at pH 11. In this case, desorption is greater (89 %) than that for kaolinite (66 %) at the same pH. For both clays, minimum desorption occurs at pH 5 which is to be expected since maximum sorption occurs in this range. For the montmorillonite, significant desorption was noted at pH 9 as a function of time. At pH 1, both clays exhibited significant pyridine desorption. Previously sorbed pyridine desorbs from the clays as a function of time and solution pH with maximum desorption at pH 1 and 11 and minimum near pH = pK_a = 5.25. Pyridine desorption was found to be much slower than sorption at comparable pH and clay-pyridine ratio. The extent of desorption is also directly related to the number of stages and/or the volume of solution. Zeta potential changes are greatest between pH 1-4 with coagulation and charge reversal at pH ~ 2 if the pyridine concentration is less than the cation exchange capacity (CEC).

Adsorbed pyridine has been used to investigate the acidic properties of carbon films by means of the IR spectroscopy by Zawadzki [1988]. He showed that pyridine could be adsorbed on carbon surface in four different states: physically adsorbed pyridine, hydrogen-bonded pyridine, pyridine in interaction with a Lewis acid site, and pyridine in interaction with a Brönsted acid site. Spectral changes caused by adsorption were established by comparing IR spectra of the same film before and after the adsorption. The results revealed clearly that the protons responsible for the OH stretching bands were not acidic enough to interact with pyridine. He concluded that (1) pyridine is physically adsorbed onto the surface of an unoxidized carbon film, and (2) IR spectra of pyridine adsorbed on an oxidized carbon film showed evidence both for hydrogen bonding interactions and for coordination compounds adsorbed on carbon surface. The strength of adsorption of pyridine on an oxidized carbon film was enhanced by simultaneous interactions involving surface hydroxyl groups adjacent to Lewis acid centers. (3) Although some weak protonic sites had well detected on an

oxidized carbon film by ion exchange as well as by ammonia and n-butylamine adsorption, no such intrinsic Brönsted sites were found by pyridine adsorption, since a protonated pyridine was not formed at a detectable level due to the lower basicity of pyridine. (4) IR spectra of pyridine on an oxidized carbon film that had been heated at 800°C have shown that the predominant mode of adsorption involved coordinative bonding between pyridine molecules and Lewis acidic surface sites.

Zhu et al. [1988] used Rundle spent shale for the adsorption of pyridine from dilute aqueous solution. They reported that at pH 8, Rundle-Lurgi spent shale adsorbs a significant amount of pyridine. The adsorption of pyridine from aqueous solutions onto the solids generated by the processing of Rundle oil shale showed the adsorption isotherm of Langmuir type (L-4) with two plateaux according to the system proposed by Giles et al. [1960, 1974]. The first plateau of L-4 curve was attributed to the completion of monolayer coverage and the second to the completion of a further layer of adsorbed molecules. The L-4 curve could result from the filling of the readily-available surfaces while the second part could result from the penetration of regions not initially accessible. The second stage of the curve could also be the result of the reorientation of the sorbed molecules providing for a denser packing. The Langmuir model was not satisfactory for the higher concentration region cations leached from the spent shale or present in the retort water (Na, K, Ca, NH_4) showed a marked effect on the adsorption. The adsorption was found to be controlled by factors such as pyridine co-ordination, surface protonation and ion exchange. The montmorillonite present in the spent shale was found to affect a re-orientation of the adsorbed pyridine.

The chemical interactions of pyridine with the spent shale surface was shown to follow the under mentioned mechanism [Weber, 1966]:

$$Py + H^+ \rightleftharpoons PyH^+ \tag{a}$$

$$Py + M^+ - SS \rightleftharpoons -M^+ - SS \tag{b}$$

$$PyH^+ + M^+ - SS \rightleftharpoons PyH^+ - SS + M^+ \tag{c}$$

$$H^+ + PyH^+ - SS \rightleftharpoons H^+ - SS + PyH^+ \tag{d}$$

$$H^+ + M^+ - SS \rightleftharpoons H^+ - SS + M^+ \qquad \text{(e)}$$

$$Py + H^+ - SS \rightleftharpoons PyH^+ - SS \qquad \text{(f)}$$
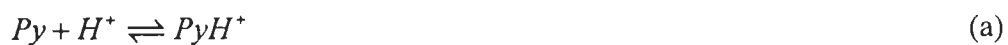
where M^+ represents the exchangeable cations on the spent shale surface (*SS*) and H^+ refers to the hydronium ion (H_3O^+). The dominant sorption reaction for pyridine was probably equation (b) where the pyridine molecules coordinate to the exchangeable cation M+, either directly by replacing the water in the primary co-ordination shell or indirectly through a water bridge. Pyridine could also be adsorbed by protonation at the spent shale surface as represented by equation (f). This reaction is feasible because the pH at the surface is usually at least 2 units lower than the pH of the bulk solution [Davies and Rideal, 1963; Bailey et al., 1968]. For the mechanism shown by equation (b), the pyridine molecule must compete with water for the ligand position around the exchangeable cations. This is possible because of its relatively high permanent dipole moment (2.1 X 11 esu). The pyridine molecule is adsorbed by phyllosilicate clays [Farmer and Mortland, 1966; Theng, 1974]. Theng [1974] noted that the principal mechanism of pyridine adsorption onto clays was by co-ordination with the exchangeable cations either directly (by replacing water in the primary hydration shell) or indirectly through a water-bridge hydrogen bond. Baker and Luh [1971] concluded that below pH 7 significant adsorption of pyridine occurs onto montmorillonite and kaolinite due simply to cation exchange of the pyridium ion. It has also been reported that the pyridine is degraded by ultraviolet light [Barnes, 1960].

Zaki et al. [1989] studied the adsorption of pyridine onto ceria surface and found that the IR spectrum resulting from Py adsorption on Al/Ce displays, in addition to the characteristic bands of Py bonded to Lewis site, a unique band at 1534 cm^{-1}. Thus the band occurs in the frequency range (1439-1550 cm^{-1}). When the band occurs at ≥ 1631 cm^{-1} it indicates the formation of Py bonded to a Brönsted site. Doping of ceria with Na$^+$, Al^{3+} and Cr^{3+} ions (at 1 atom dopant per Ce atom) largely modified the Py adsorption capacity and surface reactions, thus revealing disparate impacts on acid/base properties of the surface. They concluded that (1) ceria surfaces, produced by the

thermal decomposition at 400 °C of diammonium hexanitratocerate, exposes Lewis acid sites of at least two different acidity strengths as well as two types of OH⁻ groups. (2) high-temperature calcination of ceria (at 800 °C) weakens the surface acidity and improves the chemical reactivity of basic sites. (3) Na^+ ions have a very strong poisoning effect on the overall acid/base properties of ceria. Cr^{3+} ions have a promoting effect, whereas Al^{3+} ions help to generate Brönsted acid sites.

Martin et al. [1992] studied the adsorption of pyridine, formic acid, and acetic acid on MgO, MoO_3 and MoO_3/MgO (Mo: Mg = 1:15) samples calcined at 773 K (where no extensive reaction between the two oxides seems to take place) or 1100 K (where the $MgMoO_4$, species is formed) by FIT-IR spectroscopy. Found that pyridine get sorbed on the lewis sites on the surface of magnesia developed by molybdena. Pyridine get physisorbed shown by the bands at 1442 and 1598 cm⁻¹.

Studies on the sorption equilibria of pyridine, picoline and lutidine in aqueous solution on ion-exchange and porous resins (XAD-2, 4, 7 and 8) have been reported by Akita and Takeuchi [1993]. The sorption of pyridines best represented by Langmuir isotherm on strong acid ion-exchange resin and Freundlich isotherm adsorption of pyridines on both weak acid ion-exchange and porous resins. The pyridines were sorbed on the resins in the sequence of pyridine < 3-picoline < 3, 5-lutidine where the selectivity increased as follows: strong acid ion-exchange resin (200C) <weak acid ion-exchange resin (IRC-50) < porous resin (XAD-4). The monolayer adsorption capacity reported in the study is 4.47 mg g⁻¹ for pyridine, 4.48 mg g⁻¹ for 3-picoline and 4.2 mg g⁻¹ for that of 3-, 5- lutidine on the resins.

The adsorption of toxic and odorous pyridine on activated carbon is reported by Kumar et al. [1995] in batch and column system. The batch study was performed in the initial concentration range of 50-250 mg dm⁻³ of pyridine. At an initial concentration of 200 mg l⁻¹, 96.4 per cent (q_e = 1.203 mg g⁻¹) removal of pyridine was obtained. Equilibrium adsorption data represented by both the Freundlich and Langmuir model. They described the adsorption mechanism in three consecutive steps. First the pyridine migrate through the solution to the exterior surface of the adsorbent particles by

molecular diffusion, i.e. film diffusion, then the solute moves from particle surface into interior site of particles by pore diffusion and finally the adsorbate is adsorbed onto the active sites at the interior surface of the adsorbent particle. As the final adsorption step is very rapid the overall rate of adsorption will be controlled either by film diffusion or by internal diffusion [Smith, 1968; Weber, 1972]. The intra-particle study shown that two separate regions could be seen. The initial portion of which is due to external mass transfer followed by the region showing intraparticle diffusion mass transfer [Allen et al., 1989]. In column studies breakthrough time increased with increasing bed heights and decreasing flow rates. The BDST model was found applicable. They concluded that activated carbon can be used effectively for removal of pyridine from wastewater stream.

Batch ozonation and biological treatment method for the removal of 3-Methylpyridine (MP) and 5-ethyl-2methylpyridine (EMP), is reported by Stern et al. [1997]. They found that 90 % methylpyridines were removed. 5 moles of ozone were needed per mol of MP removed. EMP was initially oxidized much faster but the reduction of DOC only 5% when EMP was removed by 90%. 4 moles of ozone were required to remove one mole of EMP.

Ardizzone et al. [1998] studied the adsorption of aniline and pyridine at solid-liquid interfaces from n-hexane solutions onto α-Al_2O_3 and iron powders. Langmuir and the BET adsorption isotherms were to describe the adsorption process. Results were analysed on the basis of the Frumkin-Fowler-Guggenheim equation. The two solid adsorbents have been analysed by XPS determinations to assess their actual surface state and degree of hydration:hydrophilicity.

Bludau et al. [1998] used in situ FTIR spectroscopy to monitor the sorption and desorption kinetics of pyridine into and out of mordenite, ZSM-5 and silicate. Sorption and desorption of pyridine was measured through the intensity changes of the IR bands typical of sorbed pyridine. At sufficiently high temperatures 525-575 K the uniform diffusion coefficients for the whole sorption process was $D = 1 \times 10^{-12}$ and $D = 6 \times 10^{-11}$ $cm^2 s^{-1}$ for H-MOR at 525 K and H-ZSM-5 at 575 K respectively. The slow transport of

pyridine into the micropores is the rate-determining step, which may indeed be described as diffusion, but followed by a rapid reaction with the acidic Brönsted and/or Lewis sites. The values were found for the kinetics of populating both the Brönsted centres (indicated through the change in the absorbance of the typical PyB band at 1540 cm^{-1}) and the Lewis sites (monitored by the increase of the absorbance of the typical PyL band at 1450 cm^{-1}). Isosteric heat of adsorption of pyridine in Li-ZSM-5 and Na-ZSM-5 were determined to 195-155 kJmol^{-1}. and 120 kJmol^{-1} and were thus significantly higher than for benzene in H-ZSM-5 (65$\pm$5 kJmol^{-1}).

Tadjeddine et al. [1999] have investigated the geometry of the adsorption of pyridine on gold single-crystal electrode by in situ difference frequency generation (DFG) in aromatic ring spectral range, by using the CLIO free electron laser. Pyridine adsorbs via the nitrogen lone pair, the molecular plane being tilted. The potential dependence of the vibrational modes showed evidences of a reorientation of the molecule around the potential of zero charge.

Diez and Amalvy [2003] studied the interaction of pyridine, 2-vinylpyridine, and 4-vinylpyridine with silica surfaces and found that pyridine interacts more strongly with silica clusters than its derivatives, whereas 2-vinylpyridine, in its turn, exhibits a larger interaction energy than 4-vinylpyridine. They also found that the interaction pattern is dominated in all cases by the formation of a hydrogen bond between the nitrogen atom and a hydroxyl group of the silica cluster, a second, very weak hydrogen bond is formed in some of the systems, though. It is proposed that the trend of not forming nanocomposites when using 2-vinylpyridine is mainly due to the involvement of its vinyl group in a weak hydrogen bond to an oxygen atom of the silica surface avoiding to polymerize and not due to a weak acid–base interaction nor steric effects.

Pejov and Skapin [2004] were studied the adsorption of pyridine on Lewis acid sites of microcrystalline γ-alumina by quantum chemical cluster model approach at B3LYP and HF/6-31++G (d, p) levels of theory considering both the standard and the counterpoise-corrected potential energy surfaces (PESs). Harmonic vibrational frequency shifts of pyridine $\nu 8$ and $\nu 19$ internal mode components calculated at both

levels of theory seem to excellently reproduce the experimental observations, the results for standard and counterpoise-corrected PESs being essentially identical. The interaction energies of pyridine with various clusters representing microcrystalline γ-Al$_2$O$_3$ were also calculated and the natural bond orbital and atoms in molecules analyses were performed.

Mohan et al. [2004] developed carbons; FAC (activated carbon derived from coconut fibres), SAC (activated carbon derived from coconut shells), ATFAC (activated carbon derived from acid treated coconut fibres) and ATSAC (activated carbon derived from acid treated coconut shells) and used in the adsorption study. They studied the adsorption in the lower range of pyridine concentration (1-100 mg dm^{-3}). The authors found that the Langmuir adsorption isotherm model fits the data better as compared to the Freundlich adsorption isotherm model. The adsorption of pyridine follows the first order rate kinetics. They found the effective diffusion coefficient D_i, increasing with temperature in the range of 45.27 x 10^{-10} – 237.12 x 10^{-10} m^{2}s^{-1} for all the adsorbents. The activation energy for FAC, SAC, ATFAC and ATSAC was found to be 3.66, 5.34, 18.73 and 26.18 kJmol^{-1} respectively. The authors have concluded that the adsorption occurs through a particle diffusion mechanism at temperatures 10 and 25 °C while at 40 °C it occurs through film diffusion mechanism. Similarly at concentrations 25 and 50 mg dm^{-3} the adsorption is particle diffusion controlled while at $\leq$ 50 mg dm^{-3} it is film diffusion controlled.

Mohan et al. [2005] studied the ability of activated carbons developed from coconut shell to adsorb 2Pi, 3-picoline, and 4Pi from aqueous solution. The developed carbons were designated as SAC (activated carbon derived from coconut shells with out any treatment) and ATSAC (activated carbon derived from acid treated coconut shells). They characterized and utilized the carbons for the sorption of α-picoline, β-picoline, and γ-picoline at different temperatures, particle size, pH and solid to liquid ratio. The Langmuir and Freundlich isotherm models were applied and the Langmuir model was found to best report the equilibrium isotherm data. The adsorption of α-picoline,

β-picoline, and γ-picoline followed the pseudo-second order rate kinetics. Authors have concluded that in majority of cases, the adsorption is controlled by particle diffusion at temperatures 10 and 25 °C while at 40 °C it is controlled by film diffusion mechanism. Similarly at concentrations 25 and 50 mg dm^{-3} the adsorption was governed by particle diffusion in most of the cases while at > 50 mg dm^{-3} it was film diffusion controlled. The overall capacity of ATSAC was higher than SAC. The sorption capacity of γ-picoline was found more followed by α-picoline and β-picoline. The authors reported that the sorption followed the order α-picoline $<$ β-picoline $<$ γ-picoline Further the sorption followed the order a-picoline The authors reported that, 40-50% of the ultimate adsorption occurs within the first hour of contact for the adsorption of α-picoline, β-picoline and γ-picoline and the saturation is reached in 48 h.

The adsorption of pyridine on low cost adsorbent which is available easily and abundantly was studied by Lataye et al. [2006]. The authors studied the adsorption of pyridine from aqueous solutions, using BFA using batch adsorption system. The influence of various parameters, such as initial pH (pH$_0$), adsorbent dose (*m*), contact time (*t*), initial concentration (*C$_0$*), and temperature (*T*), on the removal of Py from the aqueous solutions have been studied. The study was performed in the wide range of initial concentration i.e. $50 - 600$ mg dm^{-3}. The maximum removal of Py is determined to be 99% at lower concentrations (<50 mg dm^{-3}) and 95% at higher concentrations (600 mg dm^{-3}), using a BFA dosage of 25 kg m^{-3} at normal temperature. They conducted the studies on Py adsorption equilibrium and kinetics. The adsorption equilibrium analyses were performed, using the Langmuir, Freundlich, Redlich-Peterson, and Temkin isotherm equations. The authors found that the Langmuir equation is determined to be the best to represent the equilibrium sorption data. They have also reported the thermodynamic studies, revealed that the adsorption of Py on BFA is endothermic in nature and that the isosteric heat of adsorption decreases as the equilibrium uptake of Py on the BFA surface increases (269.92 and 187.63 kJ kg^{-1} for the equilibrium Py concentration on the adsorbents in the range of 4-20 mg g^{-1}). The

authors also studied the desorption of Py from Py-loaded BFA with several solvents, showed that only 68.70% and 51% of Py could be recovered, using ethyl alcohol and 0.1 N H_2SO_4, respectively.

Lataye et al. [2007a] reported the use of BFA and RHA the agri-wastes, abundantly available at a throw-away price from the particulate collection equipment attached to the flue gas line of the boilers/furnaces operating on bagasse and rice husk as fuels as adsorbents for the removal of pyridine and its derivative 2-picoline. These agri-wastes have excellent mesoporous structure and very high affinity towards a large number of solutes (adsorbates) in aqueous solutions and waste waters. The authors also reported the use of granular activated carbon as an adsorbent for the removal of pyridine and picoline. The overall adsorptive uptake was in the order of BFA > GAC > RHA for that of pyridine and its derivatives.

Lataye et al. [2007b], reported the study on adsorption of Py from aqueous solutions using RHA, a solid waste generated from rice husk-fired boilers, as an adsorbent. The authors have studied the effect of various parameters, such as adsorbent m, pH_0, t, C_0) and T on the removal of Py from the aqueous solutions in batch mode. The range of the initial concentration studied is 50-600 mg dm^{-3}. The maximum removal of Py is found to be ~96 % at lower concentrations (< 50 mg dm^{-3}) and ~80 % at higher concentrations (600 mg dm^{-3}) using 50 kg m^{-3} of RHA dosage at normal temperature. The equilibrium data was tested by using Langmuir, Freundlich and Redlich-Peterson isotherm equations by using non-linear regression analysis. The authors reported that Langmuir and Redlich-Peterson equation found to best to represent the equilibrium sorption data. The adsorption of Py on RHA is found to be endothermic in nature.

The adsorption of pyridine by using granular activated carbon as an adsorption was reported by Lataye et al. [2007c]. The effect of various parameters like initial pH pH_0, adsorbent dose m, t, C_0 and T was studied using batch study. The maximum removal of Py is found to be ~ 97 % at lower concentrations (< 50 mg dm^{-3}) and 84 %

at higher concentrations (600 mg dm^{-3}) using 30 kg m^{-3} of GAC dosage at normal temperature. The equilibrium data was fitted to by using Langmuir, Freundlich and Redlich-Peterson isotherm equations solving by using non-linear regression analysis. The authors reported that the adsorption data can be represented satisfactorily by Langmuir and Redlich-Peterson isotherm equations. Temperature studies revealed that the adsorption of Py onto GAC is endothermic in nature.

The adsorption of 2-picoline from aqueous solutions onto bagasse fly ash (BFA), a solid waste collected from the particulate collection equipment attached to the stacks of bagasse fired boilers, is reported by Lataye et al. [2007d]. The authors have studied the influence of pH pH$_0$, adsorbent dose m, t, C$_0$ and T on the adsorption of 2-picoline from the aqueous solutions using batch adsorption experiments. The equilibrium adsorption study is carried out by using Langmuir, Freundlich, Redlich-Peterson and Temkin isotherm equations and kinetic study for 2-picoline adsorption onto BFA is carried out using first order and second order kinetic models. The adsorption of 2-picoline on bagasse fly ash follows second order kinetics and the equilibrium adsorption increases with increasing initial concentration. The maximum removal of 2-picoline is found to be 98 % at lower concentrations (< 50 mg dm^{-3}) and 49 % at higher concentrations (600 mg dm^{-3}) using 5 kg m^{-3} of BFA dosage at normal temperature and natural pH$_0$ (~6.5). They found that, equilibrium sorption isotherm data can be well represented by the Langmuir and Redlich-Peterson isotherm equations. They also reported the thermodynamic study, isosteric heat of adsorption and desorption study.

Lataye et al. [2007e] reported the adsorption of Py from synthetic aqueous solutions by RHA and GAC. Batch sorption studies have been carried out to evaluate the effect of various parameters, pH pH$_0$, adsorbent dose m, t, C$_0$ and T on the removal of Py. The maximum uptake of Py is found to be ~1 mg g^{-1} and ~10 mg g^{-1} at lower concentrations (< 50 mg dm^{-3}) and ~2 mg g^{-1} and ~17 mg g^{-1} at higher concentrations (600 mg dm^{-3}) using 50 kg m^{-3} and 30 kg m^{-3} of RHA and GAC dosage, respectively,

at the room temperature of 30±1 °C. Adsorption of Py found to be endothermic in nature and the equilibrium data can be adequately represented by Toth and Redlich-Peterson isotherm equation. Py could be recovered from the spent adsorbents by using acidic water and 0.1N H_2SO_4. SBFA is found to be more effective and efficient than either RHA or GAC for Py removal. The overall adsorption of Py on RHA and GAC is found to be in the order of GAC>RHA. Spent RHA can simply be filtered, dried and used in the boiler furnaces/incinerators.

The batch adsorption experiments were carried out to calculate the adsorption capacities of rice husk ash (RHA) and commercial grade granular activated carbon (GAC) for the adsorption of α-picoline from aqueous solutions by Lataye et al. [2007f]. The authors studied the effect of various parameters like pH_0, *m*, t, C_0 and *T* on the adsorption of Pi from the aqueous solutions were studied. The maximum uptake of Pi is observed to be 2.34 mg g^{-1} at lower concentration (50 mg dm^{-3}) and 15.46 mg g^{-1} at higher concentration (600 mg dm^{-3}) using 20 kg m^{-3} of RHA and the maximum uptake of Pi by GAC is observed to be 4.55 mg g^{-1} at lower concentration (50 mg dm^{-3}) and 36 mg g^{-1} at higher concentration (600 mg dm^{-3}) using 10 kg m^{-3} of GAC at normal temperature. The equilibrium data reported to be represented by Radke-Prausnitz and Toth isotherm equations for adsorption onto RHA and Radke-Prausnitz, Redlich-Peterson and Toth isotherm equations for adsorption onto GAC. The values of change in Gibb's free energy (ΔG_{ad}^0), enthalpy (ΔH^0) and entropy (ΔS^0) were calculated. Thermodynamic study revealed that the adsorption of Pi onto RHA and GAC is an endothermic process. Isosteric heat of adsorption is found to be decreasing with increasing surface loading. The acidic water and dilute acids showed higher desorption efficiency for Pi from RHA and GAC. Thus GAC can be regenerated by using acidic water and acids. However, RHA can be disposed off by using it as a fuel in furnaces to recover its energy value.

2.3   BIOLOGICAL TREATMENT OF PYRIDINE AND ITS DERIVATIVES

Pyridine and its derivatives can also be removed or degraded by using biological methods of treatment. The critical review on the biological treatment of pyridine and its derivatives has been discussed in this section.

Houghton and Cain [1972] studied the degradation of pyridine and the three isomeric hydroxypyridines micro-organisms that were capable of utilizing pyridine compounds as carbon and energy source isolated from soil and sewage. Three species of *Achromobacter* produced pyridine-2, 5-diol from 2- or 3-hydroxypyridine whereas an uncommon *Agrobacterium* sp. (N.C.I.B. 10413) produced pyridine-3, 4-diol from 4-hydroxypyridine. On the basis of chemical isolation, induction of the necessary enzymes in washed suspensions and the substrate specificity exhibited by the isolated bacteria, the initial transformations proposed are: 2-hydroxypyridine $\rightarrow$ pyridine-2,5-diol; 3-hydroxypyridine $\rightarrow$ pyridine-2,5-diol and 4-hydroxypyridine $\rightarrow$ pyridine-3,4-diol. A selected pyridine-utilizer, *Nocardia* Zl, did not produce any detectable hydroxy derivative from pyridine, but carried out a slow oxidation of 3-hydroxypyridine to pyridine-2, 3-diol and pyridine-3, 4-diol. Addition of the isomeric hydroxypyridines to a model hydroxylating system resulted in the formation of those diols predicted by theory.

Cain et al. [1974] studied the microbial metabolism of 2 and 3-hydroxypyridines by the maleamate pathway in *Archromobacter* sp. They used washed suspensions of two *Achromobacter* species (G2 and 2L), capable of growth upon 2- and 3-hydroxypyridine respectively as sources of C and N, rapidly oxidized their growth substrate pyridine-2, 5-diol (2, 5-dihydroxypyridine) and the putative ring-cleavage product maleamate without a lag. Extracts of both bacteria oxidized pyridine-2, 5-diol with the stoicheiometry of an oxygenase forming 1 mol of NH_3 mol^{-1} of substrate. Heat treated extracts, however, formed maleamate and formate with little free NH_3. The conversion of maleamate into maleate plus NH_3 by extracts of strain 2L, fractionated with $(NH_4)_2SO_4$, and the metabolism of maleamate and maleate to

fumarate by extracts of both strains demonstrated the existence of the enzymes catalysing each reaction of the maleamate pathway in these bacteria. The pyridine-2, 5-diol dioxygenase (mol.wt. approx. 340000) in extracts of these *Achromobacter* species required Fe^{2+} (1.7 pM) to restore full activity after dialysis or treatment with chelating agents; the enzyme from strain 2L also had a specific requirement for L-cysteine (6.7 mM), which could not be replaced by GSH or dithiothreitol. The oxygenase was strongly inhibited in a competitive manner by the isomeric pyridine-2, 3- and -3, 4-diols.

Pyridine degradation was tested by three types of assay: (i) pyridine disappearance was followed by $\bullet E_{257}$ (e for pyridine=3240lPmol^{-1} cm^{-1}) or manometrically by O_2 uptake; (ii) NAD^+ or $NADP^+$ was included and increase in $\bullet E_{340}$ or O_2 uptake determined; or (iii) NADH or NADPH were included and $-\bullet E_{340}$ determined in the presence and absence of pyridine. Only high-speed supernatant could be tested by this spectrophotometric method because of the high NAD (P) H oxidase activity of crude extracts. Pyridine oxidation could be measured manometrically when the flasks contained a reduced nicotinamide nucleotide-regenerating system [Watson et al., 1974].

Watson and Cain [1975] used *Bacillus* sp. and *Nocardia* sp. (strain ZI), isolated from soil by enrichment with 0.1 % (v/v) pyridine and grew rapidly on this compound as sole C, N and energy source. Treatment of cells with toluene led to rapid loss of the ability to oxidize pyridine. In the presence of 10mM-semicarbazide at pH 6.0, *Nocardia* Zl accumulated a semialdehyde identified as its 2,4-dinitrophenylhydrazone by chromatography, mixed melting point, mass spectrometry and isotope trapping from [2,6-'4 C] pyridine as glutarate semialdehyde. Extracts of this bacterium prepared from cells grown with pyridine or exposed to the gratuitous inducer 2-picoline, contained high activities of a specific glutarate semialdehyde dehydrogenase. Cells grown with pyridine or glutarate also contained a glutaric dialdehyde dehydrogenase, an acyl-CoA synthetase and elevated amounts of isocitrate lyase but no glutaryl-CoA

dehydrogenase. Bacillus 4 accumulated in the presence of 10 mM-semicarbazide several acidic carbonyl compounds from pyridine among which was succinate semialdehyde. Extracts of this bacillus after growth of the cells with pyridine contained an inducible succinate semialdehyde dehydrogenase in amounts at least 50-fold over those found in succinate-grown cells. Two mutants of this bacillus, selected for their inability to grow on pyridine were deficient in succinate semialdehyde dehydrogenase. In the presence of 0.2 mM-KCN, washed suspensions of Bacillus 4 accumulated formate and possibly formamide from pyridine. The use of [14C] pyridine showed that formate was derived from C-2 of the pyridine ring. The organism had a specific formamide amidohydrolase cleaving formamide quantitatively to formate and NH_3. Formate was further oxidized by the particle fraction.

Rogers et al. [1985] have studied the microbiological degradation of a mixture of alkylpyridines in groundwater maintained under aerobic and anaerobic conditions. A marked difference was observed between the aerobic and anaerobic degradation rates. In the presence of a soil inoculum and under aerobic conditions, the residual alkylpyridine concentrations generally approached zero concentration within 10 to 31 days of incubation, whereas under anaerobic conditions the concentrations of residual alkylpyridines only decreased between 40 and 80 % over a 33 day incubation period. Biodegradation rates under aerobic conditions were greatly affected by the specific ring substitution of structural isomers within a given weight class. A similar effect was not observed for anaerobic degradation rates.

Sims et al. [1986] studied the degradation of pyridine by *Micrococcus luteus*, isolated from soil by enrichment culture. The organism oxidized pyridine for energy and released N contained in the pyridine ring as ammonium. The organism could not grow on mono- or disubstituted pyridinecarboxylic acids or hydroxy-, chloro-, amino-, or methylpyridines. Cell extracts of *M. luteus* could not degrade pyridine, 2-, 3-, or 4-hydroxypyridines or 2, 3-dihydroxypyridine, regardless of added cofactors or cell particulate fraction. The organism had a NAD-linked succinate-semialdehyde

dehydrogenase which was induced by pyridine. Cell extracts of *M. luteus* had constitutive amidase activity, and washed cells degraded formate and formamide without a lag. Cells of *M. luteus* were permeable to pyridinecarboxylic acids, monohydroxypyridines, 2, 3-dihydroxypyridine, and monoamino- and methylpyridines. The results provide new evidence that the metabolism of pyridine by microorganisms does not require initial hydroxylation of the ring and that permeability barriers do not account for the extremely limited range of substrate isomers used by pyridine degraders.

The biodegradation of pyridine was studied by Lee et al. [1994] by using freely suspended and Ca-alginate-immobilized cells of *Pimelobacter* sp. When the pyridine concentration was up to 2 g dm^{-3}, freely suspended cells completely degraded pyridine regardless of the initial cell concentrations used. However, when the pyridine concentration increased to 4 g dm^{-3}, the initial cell concentration in freely suspended cell culture should be higher than 1.5 g dry cell weight dm^{-3} for complete degradation of pyridine. In addition, a freely suspended cell culture with a high initial cell concentration resulted in a high volumetric pyridine-degradation rate, suggesting the potential use of immobilized cells for pyridine-degradation. When the immobilized cells were used for pyridine-degradation, neither specific pyridine-degradation rate nor tolerance against pyridine was improved. However, a high volumetric pyridine-degradation rate in the range 0.082-0.129 g dm^{-3} hr^{-1} could be achieved by the immobilized cells because of the high cell concentration. Furthermore, when the immobilized cells were reused in degrading pyridine at a concentration of 2-4 g dm^{-3} they did not lose their pyridine-degrading activity for 2 weeks. The authors found that Pyridine at the concentration up to 6 g dm^{-3} could be degraded completely within 70 h. However, when the pyridine concentration increased to 10 g dm^{-3}, immobilized cells, like freely suspended cells, could not degrade pyridine completely.

Rhee et al. [1996] investigated the effect of the presence of supplementary glucose or acetate on the growth and pyridine-degrading activity of freely suspended

and calcium-alginateimmobilized *Pimelobacter* sp. Although the supplementary carbon sources could be degraded simultaneously with pyridine, *Pimelobacter* sp. exhibited a preference for pyridine over supplementary carbon sources. Thus, the pyridine-degrading activity of the freely suspended cells was not decreased significantly by the addition of either glucose (1.5-6 mM) or acetate (6-24 mM) to the pyridine (6-24 mM). In the semi-continuous immobilized cell culture, immobilized cells also exhibited a preference for pyridine over supplementary carbon sources and did not switch their substrate preference throughout the culture. Owing to a high cell concentration, the volumetric pyridine degradation rate at 24 mM pyridine in the immobilized cell culture was approximately six times higher than that in the freely suspended cell culture. Furthermore, the immobilized cells could be reused 16 times without losing their pyridine-degrading activity during the culture period tested. Taken together, the use of immobilized *Pimelobacter* sp. For the degradation of pyridine is quite feasible because of the preference for pyridine over supplementary carbon sources, the high volumetric pyridine degradation rate, and the reusability of immobilized cells. Concluded that, the use of immobilized *Pimelobacter* sp. for the degradation of pyridine in retort water is feasible because of the preference for pyridine over supplementary carbon sources, the high volumetric pyridine degradation rate, and the reusability of the immobilized cells.

Rhee et al. [1997] studied the anaerobic and aerobic degradation of pyridine by a newly isolated denitrifying bacterium. New denitrifying bacteria that could degrade pyridine under both aerobic and anaerobic conditions were isolated from industrial wastewater. The successful enrichment and isolation of these strains required selenite as a trace element. These isolates appeared to be closely related to *Azoarcus* species according to the results of 16S RNA sequence analysis. An isolated strain, pF6, metabolized pyridine through the same pathway under both aerobic and anaerobic conditions. Since pyridine induced NAD-linked glutarate-dialdehyde dehydrogenase and isocitratase activities, it is likely that the mechanism of pyridine degradation in strain pF6 involves N–C-2 ring cleavage. Strain pF6 could degrade pyridine in the

31

presence of nitrate, nitrite, and nitrous oxide as electron acceptors. In a batch culture with 6 mM nitrate, degradation of pyridine and denitrification were not sensitively affected by the redox potential, which gradually decreased from 150 to 2200 mV. In a batch culture with the nitrate concentration higher than 6 mM, nitrite transiently accumulated during denitrification significantly inhibited cell growth and pyridine degradation. Growth yield on pyridine decreased slightly under denitrifying conditions from that under aerobic conditions. Furthermore, when the pyridine concentration used was above 12 mM, the specific growth rate under denitrifying conditions was higher than that under aerobic conditions. Considering these characteristics, a newly isolated denitrifying bacterium, strain pF6, has advantages over strictly aerobic bacteria in field applications. Concluded that, a newly isolated denitrifying bacterium, strain pF6, has potential for use in the biodegradation of pyridine in the environment.

The study on the degradation and heterocyclic nitrification of pyridine by *Bacillus coagulans* was reported by Uma and Sandhya [1997]. The gram-positive, pyridine-degrading microorganism were isolated from contaminated soil by enrichment culture technique. Pyridine was used as source of carbon, nitrogen and energy. *Bacillus coagulans* reduce nitrogen from aromatic ring to ammonia and subsequently heterotrophically to nitrite and nitrate. The maximum degradation of pyridine was 94.1 % within 72 h at 30 °C with a 7.57 h doubling time.

Uma and Sandhya [1998] used *Bacillus coagulans* strain isolated from contaminated soil immobilised on activated carbon for degradation of pyridine, toluene and methylene chloride containing synthetic wastewaters in a packed bed reactor. Pyridine was supplied as the only source of nitrogen in the wastewaters. Continuous runs in a packed bed laboratory reactor showed that immobilized *B. coagulans* can degrade pyridine along with other organics rapidly and the effluent ammonia is also controlled in presence of "organic carbon". About 644 mg dm^{-3} of influent TOC was efficiently degraded (82.85%) at 64.05 mg dm^{-3} h^{-1}.

O'Loughlin [1999] isolated a bacterium capable of degrading 2-methylpyridine by enrichment techniques from subsurface sediments collected from an aquifer located at an industrial site that had been contaminated with pyridine and pyridine derivatives. The isolate, identified as an *Arthrobacter* sp., was capable of utilizing 2-methylpyridine, 2-ethylpyridine, and 2-hydroxypyridine as primary C, N, and energy sources. The isolate was also able to utilize 2-, 3-, and 4-hydroxybenzoate, gentisic acid, protocatechuic acid and catechol, suggesting that it possesses a number of enzymatic pathways for the degradation of aromatic compounds. Degradation of 2-methylpyridine, 2-ethylpyridine, and 2-hydroxypyridine was accompanied by growth of the isolate and release of ammonium into the medium. Degradation of 2-methylpyridine was accompanied by overproduction of riboflavin. A soluble blue pigment was produced by the isolate during the degradation of 2-hydroxypyridine, and may be related to the diazadiphenoquinones reportedly produced by other *Arthrobacter* spp. when grown on 2-hydroxypyridine. When provided with 2-methylpyridine, 2-ethylpyridine, and 2-hydroxypyridine simultaneously, 2-hydroxypyridine was rapidly and preferentially degraded; however there was no apparent biodegradation of either 2-methylpyridine or 2-ethylpyridine until after a seven day lag. The data suggest that there are differences between the pathway for 2-hydroxypyridine degradation and the pathway(s) for 2-methylpyridine and 2-ethylpyridine.

Lee et al. [2001] studied the degradation of Cells of 3-methylpyridine and 3-ethylpyridine on *Gordonia nitida* LE31. Cyclic intermediates were not detected, but formic acid was identified as a metabolite. Degradation of levulinic acid was induced in cells grown on 3-methylpyridine and 3-ethylpyridine. Levulinic aldehyde dehydrogenase and formamidase activities were higher in cells grown on 3-methylpyridine and 3-ethylpyridine than in cells grown on acetate.

Mohan et al. [2003], have studied the microbial degradation of pyridine by *Pseudomonas* (PI2), isolated from the mixed population of the activated sludge unit. Aerobic degradation of pyridine was studied with the isolated strain and the growth

parameters were evaluated. Pyridine degradation was further conformed by chromatography (HPLC) analysis. The process parameters like biomass growth and dissolved oxygen consumption were monitored during pyridine degradation. In order to conform with the plasmid capability to degrade pyridine, the requisite plasmid was isolated and transferred to DH 5a *Escherichia coli*.

Padoley [2006] studied the biodegradation of pyridine in a completely mixed activated sludge process. A potential bacterial culture (P1), isolated from garden soil and identified as *Pseudomonas pseudoalcaligenes–*KPN, was used as a starter seed to develop the biomass in a completely mixed activated sludge (CMAS) reactor and the system was evaluated for treatment of wastewater containing pyridine. The results of this study indicate that pyridine could be degraded efficiently at a loading of 0.251 kg pyridine kg $MLSS^{-1}$ d^{-1} (0.156 kg TOC kg $MLSS^{-1}$ d^{-1}) and at an optimal hydraulic retention time (HRT) of 24 h. Pyridine was used as the sole source of carbon and nitrogen by the biomass. Ammonia-nitrogen (NH_3-N) was formed due to the metabolism of the pyridine ring. In the present investigation, the performance of CMAS with reference to pyridine biodegradation and the bio-kinetic constants for the biodegradation of pyridine, in a continuous system, were computed. The results indicate that a CMAS system inoculated with *P. pseudoalcaligenes–*KPN, under optimum conditions of HRT and pyridine loading, gives a yield coefficient of (Y) 0.29, decay coefficient (K_d) 0.0011 d^{-1}, maximum growth rate constant (lmax) 0.108 d^{-1} and saturation rate constant (K_s) 5.37 mg dm^{-3} for pyridine. It is reported that the isolated *Pseudomonas pseudoalcaligenes–*KPN could degrade pyridine efficiently in the concentration range of 50-300 mg dm^{-3}.

2.4 ELECTROCHEMICAL TREATMENT OF PYRIDINE AND ITS DERIVATIVES

Electrochemical processes for pollutant removal are quite unique in the sense that they do not require any added chemical to carry out oxidation or reduction reactions, nor do they involve any hazardous materials, only inert electrodes. The whole process is clean and self-contained, does not create undesirable further waste products. The electrochemical process for the treatment of pyridine and its derivatives is discussed here in the section.

Lust et al. [1997] studied the adsorption of pyridine on Bi(111), Bi(001) and Bi(011) single crystal electrodes in 0.1 M aqueous NaF solution for concentration of pyridine ranging from 1 to 200 mM. The attractive interaction between the adsorbed molecules rises in the sequence of planes Bi (011) < Bi (111) < Bi (001) as the superficial density of atoms decreases. The absolute value of the Gibbs energy of adsorption of Py increases in the sequence of electrodes Ag < Bi (1 11) < Hg < Bi (001) < Bi (011) < Au (1 11) < Au (100) < Au(31 1). The Gibbs energy of adsorption of Py on Ag was lower (3 to 5 kJ mol^{-1}) than for Bi and Hg electrodes; this is caused mainly by the higher hydrophilicity of Ag electrodes. The adsorption activity of Py increases, when the hydrophilicity of electrodes decreases in the sequence Bi (1 11) > Hg > Bi (001) > Bi (011).

Iniesta et al. [2001] studied the electrochemical oxidation of 3-methylpyridine (3-MP) at synthetic boron-doped diamond (BDD) thin film electrode in acid media by cyclic voltammetry and bulk electrolysis. The results have shown that in the potential region of water stability there can occur direct electron transfer reactions on BDD surface that result in electrode fouling due to the formation of a polymeric film on its surface. While during electrolyses in the potential region of water decomposition, indirect oxidation reactions can take place by electrogenerated active intermediates, probably hydroxyl radicals that can avoid electrode fouling. Depending on the values of applied current density, it is possible to obtain the partial oxidation of 3-MP to nicotinic acid or the complete combustion of 3-MP to CO_2.

The percentage of 3-Methylpyridine converted into CO_2, relative to the amount of oxidized 3-MP, has been calculated fro the values of TOC using the relation :

$$\%CO_2 = \frac{\{[TOC]_0 - [TOC]_t\}/6}{[3-MP]_0 - [3-MP]_t} \times 100$$

where $[TOC]_0$ and $[TOC]_t$ are the total organic carbons (in mmol dm^{-3}) at time 0 and t respectively, $[3-MP]_0$ and $[3-MP]_t$ are the concentrations of 3-MP (in mmol dm^{-3}) at time 0 and t. The term $\{[TOC]_0 - [TOC]_t\}/6$ represents the equivalent mole number of 3-MP converted into CO_2.

The conversion of 3-MP has been defined as

$$X_{3-MP} = \frac{[3-MP]_0 - [3-MP]_t}{[3-MP]_0}$$

where $[3-MP]_0$ and $[3-MP]_t$ are the concentrations of 3-MP (in mmol dm^{-3}) at time 0 and t.

The reaction of combustion of 3-MP gives CO_2, H_2O and NH_3 near the electrode surface which, is given as:
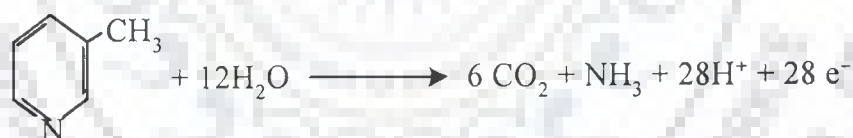
Niu and Conway [2002] have studied the adsorption and electrosorption/desorption of pyridine (Py) for potential applications to the purification of industrial waste-waters. They described the use of high-area carbon cloth (C-cloth) electrodes as quasi-3-dimensional interfaces, coupled with in situ UV–Vis spectrophotometric techniques and scanning kinetics for quantitatively monitoring the adsorption/desorption processes and simultaneously obtaining kinetic parameters. The conversion of Py to PyH^+, which decreases the removal efficiency, takes place in non-buffered electrolyte solution due to pH changes but is eliminated in a HOAc+NaOAc buffer (pH 6.8) solution. Rapid and complete removal of Py is then achieved by anodic polarization. The whole adsorption process follows pseudo-first order kinetics under

various conditions of polarization. Their investigation showed that Py, as one of the commonly occurring organic pollutants in industrial waste-waters, can be almost completely removed by adsorption on high-area C-cloth electrodes. Electrical polarization of such high-area C-cloth material greatly enhances the removal efficiency. The rate of adsorptive removal of Py is generally increased with increase of the C-cloth electrode area (as may be expected), and of the applied current or potential. Also, the electrolyte plays an important role in the removal of Py. The pH changes, which arise during electropolarization in Na_2SO_4 solution, are eliminated by using HOAc+NaOAc buffer solution.

From the derived concentration changes, the amounts, Γ (mol cm^{-2}) of Py adsorbed on the C-cloth surface can be obtained by Equation:

$$\Gamma = (c_0 - c)V/(2500m \times 10^4)$$

where c_0 and c are the concentrations of Py at the beginning and at the equilibrium adsorption state, respectively. V is the volume of solution and m the mass of the C-cloth module. The specific surface area of C-cloth is 2500 m^2 g^{-1}.

2.5 PHOTOCATALYTIC DEGRADATION OF PYRIDINE AND ITS DERIVATIVES

Zhao et al. [2004] performed the kinetic study on photo-catalytic degradation of pyridine in TiO_2 suspension system. It has been agreed that pyridine can be effectively mineralized in aerated TiO_2 slurries using near-UV irradiation. In their study, on the base of Langmuir–Hinshewood mechanism, illustrates a pseudo first-order kinetic model of the degradation with the limiting rate constant of 3.004 mg l^{-1} min^{-1} and equilibrium adsorption constant 2.763 × 10^{-2} l mg^{-1}, respectively. The degradation efficiency in alkali is a little higher than that in acid with a minimum at about pH = 5, which is explained by the formation of acid-pyridine in acidic surrounding together with the amphoteric nature of the TiO_2 surface. The promotion of H_2O_2 on the photo-degradation lies in its supplying proper amount of •OH radicals for the inducement stage before surface redox reactions.

2.6   TAGUCHI DESIGN OF EXPERIMENTAL METHODOLOGY

In the conventional optimization procedures the effect of one parameter is studied by keeping the other parameters constant, which enables to assess the impact of those particular parameters on the process performance. These procedures are time consuming, cumbersome, require more experimental data sets and can not provide information about the mutual interactions of the parameters [Beg et al., 2003]. Taguchi method of orthogonal array (OA) in DOE methodology involves the study of any given system by a set of independent variables (factors) over a specific region of interest (levels) [Mitra, 1998]. Unlike traditional DOE, which focuses on the average process performance characteristics, it concentrates on the effect of variation on the process characteristics [Phadke, 1989] and makes the product or process performance insensitive to variation by proper design of parameters. This approach also facilitates to identify the influence of individual factors, establishing the relationship between variables and operational conditions and finally establish the performance at the optimum levels obtained with a few well-defined experimental sets [Joseph and Piganatiells, 1988]. This method also determines the optimum levels of the important controllable factors based on the concept of robustness and S/N ratio [Mitra, 1998; Dehnad, 1989; Tong, 2004]. In this methodology, the desired design is obtained by selecting the best performance under conditions that produces consistent performance [Roy, 2001] and the conclusions drawn from the small-scale experiments are valid over the entire experimental region spanned by control factors and their setting levels [Phadke and Dehnad, 1988].

Analysis of the experimental data using the ANOVA (analysis of variance) and factor effects give the output that are statistically significant in finding the optimum levels. This approach not only helps in considerable saving in time and cost but also leads to a more fully developed process by providing systematic, simple and efficient methodology for the optimization of the near optimum design parameters with only a few well defined experimental sets [Taguchi, 1986; Phadke and Dehnad, 1988].

Its application created significant changes in several industrial organizations in Japan and USA in manufacturing processes and total quality control [Taguchi, 1986;

Ross, 1996]. More recently, it has been applied for the optimization of a few biochemical techniques [Cobb and Clarkson, 1994; Han, 1998], bioprocess applications [Jeney, 1999; Sreenivas Rao, 2003] and in adsorption [Srivastava et al., 2007].

Barrado et al. [1996] developed a method for the precipitation of metals as magnetic ferrite from the alkalinized solution containing Fe(II). The working conditions were optimized by using a Taguchi L_9 (3^4) experimental design in order to minimize the total residual concentration (TRC) of metal ions in solution. A statistical analysis of the experimental data revealed the most influential factor to be the Fe(II)/metal concentration ratio (F), with a 29.5% contribution, followed by pH (5.2%) and time (2.3%). On the other hand, temperature (T) had little effect on the purification efficiency (1.0%), whereas noise ($KMnO_4$) was found to contribute by as much as 22.1%. Maximal purification efficiency (99.99%) is achieved when wastewater samples are treated for 21 h at 50°C and pH 10.0 in the presence of Fe(II) in a ratio Fe(II)/total metal of 15.

Torng et al. [1998] have applied Taguchi's design of experimental methodology to improve the sequential batch reactor (SBR) process by determining the nominal values of the process parameters. They studied three controllable parameters viz. filling height, reaction time, and concentration of MLSS. The parameter to be optimised was COD value in the SBR effluent. They found that by studying these parameters the quality of wastewater effluent from SBR can be improved well.

Rao et al. [2004] optimized the parameters for xylitol production by *Candida* sp. using L_{18} OA layout. Optimal levels of physical parameters and key media components namely temperature, pH, agitation, inoculum size, corn steep liquor (CSL), xylose, yeast extract and KH_2PO_4 were determined. Among the physical parameters, temperature and agitation were found to contribute higher influence. Media components CSL, xylose concentration and KH_2PO_4 were found to play an important role in the conversion of xylose to xylitol. The yield of xylitol under optimal conditions was 78.9%.

Mohammadi et al. [2004] applied Taguchi's methodology for the separation of Cu ions from a solution using a laboratory electro-dialysis (ED) set-up. Four parameters at three levels were studied: concentration (100, 500, 1000 ppm),

temperature (25, 40, 60 °C), flow rate (0.07, 0.7, 1.2 ml/s) and voltage (10, 20, 30 V). Higher temperature, higher concentration (concentrations greater than 500 ppm have almost no effect on the performance), higher voltage and a lower flow rate are recommended as optimal operating conditions for the ED cell using platinum electrodes (CR67,MKlll)- (AR204SXR412) and CMV-AMV as ion-exchange membranes. The highest removal percentage was found to be 94.94% and 97.33% for the two types of membranes.

Ezzati et al. [2005] investigated the effect of factors influencing the separation of water in oil emulsions. A hydrophobic Polytetra-fluoro-ethylene (PTFE) membrane with 0.45 mm pore size was used. Gas oil, distilled water and Span 80 were selected as continuous phase, dispersed phase and emulsifier, respectively. A L_{16} orthogonal array (five factors in four levels) was employed to evaluate effect of water and emulsifier content in feed, operating pressure, operating temperature and feed residence time in module on the response (permeate flux and water content in permeate). It was shown that increasing emulsifier content and decreasing water content feed decrease permeate flux and water content in permeate. It was found that decreasing residence time to its lower limit causes permeate flux to increase.

Prasad et al. [2005] optimized submerged culture conditions for laccase production by *Pleurotus ostreatus* 1804 using Taguchi OA. Eight factors viz., carbon, nitrogen source (urea), 2,5-xylidine (inducer), wheat bran (lignino-cellulosic material), inoculum size, fermentation broth pH, yeast extract and phosphate source (KH_2PO_4) at three levels with a OA layout of L_{18} ($2^1 \times 3^7$) were selected for the proposed experimental design. The optimized conditions showed an enhanced laccase expression of 32.9% (from 538.8 to 803.3 U). The optimal combinations of factors obtained from the proposed DOE methodology was further validated by conducting fermentation experiments and the obtained results revealed an enhanced laccase yield of 28.3%.

Hu et al. [2005] exploited the Taguchi method for estimating the optimal operating condition of nitrogen and phosphorus (NP) removal from municipal sewage using sequencing batch reactor (SBR) and an attached cum suspended growth SBR. The effects of three controlling factors, namely batch loading rate, feed pattern (initial

feed or step feed), and mixing/aeration ratio, on NP removal were investigated under nine different experimental conditions. The total nitrogen (TN), total phosphorus (TP), total biochemical oxygen demand, and suspended solids removal efficiencies were 90.2, 83.9, 98.6, and 93.0 %, respectively, for the suspended growth SBR. The corresponding values for the attached cum suspended growth SBR were 92.6, 82.1, 98.3, and 93.1%, respectively.

Prieto et al. [2005] studied the photo-catalytic removal of color of a synthetic textile effluent, using TiO_2 suspensions under solar radiation. Following Taguchi's methodology, the reaction was conducted under different flow conditions, pH and H_2O_2 concentrations. The process shows a significant enhancement when it is carried out at high flows, alkaline media and high H_2O_2 concentration. Color removal from the effluent was reached at 55 min operating time. Following Taguchi's methodology, the most important controlling factor was H_2O_2 concentration with an influence of 33.95 %. Next important factor was flow rate, which contributes to response 29.27 %, and finally, pH with a 20.94 % (all of them at 95 % level of confidence). Noise factor had an influence of 9.87 %. Other factors have a minor contribution of 5.98 %.

Chidambara Raj [2005] optimized UV/H_2O_2 process for integration with biological waste treatment unit using by Taguchi's orthogonal design. Dosage of H_2O_2, pH, circulation rate and number of doses of oxidant were the four factors considered for optimization. For each of the four factors, experiments were run at four levels. For reduction in TOC, single dosage of hydrogen peroxide was observed to be more effective than dosing the same quantity in 2, 4 or 6 equal parts. The effect of circulation rate was found to be insignificant. If advanced oxidation processes (AOP) were to be designed as a pretreatment step before biological oxidation, 1 mole H_2O_2 mol^{-1} TOC is the optimum level of dosage. This level of addition increased biodegradability. If AOP were to be designed as a post-treatment step after biological oxidation, then 4 mole H_2O_2 mol^{-1} TOC would be the optimum level of dosage. At this level, decrease in TOC was high. Higher pH of the waste liquor generally favored reduction in TOC.

Table 2.1.1 gives the summary of the literature review on the adsorptive treatment of Py and its derivatives.

Table 2.1.1 : Studies on the adsorption of Pyridine and its derivatives

Author/ Year	Adsorbate	Adsorbents	C_0, (mg dm^{-3})	Parameters Studied	Optimum Conditions				Isotherms	% Removal	q_e
					Dose, g dm^{-3}	pH	Time	Temp, K			
Luh and Baker, 1971	Pyridine	Sodium Kaolinite and sodium montmorillonite	515	pH,		4 - 5.5	24 h	274, 297	Freundlich	46-67	-
Baker and Luh, 1971	Pyridine	Sodium Kaolinite and sodium montmorillonite	0.1 - 515	-	3% and 0.625%	4 - 5.5	17 h	274	Freundlich	-	-
Zawadzki, 1988	Pyridine	Carbon			IR study						
Zhu et al., 1988	Pyridine	Oil Shale	100-390	-	100	8	24	298	Langmuir	30	0.13-0.26
Zaki et al., 1989	Pyridine	Ceria surface			IR study						
Martin et al., 1992	Pyridine, formic acid and acetic acid	Mg and Mo oxides			IR study						
Akita and Takeuchi, 1993	Py, picoline and lutidine	Resins	-	-	25	8	24	298	Langmuir, Freundlich	-	4.47, 4.48 and 4.2

Table 2.1.1 (Contd.)

Author/ Year	Adsorbate	Adsorbents	C_0, (mg dm^{-3})	Parameters Studied	Optimum Conditions				Isotherms	% Removal	q_e
Kumar et al., 1995	Pyridine	AC	50-250	m, C_0	40	-	2 h	-	Langmuir, Freundlich	96.4	1.203
Ardizzone et al., 1998	Pyridine and aniline	α-Al$_2$O$_3$ and Iron powder	-	-	-	-	18, 30 h	298	-	-	-
Bludau et al., 1998	Pyridine	mordenite, ZSM-5 and silicate				IR study					
Pejov and Skapin, 2004	Pyridine	Alumina				IR study					
Mohan et al., 2004	Pyridine	AC, Derived from coconut shell	1-100	m, pH$_0$, T,	2	8	48 h	298	Langmuir, Freundlich	~90%	~60
Mohan et al., 2005	Py, 2-picoline, 3-picoline, 4-picoline	AC, Derived from coconut shell	1-100	m, pH$_0$, T	2	8	48 h	298	Langmuir, Freundlich	40-50%	~34
Lataye et al., 2006 (Present Study)	Pyridine	Bagasse fly ash	50 - 600	m, pH$_0$, T, C$_0$, desorption	25	6.5	6h	283-323	Langmuir, Freundlich, Temkin, Redlich-Peterson	99%	~31

Table 2.1.1 (Contd.)

Author/ Year	Adsorbate	Adsorbents	C_0, (mg dm^{-3})	Parameters Studied	Optimum Conditions				Isotherms	% Removal	q_e
Lataye et al., 2007a (Present Study)	Py, 2-picoline	BFA, RHA and GAC	50 - 600	m, pH$_0$, T, C$_0$, desorption	5 - 50	6-8	5h	283-323	Langmuir, Freundlich, Temkin, Redlich-Peterson	50-99%	-
Lataye et al., 2007b (Present Study)	Pyridine	RHA	50 - 600	m, pH$_0$, T, C$_0$, desorption	50	6-8	5h	283-323	Langmuir, Freundlich, Temkin, Redlich-Peterson	~80-96%	~12
Lataye et al., 2007c (Present Study)	Pyridine	GAC	50 - 600	m, pH$_0$, T, C$_0$, desorption	30	6-8	5h	283-323	Langmuir, Freundlich, Temkin, Redlich-Peterson	~84-97%	~20
Lataye et al., 2007d (Present Study)	2-picoline	Bagasse fly ash	50 - 600	m, pH$_0$, T, C$_0$, desorption	25	6.5	6	283-323	Langmuir, Freundlich, Temkin, Redlich-Peterson	99%	~61

2.7 SUMMARY

From the above literature survey, the following gaps are found:

➢ Maximum work has been reported on the adsorption of pyridine using various adsorbents, which are costly, viz., resins, activated carbons, etc.

➢ No work has been reported on the adsorption of Py and its derivatives using low cost adsorbents like RHA and BFA, for which no pretreatment is required except washing and sieving.

➢ The adsorption of pyridine has been studied only at a low initial concentration not more than 100 mg dm^{-3}. Since the concentration of Py and its derivatives in actual wastewaters may be > 100 mg dm^{-3}, studies on the adsorption of these compounds in the higher concentration range is required

➢ No work has been reported on the adsorption of pyridine derivatives like, 2-picoline, 4-picoline and 3-aminopyridines using BFA/RHA as adsorbents, as these are also the hazardous materials and present in the wastewater emitted from various industries

➢ No study has been reported in the literature on the desorption of pyridine and its derivatives from the loaded adsorbents.

➢ No work has been reported in the literature on the thermodynamic aspects of adsorption of pyridine and its derivatives

➢ No work is reported on the application of Taguchi's design of experiments for adsorption of pyridine and its derivatives.

ADSORPTION FUNDAMENTALS

3.1 GENERAL

Adsorption is a surface phenomenon. It is used as a separation process where a species present in a fluid phase is transferred to the solid phase and gets attached to the solid surface, if the concentration of the species in the fluid-solid boundary region is higher than that in the bulk of the fluid [Tien, 1994]. In an adsorption process, molecules or atoms or ions in the fluid phase get concentrated or accumulated on the surface of a solid, where they bond with the solid surface or are held there by weak inter-molecular forces. The accumulated or concentrated species on the surface of solid is called the adsorbate, and the porous solid material is known as an adsorbent. In this chapter, the fundamentals of adsorption onto adsorbents are presented: These fundamentals may be used for the adsorption of pyridine and its derivatives onto adsorbents.

3.2 ADSORPTION KINETIC STUDY

In order to investigate the adsorption processes, various kinetic models are used to describe the time-course of adsorption of a species onto an adsorbent. The kinetic models include pseudo-first-order, pseudo-second-order, rate expressions when the diffusional mass transfer resistances (external to solid, i.e. in the fluid phase, and internal-pore and surface diffusion) are considered to be negligible. The mass transfer based models include intra-particle diffusion model, Elovich model, Bangham model and modified Freundlich models.

3.2.1 Pseudo-First-Order Model

The sorption of organic molecules from a liquid phase to a solid phase can be considered as a reversible process with equilibrium being established between the

solution and the solid phase. Assuming a non-dissociating molecular adsorption of adsorbates onto adsorbent particles, the sorption phenomenon can be described as [Fogler, 1998].

$$A \ + \ S \ \underset{k_D}{\overset{k_A}{\rightleftharpoons}} \ A.S \qquad (3.2.1)$$

where, A is adsorbate and S is the active site on the adsorbent and AS is the activated complex. k_A and k_D are the adsorption and desorption rate constants, respectively. It can be shown using first order kinetics that with no adsorbate initially present on the adsorbent (i.e. $C_{AS0} = 0$ at t=0), the fractional uptake of the adsorbate by the adsorbent can be expressed as

$$\frac{X_A}{X_{Ae}} = 1 - \exp\left[k_A C_S + \frac{k_A}{K_S} \right] t \qquad (3.2.2)$$

where, X_{Ae} = fraction of the adsorbate adsorbed on the adsorbent under equilibrium condition (i.e. C_{ASe} / C_{A0})

$$K_S = k_A / k_D$$

C_S = adsorbent concentration in the solution

Thus, the plot of $\ln\left(1 - \frac{X_A}{X_{Ae}}\right)$ versus t for various values of C_{A0} at a constant C_S will give a straight line which will be coincident on the ordinate at $t=0$. Constants k_A and k_D can be obtained using relevant relations and the slope of each curve for a given value of C_S. Equation (3.2.2) can be transformed as [Srivastava et al., 2006b].

$$\log(q_e - q_t) = \log q_e - \frac{k_f}{2.303} t \qquad (3.2.3)$$

where, $\quad k_f = \left(k_A C_S + \frac{k_A}{k_S} \right);$ \qquad (3.2.4)

$$q = X_A, \text{ and } q_e = X_{Ae}$$

This equation is the so-called Lagergren equation [Lagergren, 1898]. This equation is, however, valid only for the initial period of adsorption. Various investigators have erroneously fitted this equation to the adsorbate uptake data for extended periods, ignoring the data of the initial period. A plot of $\log(q_e - q_t)$ versus t for the initial period enables the determination of the kinetic constants.

Experimental results don't follow pseudo-first order model for the whole period because they differ in two important aspects: (i) $k_f(q_e - q_t)$ does not represent the number of available sites, and (ii) $\log q_e$ was not equal to the intercept of the plot of $\log(q_e - q_t)$ against t [Ho and Mckay, 1999].

3.2.2 Pseudo-Second-Order Model

For cellulose based sorbents having fibers, which may have polar functional groups, chemical bonding of polar functional groups may occur with solute ions and these groups may impart cation exchange capacity to the adsorbents [Ho and Mckay, 1998, 1999, 2000]. For such sorption systems, the rate of sorption to the surface should be proportional to a driving force times an area, and the sorption rate equation may be given as:

$$\frac{dq}{dt} = k_S(q_e - q_t)^2 \qquad (3.2.5)$$

where k_S is the pseudo second order rate constant (g mg^{-1} min^{-1}), q_e the amount of solute ions adsorbed at equilibrium(mg g^{-1}) and q_t is the amount of solution ions adsorbed on the sorbent at any time, t (mg g^{-1}).

This equation can be integrated with $q_t = 0$ at $t = 0$, to give

$$q_t = \frac{k_S q_e^2 t}{1 + k_S q_e t} \qquad (3.2.6)$$

As has been pointed out by Ho [2006] and Ho and Ofamaja [2006b] this equation can be linearized to give at $t = 0$ Eq. (3.2.5) gives the initial sorption rate

$$\frac{t}{q_t} = \frac{1}{k_S q_e^2} + \frac{1}{q_e} t \qquad (3.2.7)$$

At $t \to 0$, $q_t \to 0$ and Eq. (3.2.5) gives the initial sorption rate,

$$\left. \frac{dq}{dt} \right|_{t \to 0} = h = k_S q_e^2 \tag{3.2.8}$$

where h, the initial sorption rate, has the units of mg g^{-1} min^{-1}.

The adsorption capacity depends upon the initial sorbate concentration, C_o system temperature, T, solution pH, sorbate particle size, sorbate dose, m, sorbate characteristics, etc., the kinetic model is concerned only with the effect of observable parameters on the overall rate [Ho, 2006].

The linearized plot of t/q_t versus t is the so-called ratio correlation in that t is present in both the ordinate and abscissa of the plot of course would yield a perfect correlation coefficient would be 1.0 in all cases. Therefore, this kinetic expression would become best fit if compared with first-order or other kinetic expressions used in the sorption studies [Lyberatos, 2006]. Therefore, it is not appropriate to use the coefficient of determination of linear regression method for comparing the best-fitting of kinetic models. Non-linear fitting could be adopted to obtain the kinetic parameters [Ho, 2006].

Eq. 3.2.6 seems to be valid at low and high times of sorption. At $t \to \infty$, $q_t \to q_e$ and at $t \to 0$, $q_t \to 0$.

For very fast adsorption situation, it is too difficult to measure the adsorption rate in the time-scale of the kinetic experiments. In such situations, it is better to provide a qualitative discussion of the kinetic results.

The q_e and the h alongwith the k_S can be determined experimentally from the slope and intercept of the plot of t/q_t versus t.

3.2.3 Intra-particle Diffusion Study

A functional relationship common to most of the treatments of intraparticle transport is that uptake varies almost proportionally with the square root of time, ($t^{0.5}$),
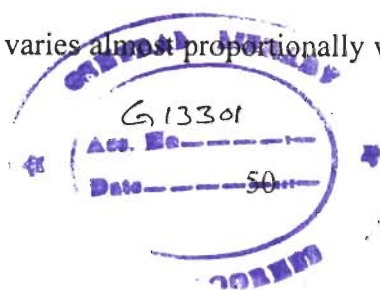
rather than time, (t), itself [Weber and Morris, 1963; McKay et al., 1980; Allen et al., 1989], i.e.

$$q_t = k_{id} t^{0.5} + I \qquad (3.2.9)$$

where, k_{id} is the intra-particle diffusion rate constant (mg g^{-1} min$^{-1/2}$) and I (mg g^{-1}) is a constant that gives an idea about the thickness of the boundary layer, i.e., the larger the value of I, the greater is the boundary layer effect. The mathematical dependence of fractional uptake of adsorbate on $t^{0.5}$ is obtained if the sorption process is considered to be influenced by diffusion in the cylindrical (or spherical) particle and the convective diffusion in the adsorbate solution. It is assumed that the external resistance to mass transfer surrounding the particles is significant only in the early stages of adsorption.

Many investigators [Allen et al., 1989; Mall et al., 2005a, b] have represented the data points of q versus $t^{0.5}$ by two straight lines- the first straight portion depicting macro-pore diffusion and the second representing micro-pore diffusion. Extrapolation of the linear portions of the plots back to the ordinate gives the intercepts, which provide the measure of the boundary layer thickness. The deviation of straight lines from the origin is attributed to the difference in the rate of mass transfer between the initial and final stages of adsorption. Further, such deviation of straight line from the origin indicates that the pore diffusion is not the sole rate-controlling step. The slope of the Weber and Morris plots: q versus $t^{0.5}$, are defined as a rate parameter (k_{id}), characteristic of the rate of adsorption in the region where intra-particle diffusion is rate controlling. The higher the value of k_{id} the higher is the intraparticle diffusion rate.

3.2.4 The Elovich Model

The Elovich equation is given as follows (Cheung et al. 2000, Onal, 2006):

$$\frac{dq_t}{dt} = \alpha e^{-\beta q_t} \qquad (3.2.10)$$

where α is the initial rate (mg g^{-1} min^{-1}) because (dq_t/d_t) approaches α when q_t approaches zero, and the parameter β (g mg^{-1}) is related to the extent of surface

coverage and activation energy for chemisorptions (Teng and Hsieh, 1999).

For $q_t = 0$ at $t = 0$, equation can be integrated as:

$$q_t = \frac{1}{\beta}\ln(t + t_0) - \frac{1}{\beta}\ln(t_0) \tag{3.2.11}$$

where $t_0 = 1/\alpha\beta$. If t is much larger than t_0. Eq. (3.2.10) can be simplified as:

$$q_t = \frac{1}{\beta}\ln(\alpha\beta) + \frac{1}{\beta}\ln t \tag{3.2.12}$$

The constants of Elovich equation can be determined from the plot of $\ln t$ Vs q_t.

3.2.5 Bangham's Equation

Bangham's equation can be used to check the whether pore-diffusion is the only rate-controlling step or not in the adsorption system (Aharoni et al., 1979).

$$\log\log\left(\frac{C_0}{C_0 - q_t m}\right) = \log\left(\frac{k_{0B}m}{2.303V}\right) + \alpha\log(t) \tag{3.2.13}$$

where, $\alpha\,(<1)$ and k_{0B} are constants.

If the experimental data are represented by Eq. (3.2.12), then it is an indication that the adsorption kinetics is limited by the pore diffusion.

3.2.6 Modified Freundlich Equation

The modified Freundlich equation was originally developed by Kuo and Lotse (1973). It is given as follows:

$$q_t = kC_0 t^{1/m} \tag{3.2.14}$$

Where q_t is the amount adsorbed (mg g^{-1}) at any time t, k the apparent adsorption rate constant (dm^3 g^{-1} min^{-1}), C_0 the initial concentration (mg dm^{-3}), t the contact time (min) and m is the Kuo-Lotse constant. Linear form of modified Freundlich equation is given as:

$$\ln q_t = \ln(kC_0) + \frac{1}{m}\ln t \tag{3.2.15}$$

The constants can be determined form the plot of $\ln q_t$ vs $\ln t$.

3.3 ADSORPTION DIFFUSION STUDY

The mathematical treatment of Boyd et al. [1947] and Reichenberg [1953] to distinguish between the particle, and film diffusion and mass action-controlled mechanism of exchange have laid the foundations of sorption/ion-exchange kinetics. In adsorption systems, the mass transfer of solute or adsorbate onto and within the adsorbent particle directly affects the adsorption rate. It is not only important to study the rate at which the solute is removed from aqueous solution in order to apply adsorption by solid particles to industrial uses but also it is necessary to identify the step that governs the overall removal rate in the adsorption process in order to interpret the experimental data. There are essentially four steps in the adsorption of a solute from the bulk liquid solution by an adsorbent.

1.   Transport of solute from the bulk of the solution to the external film surrounding the adsorbent particle(assumed to be very fast in agitated vessels)

2.   Diffusion of the adsorbate from across the external liquid film to the external surface of the adsorbent particle (film diffusion; the resistance could be neglected for properly mixed/agitated vessels)

3.   Diffusion of the adsorbate from the poremouth through the pores to the immediate vicinity of the internal adsorbent surface (pore, surface and molecular diffusion)

4.   Adsorption of the adsorbate onto the interior surface of the adsorbent.

All these processes play a role in the overall sorption of the solute from the bulk liquid solution to the internal surface of an adsorbent. In a rapidly stirred, well mixed batch adsorption, mass transport from the bulk solution to the external surface of the adsorbent is usually rapid. Therefore, the transport resistance of the adsorbate from the bulk of the solution to the exterior film surrounding the adsorbent may be small and can be neglected. In addition, the adsorption of adsorbate at surface sites (step 4) is usually very rapid, and thus offers negligible resistance in comparison to other steps, i.e. steps 2

53

and 3. Thus, these processes usually are not considered to be the rate-limiting steps in the sorption process.

In most cases, steps (2) and (3) may control the sorption phenomena. For the remaining two steps in the overall adsorbate transport, three distinct cases may occur:

Case I: external transport resistance > internal transport resistance

Case II: external transport resistance < internal transport resistance

Case III: external transport resistance ≈ internal transport resistance

In cases I and II, the overall rate is governed by the film diffusion and diffusion in the pores, respectively. In case III, the transport of solute to the boundary may not be possible at a significant rate, thereby, leading to the formation of a liquid film with a concentration gradient surrounding the adsorbent particles.

Usually, external transport is the rate-limiting step in systems which have (a) poor phase mixing, (b) dilute concentration of adsorbate, (c) small particle size, and (d) high affinity of the adsorbate for the adsorbent. In contrast, the intra-particle step limits the overall sorption for systems that have (a) a high concentration of adsorbate, (b) a good phase mixing, (c) large particle size of the adsorbents, and (d) low affinity of the adsorbate for the adsorbent.

3.3.1 Sorption Kinetics

Kinetic data could be treated by the model given by Boyd et al. [1947] which is valid under the experimental conditions used. 'Intraparticle transport' first proposed by Weber and Morris [1963] for column adsorption using GAC, comprises of surface diffusion and pore diffusion (including bulk or molecular diffusion). All these diffusion terms may be combined t give "intraparticle diffusion."

Several researchers [Gilliland et al., 1974; Sudo et al., 1978; Suzuki and Fujii, 1982; Fredrich et al., 1989; Seidel and Carl, 1989; Tien, 1994; Swamy et al., 1998] and have shown that the surface diffusion coefficient is strongly dependent on the concentration of the adsorbed phase. However, for the simplification of the sorption transport, surface diffisivity is taken as invariant with the adsorbed phase concentration

[Merck et al., 1980; Crittenden et al., 1986]. Combining surface and pore diffusion (including molecular diffusion) into a single effective diffusion term, we can use effective diffusivity, D_e to represent intra-particle diffusion. Also, ignoring the variation of pore solution concentration with time, we can write the general equation of continuity of the solute A in a cylindrical and spherical coordinate system as follows:

Cylindrical Particles: $\dfrac{\partial C_A}{\partial t} + \dfrac{1}{r}\dfrac{\partial}{\partial r}(rN_{Ar}) + \dfrac{1}{r}\dfrac{\partial N_{A\theta}}{\partial \theta} + \dfrac{\partial N_{Az}}{\partial r} = R_A$ (3.3.1)

Spherical particles: $\dfrac{\partial CA}{\partial t} + \dfrac{1}{r^2}\dfrac{\partial}{\partial r}(r^2 N_{Ar}) + \dfrac{1}{r\sin\theta}(N_{A\theta}\sin\theta) + \dfrac{1}{r\sin\theta}\dfrac{\partial N_{A\phi}}{\partial \theta} + \dfrac{\partial N_{Az}}{\partial r} = R_A$

(3.3.2)

where, r, θ, z and ϕ are the coordinate parameters for the cylindrical and spherical systems; and R_A is the rate of production of A by chemical reaction; taken to be zero in the present case. Assuming diffusion to take place radially with diffusion in θ, ϕ and z directions to be zero, the equations (3.3.1 and 3.3.2) become,

$\dfrac{\partial C_A}{\partial t} + \dfrac{1}{r}\dfrac{\partial}{\partial r}(rN_{Ar}) = 0$ (3.3.3)

$\dfrac{\partial C_A}{\partial t} + \dfrac{1}{r}(r^2 N_{Ar}) = 0$ (3.3.4)

Since $N_{Ar} = -D_e\dfrac{\partial C_A}{dr}$ for dilute solutions, the above equation can be written as

$\dfrac{\partial C_A}{\partial t} + \dfrac{1}{r}(-rD_e\dfrac{\partial CA}{dr}) = 0$ (3.3.5)

$\dfrac{\partial C_A}{\partial t} + \dfrac{1}{r^2}\dfrac{\partial}{\partial r^2}(-r^2 De\dfrac{\partial C_A}{\partial r}) = 0$ (3.3.6)

Equation (3.3.5) and (3.3.6) can be solved with the following initial and boundary conditions:

$C_A(r,0) = C_{A0}$,

$C_A(R,t) = C_A^*$

$\underset{r\to 0}{Lt}\, C_A(r,t) = $ bounded

where, R is the radius of the cylinder/sphere.

The detailed solution for the cylindrical and spherical coordinate systems have been given by Skelland [1974] and Crank [1965]. For cylindrical coordinates, the solution for $C_{A0} = 0$, i.e. the initial condition of the adsorbate in the adsorbent can be taken as zero, is given as:

$$\frac{C_A'}{C_A^*} = 1 - \frac{2}{R} \sum_{n=1}^{\infty} \left[\frac{J_0(b_n r)}{b_n J_1(b_n R)} exp(-D_e b_n^2 t) \right] \tag{3.3.7}$$

where $b_n s$ are the roots of $J_0(b_n R) = 0$ and $J_0(b_n, R)$ is the Bassel function of the first kind of order zero. Using average adsorbate concentration in the adsorbent, we get,

$$F(t) = \frac{\overline{C_A}}{C_A^*} = \frac{X_A}{X_{Ae}} = 1 - \frac{4}{R^2} \sum_{n=1}^{\infty} \left[\frac{1}{b_n^2} (-D_e b_n^2 t) \right] \tag{3.3.8}$$

where, X_A and X_{Ae} are the fraction of the adsorbate adsorbed at time t and at time $t = \infty$, respectively, and $F(t)$ is the fractional uptake.

In the above equation of this section C represents the concentration of the sorbate onto the sorbent surface, i.e. q_t and $\overline{C}$ represents the average surface concentration of the solute (i.e. $\overline{q_t}$) and C* represents the solute concentration at the centre of the sorbent particles.

Similarly, for spherical adsorbent particle, we get [Reichenberg, 1953; Helfferich, 1962; Skelland, 1974]:

$$F(t) = \frac{X_A}{X_{Ae}} = 1 - \frac{6}{\pi^2} \sum_{n=1}^{\infty} \frac{1}{b_n^2} exp(-D_e b_n^2 t)] \tag{3.3.9}$$

where, $b_n s$ are the roots of $J_0(bn_p R) = 0$

Vermeulen's approximation [Vermeulen, 1953] of equation (3.3.9) leads to the whole range $0 < F(t) < 1$, for adsorption on to spherical particles. This approximation is given as:

$$F(t) = \left[1 - exp\left(\frac{-\pi^2 D_e t}{R_a^2} \right) \right]^{1/2} \tag{3.3.10}$$

This equation could further be simplified to cover most of the data points for

calculating effective particle diffusivity, i.e.

$$\ln\left[\frac{1}{(1 - F^2(t))}\right] = \frac{\pi^2 D_e t}{R_a^2} \tag{3.3.11}$$

The D_e can be calculated from the slope of the plot of $\ln\left[1/(1 - F^2(t))\right]$ versus t.

3.4 ADSORPTION EQUILIBRIUM STUDY

The successful representation of the dynamic adsorption of solute from a solution onto an adsorbent depends upon the equilibrium between the two phases. Adsorption equilibrium is established when the amount of adsorbate adsorbed on the solid surface of adsorbent is equal to the amount desorbed. At its equilibrium condition the amount of solute adsorbed on the solid adsorbent surface and the solution concentration remain constant. The relationship between the amount of adsorbate adsorbed and the adsorbate concentration remaining in solution is described by an isotherm. The adsorption isotherm can be depicted by plotting solid phase concentration against liquid phase concentration graphically. To optimize the design of an adsorption system for the adsorption of adsorbates, it is important to establish the most appropriate correlation for the equilibrium curves. Equilibrium isotherms are measured to determine the capacity of the adsorbent for the adsorbate. Various isotherm equations like those of Langmuir, Freundlich, Temkin and Redlich-Peterson (R-P) have been used in the literature to describe the equilibrium characteristics of adsorption from liquid solutions. In the present study Toth and Radke-Prausnitz isotherm equations have also been used alongwith the above isotherm equations to test the adequacy and appropriateness of these isotherm equations to represent the experimental equilibrium sorption data.

3.4.1 Langmuir, Freundlich and Redlich-Peterson (R-P) Isotherms

To optimize the design of an adsorption system for the adsorption of adsorbates, it is important to establish the most appropriate equilibrium correlation. Various isotherm equations like those of Langmuir [1918] and Freundlich [1906], Redlich–

Peterson [1959] and Temkin [1940] have been used to describe the equilibrium characteristics of adsorption. For low adsorbate loadings, Henry's law is valid. The Freundlich isotherm is derived by assuming a heterogeneous surface [Halsey and Taylor, 1947] with a non-uniform distribution of heat of adsorption over the surface. Whereas, in the Langmuir theory, the basic assumption is that the sorption takes place at specific homogeneous sites within the adsorbent. The Langmuir equation assumes monolayer sorption onto a surface with a finite number of identical sites, and is given by:

$$q_e = \frac{q_m K_L C_e}{1 + K_L C_e} \quad \text{or} \quad \frac{C_e}{q_e} = \frac{1}{K_L q_m} + \frac{C_e}{q_m} \qquad (3.4.1)$$

where, q_m is the monolayer adsorption capacity (mg g^{-1}) and is a constant, and K_L is a constant related to the free energy of adsorption ($K_L - e^{-\Delta G/RT}$) and is the reciprocal of the concentration at which the adsorbent is half-saturated. C_e is the equilibrium liquid phase concentration (mg dm^{-3}). A plot of either C_e/q_e versus C_e or the multiple regression fit of the equation with the experimental data enables the determination of the constants. The Freundlich equation is given by:

$$q_e = K_F C_e^{1/n} \quad \text{or} \quad \ln q_e = \ln K_F + \frac{1}{n} \ln C_e \qquad (3.4.2)$$

where, K_F is a constant indicating the adsorption capacity of the adsorbent (dm^3 g^{-1}) and (1/n) is a constant giving the intensity of adsorption. These constants can be calculated from the plot of ln(C_e) versus ln(q_e). The Redlich-Peterson equation is written as:

$$q_e = \frac{K_R C_e}{1 + a_R C_e^{\beta}} \qquad (3.4.3)$$

where, K_R (dm^3 g^{-1}) and a_R (dm^3 mg^{-1}) are the R-P isotherm constants and β is the exponent which lies between 0 and 1. For high concentrations, Eq. (3.4.3) reduces to Freundlich isotherm with $K_F = K_R/a_R$ (dm^3 mg^{-1}), and heterogeneity factor $(1/n) = (1-\beta)$. For $\beta = 1$ Eq. (3.4.3) reduces to Langmuir equation, with $K_L = a_R$. For $\beta = 0$, Eq. (3.4.3) reduces to the Henry's equation, i.e.

$$q_e = \frac{K_R C_e}{1 + a_R} \qquad (3.4.4)$$

For very small C_e values, Eq. (3.4.1) also reduces to the Henry's equation with

$$q_e = q_m K_L C_e \qquad (3.4.5)$$

Thus at low loadings we have

$$\frac{K_R}{1 + a_R} = q_m K_L \qquad (3.4.6)$$

The R-P isotherm incorporates three parameters and can be applied to the homogeneous or heterogeneous systems. By rearranging Eq. (3.4.3) and taking logarithms of both the sides of the rearranged equation, we get

$$\ln(K_R \frac{C_e}{q_e} - 1) = \ln a_R + \beta \ln C_e \qquad (3.4.7)$$

Since K_R is unknown, Eq. (3.4.7) can be fitted to experimental data by maximizing the correlation coefficient between the predicted values of q_e from Eq. (3.4.7) and the experimental data using the solver add-in function of the MS excel, assuming various values of K_R.

3.4.2 Temkin Isotherm

Temkin isotherm contains a factor that explicitly takes into account the interactions between the adsorbing species and the adsorbent. This isotherm assumes that (i) the heat of adsorption of all the molecules in the layer decreases linearly with coverage due to adsorbate-adsorbate interactions, and (ii) that the adsorption is characterized by a uniform distribution of binding energies up to some maximum binding energy [Temkin and Pyzhev, 1940; Kim et al., 2004]. Temkin isotherm is represented by the following equation:

$$q_e = \frac{RT}{b} \ln(K_T C_e) \qquad (3.4.8)$$

Eq. (3.4.9) can be expressed in its linear form as:

$$q_e = B_T \ln K_T + B_T \ln C_e \qquad (3.4.9)$$

where, $B_T = \dfrac{RT}{b}$ and is related to the heat of adsorption. (3.4.11)

b and K_T is the equilibrium binding constant (dm^3 mol^{-1}) corresponding to the maximum binding energy. A plot of q_e versus $\ln C_e$ enables the determination of the isotherm constants K_T and B_T.

3.4.3 Toth Isotherm

This is one of the empirical equations which satisfies the limits of low and high solute concentrations in the solution and possess the correct Henry law type behaviour. This equation describes well many systems with sub-monolayer coverage. Toth equation [Toth, 1971] is given as:

$$q_e = \frac{q_e^\infty C_e}{\left[1/K_{th} + C_e^{Th}\right]^{1/Th}} \quad \text{or} \quad \left[\frac{C_e}{q_e}\right]^{Th} = \frac{1}{(q_e^\infty)^{Th} K_{Th}} + \frac{(C_e)^{Th}}{(q_e^\infty)^{Th}} \quad (3.4.11)$$

where, q_e^∞, monolayer adsorptive uptake, mg g^{-1}, K_{Th}, Toth isotherm constant, (mg dm^{-3})Th, and Th is, dimensionless Toth isotherm constant characterizes the heterogeneity of the adsorbents surface and is usually less than unity. The more it deviates from the unity, the larger is the heterogeneity of the adsorbent. When $Th = 1$ the Toth isotherm Eq. (3.4.11) reduces to Langmuir Eq. (3.4.2).

3.4.4 Radke-Prausnitz Isotherm

Radke and Prausnitz equation is given as [Radke and Prausnitz, 1972]:

$$q_e = \frac{K_{RP} k_{rp} C_e}{1 + K_{RP} C_e^P} \quad \text{or} \quad \frac{C_e}{q_e} = \frac{1}{K_{RP} k_{rp}} + \frac{C_e^P}{k_{rp}} \quad (3.4.12)$$

where, K_{RP} (dm^3 g^{-1}) and k_{rp} [(mg g^{-1})/(mg dm^{-3})$^{1/P}$] are Radke-Prausnitz constants and P is a dimensionless exponent. For $P = 1$, Eq. (3.4.12) reduces to the Langmuir Eq. (3.4.2).

The traditional approach of determining the isotherm parameters by linear regression of isotherm equations gives very good fits to the experimental data as most

of their regression correlation coefficients are close to unity. However, the correlation coefficient, R^2 yields the best-fit isotherm constants based on the linearized isotherm plots which has the disadvantage in that it may not provide the best isotherm constants to correlate the original isotherm equation with experimental data points. In addition, since the R^2 factor is based on the square of the difference between theoretical and experimental points, it will result in higher weigthing to the higher C_e value data points. Consequently it will give a better fit correlation to the higher C_e value data point. It would be better to use non-linear regression analysis for fitting the isotherm equations to the experimental data.

3.5   FACTORS CONTROLLING ADSORPTION

The amount of adsorbate adsorbed by an adsorbent from aqueous solution is depend upon a number of factors which are discussed below.

3.5.1   Nature of Adsorbent

The adsorption capacity of an adsorbent depends upon its physicochemical characteristics, specific surface area and its affinity for the adsorbate. Adsorption capacity is directly proportional to the exposed surface of the adsorbent. For the non-porous adsorbents, the adsorption capacity is inversely proportional to the particle diameter whereas for porous material it is practically independent of particle size. However, for porous substances particle size affects the rate of adsorption. For substances like GAC, the breaking of large particles to form smaller ones open up previously sealed channels making more surface accessible to the adsorbent.

Pore sizes are classified in accordance with the classification adopted by the International Union of Pure and Applied Chemistry (IUPAC) [IUPAC, 1982], that is, micro-pores (diameter (d) < 20 Å), meso-pores (20 Å < d < 500 Å) and macro-pores (d > 500 Å). Micro-pores can be further divided into ultra-micropores (d < 7 Å) and super micro-pores (7 Å < d < 20 Å). For liquids, the adsorption of organic molecular would generally be facilitated by mesopores, which effect faster intra-particle migration of the adsorbate.

3.5.2 Adsorbent dose

The removal increases rapidly with an increase in the adsorbent dose. An increase in the sorption with an increase in the adsorbent dose can be attributed to the increase in the mesoporous surface area available for sorption, and hence, the availability of more adsorption sites. However, the unit adsorption decreases with an increase in m. The decrease in sorption capacity per unit weight of adsorbent is because of the fact that an increase in the sorbent dose at a constant concentration and volume leads to the saturation of sorption sites through the sorption process [Shukla et al., 2002; Yu et al., 2003; Lataye et al., 2006; Lataye et al., 2007d]. Also, particle-particle interaction such as aggregation at higher m leads to a decrease in the total surface area of the sorbent and an increase in the diffusional path length [Shukla et al., 2002, Ozacar 2005; Lataye et al., 2006; Lataye et al., 2007d]. The incremental uptake of adsorbate is very small after a particular dose, as the surface concentration and the bulk solution concentration of adsorbate come to equilibrium to each other [Mall et al., 2005a, b].

3.5.3 pH of Solution

The surface charge as well as the degree of ionization is affected by the pH of the solution. Since the hydrogen and hydroxyl ions adsorb readily on the adsorbent surface, the adsorption of other molecules and ions is strongly affected by pH. Generally a surface adsorbs anions favourably at low pH and cations at high pH.

3.5.4 Contact Time

In physical adsorption, most of the adsorbate species are adsorbed within a short interval of contact time. However, strong chemical binding of adsorbate with adsorbent requires a longer contact time for the attainment of equilibrium. Available adsorption results reveal that the uptake of adsorbate species is fast at the initial stages of the contact period, and thereafter, it becomes slower near the equilibrium. In between these two stages of the uptake, the rate of adsorption is found to be nearly constant. This may be due to the fact that a large number of active surface sites are

available for adsorption at initial stages and the rate of adsorption is a function of available vacant site. During the course of adsorption, the concentration of the available vacant sites decreases and the repulsion between solute molecules on the surface and solution increases thereby reducing the adsorption rate.

3.5.5   Initial Concentration of Adsorbate

A given mass of adsorbent can adsorb only a fixed amount of adsorbate. So the initial concentration of the adsorbate in the solution is very important. The amount adsorbed decreases with an increase in the adsorbate concentration as the resistance to the uptake of solute from the solution decreases with an increase in the solute concentration. Therefore, the rate of adsorption increases because of the increasing driving force.

3.5.6   Temperature

Temperature dependence of adsorption is of complex nature. Adsorption processes are generally exothermic in nature and the extent and rate of adsorption in most cases decreases with increasing temperature. This trend may be explained on the basis of rapid increase in the rate of desorption or alternatively explained on the basis of Le-Chatelier's principle.

Some of the adsorption studies show increased adsorption with increasing temperature. This increase in adsorption is mainly due to an increase in number of adsorption sites caused by breaking of some of the internal bonds near the edge of the active surface sites of the adsorbent. Also, if the adsorption process is controlled by the diffusion process (intraparticle transport-pore diffusion), then the sorption capacity increases with an increase in temperature due to endothermicity of the diffusion process. An increase in temperature results in an increased mobility of the ions and a decrease in the retarding forces acting on the diffusing ions. These result in the enhancement in the sorption capacity of the adsorbents.

3.5.7 Degree of Agitation

Agitation in batch adsorption is important to ensure proper contact between the adsorbent and the adsorbate in the solution. At lower agitation speeds, the stationary liquid film around the particle is thicker and the resistance to transport is large. Thus, the process is external mass transfer controlled. With the increase in agitation (or proper mixing) this film thickness decreases and the film resistance to mass transfer gets reduced and after a certain agitation speed, the process becomes intraparticle diffusion controlled. Whatever is the extent of agitation, the solution inside the pores remains unaffected and hence, for intraparticle mass transfer controlled processes agitation has no effect on the rate of adsorption.
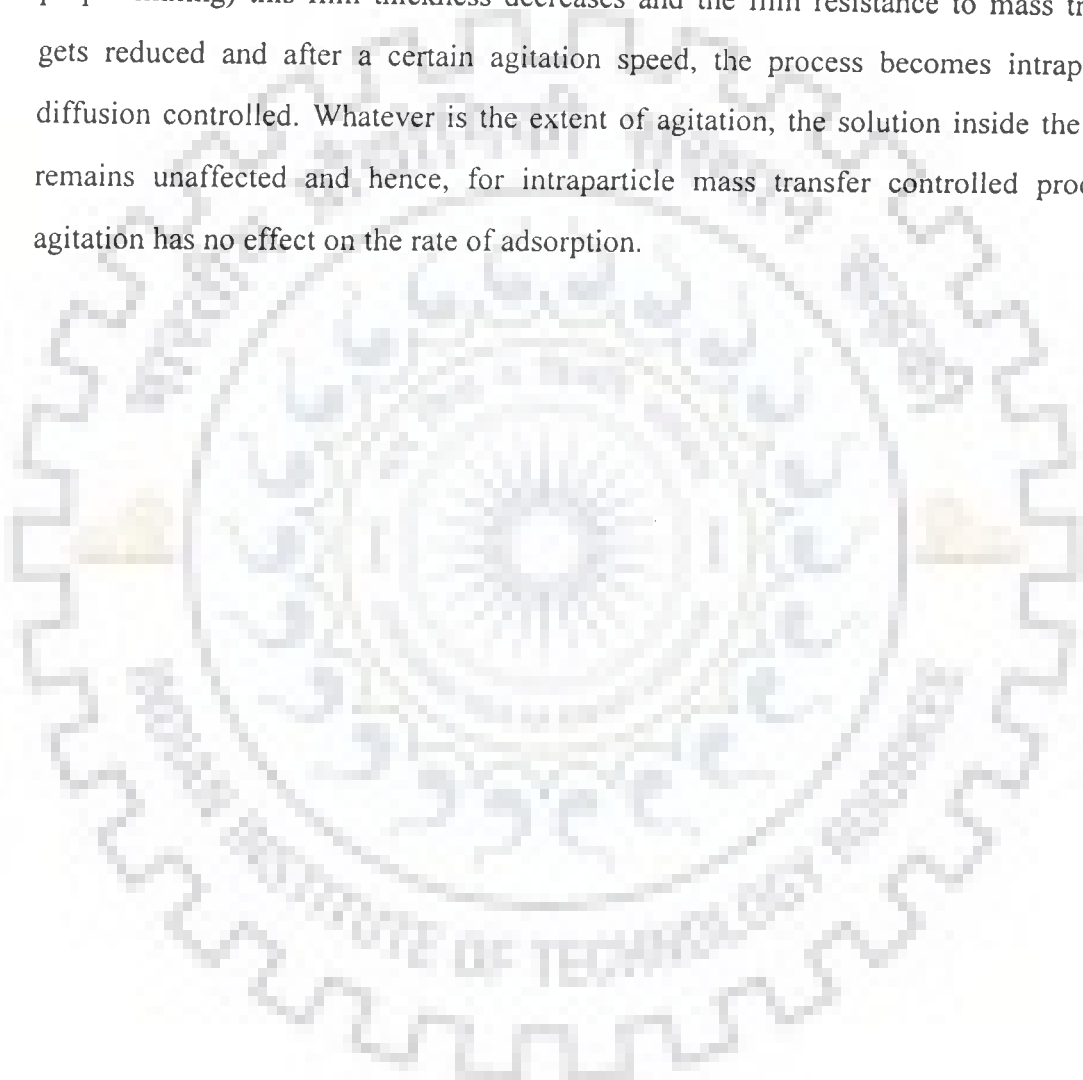
EXPERIMENTAL PROGRAMME

This chapter deals with the materials and methods of analysis, and the experimental procedures adopted to collect the experimental data.

4.1   MATERIALS

4.1.1   Adsorbents

Adsorption of Py and its derivatives was studied using three adsorbents, namely, bagasse fly ash (BFA), rice husk ash (RHA) and the commercial grade granular activated carbon (GAC). BFA was obtained from a nearby sugar mill (Deoband sugar Mills, U.P., India), sieved and a mass fraction between $-600 + 180$ µm was used for the sorption study. RHA was obtained from Bhawani Paper Mills, Raebareli, U.P. (India). RHA was sieved and a mass fraction between $-600 + 180$ µm was used for the sorption study. Coconut-based GAC was purchased from ZeoTech Adsorbents Pvt. Ltd., New Delhi, India and was sieved. The size range of $-1700 + 500$ µm was used for the sorption of Py from the aqueous solutions. BFA and RHA were washed with hot water (70 °C) dried and sieved. GAC was used as procured, except sieving as indicated above. The samples were sieved using IS sieves (IS 437,1979).

4.1.2   Adsorbates

All the chemicals used in the study were of analytical reagent (AR) grade. Pyridine (Py) was procured from, E. Merck (India), Mumbai (India). 2-Picoline (2Pi) and 4-Picoline (4Pi) were procured from Acros Organics (USA) and 3-Aminopyridine (AmPy) was procured from HiMedia Laboratories, Mumbai (India). The stock aqueous solutions of 1000 mg dm^{-3} concentration were prepared for each of the compound by taking respective amount of chemicals in double distilled water (DDW). The

concentration range of sorbate test solutions prepared from the stock solutions varied between 50 and 600 mg dm^{-3}. These test solutions were prepared by diluting the stock solutions of Py, 2Pi, 4Pi and AmPy with DDW.

4.1.3   Other Chemicals

All other chemicals used in the study viz., acids, alkalies, KNO_3, KBr, etc were supplied by S.D. Fine Chemicals, Mumbai, India.

4.2   ADSORBENT CHARACTERISATION

The physico-chemical characteristics of the three adsorbents were determined by using standard procedure as detailed below:

4.2.1   Proximate Analysis

Proximate analyses of the adsorbents were carried out using the procedure given in IS 1350:1984.

A small amount of the adsorbent was finely ground and a representative sample was then taken for analysis. Sample was divided into two portions. The first portion of the sample was placed in a silica crucible and its moisture was determined. To determine the moisture content, sample was weighed and kept in oven at 105 ^{0}C, for 1 h. After 1 h the dry weight of sample was taken and % moisture was determined from the difference of initial weight and final weight (dry weight). After that, the sample was heated to 750 ^{0}C in a muffle furnace and maintained at this temperature for 2 h or more till a constant weight of the residue was obtained. The weight of the residue represented the ash content of the adsorbent. The second portion of the sample was placed in a crucible, covered with a lid and heated in the furnace at 600 ^{0}C for six minutes and thereafter at 950 ^{0}C in the furnace for another six minutes. Thereafter the crucible was kept in a dessicator for cooling and then the crucible was weighed. The difference in weights was due to the loss of volatilities and moisture in the sample. The volatile matter was found by subtracting the corresponding moisture determined previously. Chemical analyses of the adsorbents were carried out as per IS 355: 1984.

4.2.2 Chemical Analysis

Chemical analysis of the adsorbents were carried out as per IS 355 : 1984. The concentrations of Py, 2Pi, 4Pi and AmPy in the aqueous solutions were determined by using a Perkin Elmer Lambda 35 double beam spectrophotometer. The absorbance versus wavelength plots were made for all the adsorbate, namely pyridine, 2-picoline, 4-picoline and 3-aminopyridine. The wavelength at which maximum absorbance was obtained was taken as λ_{max}. The λ_{max} was found as 256, 262, 254 and 290 nm, respectively, for pyridine, 2-picoline, 4-picoline and 3-aminopyridine. The absorbance at the respective λ_{max} were determined for the aqueous solutions of the adsorbates and the plots were made as absorbance versus concentration. The linear portion of these plots were taken as the calibration curves and used for the determination of the actual adsorbate concentration in the solution. Wherever necessary, the solutions were diluted with double-distilled water (DDW) to have their concentrations in the linear range of the calibration curve.

4.2.3 Particle Size

Particle size analyses of the adsorbents were carried out as per IS 2720 (part-4), 1985 using standard sieves.

4.2.4 Density

Bulk density of the adsorbents were determined by using MAC bulk density meter.

4.2.5 Ultimate or CHN analysis

The ultimate analysis was performed on finely ground and oven-dried adsorbents to determine the weight fractions of carbon, hydrogen and nitrogen using Elementar Vario EL III (Elementar Analysensysteme GmbH, Germany).

4.2.6 Point of Zero Charge (pH_{PZC})

The point of zero charge of the adsorbents was determined by the Solid addition method [Balistrieri and Murray, 1981]. To a series of 0.1 dm³ conical flasks 0.045 dm³

of KNO_3 solution of known strength was transferred. The pH_0 values of the solution were roughly adjusted from 2 to 12 by adding either 0.1N HCl or NaOH. The total volume of the solution in each flask was made exactly to 0.05 dm^3 by adding the KNO_3 solution of the same strength. The pH_0 of the solutions were then accurately noted. One gram of BFA/RHA/GAC was added to each flask, which were securely capped immediately. The suspensions were then manually shaken and allowed to equilibrate for 48 h with intermittent manual shaking. The pH values of the supernatant liquid were noted. The difference between the initial and final pH (pH_f) values ($\Delta pH = pH_0 - pH_f$) was plotted against the pH_0. The point of intersection of the resulting curve at which $\Delta pH = 0$ gave the pH_{PZC}. The procedure was repeated for different concentrations of KNO_3.

4.2.7 X-Ray Diffraction (XRD) Analysis

The structures of the different adsorbents were studied with the help of a X-ray diffractometer (Bruker AXS, Diffraktometer D8, Germany) available in the Institute Instrumentation Centre (IIC), IIT, Roorkee, India. The XRD analysis was done using Cu-Kα as a source and Ni as a filter. Goniometer speed was kept at 2° min^{-1}. The range of scanning angle (2θ) was kept at 10-90°. The intensity peaks indicate the values of 2 θ, where Bragg's law is applicable. The identification of compounds was determined by using the ICDD library.

4.2.8 Scanning Electron Microscopic Analysis

To understand the morphology of the adsorbents before and after the adsorption of pyridine, 2-picoline 4-picoline and 3-aminopyridine, the scanning electron microscope (SEM) micrographs were taken using LEO, Model 435 VP, England. The adsorption particles were first gold coated to make the sample conductive, using Sputter Coater, Edwards S150, then the SEMs were taken at various magnification.

4.2.9 Pore Size Distribution Analysis

Textural characteristics of adsorbents were determined by nitrogen adsorption at 77.15 K to determine the specific surface area and the pore diameter using an ASAP 2010 Micromeritics instrument and by Brunauer-Emmett-Teller (BET) method (Brunauer et al., 1938), using the software of Micromeritics. Nitrogen was used as cold bath (77.15 K). The Barrett-Joyner-Halenda (BJH) method (Barret et al., 1951) was used to calculate the mesopore distribution.

4.2.10 Fourier Transform Infra Red (FTIR) Spectral Analysis

FTIR spectrometer (Thermo nicolet, Model Magna 760) was employed to determine the presence of functional groups in the adsorbents before and after the adsorption of pyridine and its derivatives at room temperature. Pellet (pressed-disk) technique has been used for this purpose. The sample was mixed with KBr (IR spectroscopy, grade) thoroughly and pellet was made by using a special mold provided to make pellet under the pressure of 15 ton. The spectral range was from 4000 to 400 cm^{-1}.

4.2.11 Calorific Value

Calorific value of the adsorbents was determined by using a Digital Bomb Calorimeter supplied by Toshniwal Brothers (Delhi) Pvt. Ltd., Gurgaon, Haryana, India.

4.3 BATCH EXPERIMENTAL PROGRAMME

A temperature controlled orbital shaker (Remi Instruments, Mumbai) was used for the batch adsorption study. The temperature range for the studies was from 283 to 323 K. All the batch studies were performed at the shaking rate of 150 revolutions per minute (rpm). For each experimental run, 0.050 dm^3 aqueous solution of the known concentration of Py, 2Pi, 4Pi and AmPy was taken in a 0.25 dm^3 conical flask containing a known mass of the adsorbent. These flasks were agitated at a constant

shaking rate of 150 rpm in a temperature controlled orbital shaker maintained at a constant temperature. The pH_0 of the adsorbate solution was adjusted using 1 N H_2SO_4 or 1 N NaOH aqueous solution without any further adjustment during the sorption process. To check whether the equilibrium has been attained, the samples were withdrawn from the flasks at different time intervals, centrifuged using a Research Centrifuge (Remi Instruments, Mumbai) at 5000 rpm for 5 min and then the supernatant liquid was analyzed for residual concentration of respective compound using Perkin Elmer Lambda 35 double beam spectrophotometer.

4.3.1 Effect of Initial pH (pH_0)

The sorption of pyridine, 2-Picoline, 4-Picoline and 3-Aminopyridine by the adsorbents was studied over a pH_0 range of 2-12 at 303 K and over a contact time of 5 h. C_o used was 300 mg dm^{-3} for pyridine and 100 mg dm^{-3} for 2Pi, 4Pi and AmPy. The optimum adsorbent dosage were used in the study.

4.3.2 Batch Kinetic Study

To study the adsorption kinetics, 0.05 dm^3 of the aqueous solution containing 50-600 mg dm^{-3} of the specific adsorbate was taken in a series of conical flasks. Preweighed amounts of the adsorbents were added to different flasks. The flasks were kept in a temperature-controlled shaker and the aqueous solution-adsorbent mixtures were stirred at 150 rpm. At the end of the predetermined time, t, the flasks were withdrawn, their contents were centrifuged, and the supernatant analyzed for the respective sorbate concentration. Adsorption kinetics was followed for 24 h and it was observed that after 1 h, there was gradual but very slow removal of the adsorbate from the solution. In order to understand the kinetics of adsorption of the sorbates, various kinetic models, like pseudo-first-order, pseudo-second-order, intra-particle diffusion, Elovich, Bangham and modified Freundlich models were studied.

4.3.3   Adsorption Equilibrium Study

Experiments were carried out at the optimum pH_0 by contacting a fixed amount of adsorbent with 0.50 dm^3 of the respective sorbate solutions having C_0 in the range of 50-600 mg dm^{-3}. After 5 h contact time the mixture was centrifuged the supernatant was analyzed for finding out the residual sorbates concentration. The sorbet uptake by the adsorbent was determined as:

$$q_e = \frac{(C_0 - C_e)V}{W} \qquad (4.1)$$

where q_e is equilibrium amount of adsorbate adsorbed (mg g^{-1}), C_0 is initial concentration of adsorbate in aqueous solution (mg dm^{-3}), C_e equilibrium concentration (mg dm^{-3}), V is volume of aqueous solution (dm^3) and W is the weight of adsorbent (g).

Three two-parameter models, viz., Langmuir, Freundlich, and Temkin, and three three-parameter models, viz., Redlich-Peterson, Toth and Radke-Prausnitz were used to correlate the experimental equilibrium adsorption data.

4.3.4   Effect of Temperature and Estimation of Thermodynamic Parameters

The effect of temperature on the sorption characteristics was investigated by determining the adsorption isotherms at 283, 293, 303, 313 and 323 K. Isosteric heats of adsorption at various surface coverages have been determined using classical thermodynamic equations. C_o was varied from 50 mg dm^{-3} to 600 mg dm^{-3} but the pH_0 of the solutions was maintained at 6.0.

4.3.5   Analysis of Pyridine and its Derivatives and Error Analysis

The concentration of pyridine, 2-picoline, 4-picoline and 3-aminopyridine in the liquid sample was determined by a Perkin Elmer Lambda 35 double beam spectrophotometer at the wavelengths of 256, 262, 254 and 290 nm respectively. Before the analysis, the samples were diluted with double distilled water as per the requirement.

The percentage removal of the respective compound and equilibrium adsorption

uptake in solid phase, q_e (mg g^{-1}), were calculated using the following relationships:

$$\text{Percentage removal} = 100\frac{(C_0 - C_e)}{C_0} \tag{4.2}$$

Amount of adsorbate adsorbed per g of adsorbent,

$$q_e = \frac{(C_0 - C_e)V}{W} \tag{4.3}$$

where, C_o is the initial concentration (mg dm^{-3}), C_e is the equilibrium concentration (mg dm^{-3}), V is the volume of the solution (dm^3) and W is the mass of the adsorbent (g).

Two different error functions of non-linear regression basin were employed in this study to find out the most suitable kinetic and isotherm models to represent the experimental data. The hybrid fractional error function (HYBRID) (Porter et al., 1999) and the Marquardt's percent standard deviation (MPSD) error function (Marquardt, 1963) and Chi-square (χ^2) (Ho, 2004) have been used previously by a number of researchers in the field. These error functions are given as

$$HYBRID = \frac{100}{n-p}\sum_{i=1}^{n}\left[\frac{(q_{e,\exp} - q_{e,calc})^2}{q_{e,\exp}}\right]_i \tag{4.4}$$

$$MPSD = 100\sqrt{\frac{1}{n-p}\sum_{i=1}^{n}\left(\frac{(q_{e,\exp} - q_{e,calc})}{q_{e,\exp}}\right)_i^2} \tag{4.5}$$

$$\chi^2 = \sum\frac{(q_{e,\exp} - q_{e,calc})^2}{q_{e,calc}} \tag{4.6}$$

where, n is number of data points, P is number of unknown parameters, $q_{e,exp}$ is the experimental adsorption capacity (mg g^{-1}) and $q_{e,calc}$ is the adsorption capacity calculated by isotherm model (mg g^{-1}).

4.3.6 Multi-stage Adsorption Study

Multi-stage adsorption study was carried out for the removal of Py, 2Pi, 4Pi and AmPy from aqueous solutions using BFA, RHA and GAC. The filtrate obtained from

the first stage (after shaking the effluent with respective adsorbents at optimum dosage) was again treated with fresh adsorbent at optimum dosage in the next stage. The same procedure was repeated until the minimum/zero residual concentration of adsorbate was not achieved. The pH_0 of the solution was maintained at optimum in all the stages. The optimum dosage used in the multistage adsorption study are given in Table 4.3.1 below.

Table 4.3.1: Optimum dosage used in multistage adsorption study.

S.N.	Adsorbate	Initial Concentration (mg dm^{-3})	Optimum Dosage (g dm^{-3})		
			BFA	RHA	GAC
1	Pyridine	100	8	30	20
2	2-picoline	100	5	20	10
3	4-picoline	100	5	20	10
4	3-aminopyridine	100	8	30	20

4.3.7 Batch Desorption Study

From the point of view of the recovery of the adsorbate and the regeneration of the adsorbent, the desorption characteristics of Py from loaded BFA, RHA and GAC have been studied. Several solvents, viz. distilled water (various pH), soil+water (the amount of soil used was in the proportion of 1:5 i.e. 1 part of adsorbent to 5 part of soil), ethyl alcohol, 0.1N H_2SO_4, 0.1N HNO_3, 0.1N NaOH have been used as the desorbing solvents. Ethyl alcohol was chosen as a solvent since Py and its derivatives are soluble in alcohol. The desorption experiments were carried out by mixing a fixed amount of Py, 2pi, 4Pi and AmPy loaded BFA, RHA and GAC with 0.05 dm^3 of the chosen solvent and agitated in an orbital shaker for 5 h at 150 rpm. After 5 h, the mixture was centrifuged and the supernatant was analysed for the Py, 2pi, 4Pi and AmPy concentration and the amount of respective adsorbate desorbed was determined. The desorption study was performed the temperature of 303 and 288 K.

4.4 ADSORPTION STUDY USING TAGUCHI'S DESIGN OF EXPERMENTAL METHODOLOGY

4.4.1 Selection of Process Parameters

Batch experiments are conducted to identify various process parameters pertaining to adsorptive removal of pyridine, 2-picoline, 4-picoline and 3-aminopyridine from aqueous solutions by bagasse fly ash (BFA), rice husk ash (RHA) and commercial grade granulated activated carbon (GAC). The Taguchi's design of experiment has been used in the present study for the removal of Py, 2Pi, 4Pi and AmPy in single, binary (in combination of Py-2Pi, Py-4Pi and 2Pi-4Pi) and ternary (in combination of Py-2Pi-4Pi) mixtures. The various parameters which affect the removal efficiency of sorbates from the aqueous solution are:

1. Number and concentration of compounds in the solution,
2. Initial pH (pH_0) of the solution,
3. Amount and particle size of adsorbent in the solution,
4. Volume in the solution,
5. Contact time between adsorbent and the aqueous solution, and
6. Temperature of the solution.

4.4.2 Experimental Conditions

The entire experimentation has been carried out in a phased manner. Each phase of experiment has been carried out using appropriate orthogonal array (OA) and steps suggested by Taguchi. The selection of OA and their analysis procedure are discussed in the other Chapter V.

Experiments were performed to maximize the total amount of adsorbate adsorbed from the aqueous solutions of pyridine, 2-picoline, 4-picoline in different combinations by BFA, RHA and GAC in a batch adsorption process. In single and binary adsorption system four significant parameters have been used at three levels each. The process parameters, their designations and levels for single and binary systems are given in Table 4.4.1 and 4.4.2 respectively. In ternary system seven process

parameters have been selected for this phase of experimentation. In addition, it has been decided to study three two-parameter interactions. These process parameters, their designations and levels are given in Table 4.4.3.

4.4.3 Selection of Orthogonal Array (OA) and Parameter Assignment

Before selecting a particular OA for an experiment two items must be established a priori (Ross, 1988):

(i)   The number of parameters and interactions of interest

(ii)   The number of levels for the parameters of interest

Table 4.4.1. Process parameters for single component adsorption study using Taguchi's OA (L_9 (3^4)).

Factors	Parameters	Units	Levels								
			BFA			RHA			GAC		
			1	2	3	1	2	3	1	2	3
A	C_0	mg dm^{-3}	50	100	150	50	100	150	50	100	150
B	m	g dm^{-3}	4	8	12	20	30	40	10	20	30
C	T	K	293	303	313	293	303	313	293	303	313
D	t	min	30	60	90	30	60	90	30	60	90

Table 4.4.2 Process parameters for binary adsorption study using Taguchi's OA (L_9 (3^4)).

Factors	Parameters	Units	BFA			RHA			GAC		
			Levels			Levels			Levels		
			1	2	3	1	2	3	1	2	3
A	$C_{0,1}$	mg dm^{-3}	0	50	100	0	50	100	0	50	100
B	$C_{0,2}$	g dm^{-3}	0	50	100	0	50	100	0	50	100
C	Dose	K	4	8	12	20	30	40	10	20	30
D	Time	min	30	60	90	30	60	90	30	60	90

Table 4.4.3   Process parameters for multi-component adsorption study using Taguchi's OA (L_{27} (3^{13})).

Factors	Parameters	Units	Levels								
			BFA			RHA			GAC		
			1	2	3	1	2	3	1	2	3
A	$C_{0, Py}$	mg dm^{-3}	0	50	100	0	50	100	0	50	100
B	$C_{0, 2Pi}$	mg dm^{-3}	0	50	100	0	50	100	0	50	100
C	$C_{0, 4Pi}$	mg dm^{-3}	0	50	100	0	50	100	0	50	100
D	Temp	K	293	303	313	293	303	313	293	303	313
E	pH_0	-	4	6	8	4	6	8	4	6	8
F	m	g dm^{-3}	4	8	12	20	30	40	10	20	30
G	Time	min	30	60	90	30	60	90	30	60	90

The OA selected must satisfy the total degrees of freedom of the OA ≥ total degree of freedom required for the experiment

The number of parameters and their ranges for each phase of experiment have already been given in the previous paragraphs. It is decided to study each selected parameter at three levels, because non-linear behaviour (if any) of the parameters of a process can only be determined if more than two levels are used (Byrne and Taguchi, 1987). The OA's selected for the experiments are discussed in Chapter V.

Four significant process parameters have been selected for single and binary experimentation. These process parameters, their designations and levels are given in Table 4.4.1-Table 4.4.2. With four parameters each at three levels, the total DOF required is 8 [= 4 x (3 − 1)], since a three level parameter has 2 DOF (No. of levels-1). Hence, an L_9 (3^4) OA (a standard 3-level OA) has been selected for these phases of work. The L_9 OA with assignment of parameters is shown in Table 4.4.4.

Table 4.4.4 Column assignment for the various factors in the Taguchi's L$_9$ (3^4) orthogonal array.

Order of Expt.	Run	Factors			
		A	B	C	D
6	1	2	3	1	2
5	2	2	2	3	1
7	3	3	1	3	2
2	4	1	2	2	2
8	5	3	2	1	3
9	6	3	3	2	1
3	7	1	3	3	3
4	8	2	1	2	3
1	9	1	1	1	1

Seven process parameters have been selected for the phase-I of experimentation. In addition, it has been decided to study three two-parameter interactions. These process parameters, their designations and levels are given in Table 4.4.5. With seven parameters each at three levels and three second order interactions, the total DOF required is 26 [= 7 x (3 − 1) + 3 x 4], since a three level parameter has 2 DOF (No. of levels-1) and each two-parameter interaction term has 4 DOF (2 x 2). Hence, an L$_{27}$ (3^{13}) OA (a standard 3-level OA) has been selected for this phase of work. The L$_{27}$ OA with assignment of parameters and interactions is shown in Table 4.4.5. The parameters and interactions have been assigned to specific columns of the OA using the Triangular Table (Ross, 1988).

Table 4.4.5. Column assignment for the various factors and three interactions in the Taguchi's $L_{27}(3^{13})$ orthogonal array.

Exp. no.	1	2	3	4	5	6	7	8	9	10	11	12	13	R1	R2	R3	S/N Ratio (dB)
	A	B	AxB	AxB	C	AxC	AxC	BxC	D	E	BxC	F	G				
1	0	0	0	0	0	0	0	0	0	0	0	0	0	Y11	Y12	Y13	S/N (1)
2	0	0	0	0	1	1	1	1	1	1	1	1	1	-	-	-	-
3	0	0	0	0	2	2	2	2	2	2	2	2	2	-	-	-	-
4	0	1	1	1	0	0	0	1	1	1	2	2	2	-	-	-	-
5	0	1	1	1	1	1	1	2	2	2	0	0	0	-	-	-	-
6	0	1	1	1	2	2	2	0	0	0	1	1	1	-	-	-	-
7	0	2	2	2	0	0	0	2	2	2	1	1	1	-	-	-	-
8	0	2	2	2	1	1	1	0	0	0	2	2	2	-	-	-	-
9	0	2	2	2	2	2	2	1	1	1	0	0	0	-	-	-	-
10	1	0	1	2	0	1	2	0	1	2	0	1	2	-	-	-	-
11	1	0	1	2	1	2	0	1	2	0	1	2	0	-	-	-	-
12	1	0	1	2	2	0	1	2	0	1	2	0	1	-	-	-	-
13	1	1	2	0	0	1	2	1	2	0	2	0	1	-	-	-	-
14	1	1	2	0	1	2	0	2	0	1	0	1	2	-	-	-	-
15	1	1	2	0	2	0	1	0	1	2	1	2	0	-	-	-	-
16	1	2	0	1	0	1	2	2	0	1	1	2	0	-	-	-	-
17	1	2	0	1	1	2	0	0	1	2	2	0	1	-	-	-	-
18	1	2	0	1	2	0	1	1	2	0	0	1	2	-	-	-	-
19	2	0	2	1	0	2	1	0	2	1	0	2	1	-	-	-	-
20	2	0	2	1	1	0	2	1	0	2	1	0	2	-	-	-	-
21	2	0	2	1	2	1	0	2	1	0	2	1	0	-	-	-	-
22	2	1	0	2	0	2	1	1	0	2	2	1	0	-	-	-	-
23	2	1	0	2	1	0	2	2	1	0	0	2	1	-	-	-	-
24	2	1	0	2	2	1	0	0	2	1	1	0	2	-	-	-	-
25	2	2	1	0	0	2	1	2	1	0	1	0	2	-	-	-	-
26	2	2	1	0	1	0	2	0	2	1	2	1	0	-	-	-	-
27	2	2	1	0	2	1	0	1	0	2	0	2	1	Y27,1	Y27,2	Y27,3	S/N (27)

4.5 ANALYSIS AND DISPOSAL OF SPENT ADSORBENTS

The spent adsorbents obtained as a result of adsorption of Py, 2Pi, 4Pi and AmPy were characterized by proximate, chemical, ultimate, FTIR, XRD, SEM, and Thermogravimetric analyses. Proximate and chemical analysis of the spent BFA, RHA and GAC were carried out as per IS 1350: 1984 and IS 6392 (part-I) 1973, respectively. Ash content in the spent adsorbent was evaluated by combustion in a muffle furnace at 775 $^{\circ}$C for 1 h as also the residue obtained after TGA at 900 $^{\circ}$C. The heating values of the blank and spent BFA, RHA and GAC were determined by preparing a suitable pellet and combusting it in a standard adiabatic bomb calorimeter. The FTIR spectra of the spent adsorbents were recorded on a FTIR Spectrometer (Thermo Nicolet, USA, Software used: NEXUS) in the 4000 – 400 cm^{-1} wave number range using KBr pellets.

4.5.1 Thermal Analysis

The thermal degradation (gasification) characteristics of the blank and spent adsorbents were studied using the thermo-gravimetric (TGA) and differential Thermal (DTA) analysis techniques. The thermal degradation of the adsorbents was carried out non-isothermally using the TGA analyzer from Perkin Elmer (Pyris Diamond).

In the present study, the operating pressure was kept slightly positive. The samples were prepared carefully after crushing and sieving so as to obtain homogeneous material properties. The sample was uniformly spread over the crucible base in all the experiments and the quantity of sample taken was 5-10 mg in all the runs. Experimental runs were taken under both nitrogen and air (oxidizing) atmospheres at 100 K min^{-1} heating rate. The tests were conducted over a temperature range of temperature from the ambient temperature to 1000 $^{\circ}$C. Flow rate of nitrogen/air was maintained at 400 ml min^{-1}.

The weight loss at the constant heating rate was continuously recorded and downloaded using the software, Muse, Pyris Diamond. The instrument also provided the continuous recording of the results of the differential thermal gravimetry (DTG) and differential thermal analysis (DTA) as a function of sample temperature and time. The TG, DTG and DTA curves obtained in each case were analyzed to understand the behavior of thermal degradation.

TAGUCHI'S DESIGN OF
EXPERIMENTAL METHODOLOGY

5.1   EXPERIMENTAL DESIGN METHODOLOGY

The design of experiments is an optimization technique to define and investigate all possible conditions in an experiment involving multiple factors. Taguchi [1986] techniques are also optimization techniques. In Taguchi's methodology, experiments are designed using specially constructed tables known as "orthogonal arrays" (OA) for laying out of experiments. These OA's are also generalized Graeco-Latin squares. To design an experiment is to select the most suitable OA and to assign the parameters and interactions of interest to the appropriate columns. In the method, linear graphs and triangular tables suggested by Taguchi are used, which make the assignment of parameters quite simple.

In the Taguchi's method used in our studies, the results of the experiments are analyzed to achieve one or more of the following objectives [Ross, 1988]:

1.   To establish the best or the optimal condition to obtain the total uptake of pyridine and its derivatives in single, binary and tertiary systems by BFA, RHA and GAC in array of systems having various combinations.

2.   To estimate the contribution of individual parameters and interactions on the optimized sorption uptake of adsorbate and

3.   To estimate the response under the optimal conditions.

The optimum conditions are identified by studying the main effects of each of the parameters. The main effects indicate the general trend of influence of each parameter on the sorption process. The knowledge of contribution of individual parameters is a key in deciding the nature of control to be established in the process. The analysis of variance (ANOVA) is applied to the experimental results in

determining the percent contribution of each parameter against a stated confidence level. The control of parameters can be determined by studying ANOVA table for a given analysis.

There are two different approaches to carry out the complete analysis. In the standard approach, the results of a single run or the average of repetitive runs are processed through main effect and ANOVA analysis (raw data analysis). In the second approach multiple runs are taken and the signal-to-noise (S/N) ratio for the same steps are used in the analysis. The S/N ratio is a concurrent quality metric linked to the loss function [Barker, 1990], and by maximizing the S/N ratio, the loss associated can be minimized.

The S/N ratio determines the most robust set of operating conditions from variation within the results. The S/N ratio is treated as a response of the experiment. The outer OA is used to force the noise variation into the experiment i.e., the noise is intentionally introduced into the experiment. However, processes are often subjected to many noise factors that in combination strongly influence the variation of the response. For extremely 'noisy' systems, it is not generally necessary to identify specific noise factors and to deliberately control them during experimentation. It is sufficient to generate repetitions at each experimental condition of the controllable parameters and analyze them using an appropriate S/N ratio [Byrne and Taguchi, 1987].

In the present investigation, both the analyses: the raw data analysis and the S/N data analysis have been carried out. The effects of the selected parameters on the selected quality characteristic, total pyridine adsorbed in mg on the adsorbent per g of adsorbent (q_{tot}), have been investigated through the plots of the main effects based on the raw data. The optimum conditions for the quality characteristic have been established through S/N data analysis aided by the raw data analysis. No outer array has been used and instead, experiments have been repeated three times at each experimental condition under batch study.

5.2 LOSS FUNCTION, SIGNAL-TO-NOISE RATIO AND THEIR INTER-RELATIONSHIP

5.2.1 Loss Function

Taguchi defines the loss-function as a quantity proportional to the deviation from the nominal quality characteristic. He found the following quadratic form to be a practical workable function, viz.

$$L(y) = k\,(y - m_T)^2$$
(5.2.1)

where, L = loss in monetary unit

m_T = value at which the characteristic should be set

y = actual value of the characteristic

k = constant depending on the magnitude of the characteristic and the monetary unit involved

The difference between Taguchi Loss-function and the traditional quality control approach is graphically shown in Figs. (5.2.1a, b) [Ross, 1988]. The loss function represented in Eq. (5.2.1) is a continuous function and not a sudden step as in the case of traditional approach (Fig. (5.2.1b)). This consequence of the continuous loss function illustrates the point that merely quality characteristic does not necessarily mean that process is of good quality as shown in Fig. (5.2.1a). The loss must be zero when the quality characteristic of a product target value is met.

5.2.1.1 Average loss-function for the adsorption process

In the adsorption process, the average loss per unit can be expressed as:

$$L(y) = [\,k\,(y_1 - m_T)^2 + k\,(y_2 - m_T)^2 + \ldots + k\,(y_n - m_T)^2\,]$$
(5.2.2)

where, $y_1, y_2, \ldots\ldots, y_n$ = actual value of the characteristic for the parameter 1, 2, ... n, respectively

n = number of parameter in a given sample and

m_T = best value of the parameter

The Eq. (5.2.2) can be simplified as:

$$L(y) = [k(y_1 - m_T)^2 + k(y_2 - m_T)^2 + ... + k(y_n - m_T)^2]$$

$$= k(MSD_{NB}) \tag{5.2.3}$$

where, MSD_{NB} = Mean squared deviation or the average of squares of all deviations

from the target or nominal value

NB = Nominal-is-best.

This equation is used on the basis of the loss function for manufacturing units proposed by Roy [1990].

5.2.1.2 Other loss-functions

The loss-function can also be applied to parametric characteristics other than the situation where the nominal value is the best value (m_T).

The loss-function for a 'lower-is-better' type of parametric characteristic (LB) is shown in Fig. (5.2.2a). The loss-function is identical to the 'nominal-is-best' type of situation when $m_T = 0$, which is the best value for 'lower-is-better' characteristic (no negative value). The loss-function for a 'higher-is-better' type of parametric characteristic (HB) is also shown in Fig. (5.2.2b), where also $m_T = 0$.

5.2.2 Signal-to-Noise (S/N) Ratio

The loss-function discussed above is an effective figure of merit for making engineering design decisions. However, to establish an appropriate loss function with its k value to use as a figure of merit is not always cost-effective and easy. Recognizing the dilemma, Taguchi created a transform for the loss function that is named as the signal-to-noise (S/N) ratio [Barker, 1990].
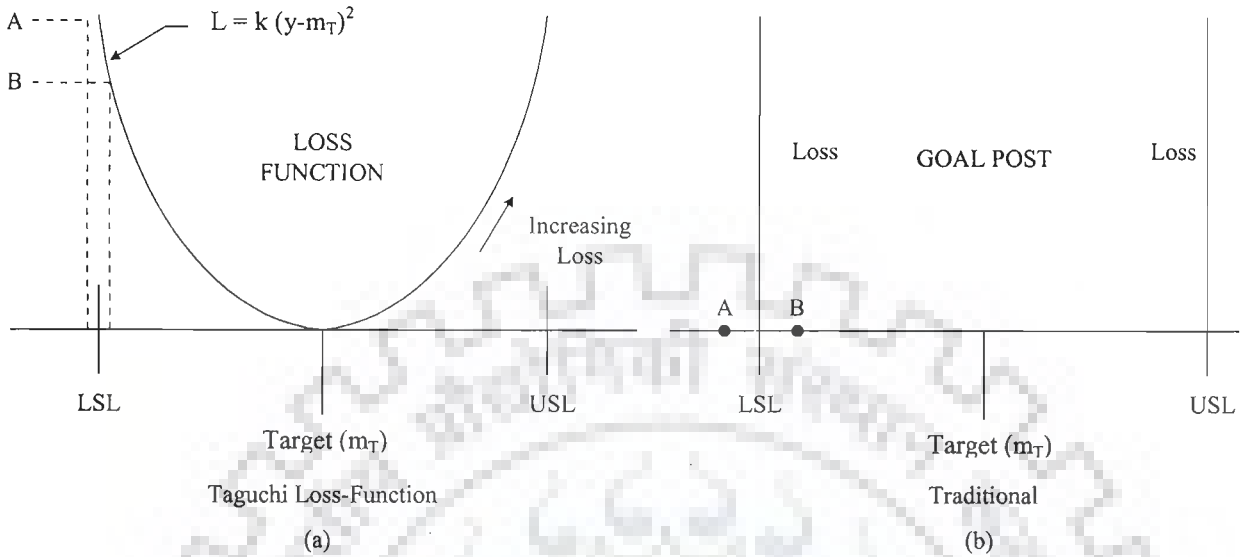
Fig. 5.2.1. (a) Taguchi Loss-function and (b) Traditional Approach [Ross, 1988]
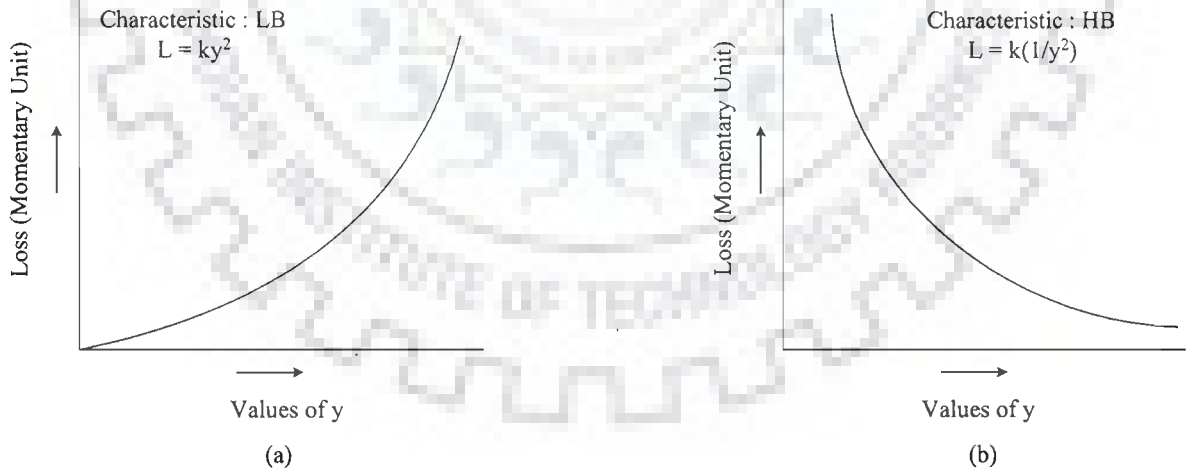
Fig. 5.2.2. (a) Loss-function for LB and (b) HB Characteristics (Ross, 1988)

The S/N ratio, as stated earlier, is a concurrent statistic. A concurrent statistic is able to look at two characteristics of a distribution and roll these characteristics into a single number or figure of merit. The S/N ratio combines both the parameters (the mean level of the quality characteristic and variance around this mean) into a single metric [Barker, 1990]. A high value of S/N ratio implies that the signal is much higher than the random effects of noise factors. Process operation consistent with highest S/N ratio always yields optimum quality with minimum variation [Barker, 1990].

The S/N ratio consolidates several repetitions (at least two data points are required) into one value. The equations for calculating S/N ratios for 'lower-is-better' (LB), 'higher-is-better' (HB) and 'nominal-is-best' (NB) type of characteristics are [Ross, 1988]:

(i)   *Lower is better (LB)*

$$(S/N)_{LB} = -10\log\left(\frac{1}{R}\sum_{j=1}^{R} y_j^2\right)$$

(5.2.4)

where, y_j = value of the characteristic in an observation j;

R = number of observations or number of repetitions in a trial.

Alternatively [Roy, 1990],

$$(S/N)_{LB} = -10\log(MSD_{LB})$$

(5.2.5)

where, $MSD_{LB} = \left(y_1^2 + y_2^2 + ... + y_R^2\right)/R$

Here target value $m_T = 0$.

(ii) Higher is better (HB)

$$(S/N)_{HB} = -10\log\left(\frac{1}{R}\sum_{j=1}^{R}\frac{1}{y_j^2}\right)$$

(5.2.6)

where, y_j and R have the same meaning as given above.

Alternatively (Roy, 1990),

$$(S/N)_{HB} = -10\log(MSD_{HB})$$

(5.2.7)

where, $MSD_{HB} = \left(\dfrac{1}{y_1^2} + \dfrac{1}{y_2^2} + ... + \dfrac{1}{y_R^2} \right) \Big/ R$

Here target value $m_T = 0$.

(iii) 'Nominal- is- best' (NB)

$$(S/N)_{NB} = -10\log\left(\frac{1}{R} \sum_{j=1}^{R} (y_j - y_0)^2 \right) \tag{5.2.8}$$

where, y_0 = nominal value of the characteristic, and other terms y_j and R have their usual meanings.

Alternatively (Roy, 1990),

$$(S/N)_{NB} = -10\log(MSD_{NB}) \tag{5.2.9}$$

where, $MSD_{NB} = \left((y_1 - y_0)^2 + (y_2 - y_0)^2 + ... + (y_R - y_0)^2 \right) \Big/ R$

Mean squared deviation (MSD) reflects the deviation from the target value. MSD expressions are different for various characteristics. For the 'nominal-is-best' characteristic, the quality standard definition of MSD is used. For 'lower-is-better', the unstated target value is zero, and 'higher-is-better', the inverse of each large value becomes a small value and again, the unstated target value is zero.

5.2.3 Relationship between S/N Ratio and Loss-Function

Fig. 5.2(a) shows a single sided quadratic loss-function with minimum loss at the zero value of the desired characteristic. It is seen that the loss grows with an increase in y. Since loss is to be minimized, the target value for y is zero.

The basic loss-function is:

$$L(y) = k(y - m_T)^2 \tag{5.2.10}$$

If $m_T = 0$,

$$L(y) = k(y^2) \tag{5.2.11}$$

The loss may be generalized by using k = 1 and the expected value of loss may be found by summing all the losses for a population and dividing it by the number of

samples (R) taken from this population. Thus, [Barker, 1990]:

$$EL = Expected \ Loss = \frac{\sum y_i^2}{R} \qquad (5.2.12)$$

The negative of the above demerit expression produces a positive quality function. This is the thought process that goes into the creation of S/N ratio from the basic quadratic loss-function. Taguchi suggested that the noise (loss function) may be written as:

$$(S/N)_{LB} = 10 \log_{10}(\sum y_i^2 / R) \qquad (5.2.13)$$

The same thought pattern follows in the creation of other S/N ratios.

5.3 STEPS IN EXPERIMENTAL DESIGN AND ANALYSIS OF ADSORPTION

The Taguchi experimental design and analysis steps are discussed below.

5.3.1 Selection of Orthogonal Array (OA)

In selecting an appropriate OA, the pre-requisites are the [Ross, 1988; Roy, 1990]:

(i)   selection of process parameters and/or interactions to be evaluated, and

(ii)   selection of number of levels for the significant parameters.

Determination of parameters which need to be investigated depends upon adsorbate removal response by the adsorbents of interest. Amongst the several methods suggested by Taguchi, for the following methods are generally used [Ross, 1988]:

(a)   Brainstorming,

(b)   Flow charting, and

(c)   Cause-effect diagrams

The total degree of freedom (DOF) of an experiment is a direct function of the total number of trials. If the number of levels of a parameter increases, the DOF of the parameter as also the total number of trails (N) increase. For each parameter, two levels are recommended to minimize the size of the experiment [Ross, 1988]. If curved or

higher order polynomial relationship between the parameters under study and the response is expected, at least three levels for each parameter should be considered [Barker, 1990]. Thus, either two-level arrays or three-level arrays are to be used. The standard arrays are [Taguchi and Wu, 1979]:

(i)   Two-level arrays: L_4, L_8, L_{12}, L_{16}, L_{32}

(ii)   Three-level arrays: L_9, L_{18}, L_{27}

The number in the array designation indicates the number of trials in that array. The DOF available in an OA is given as [Ross, 1988]:

$$f_{L_N} = N - 1 \qquad\qquad (5.3.1)$$

where, f_{L_N} = total degrees of freedom of an OA,

L_N = OA designation, and

N = number of trials

The following inequality must be satisfied for any OA [Ross, 1988]:

$$f_{L_N} \geq \text{Total DOF required for parameters and interactions.}$$

Depending on the number of levels in the parameters and total DOF required for the experiment, a suitable OA is selected.

5.3.2   Assignment of Parameters and Interactions to the OA

The OA's have several columns available for assignment of parameters and some columns subsequently can estimate the effect of interactions of these parameters. Generally the assignment of parameters and interactions to arrays are done with the aid of [Ross, 1988; Roy, 1990]:

(a) Linear graphs, and

(b) Triangular tables

Each OA has a particular set of linear graphs and a triangular table associated with it. The linear graphs indicate various columns to which parameters may be assigned and the columns subsequently evaluate the interaction of these parameters.

The triangular tables contain all the possible interactions between parameters (columns). Using the linear graphs and/or the triangular table of the selected OA, the parameters and interactions are assigned to the columns of the OA.

5.3.3   Selection of Outer Array

Taguchi separates factors (parameters) into two main groups: controllable and uncontrollable (noise) factors. Noise factors, Noise factors, are nuisance variables that are difficult, impossible, or expensive to control [Byrne and Taguchi, 1987]. The noise factors are responsible for the performance variation of a process. Taguchi recommends the use of outer array for the noise factors and inner arrays for controllable factors. If an outer array is used, the noise variation is forced into the experiment. However, experiments against the trial conditions of the inner-array (the OA used for the controllable factors) may be repeated and in this case the noise variation is into the experiment [Byrne and Taguchi, 1987]. The outer array, if used will have the same assignment considerations. However, the outer array should not be as complex as the inner array because the outer array is noise only which is controlled only in the experiment [Ross, 1988].

5.3.4   Experimentation and Data Collection

The experiment is conducted against each of the trial conditions of the inner array. Each experiment at a trial condition is repeated simply (without using any outer array) or according to the outer array used. Randomization strategies (Ross, 1988) should be considered during the experiment. The data (raw data) are recorded against each trial condition and S/N ratios of the repeated data points are calculated and recorded against each trial condition.

5.3.5   Data Analysis

The following methods have been used in the analysis of data in the present study.

(i)   Plot of average response curves

(ii)   ANOVA for Raw data

(iii)   ANOVA for S/N data.

The plot of average responses at each level of a parameter indicates the trend. It is a pictorial representation of the effect of a parameter on the response. The change in the response characteristic with the change in levels of a parameter can easily be visualized from these curves. Typically, ANOVA for OA's are conducted in the same manner as other structured experiments [Ross, 1988]. The S/N ratio is treated as a response of the experiment, which is a measure of the variation within a trial when noise factors are present. A standard ANOVA can be conducted on the S/N ratio which will identify the significant parameters (mean and variation).

5.3.6   Parameter Design Strategy

5.3.6.1 Parameter classification and selection of optimal levels

When the ANOVA on the raw data (identifies control parameters which affect the average) and S/N data (identifies control parameters which affect the variation) are completed, the control parameters may be put into four classes (Ross, 1988):

Class I   Parameters which affect both the average and the variation

Class II   Parameters which affect variation only

Class III   Parameters which affect average only

Class IV   Parameters which affect nothing.

The parameter design strategy is to select the proper levels of class I and class II parameters to reduce variation and class III parameters to adjust the average to the target value. Class IV parameters may be set at the most economical levels since nothing is affected.

5.3.6.2 Prediction of the mean

After determination of the optimum condition, the mean of the response (μ) at the optimum condition is predicted. This mean is estimated only from the significant parameters. The ANOVA identifies the significant parameters. Suppose, parameters A

and B are significant, and A_2, B_2 (second level of A = A_2, second level of B = B_2) are the optimal treatment conditions. Then, the mean at the optimal condition (optimal value of the response characteristic) is estimated as (Ross, 1988):

$$\mu = \overline{T} + (\overline{A}_2 - \overline{T}) + (\overline{B}_2 - \overline{T})$$

$$= \overline{A}_2 + \overline{B}_2 - \overline{T} \qquad (5.3.2)$$

where, $\overline{T}$ = overall mean of the response

$\overline{A}_2$, $\overline{B}_2$ represent average values of the responses at the second levels of parameters A and B, respectively,

We may find that the prescribed combination of parameter levels (optimal treatment condition) is identical to one of those in the experiment. If this situation exists, then the most direct way to estimate the mean for that adsorption condition is to average all the results for the trials which are set at those particular levels.

5.3.6.3 Determination of confidence interval

The estimate of the mean (μ) is only a point estimate based on the average of results obtained from the experiment. Statistically, this provides a 50 % chance of the true average being greater than μ and a 50% chance of the true average being less than μ. It is therefore customary to represent the values of a statistical parameter as a range within which it is likely to fall for a given level of confidence (Ross, 1988). This range is termed as the confidence interval (CI). In other words, the confidence interval is a maximum and minimum value between which the true average should fall at some stated percentage of confidence [Ross, 1988].

The following two types of confidence intervals are suggested by Taguchi in regard to the estimated mean of the optimal treatment condition [Ross, 1988]:

(i)   Around the estimated average of a treatment condition predicted from the experiment. This type of confidence interval is designated as CI_{POP} (confidence interval for the population).

(ii) Around the estimated average of a treatment condition used in a confirmation experiment to verify predictions. This type of confidence interval is designated as CI_{CE} (confidence interval for a sample group).

The difference between CI_{POP} and CI_{CE} is that CI_{POP} is for the entire population, i.e., all the experiments conducted under the specified conditions, and CI_{CE} is for only a sample group of data obtained under the specified conditions. Because of the smaller size (in confirmation experiments) relative to the entire population, CI_{CE} must be slightly wider. The expressions for computing the confidence interval are [Ross, 1988, Roy, 1990]:

$$CI_{POP} = \sqrt{\frac{F_\alpha (1, f_e) V_e}{n_{eff}}}$$ (5.3.3)

$$CI_{CE} = \sqrt{F_\alpha (1, f_e) V_e \left[\frac{1}{n_{eff}} + \frac{1}{R} \right]}$$ (5.3.4)

where, $F_\alpha (1, f_e)$ = The F-ratio at a confidence level of $(1 - \alpha)$ against DOF, 1 and error DOF f_e.

V_e = Error variance (from ANOVA),

$$n_{eff} = \frac{N}{1 + [\text{Total DOF associated in the estimate of the mean}]},$$ (5.3.5)

And other symbols have their meanings.

It can be seen from Eq. (5.3.4), that as R approaches infinity, i.e., the entire population, the value 1/R approaches zero, and $CI_{CE} = CI_{POP}$. As R approaches 1, the CI_{CE} becomes wider.

5.3.6.4 Confirmation experiments

The confirmation experiment is the final step in verifying the conclusions from the previous round of experimentation. The optimum conditions are set for the significant parameters (the insignificant parameters are set at economic levels) and a

93

selected number of tests are conducted under constant specified conditions. The average of the results of the confirmation experiments is compared with the anticipated average based on the parameters and levels tested. The confirmation experiment is a crucial step and is highly recommended to verify the experimental conclusions [Ross, 1988].

5.4   ANALYSIS OF L_9 ORTHOGONAL ARRAY

The L_9 OA along with the process parameters assigned are shown in Table 4.4.4 (Chapter-IV). This array has been used for the experimentation in single and binary (solute) sorption systems. The experiment in each trial condition has been repeated three times. Thus, three responses for each trial condition have been recorded. These responses (raw data) are represented by y_{ij}, i = 1, 2, ……, 9, and j = 1, 2, 3 and are shown in the 'Response' column under R_1, R_2 and R_3 (Table 4.7.2). The S/N ratios are represented by S/N (i), i = 1, 2,…,9. Since nine experiments are specified in the L_9 OA, so there are a total of 27 and (= 3 x 9) responses (raw data points) and 9 (one S/N ratio against each trial condition) S/N ratios.

5.5   ANALYSIS OF L_{27} ORTHOGONAL ARRAY

The L_{27} OA along with the process parameters assigned is shown in Table 4.4.5. This array has been used for the experimentation. The experiment in each trial condition has been repeated three times. Thus, three responses for each trial condition have been recorded. These responses (raw data) are represented by y_{ij}, i = 1, 2, ……, 27 and j = 1, 2, 3 and are shown in the 'Response' column under R1, R2 and R3 (Table 4.4.5, Chapter-IV). The S/N ratios are represented by S/N (i), i = 1, 2, ……, 27. Since twenty seven experiments are specified in the L_{27} OA, so therefore, the total responses are 81 (= 3 x 27) (raw data points) and 27 (one S/N ratio against each trial condition) S/N ratios.

5.5.1 Raw Data Analysis

5.5.1.1 Level totals and their averages

For parameter A (Table 4.4.4, Chapter-IV), the level totals of the response raw data at A_1, A_2 and A_3 are calculated by adding the responses corresponding to the levels L_1, L_2 and L_3 respectively. For example

A(1) = Level total due to parameter A at level L_1

$$= (y_{11} + y_{12} + y_{13}) + (y_{21} + y_{22} + y_{23}) + ... + (y_{91} + y_{92} + y_{93})$$

where, y_{ij} = response of trial i and repetition j.

i.e., y_{11} = response of trial 1 and repetition 1.

Similarly, other level totals A(2), A(3) are calculated. The same procedure is followed to find the following level totals :

$B(1)$, $B(2)$, $B(3)$

$C(1)$, $C(2)$, $C(3)$

$D(1)$, $D(2)$, $D(3)$

$E(1)$, $E(2)$, $E(3)$

The interaction terms: (A x B), (B x C) and (A x C) each appear in two columns Table 4.4.5 (Chapter-IV).

(A x B) in columns 3 and 4

(B x C) in columns 8 and 11

(A x C) in columns 6 and 7.

Both the columns for each interaction should be considered to find the level totals. For example, the level totals AB(1), AB(2) and AB(3) against (A x B) is calculated as follows (Roy, 1990):

AB(1) = sum of level totals due to interaction A x B at level L_1 in columns 3 and 4.

In this calculation 54 data points are added. In each column, data points for 9 trial conditions are 27 (= 3 x 9). Again in each column each level of a parameter or an

interaction (2nd order) appears 9 times. Following the same procedure, the other level totals AB(2), AB(3) are calculated. The same procedure is applied to other interactions (B x C and A x C) also.

The average values of the response due to the parameters and interactions are calculated as follows (Roy, 1990):

$\overline{A}(1)$ = Average effect due to parameter A at level 1 (L_1)

$$= \frac{A(1)}{27} \text{ [since 27 data points are added to find A(1)].}$$

Similarly, $\overline{A}(2), \overline{A}(3)$ and average effects due to other parameters are calculated.

The average effect due to the interaction A x B is calculated as

$$\overline{AB}(1) = \frac{AB(1)}{54}$$

Here, 54 data points (27 in each column) are added to find AB(1).

Similarly, the average effects at other levels (L_2 and L_3) and for other interactions (B x C and A x C) are calculated.

5.5.1.2 Main effects due to parameters and interactions

The main effects of parameter A when level changes from L_1 to L_2 and L_2 to L_3 and L_3-L_1 are [Roy, 1990]:

Main effect of parameter A when A changes

from level 1 to level 2 ($L_1 \rightarrow L_2$) = Distance in average values of the response between Level 2 and Level 1 of parameter A

$$= \overline{A}(2) - \overline{A}(1)$$

Main effect of parameter A when A changes

from level 2 to level 3 ($L_2 \rightarrow L_3$) = Distance in average values of the response between Level 3 and Level 2 of parameter A

$$= \overline{A}(3) - \overline{A}(2)$$

The main effects of other parameters and interactions are also calculated in the similar fashion.

5.5.1.3 Analysis of Variance (ANOVA) [Roy, 1990]

ANOVA calculation follows the following procedure:

Step 1. Total of all results (T_T)

$$T_T = \sum_{i=1}^{n} \sum_{j=1}^{R} y_{ij} \; ;$$

n = Total number of trials = 27

R = Total number of repetitions = 3

Step 2. Correction factor (C.F.)

$$C.F. = T_T^2 / N$$

where, N = Total number of experiments = R x n = 27 x 3 = 81

Step 3. Total sum of squares (SS_T)

$$SS_T = \sum_{i=1}^{n} \sum_{j=1}^{R} y_{ij}^2 - C.F.$$

Step 4. Sum of squares due to a parameter (SS)

$$SS_A = \left[\frac{A(1)^2}{N_{A_1}} + \frac{A(2)^2}{N_{A2}} + \frac{A(3)^2}{N_{A3}} \right] - C.F.$$

where, $N_{A_1}, N_{A_2}, N_{A_3}$ are number of trials with parameter A at level 1, 2 and 3, respectively. The sum of squares SS_B, SS_C, SS_D, etc., are also calculated in the similar way.

Since the interaction terms appear in two columns as specified in Table 4.4.5 (Chapter-IV), the sum of squares due to interactions must consider both the columns [Roy, 1988]. Thus, to find $SS_{A \times B}$, effects of columns 3 and 4 are considered

$SS_{A \times B} = SS_{A \times B}$ due to column 3 + $SS_{A \times B}$ due to column 4

$SS_{B \times C} = SS_{B \times C}$ due to column 8 + $SS_{B \times C}$ due to column 11

$SS_{A \times C} = SS_{A \times C}$ due to column 6 + $SS_{A \times C}$ due to column 7

Step 5. Error sum of squares (SS_e)

$$SS_e = SS_T - (SS_A + SS_B + SS_C + SS_D + SS_E + SS_F + SS_G + SS_{AxB} + SS_{BxC} + SS_{AxC})$$

The symbol 'e' stands for error term.

Step 6. Total and parameter degrees of freedom (DOF)

$$f_T = Total\ DOF = (\text{Total number of trials} - 1)$$

$$= (R \times n - 1) = (3 \times 27 - 1) = 80$$

$$f_A = \text{DOF of parameter A}$$

$$= (\text{Number of levels of parameter A}) - 1 = 3 - 1 = 2$$

Similarly,

$$f_B = 2,\ f_C = 2,\ f_D = 2,\ f_E = 2,\ f_F = 2,\ \text{and}\ f_G = 2.$$

Here, the DOF for the interaction terms are calculated as [Ross, 1988]:

DOF of interaction term = Product of DOF of the interacting parameters

So, the DOF of A x B, B x C and A x C are :

$$f_{A \times B} = f_A \times f_B = 2 \times 2 = 4$$

$$f_{B \times C} = f_B \times f_C = 2 \times 2 = 4$$

$$f_{A \times C} = f_A \times f_C = 2 \times 2 = 4$$

A, B, C are three level parameters each having DOF of 2 (= 3 − 1)

$$f_e = \text{error DOF} = f_T - (f_A + f_B + f_C + f_E + f_F + f_G + f_H + f_{AxB} + f_{BxC} + f_{AxC})$$

$$= 80 - 26 = 54$$

Step 7. Mean square of variance (V_m)

$$V_A = \text{Variance due to parameter A} = SS_A / f_A$$

$$V_B = SS_B / f_B,\ V_C = SS_C / f_C, \text{etc.}$$

$$V_e = \text{Variance due to error} = SS_e / f_e$$

Step 8. Percentage contribution (P)

$$P_A = \text{\% contribution of parameter A towards mean of the response}$$

$$= SS_A / SS_T$$

Similarly,

$$P_B \;=\; SS_B \,/\, SS_T \,, \; P_C \;=\; SS_C \,/\, SS_T \,,\; \text{etc.}$$

Step 9. F-ratios

$$F_A \;=\; V_A \,/\, V_e \,, \; F_B \;=\; V_B \,/\, V_e \,,\; \text{etc.}$$

where, F_A, F_B, F_C, etc. are F-series due to parameters A, B, C, etc., respectively.

Step 10. Pooling

If the calculated F-ratio (Step 9) for a parameter is less than F-ratio tabulated [Ross, 1988] at a stated confidence level (95% confidence level) then the effect of the parameter is insignificant and the parameter is pooled. If a parameter is pooled, the sum of square due to the parameter is added to the error sum of error and the other ANOVA terms are modified. If parameter A is pooled,

$$SS_e \text{ (pooled)} = SS_e + SS_A$$

$$f_e \text{ (pooled)} = f_e + f_A$$

$$V_e \text{ (pooled)} = SS_e \text{ (pooled)} \,/\, f_e \text{ (pooled)}$$

Step 11. Pure sum of squares (SS')

If parameter A is significant

$$SS_A = SS_A - (V_e \times f_A)$$

Similarly, for other significant parameters pure sum of squares can be calculated. The subtracted amount of sum of squares must be added to the error sum of squares in order that the total sum of square is unchanged.

$$SS_e = SS_e + (V_e \times f_A)$$

Step 12. Modified percentage contribution

After pooling of the insignificant parameters, the percentage contribution of significant parameters is calculated. If parameter A is significant, the percent contribution is calculated as:

$$P_A \;=\; \frac{SS_A'}{SS_T} \times 100$$

Similarly,

$$P_B = \frac{SS_B'}{SS_T} \times 100 \,, \; P_C = \frac{SS_C'}{SS_T} \times 100 \,, \text{etc.}$$

P_e = Percentage contribution of error term

$$= \frac{SS_e'}{SS_T} \times 100$$

P_T = Total percentage contribution

$$= P_A + P_B + P_C + P_D + P_E + P_F + P_G + P_e$$

where P_A, P_B, P_C, etc. are percent contributions due to parameters A, B, C, etc..

5.5.2 S/N Data Analysis

5.5.2.1 Conversion of raw data into S/N ratio

Let S/N(i), i = 1, 2, ..., 27, be the S/N ratios in dB of the raw data against the trial conditions and y_{ij}, i = 1, 2, ..., 27 and j = 1, 2, 3, are the raw data (Table 4.4.5, Chapter-IV)

For each ith trial condition, there are three responses (raw data) for three repetitions, j = 1, 2, 3.

Case I: If the response of the selected quality characteristic is 'lower-the-better' (LB) type, the S/N ratio against each trial condition is calculated

$$(S/N)_{LB} = -10 \log \left[\frac{1}{R} \sum_{j=1}^{R} y_j^2 \right]$$

Case II: If the response is 'higher-the-better' (HB) type, the S/N ratios are calculated

$$(S/N)_{HB} = -10 \log \left[\frac{1}{R} \sum_{j=1}^{R} \frac{1}{y_j^2} \right]$$

Case III: If the response is 'nominal-the-best' (NB) type, the S/N ratios are calculated

$$(S/N)_{NB} = -10 \log \left[\frac{1}{R} \sum_{j=1}^{R} (y_j - y_0)^2 \right]$$

The raw data are converted to S/N ratios using the LB, HB, NB signal-to-noise ratio formula. The choice depends on the type of the quality characteristic. Thus, for the L_{27} OA after consolidation of the repeated responses (raw data) of a trial condition into a single metric (the S/N ratio) total of twenty seven responses are found (l = 1, 2,......,27) instead of eighty one responses in raw data analysis.

(ii)   Analysis

The use of S/N ratio as response presents a minor difference in the analysis procedure (raw data analysis) discussed above. The use of S/N ratio reduces the total degrees of freedom of the entire experiment.

For the L_{27} OA with S/N ratios as responses, the total DOF of the experiment becomes [Roy, 1990]:

f_T = (Number of trial conditions-1)

= 27 – 1 = 26

The rest of the analysis follows the same steps as discussed above. Same steps have been used for the design of experiments for single and binary sorption systems for the removal of Py, 2Pi, 4Pi, and AmPy from aqueous solutions.

RESULTS AND DISCUSSION

6.1 GENERAL

This chapter presents the results and discussion on the adsorption of pyridine (Py), 2-picoline (2Pi), 4-picoline (4Pi) and 3-aminopyridine (AmPy) from aqueous solutions onto bagasse fly ash (BFA), rice husk ash (RHA) and commercial grade granular activated carbon (GAC). This chapter has been divided into the following sections:

1. Characterization of adsorbents,

2. Batch adsorption,

3. Optimization of parameters for single and multi-component batch adsorption using Taguchi's design of experimental (DOE) methodology,

4. Multi-stage batch adsorption of Py, 2Pi, 4Pi and AmPy,

5. Desorption of Py, 2Pi, 4Pi and AmPy from spent adsorbents, and

6. Thermal oxidation characteristics of spent adsorbents.

6.2 CHARACTERIZATION OF ADSORBENTS

6.2.1 Physico-chemical Characterisation of Adsorbents

The fractional sieve analysis of the particles of BFA showed: -600+425 μm: 31.42%; -425+180 μm: 68.43%. The average particle diameter was found to be 381.45 μm. The fractional sieve analysis of the particles of RHA showed: -600+425 μm: 36.72%; -425+300μm: 49.68%; -300+180 μm: 13.60%. The average particle diameter was found to be 412 μm. The fractional sieve analysis of the GAC particles showed: -1700+1000 μm: 83.50 % and -1000+500 μm: 16.50%. The average particle diameter was found to be 1271 μm. GAC had highest particle size among the three adsorbents. The physico-chemical characteristics of the three adsorbents are presented in Table 6.2.1.

Table 6.2.1. Physico-chemical characteristics of adsorbents.

Characteristics	BFA	RHA	GAC
Proximate analysis			
Moisture (%)	4.91	1.1	4.41
Volatile matter (%)	14.63	7.36	3.32
Ash (%)	28.3	80.58	51.9
Fixed Carbon (%)	52.16	10.96	40.37
Bulk density (kg/m^3)	133.3	175.3	506.7
Heating value (MJ/kg)	28.73	21.8	20.12
Average particle size (µm)	381.45	412	1271
Chemical analysis of ash			
Insoluble (%)	78.35	65.17	86
SiO$_2$ (%)	2.46	12.6	0.41
Fe$_2$O$_3$ & Al$_2$O$_3$ (%)	2.92	3.38	5.45
CaO (%)	14	17.4	1.75
MgO (%)	1.09	0.96	4.5
Others	1.18	0.49	1.89
Ultimate analysis of adsorbents			
Carbon (%)	56.03	13.14	41.61
Hydrogen (%)	0.78	0.194	0.237
Surface area of pores (m^2/g)			
(i) BET	244.54	65.36	171.05
(ii) BJH			
(a) adsorption cumulative	62.29	52.35	131.98
(b) desorption cumulative	36.19	26.62	94.33
BJH cumulative pore volume (cm^3/g)			
(i) Single Point Total	0.134	0.0388	0.1327
(ii) BJH adsorption	0.053	0.0386	0.1231
(iii) BJH desorption	0.051	0.0352	0.1081
Average pore diameter (Å)			
(i) BET	22.5	34.66	31.03
(ii) BJH adsorption	33.78	43.27	37.3
(iii) BJH desorption	56.12	58.34	45.86

BFA   **RHA**

GAC

Fig. 6.2.1. Photograph of BFA, RHA and GAC.

It is observed that BFA has the lowest bulk density among the adsorbents. The amount of ash is very high in RHA as compared to that of BFA and GAC. High amount of ash indicates inorganic nature of RHA. Similar properties of RHA have been reported by Nakbanpote et al. [2000] and Srivastava et al. [2006a]. The amount of carbon content is highest in BFA followed by GAC and RHA. Due to low carbon content, RHA is expected to have low porosity and thereby low surface area. The chemical analysis of adsorbents shows the presence of different oxides. Silicon and calcium oxides are found to be the major components in all the adsorbents. Other constituents present are oxides of iron and magnesium. Ultimate analysis of BFA, RHA and GAC showed 56.03, 13.14 and 41.61% carbon; 0.78, 0.19 and 0.24% hydrogen; respectively and oxygen by balance was found to be 43.2 %, 86.7 % and 58.1 % respectively.

The morphologies of blank and Py, 2Pi, 4Pi and AmPy-loaded BFA, RHA and GAC were examined by scanning electron microscopy (SEM) and X-ray diffraction (XRD) analysis. The SEMs of the blank and Py, 2Pi, 4Pi and AmPy-loaded BFA, RHA and GAC are shown in Fig. 6.2.2 through 6.2.4. These figures reveal the surface texture and porosity of the blank and loaded adsorbents. SEM micrographs of BFA at 1000X magnification (Fig. 6.2.2) show the fibrous structure and strands of the fibre. It can be inferred from these figures that the surface texture of the blank adsorbents changes after the adsorption of Py and its derivatives. Similar changes after adsorption can be observed in the micrographs of blank and loaded RHA and GAC (Figs. 6.2.3 and 6.2.4).

XRD patterns of blank and loaded adsorbents are shown in Figs. 6.2.5 - 6.2.7. The d-spacing values provided by the XRD spectra of BFA (Fig. 6.2.5) reflect the presence of Silica (SiO_2), Wollastonite ($CaSiO_3$), Aragonite ($CaCO_3$) and Akdalaite [$(Al_2O_3)_4.H_2O$] whereas Cristobalite (SiO_2), Margaritasite [$(Cs,K,H_3O)_2(UO_2)2V_2O_8.(H_2O)$] and Macedonite ($PbTiO_3$) were the major components identified in RHA (Fig. 6.2.6). XRD spectra of GAC (Fig. 6.2.7) shows the presence of Moganite (SiO_2), Akdalaite [$(Al_2O_3)_4.H_2O$], Tamarugite [$NaAl(SO_4)_2.6H_2O$] Fersilicate (FeSi) and Majorite [$Mg_3(Fe,Al,Si)_2(SiO_4)_3$] as major components.
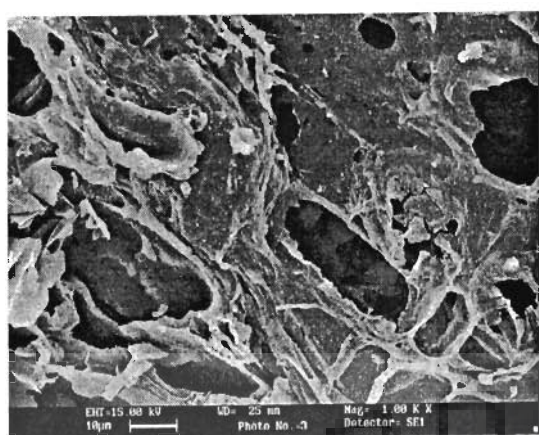
BFA - Blank
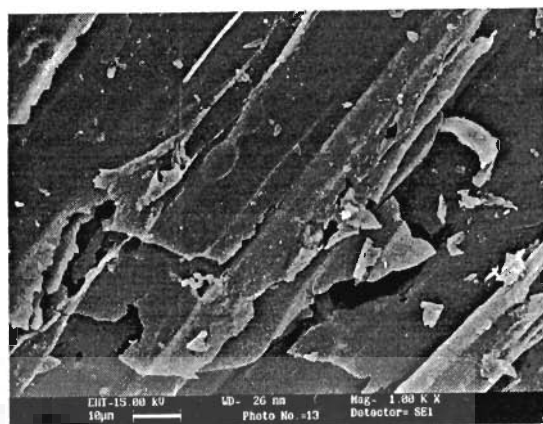
BFA – Py
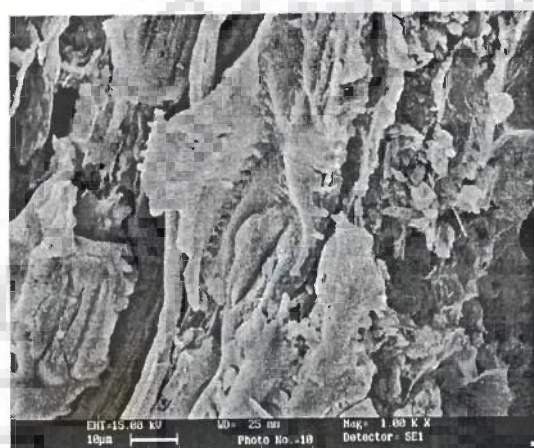
BFA – 2Pi
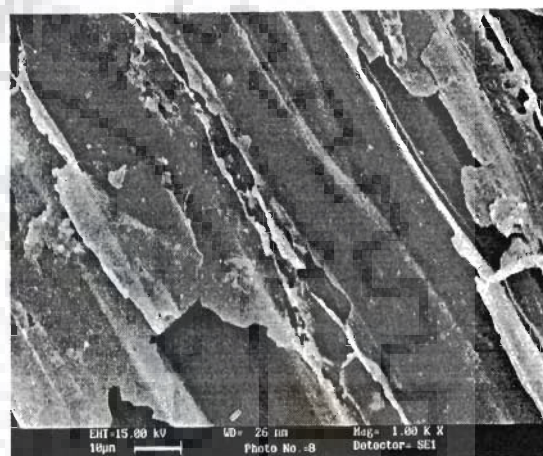
BFA – 4Pi
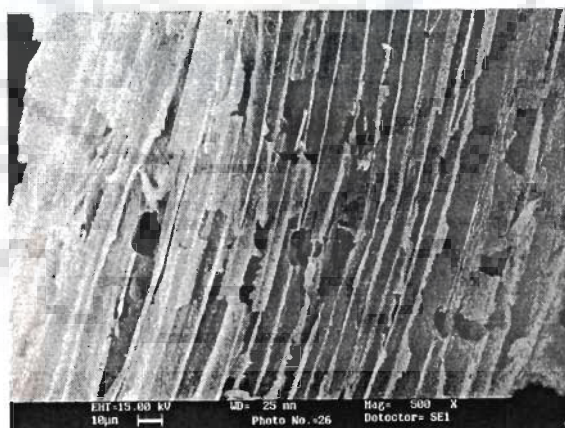
BFA – AmPy

Fig. 6.2.2. SEM of blank and Py and its derivatives loaded BFA at 1000X.
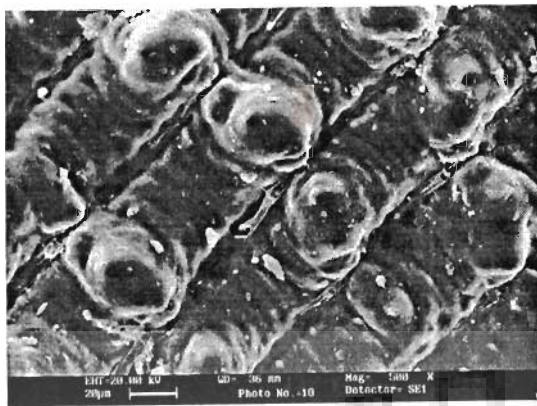
RHA – Blank
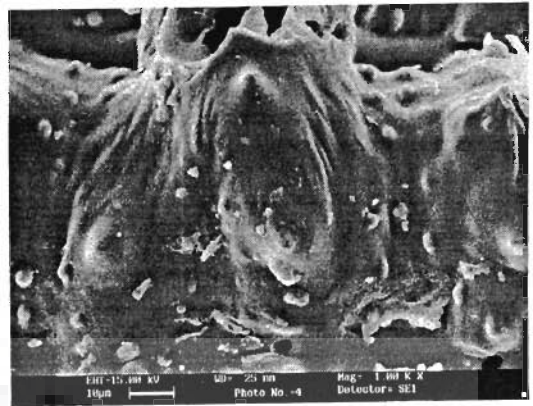
RHA – 2Pi

RHA – Py
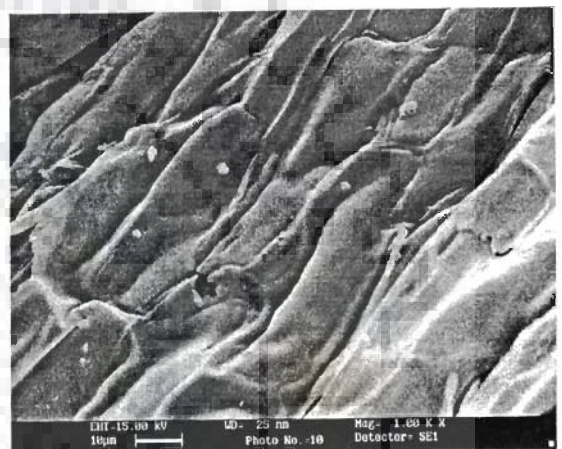
RHA – 4Pi

RHA – AmPy

Fig. 6.2.3. SEM of blank and Py and its derivatives loaded RHA at 1000X.
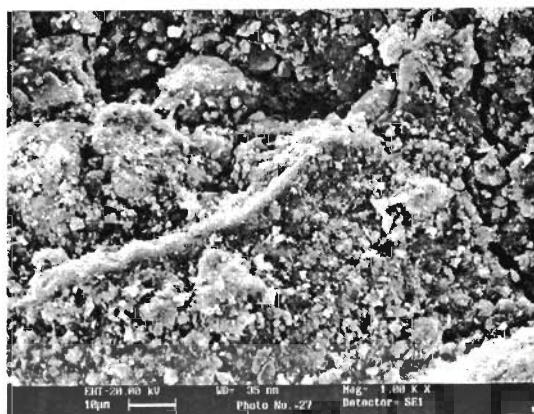
GAC – Blank
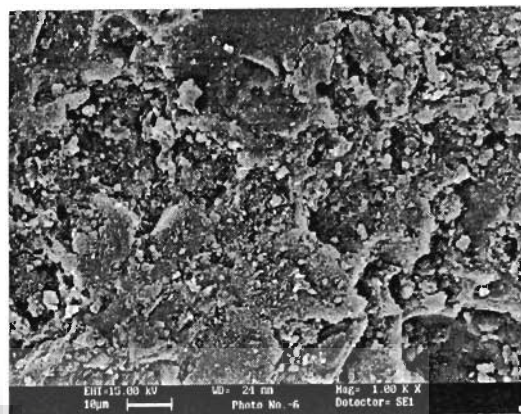
GAC – 2Pi
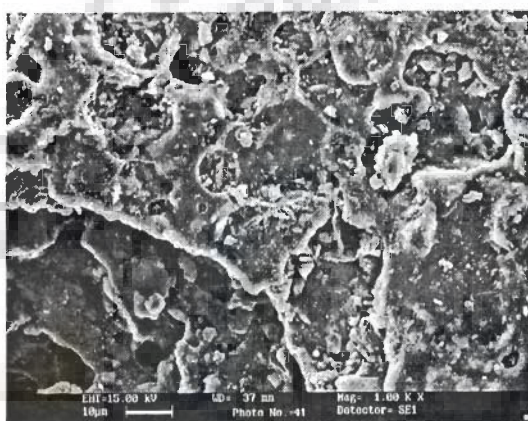
GAC – Py
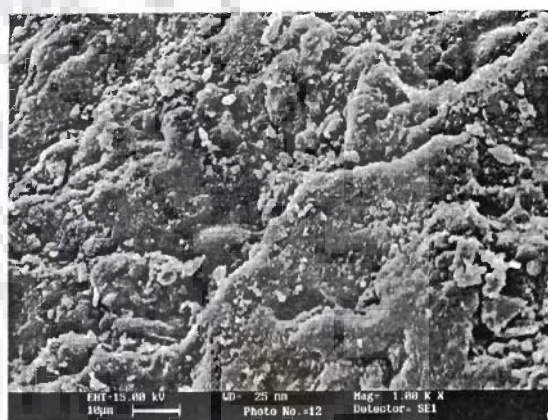
GAC – 4Pi
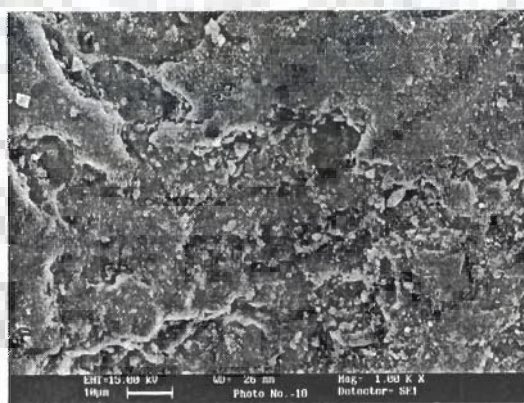
GAC – AmPy

Fig. 6.2.4. SEM of blank and Py and its derivatives loaded GAC at 1000X.
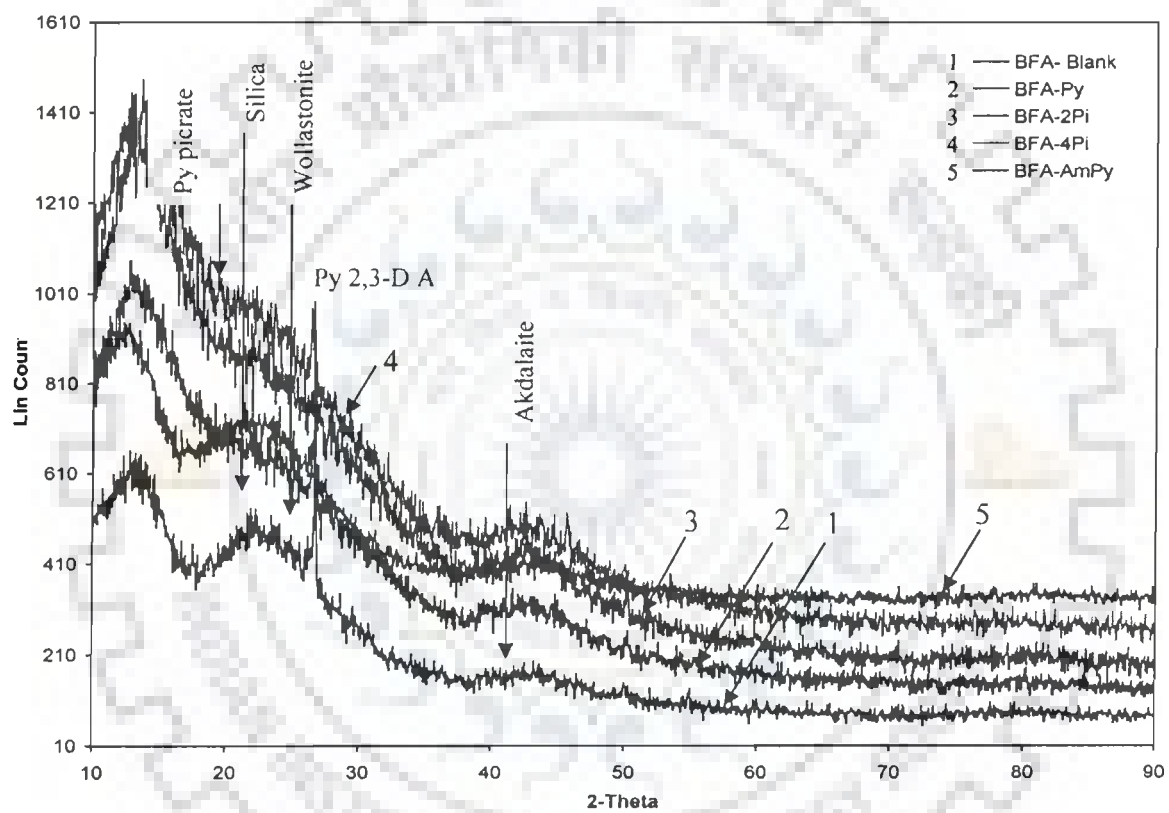
Fig. 6.2.5. X-ray diffraction of Blank and Py and its derivatives loaded BFA
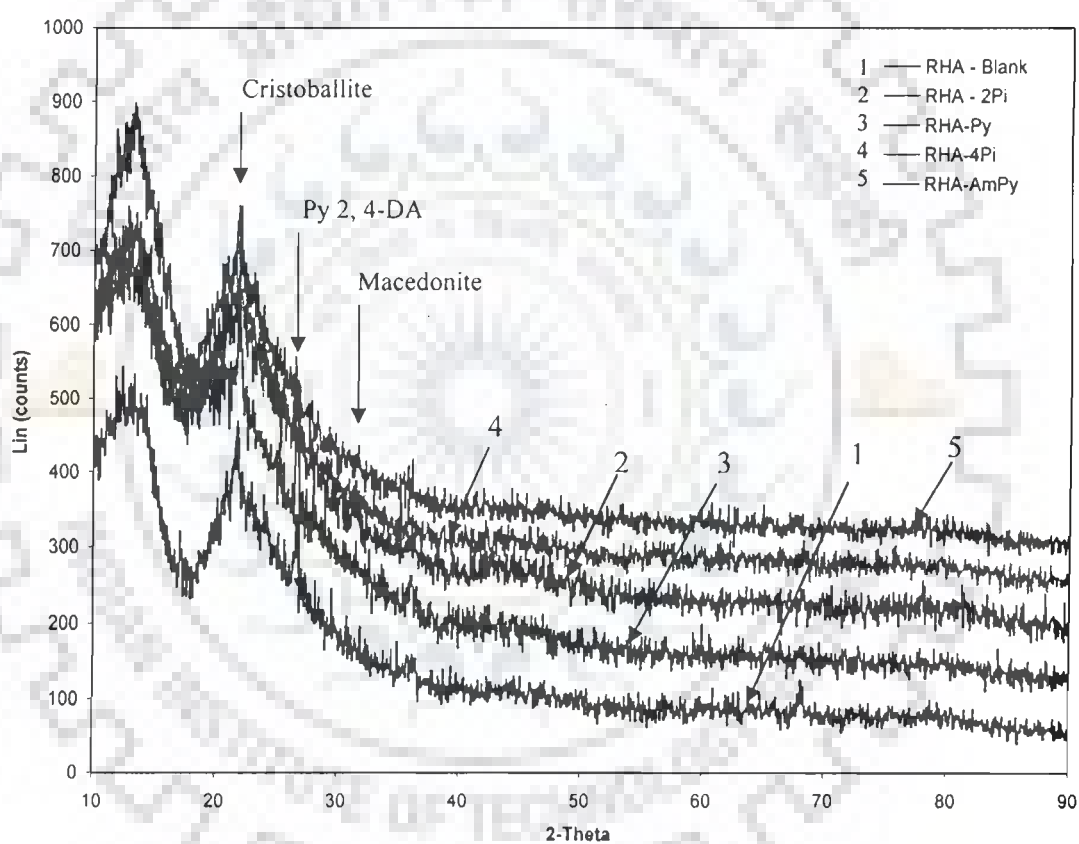
Fig. 6.2.6. X-ray diffraction of Blank and Py and its derivatives loaded RHA
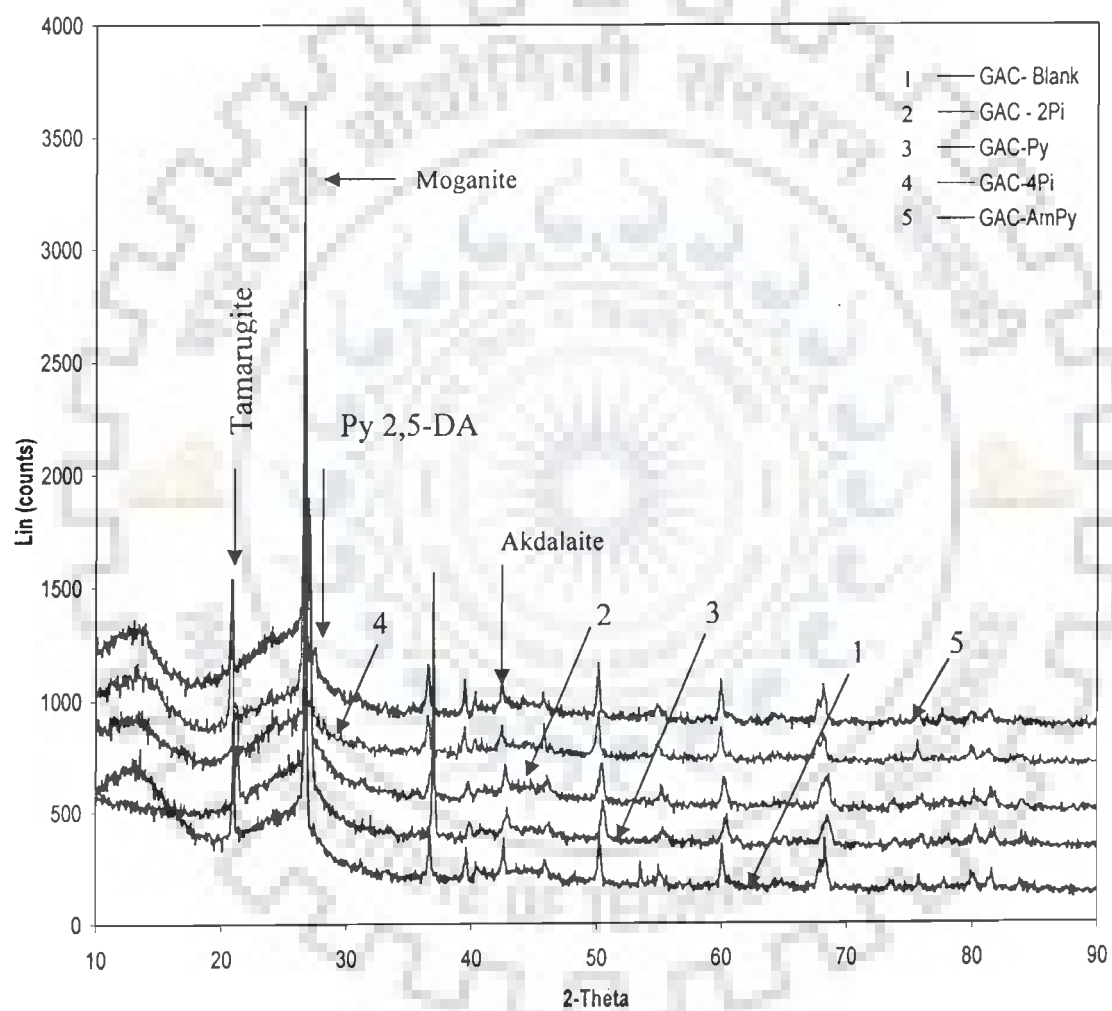
Fig. 6.2.7. X-ray diffraction of Blank and Py and its derivatives loaded GAC

The broad peak in the XRD spectra of all the three adsorbents indicates the presence of amorphous form of silica. Major pyridine compounds in loaded BFA, RHA and GAC identified are pyridine 2, 3-diacarboxylic acid or quinolinic acid ($C_7H_5NO_4$), pyridine 2, 4-dicarboxylic acid hydrate ($C_7H_5NO_4 \cdot H_2O$) and pyridine 2, 5-diacarboxylic acid hydrate ($C_7H_5NO_4 \cdot H_2O$) at $2\theta \approx 27\text{-}28°$. The main compounds and some of the pyridine compounds are shown in Fig. 6.2.5 to Fig. 6.2.7 as Py 2, 3-DA, Py 2, 5-DA etc. The other compounds identified were zinc-picoline ($C_{20}H_{28}N_6S_2Zn$) and pyridine picrate ($C_{12}H_8N_4O_7$) at $2\theta \sim 24.4°$ and 21° in Py and its derivative loaded adsorbents.

6.2.2 Pore Size Distribution of Adsorbents

BJH method is the most popular method used for the evaluation of the mesoporous structure of the adsorbents. Pore sizes are classified in accordance with the classification adopted by the International Union of Pure and Applied Chemistry (IUPAC) [IUPAC, 1982], that is, micro-pores (diameter (d) < 20 Å), meso-pores (20 Å < d < 500 Å) and macro-pores (d > 500 Å). Micro-pores can be divided into ultra micro-pores (d < 7 Å) and super micro-pores (7 Å < d < 20 Å). Because of the larger sizes of liquid molecules, the adsorbents for liquid phase adsorbates should have predominantly mesoporous in the structure.

Pore size distributions of BFA, RHA and GAC are given in Fig. 6.2.8 and analysis results are given in Table 6.2.1. The BET surface area of BFA, RHA and GAC are 244.54, 65.36 and 171.05 m^2 g^{-1}, respectively. Barrett-Joyner-Halenda (BJH) adsorption/desorption surface area of pores is found to be 62.29/36.19 m^2 g^{-1}. The single point total pore volume of pores (< 3560 Å) is 0.134 cm^3 g^{-1}, whereas cumulative pore volume of pores (17 < d < 3000 Å) is 0.053 $cm^3 g^{-1}$. The average pore diameter by BET method is found to be 22.50 Å whereas the BJH adsorption/desorption average pore diameter is found to be 33.78 Å/56.12 Å. Micropores (d < 20 Å) account for 35.6% (27.19 m^2 g^{-1}) of the pore surface area and 19% (0.01 cm^3 g^{-1}) of the pore volume and the mesopores (20 Å < d < 500 Å) account for 64.2% (39.97 m^2 g^{-1}) of the pore surface area and 74% (0.04 cm^3 g^{-1}) of the pore volume. The macropores (d > 500 Å) account for only 0.2% (0.1 $m^2 g^{-1}$) of the pore surface area and 7% (0.004 $cm^3 g^{-1}$) of the pore volume.
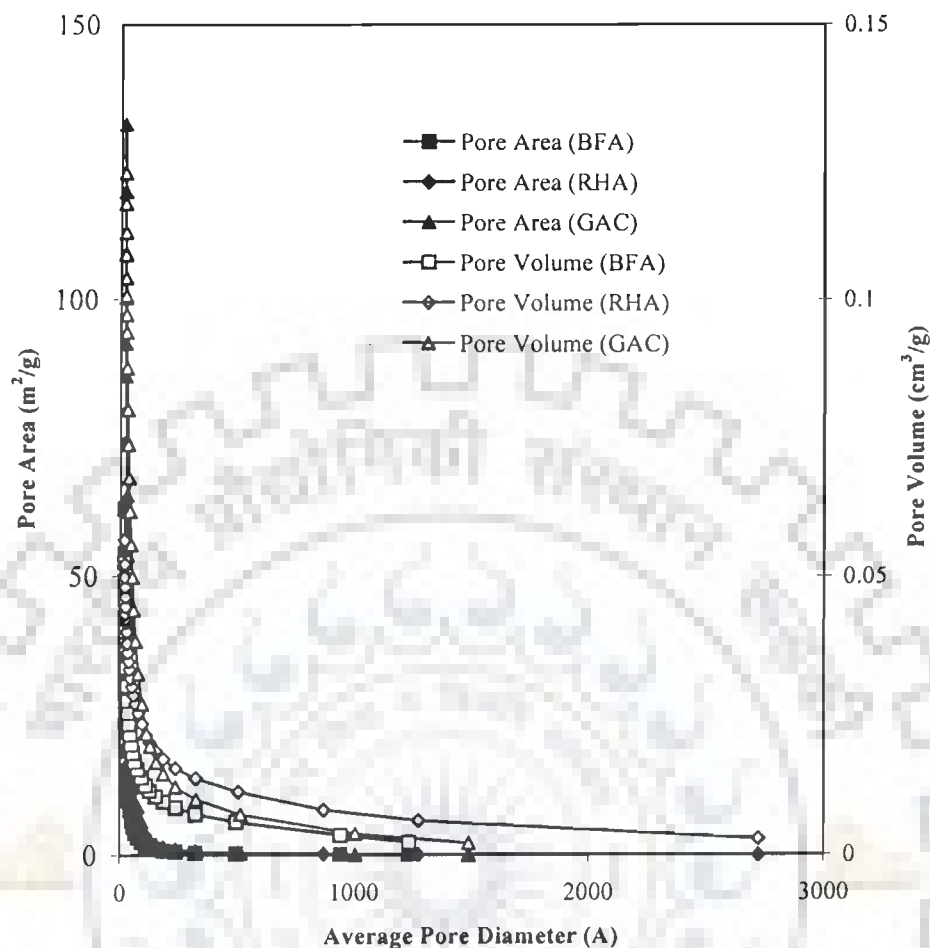
Fig. 6.2.8. Pore size distribution of BFA, RHA and GAC.

The BET pore surface area of RHA is found to be 65.36 m^2g^{-1}, whereas the Barrett-Joyner-Halenda (BJH) adsorption/desorption surface area of pores is found to be 52.35/26.62 m^2g^{-1}. The single point total pore volume of pores (< 2530 Å) is 0.0567 $cm^3 g^{-1}$, whereas cumulative pore volume of pores (17 < d < 3000 Å) is 0.0566 cm^3g^{-1}. The average pore diameter by BET method is found to be 34.66 Å whereas the BJH adsorption/desorption average pore diameter is found to be 43.27 Å/58.34 Å. Micropores (d < 20 Å) account for 36.1% (18.9 m^2g^{-1}) of the pore surface area and 15% (0.0084 cm^3g^{-1}) of the pore volume, and the mesopores (20 Å < d < 500 Å) account for 63.5% (33.2 $m^2 g^{-1}$) of the pore surface area and 71% (0.04 cm^3g^{-1}) of the pore volume

114

The macropores (d > 500 Å) account for only 0.4% (0.2 m^2g^{-1}) of the pore surface area and 14% (0.0081 cm^3g^{-1}) of the pore volume.

The BET surface area of GAC is found to be 171.052 m^2g^{-1}, whereas BJH adsorption/desorption surface area of pores is found to be 131.9816/94.3321 m^2g^{-1}. The single point total pore volume of pores (< 3400 Å) is 0.133 cm^3g^{-1}, whereas cumulative pore volume of pores (17 < d < 3000 Å) is 0.123 cm^3g^{-1}. The average BET pore diameter is 31.028 Å, whereas the BJH adsorption/desorption average pore diameter is 37.30 Å/45.86 Å. 23.9% (31.6 $m^2 g^{-1}$) of the pore surface area (d < 20 Å) and 12% (0.015 $cm^3 g^{-1}$) of the pore volume is covered by the micropores, 75.8% (100.0 $m^2 g^{-1}$) of the pore surface area accounts for the mesopores (20 Å < d < 500 Å) and 82% (0.101 $cm^3 g^{-1}$) of the pore volume, and only 0.3% (0.4 $m^2 g^{-1}$) of the pore surface area (d > 500 Å) and 6% (0.007 $cm^3 g^{-1}$) of the pore volume are covered by the macropores. A comparison of the pore analysis data shows that the BET surface area of BFA is largest (244 $m^2 g^{-1}$) followed by that of GAC (171) and RHA 65 m^2g^{-1} RHA distribution analysis of adsorbents shows that the micropores (d < 20 Å) of GAC have a minimum pore area of 24% followed by almost equal values of BFA and RHA (~36%) The GAC is found to be predominantly mesoporous (76% of pore area) followed by similar area of BFA and RHA (~ 64%). The highest mesopore are is that of GAC (~6%) while almost no macropores are present in BFA and RHA. The BET average pore diameter of BFA < GAC < RHA. Based on this analysis, it can be safely said that the RHA and GAC have predominantly mesoporous structure.

6.2.3   FTIR Spectroscopy of the Adsorbents

The chemical structure of the adsorbents is of vital importance in understanding the sorption process. The sorption capacity of adsorbents is strongly influenced by the chemical structure of their surface. The carbon-oxygen functional groups are by far the most important structures in influencing the surface characteristics and surface behavior of adsorbents. BFA and RHA have similar spectra as shown in Figs. 6.2.9 and 6.2.10. A broad band between 3100 and 3700 cm^{-1} in all the adsorbents is indicative of the

presence of both free and hydrogen bonded OH groups on the adsorbent surface [Kamath and Proctor, 1998]. This stretching is due to both the silanol groups (Si–OH) and adsorbed water (peak at 3400 cm^{-1}) on the surface [Abou-Mesalam, 2003]. C-O group stretching from aldehydes and ketones can also be inferred from peaks in the region of 1600 cm^{-1}. These FTIR spectra also show transmittance around ~1100 cm^{-1} region due to the vibration of the C–O group in lactones [Davila-Jimenez et al., 2005] and due to Si–O–Si and –C–O–H stretching and –OH deformation. The band around ~1400 cm^{-1} in all the adsorbents may be attributed to the carboxyl-carbonate structures. The functional groups suggested most often are (i) carboxyl groups, (ii) phenolic hydroxyl groups, (iii) carbonyl groups (e.g. quinone-type), and (iv) lactone groups (e.g. fluorescein-type) [Ricordel et al., 2001]. Zawadzki [1988] showed that pyridine is adsorbed on carbon surface in four different states: physically adsorbed pyridine, hydrogen-bonded pyridine, pyridine in interaction with a Lewis acid site, and Bronsted acid site. Figs. 6.2.9 to Fig. 6.2.11 show the FTIR spectra of the blank various adsorbate and loaded adsorbents. Two clear peaks around 1400 to 1500 cm^{-1} and 1620 to 1650 cm^{-1} can be identified which seemed to be affected due to Py-adsorption onto BFA, RHA and GAC. The peak around 1400 cm^{-1} in the range 1400 to 1500 cm^{-1} is the characteristic band of Py bonded to Lewis site. The peaks around 1634 cm^{-1} in the range of 1600 to 1650 cm^{-1} are due to the bond of pyridine and its derivatives to the Bronsted site. Similar results were reported by Zawadzki [1988] and Zaki et al. [1989]. These peaks are normally attributed to adsorbed bound water onto the sorbent surface. The peak around 1400 cm^{-1} corresponds to bound water coordinated to cations. This may also be attributed to single C-N bond (not to hydrogen). The peak around 1630 cm^{-1} is attributed to hydrogen bending vibrations reflecting the presence of bound water. Peak around 1600 cm^{-1} may also be due to conjugated hydrocarbon bonded carboxyl groups. Upon Py adsorption, these peaks get slightly shifted with the increase in transmittance. The peak shift from about 1620 to 1633 cm^{-1} may be due to NH deformation and R-N-H bending vibrations.
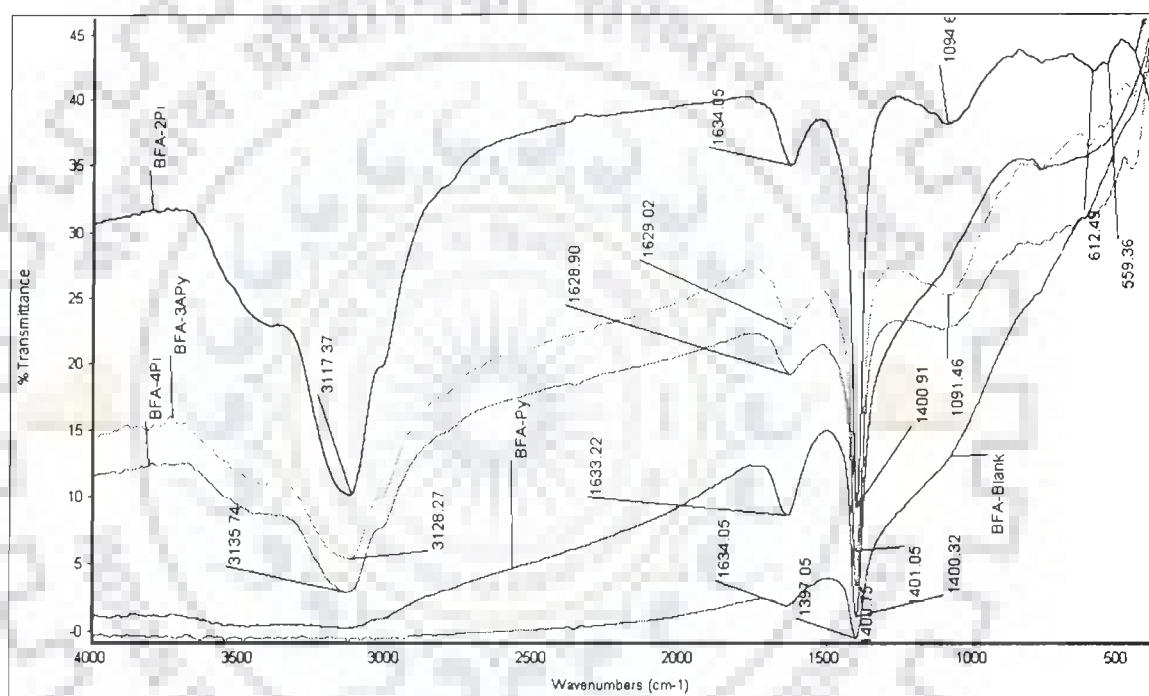
Fig 6.2.9. FTIR spectra of blank and Py and its derivatives loaded BFA
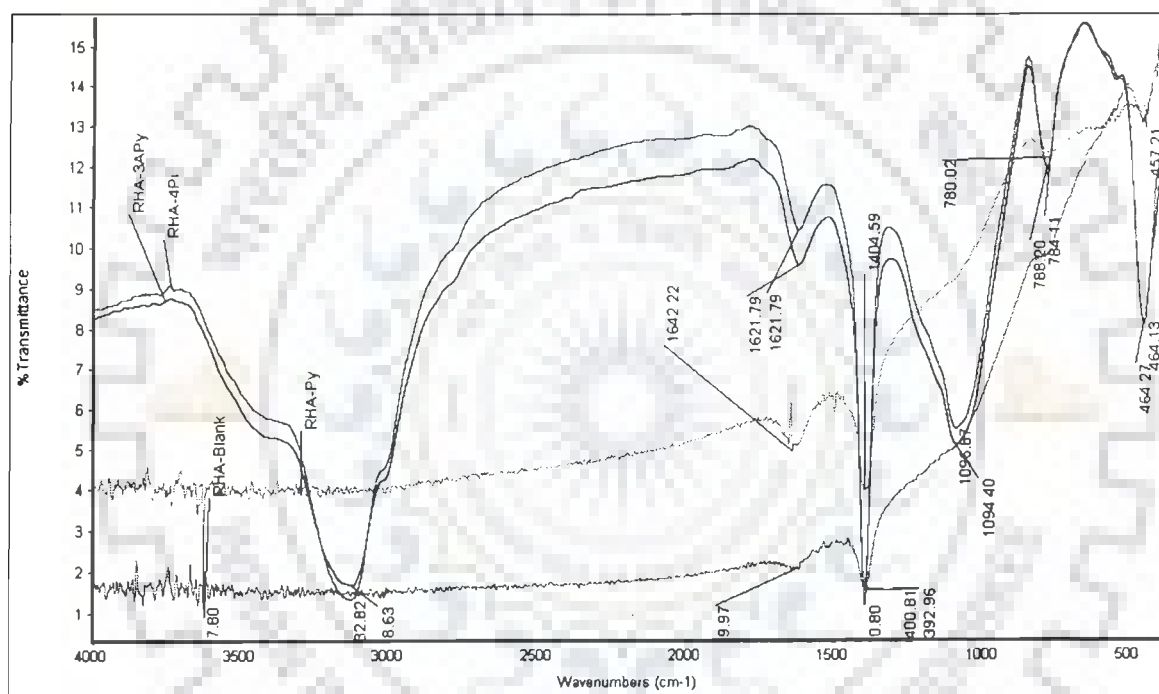
Fig 6.2.10 FTIR spectra of blank and Py and its derivatives loaded RHA
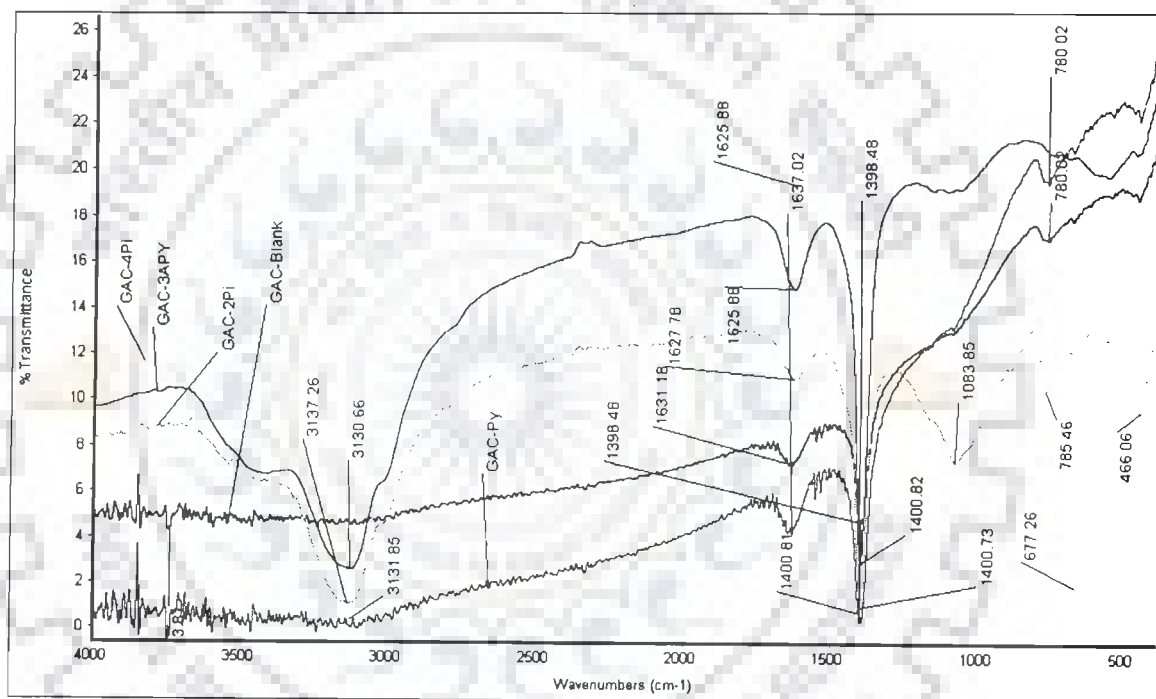
Fig 6.2.11 FTIR spectra of blank and Py and its derivatives loaded GAC

6.2.4 The point of zero charge (pH_{PZC}) of the adsorbents

Adsorption of cations is favored at pH > pH_{PZC}, while the adsorption of anions is favored at pH < pH_{PZC}. The specific adsorption of cations shifts pH_{PZC} towards lower values, whereas the specific adsorption of anions shifts pH_{PZC} towards higher values. Fig. 6.2.12 shows that for all the concentrations of KNO_3, the pH_{PZC} for BFA, RHA and GAC are found to be 9.0, 10.15 and 9.25, respectively.
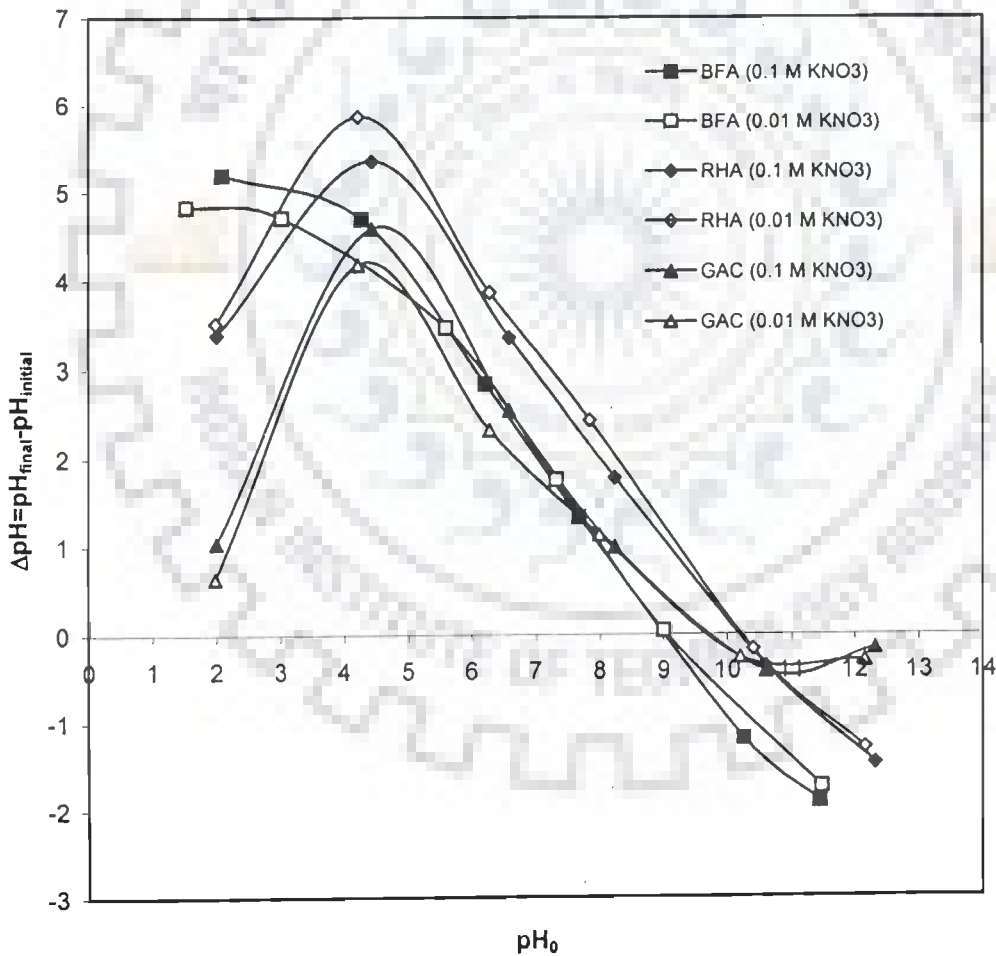
Fig. 6.2.12. Point of zero charge pH $_{pzc}$ of adsorbents.

120

6.3 BATCH ADSORPTION OF PYRIDINE AND ITS DERIVATIVES ONTO BFA, RHA AND GAC

Batch adsorption studies have been conducted for the removal of Pyridine (Py), 2-Picoline (2Pi), 4-Picoline (4Pi) and 3-Aminopyridine (AmPy) from aqueous solutions by BFA, RHA and GAC. Effect of various parameters viz. adsorbent dose (m), initial pH (pH_0), contact time (t), initial concentration (C_0), temperature (T) on the adsorption of Py, and its derivatives onto these adsorbents have been discussed in this section.

6.3.1 Effect of Adsorbent Dosage (m)

The effect of adsorbent dosage (m) on the amount adsorbed (mg g^{-1} of adsorbent (q_e)), and the removal of Py (C_0= 300 mg dm^{-3}), 2Pi, 4Pi and AmPy (C_0 = 100 mg dm^{-3}) by BFA, RHA and GAC are shown in Figs. 6.3.1 - 6.3.3. From the figures, it is found that the removal for a fixed concentration increases with an increase in amount of adsorbent but the capacity of the adsorbent for the sorption of adsorbate, i.e. the amount of adsorbate sorbed per unit weight of adsorbent, decreases with an increase in adsorbent dose. The increase in the removal of adsorbate with an increase in m for a fixed C_0 can be attributed to the greater surface area and increased number of adsorption sites [Srivastava et al, 2005b; Ho and Ofomaja, 2006a; Lataye et al., 2006]. The decrease in adsorption capacity with an increase in m can be ascribed to the unsaturation of adsorption sites through the adsorption reaction [Shukla et al., 2002; Yu et al., 2003] and the adsorbent particle-particle interaction leading to solids aggregation. Such particle aggregation will lead to a decrease in total surface area of the sorbent and an increase in diffusional path length [Perlinger and Eisenreich, 1991; Ozacar and Sengil, 2005]. Particle-particle interaction may also desorb some of the sorbates that is only loosely and reversibly bound to the adsorbent surface.

121
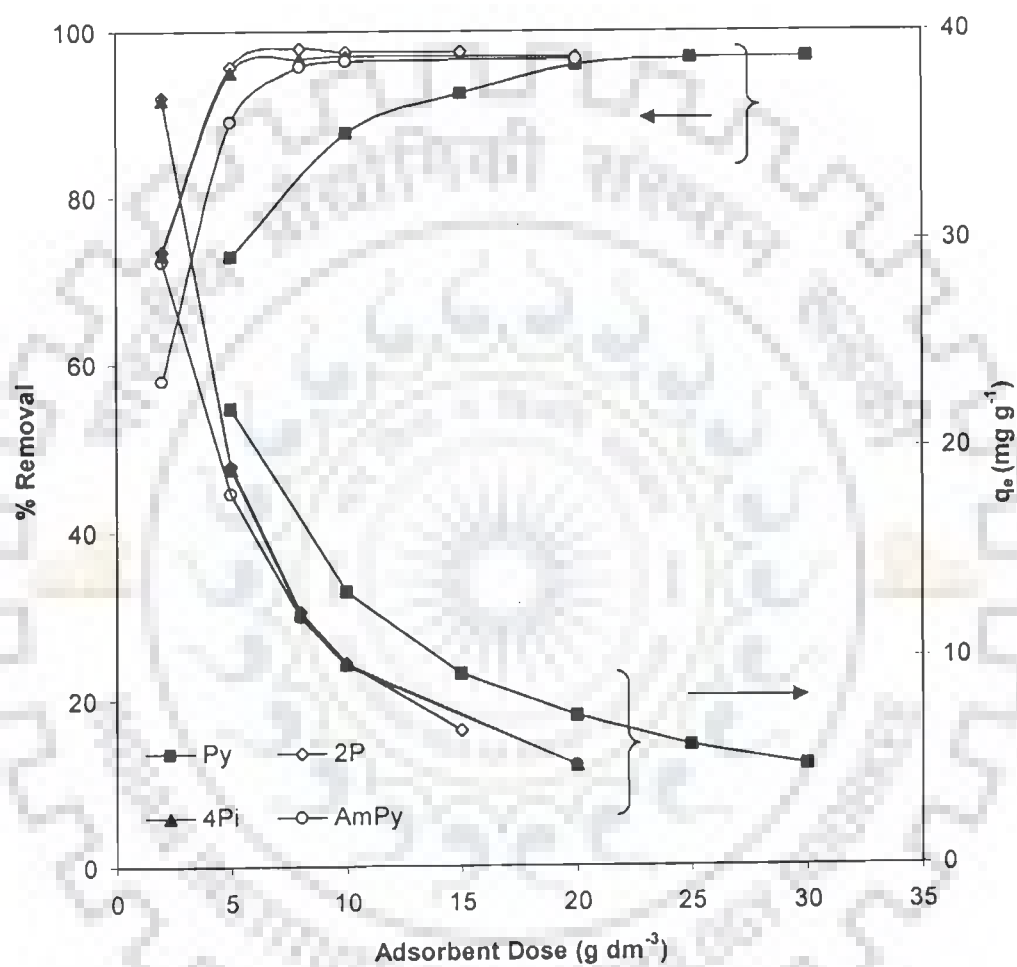
Fig. 6.3.1. **Effect of BFA dose on the removal of Py (C_0 = 300 mg dm^{-3}) and 2Pi, 4Pi and AmPy (C_0 = 100 mg dm^{-3}), pH_o = 6, T = 303 K, t = 5 h.**

122
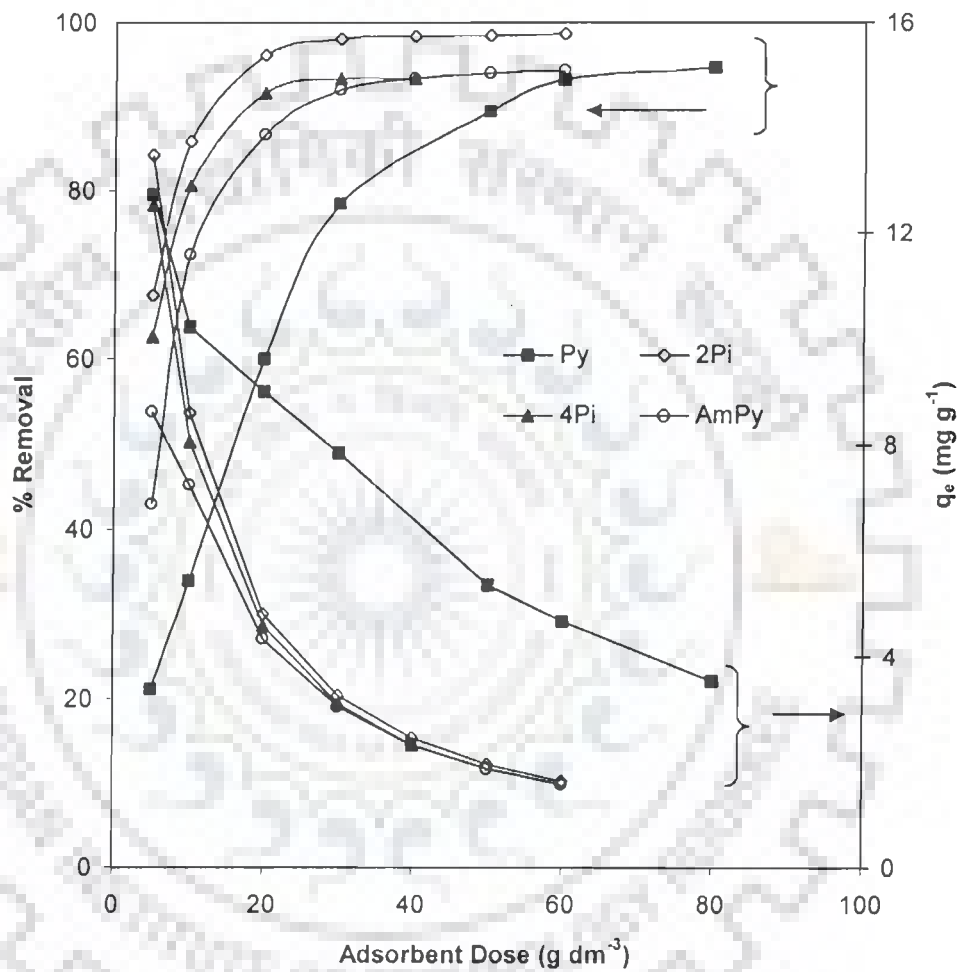
Fig. 6.3.2. **Effect of RHA dose on the removal of Py (C_0 = 300 mg dm^{-3}) and 2Pi, 4Pi and AmPy (C_0 = 100 mg dm^{-3}), pH_o = 6, T = 303 K, t = 5 h.**
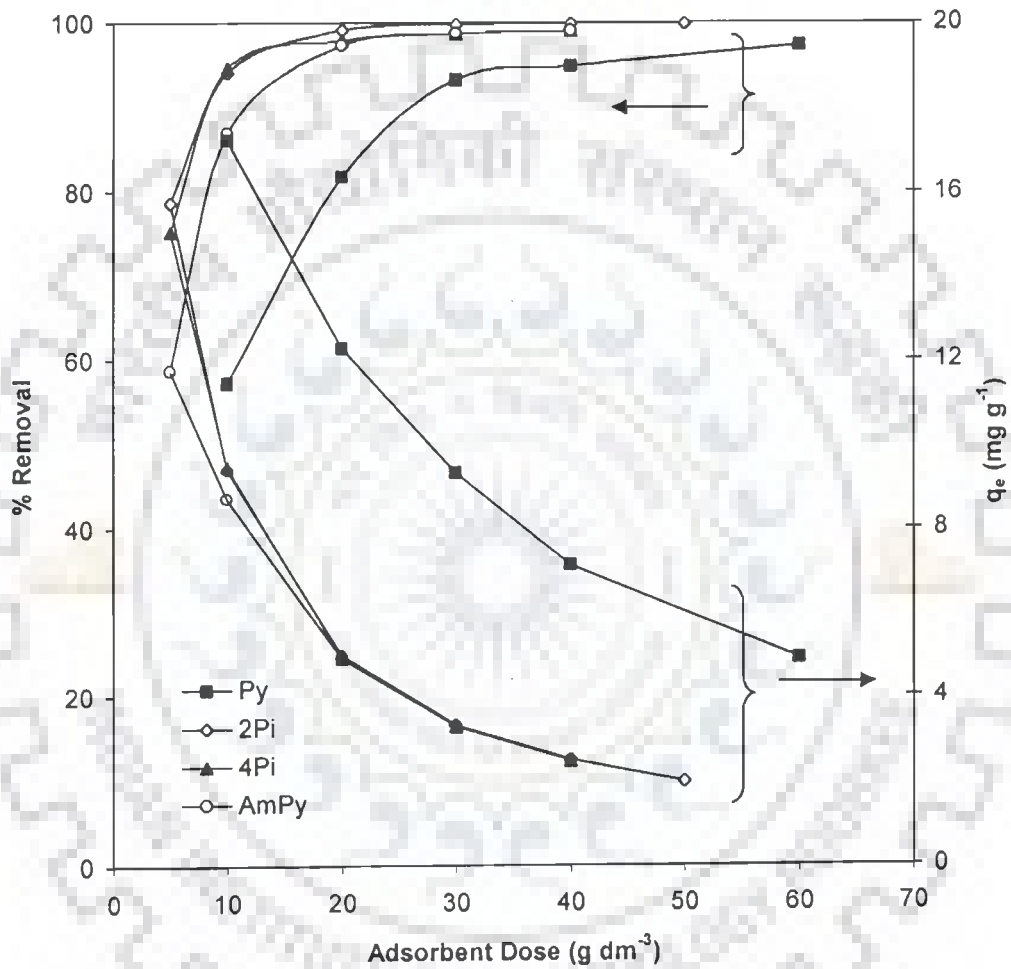
Fig. 6.3.3. Effect of GAC dose on the removal of Py (C_0 = 300 mg dm^{-3}) and 2Pi, 4Pi and AmPy (C_0 = 100 mg dm^{-3}), pH_o = 6, T = 303 K, t = 5 h.

The Py removal by BFA is observed to increase with an increase in m upto ~ 25 g dm^{-3} and beyond m = 25 g dm^{-3}, the removal remains almost unaffected by the BFA dosage. At m < 25 g dm^{-3}, the adsorbent surface becomes saturated with Py and the residual concentration in the solution is large. For m > 25 g dm^{-3}, the incremental Py removal becomes very low as the surface Py concentration and the solution of Py concentration come to equilibrium with each other. Thus m = 25 g dm^{-3} was chosen as the optimum dose for the removal of Py by BFA. The optimum dose for Py at C_0 = 100 mg dm^{-3} was also found out as 8 g dm^{-3}. Similarly the optimum m for BFA was determined for the other adsorbate-adsorbent systems as well. m = 5 g dm^{-3} for 2Pi, 5 g dm^{-3} for 4Pi and 8 g dm^{-3} for AmPy, for BFA for the C_0 = 100 mg dm^{-3}. The optimum dosage of RHA for the removal of Py (C_0 = 300 mg dm^{-3}) and for the removal of 2Pi, 4Pi and AmPy (C_0 = 100 mg dm^{-3}) was obtained as m = 50 g dm^{-3} (30 g dm^{-3} for Py C_0 = 100 mg dm^{-3}), 20 g dm^{-3}, 20 g dm^{-3} and 30 g dm^{-3}, respectively. The optimum dosage of GAC for the removal of Py (C_0 = 300 mg dm^{-3}), 2-Pi, 4Pi and AmPy (C_0 = 100 mg dm^{-3}) was obtained as m = 30 g dm^{-3} (20 g dm^{-3} for Py C_0 = 100 mg dm^{-3}), 10 g dm^{-3}, 10 g dm^{-3} and 20 g dm^{-3}, respectively.

6.3.2 Effect of Initial pH (pH_0)

Py behaves like a base (pKa ~ 5.23) [Gilchrist, 1985] and the transition of Py to PyH$^+$ is pH-dependent, with a maximum amount of PyH$^+$ occurring in the pH range of 4.5-6.0 (around the pKa value). The solution pH affects the surface charge of the adsorbents and, therefore, the adsorption process through dissociation of functional groups, viz. surface oxygen complexes of acid character such as carboxyl and phenolic groups or of basic character such as pyrones or chromens, on the active sites of the adsorbent [Carlos, 2004]. Py molecule is stable over a wide range of pH$_0$ [Zhu et al., 1988; Lataye et al., 2006, 2007d].

BFA and RHAcontain oxides of aluminium, calcium and silicon on the surface. The presence of these metal oxides in contact with water leads to the development of surface charge according to the pH of the solution:

$$H_2O \rightleftharpoons H^+ + OH^- \tag{a}$$

$$M + OH^- \rightarrow MOH \tag{b}$$

$$M\text{-}OH + H^+ \rightarrow M\text{-}OH_2^+ \tag{c}$$

$$M\text{-}OH + OH^- \rightarrow M\text{-}O^- + H_2O \tag{d}$$

where, M stands for Al, Ca and Si. The chemical interaction of Py with adsorbents may be explained on the basis of the explanation put forth by Weber [1966] and Zhu *et al.* [1988]:

$$PyD + H^+ \rightleftharpoons PyDH^+ \tag{e}$$

$$PyD + S \rightleftharpoons PyD\text{-}S \tag{f}$$

$$PyDH^+ + M^+\text{-}S \rightleftharpoons PyDH\text{-}S + M^+ \tag{g}$$

$$H^+ + PyDH^+\text{-}S \rightleftharpoons H^+\text{-}S + PyDH^+ \tag{h}$$

$$H^+ + S \rightleftharpoons H^+\text{-}S \tag{i}$$

$$PyD\text{-}H^+\text{-}S \rightleftharpoons PyDH^+\text{-}S \tag{j}$$
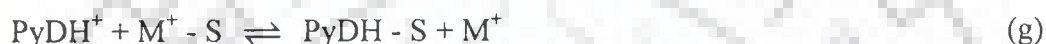
Here in the above equations PyD represents Py and its derivatives and S represents the solid adsorbents, respectively. As Niu and Conway [2002] have shown the mol % of $PyDH^+$ in the solution would be < 5 mol % at pH > 6.5. Since PyD contains nitrogen atom, which is more electronegative than in SP^2 hybridized C, PyD gets preferentially adsorbed on a positively charged surface [Niu and Conway, 2002].

At low pH (pH $\leq$ (pKa = 5.2)), the PyD is converted to $PyDH^+$ through protonation via reaction Eq. (e) resulting in the low adsorption of protonated PyD on the positively charged adsorbent surface as shown by reaction Eq. (g). At higher pH (pH $\geq$ (pKa = 5.2)), π-π dispersion interactions along with electrostatic interactions become important and PyD molecule is adsorbed onto S [Radovic et al., 1997 2000]. It may, however, be noted that BFA, RHA and GAC have a maximum affinity to PyD and $PyDH^+$ at pH ~ 6. $PyDH^+$ adsorption is at a lower rate than that of PyD molecules. Therefore, the dominant sorption reaction (at $pH_0 \approx 6$) is perhaps given by Eq. (f). Other reactions given by Eq. (e), (g-j) play insignificant role in the overall adsorption of PyD.
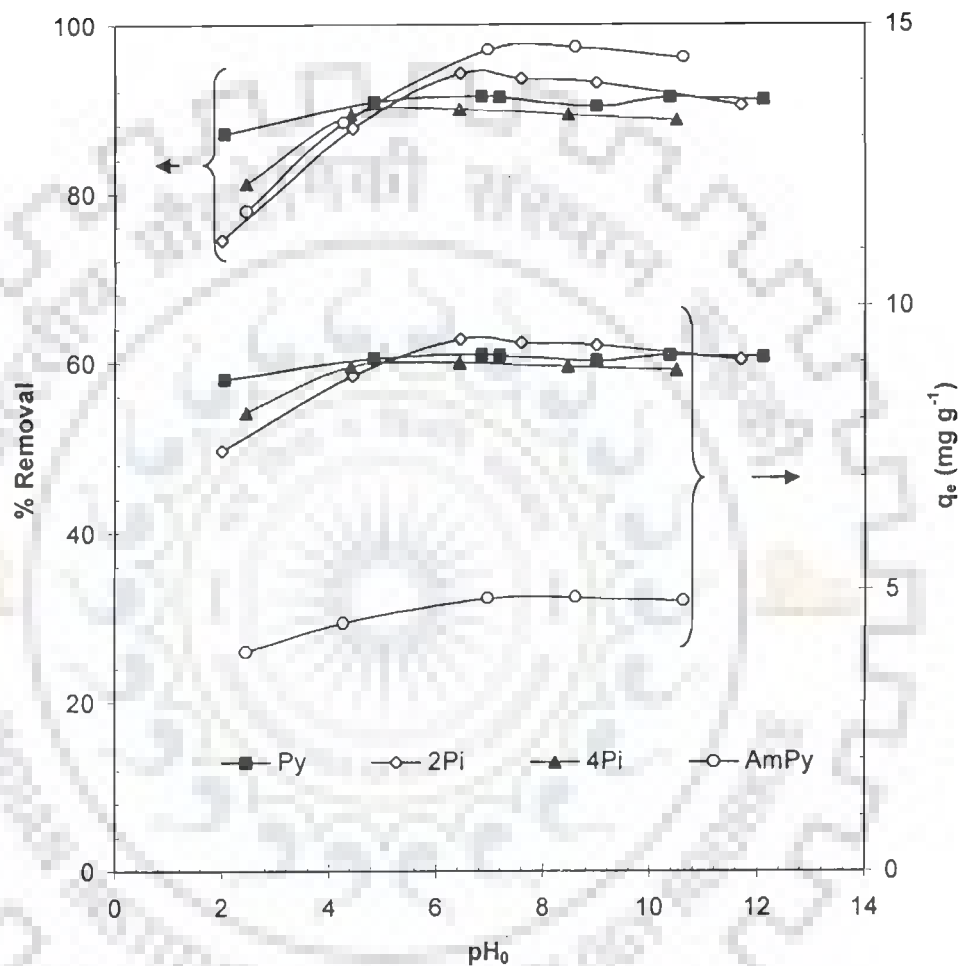
Fig. 6.3.4. Effect of initial pH on the equilibrium uptake and % removal of Py
(C_0 = 300 mg dm^{-3}, m = 25 g dm^{-3}), 2Pi, 4Pi (C_0 = 100 mg dm^{-3},
m = 5 g dm^{-3}) and AmPy (C_0 = 100 mg dm^{-3}, m = 8 g dm^{-3}) (T = 303 K,
t = 5 h) by BFA.
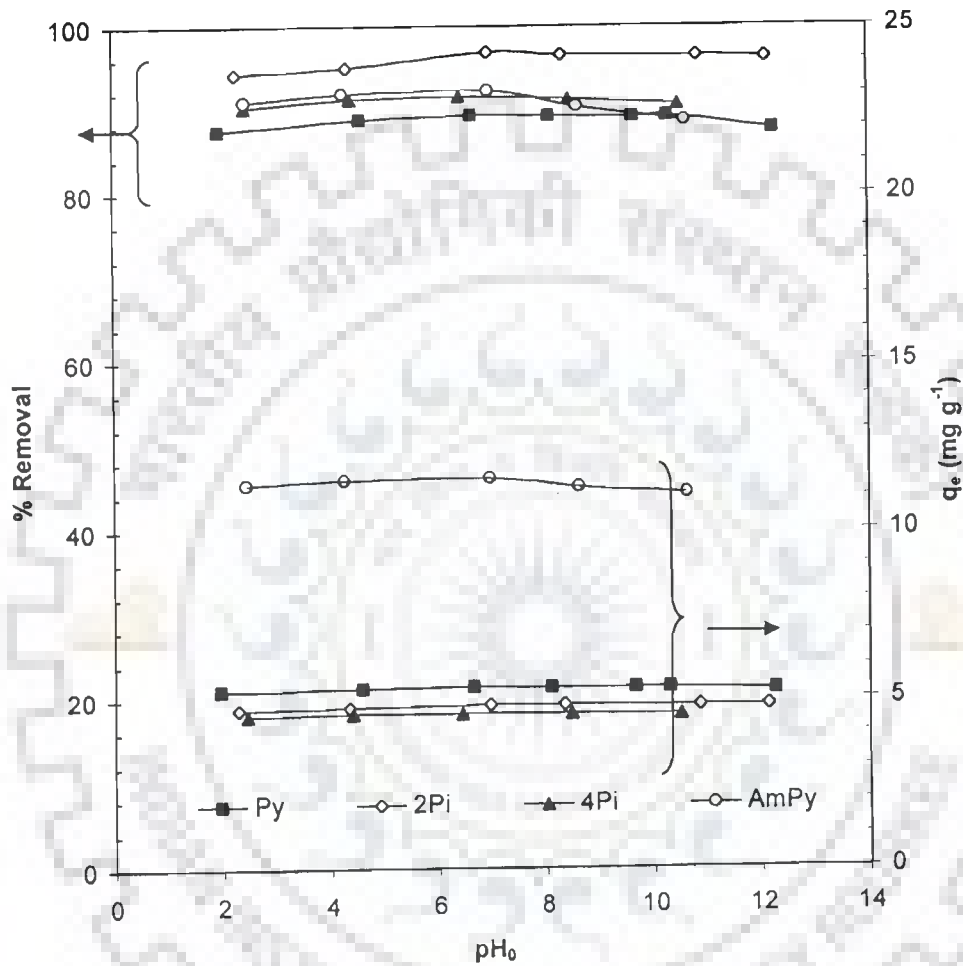
Fig. 6.3.5. Effect of initial *pH* on the equilibrium uptake and % removal of Py (C_0 = 300 mg dm^{-3}, m = 50 g dm^{-3}), 2Pi, 4Pi (C_0 = 100 mg dm^{-3}, m = 20 g dm^{-3}) and AmPy(C_0 = 100 mg dm^{-3}, m = 30 g dm^{-3}) (T = 303K, t = 5 h) by RHA.
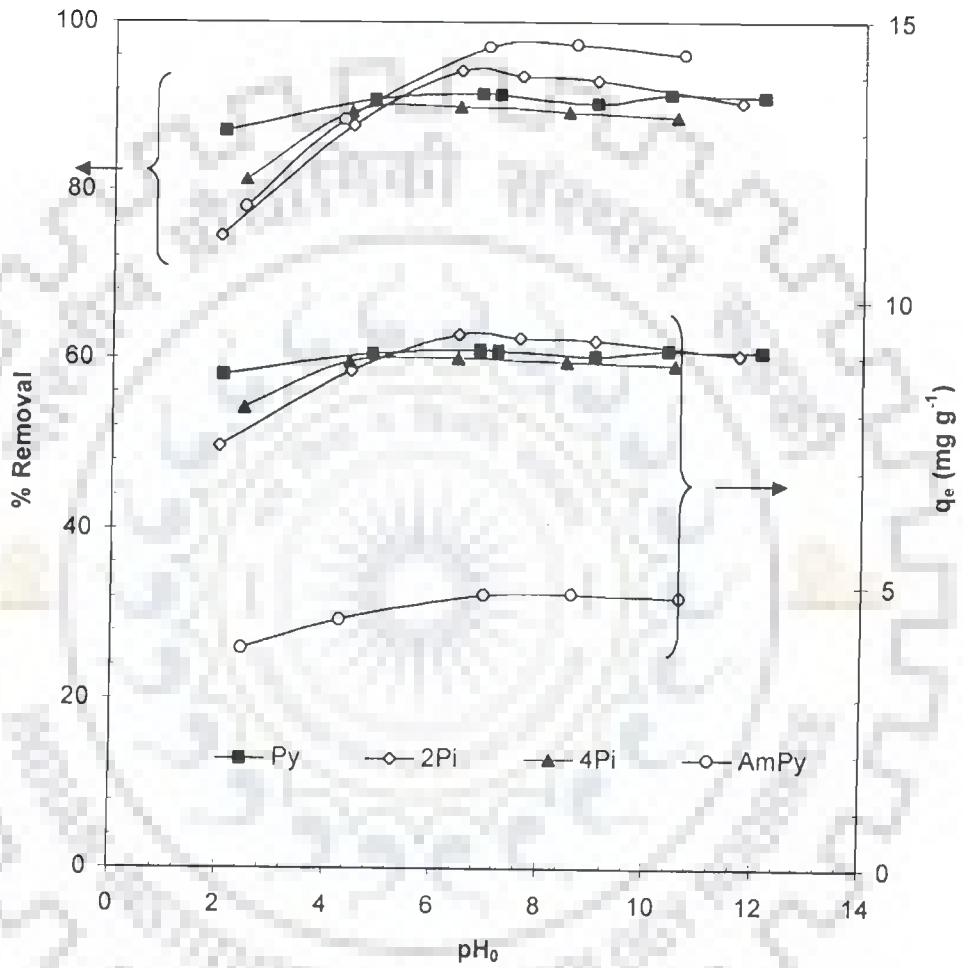
Fig. 6.3.6. Effect of initial pH on the equilibrium uptake and % removal of Py
(C_0 = 300 mg dm^{-3}, m = 30 g dm^{-3}), 2Pi, 4Pi (C_0 = 100 mg dm^{-3},
m = 10 g dm^{-3}) and AmPy (C_0 = 100 mg dm^{-3}, m = 20 g dm^{-3})
(T= 303 K, t = 5 h) by GAC.

Effect of pH_0 on the removal of Py, 2Pi, 4Pi and AmPy by BFA, RHA and GAC is shown in Figs. 6.3.4 – 6.3.6. The effect of pH_0 was studied on the removal of Py and its derivatives with the solutions of different adsorbates, viz. for Py: $C_0 = 300$ mg dm^{-3}, $m = 25$ g dm^{-3}; for 2Pi: $C_0 = 100$ mg dm^{-3}, m = 5 g dm^{-3}; for 4Pi: $C_0 = 100$ mg dm^{-3}, $m = 5$ g dm^{-3} and for AmPy: $C_0 = 100$ mg dm^{-3}, $m = 8$ g dm^{-3}. The sorbates solutions were kept at 30 °C for 5 h, after which the absorbance of the centrifuged supernatant was determined at $\lambda_{max} = 256$ nm, 262, 254 and 290, respectively for Py, 2Pi, 4Pi and AmPy and the residual concentration of the sorbates in the supernatant was found out. A maximum adsorption was found to occur at the natural pH_0 (~6 - 8). However, as the pH_0 decreased   ($pH_0 < 6$), the adsorption was found to decrease.

6.3.3   Effect of Initial Concentration (C_0)

The effect of C_0 on the adsorption of Py, 2Pi, 4Pi and AmPy is shown in Figs. 6.3.7– 6.3.9. The removal of Py and its derivatives decreased with an increase in C_0, although the total amount of adsorbate adsorbed per unit mass of adsorbent, i.e. q increased with an increase in C_0. The increase in adsorption uptake with an increase in C_0 is attributed to an increase in the driving force for adsorption and a decrease in resistance to the uptake of adsorbate by the adsorbents from the solution [Mall et al., 2005a].

6.3.4   Effect of Contact Time

The contact time, t between adsorbate and adsorbents is an important factor in the adsorption process. A rapid uptake of the adsorbate and the establishment of equilibrium in a short period signifies the efficacy of the adsorbent for its use in the wastewater treatment. In physical adsorption, most of the adsorbate species are adsorbed within a short interval of contact time. However, strong chemical binding of the adsorbate with the adsorbent requires a longer contact time for the attainment of equilibrium [Tien, 1994]. The effect of t on the removal of Py ($C_0 = 300$ mg dm^{-3} $m = 25$ g dm^{-3}), 2Pi, 4Pi ($C_0 = 100$ mg dm^{-3}, $m = 5$ g dm^{-3}) and AmPy ($C_0 = 100$ mg dm^{-3}, $m = 8$ g dm^{-3}) by BFA, RHA and GAC at $T = 303$ K, and $pH_0 = 6 - 7$ is shown in Figs. 6.3.10 - 13.3.12.
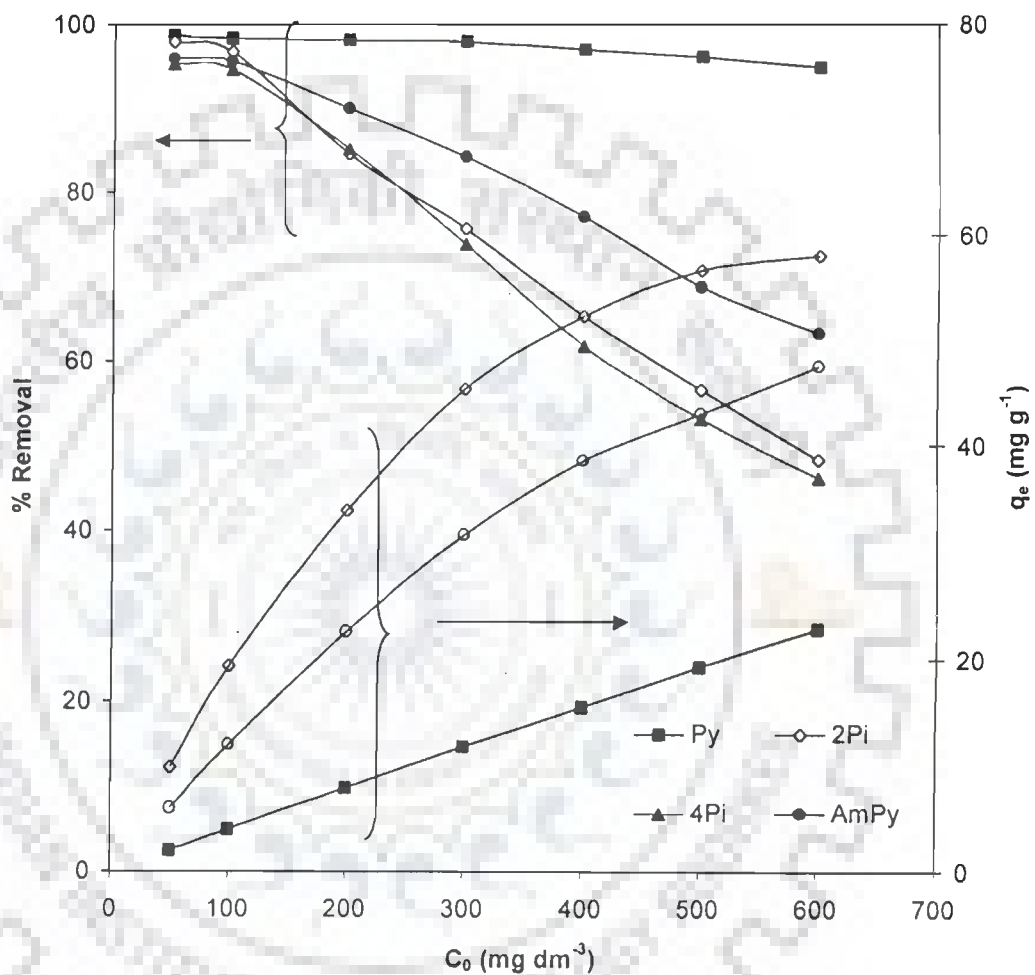
Fig. 6.3.7. Effect of initial concentration on the removal of Py (m = 25 g dm^{-3}), 2Pi, 4Pi (m = 10 g dm^{-3}) and AmPy (m = 20 g dm^{-3}) by BFA, T= 303 K, pH = Natural (6-7)
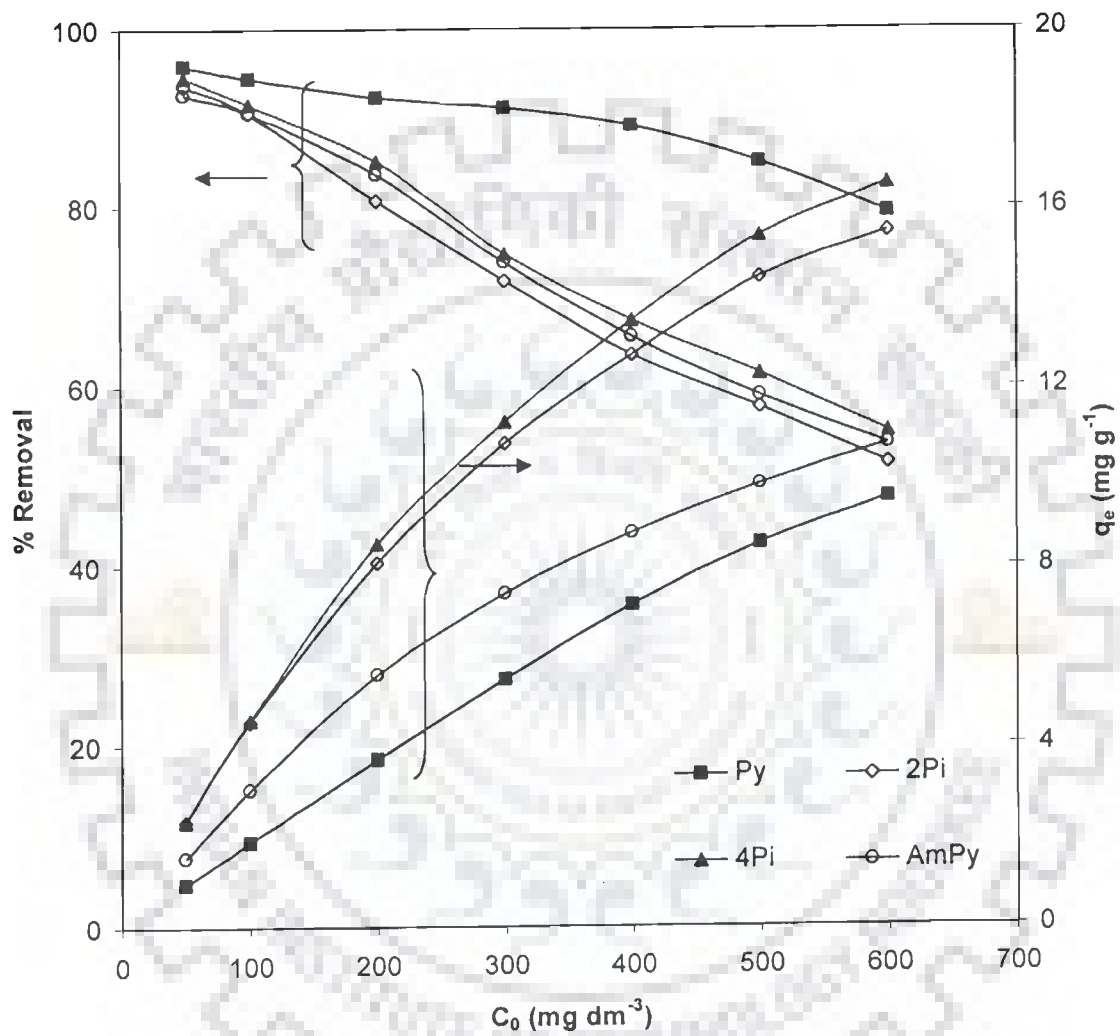
Fig. 6.3.8. Effect of initial concentration on the removal of Py (m = 50 g dm^{-3}), 2Pi, 4Pi (m = 20 g dm^{-3}) and AmPy (m = 30 g dm^{-3}), (T= 303 K, pH = Natural (6-7))by RHA.
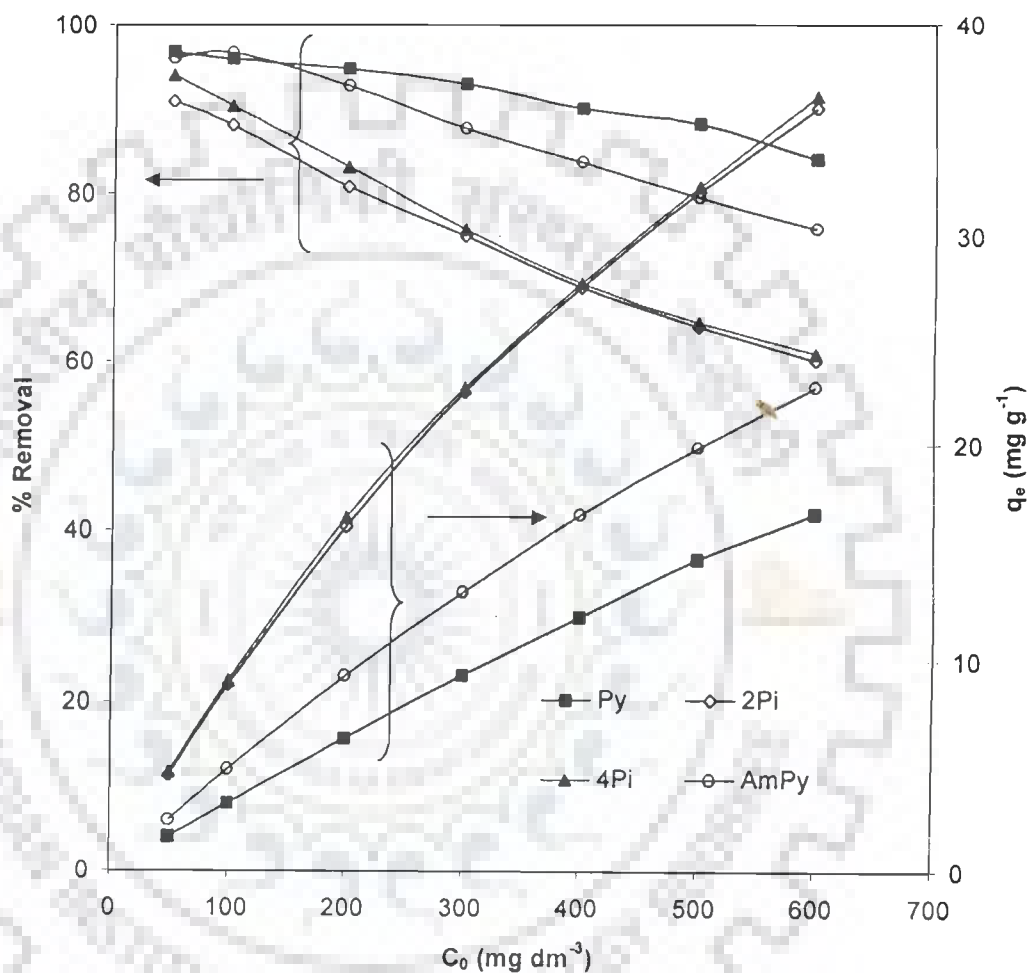
Fig. 6.3.9. Effect of initial concentration on the removal of Py (m = 30 g dm^{-3}), 2Pi, 4Pi (m = 10 g dm^{-3}) and AmPy (m = 20 g dm^{-3}), (T= 303 K, pH = Natural (6-7)) by GAC.

The figures show rapid adsorption of Py and its derivatives in the first 15 min, and thereafter, the adsorption rate decreased gradually. For BFA-Py system the adsorptive uptake is almost instantaneous: About 86.5% of Py from an aqueous solution of C_0 = 300 mg dm^{-3} is adsorbed in one min of contact, thereafter, the Py removal is low. The residual Py concentration is 6.78 % after 1 h, ~3.37% after 6 h, 3.35% after 24 h and 3.13% after 72 h contact time. Since the difference in Py removal at 6 h and 72 h is less than 0.25% of the 72 h removal, a steady-state approximation was assumed and a quasi-equilibrium situation was accepted at t = 6 h and further experiments were conducted under vigorous shaking conditions, at t = 6 h only.

Similar trends were observed for all other adsorbate-adsorbent systems also, i.e. for Pi and Py with BFA, RHA and GAC. The rate of removal is found to be very rapid during the initial 15 min, about > 90% removal was observed in all the systems in 1 h, and, thereafter, the rate of removal decreased. It is found that the adsorptive removal ceases after 5 h of contact with all the adsorbents. Besides, the adsorbates are adsorbed into the mesopores that get almost saturated with adsorbate during the initial stage of adsorption. Thereafter, the adsorbates have to traverse farther and deeper into the pores encountering much larger resistance. This is obvious from the fact that a large number of vacant surface sites are available for adsorption during the initial stage, and after a lapse of time, the remaining vacant surface sites are difficult to be occupied due to repulsive forces between the solute molecules on the solid surface and in the bulk solution phase. This results in the slowing down of the adsorption during the later period of adsorption. The residual concentrations at 5 h contact time were found to be higher by a maximum of ~1% than those obtained after 12 h contact time. Therefore, after 5 h contact time, a steady state approximation was assumed and a quasi-equilibrium situation was accepted for Pi and AmPy with, RHA and GAC. Accordingly all the batch experiments were conducted with a contact time of 5 h under vigorous shaking conditions for RHA and GAC and 6 h for BFA. Figs. 6.3.10 - 6.3.12 present the plots of the time-course of Py, 2Pi, 4Pi and AmPy onto BFA, RHA and GAC.
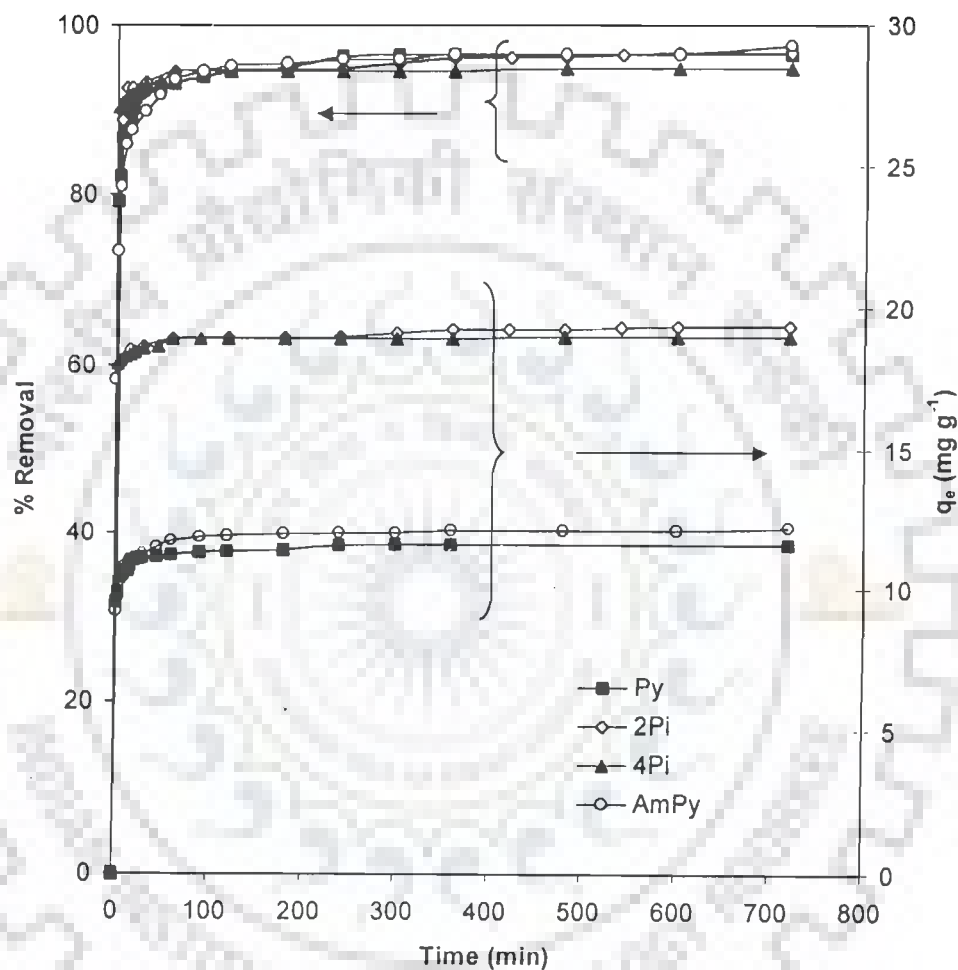
Fig.6.3.10 Effect of contact time on the removal of Py ($C_0 = 300$ mg dm^{-3} m = 25 g dm^{-3}), 2Pi, 4Pi ($C_0 = 100$ mg dm^{-3}, m = 5 g dm^{-3}) and AmPy ($C_0 = 100$ mg dm^{-3}, m = 8 g dm^{-3}) (T= 303 K, pH = (6-7)) by BFA.
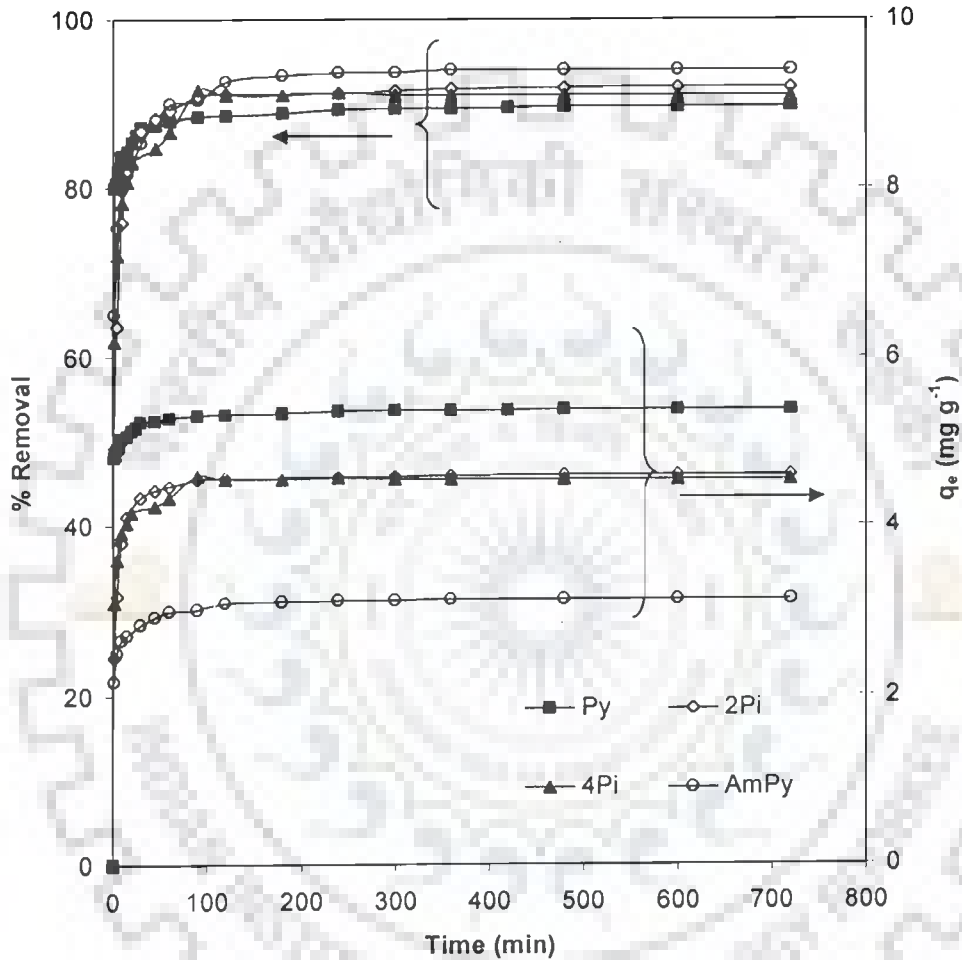
Fig. 6.3.11 Effect of contact time on the removal of Py ($C_0 = 300$ mg dm^{-3} m = 50 g dm^{-3}), 2Pi, 4Pi ($C_0 = 100$ mg dm^{-3}, m = 20 g dm^{-3}) and AmPy ($C_0 = 100$ mg dm^{-3}, m = 30 g dm^{-3}) (T= 303 K, pH = (6-7)) by RHA.
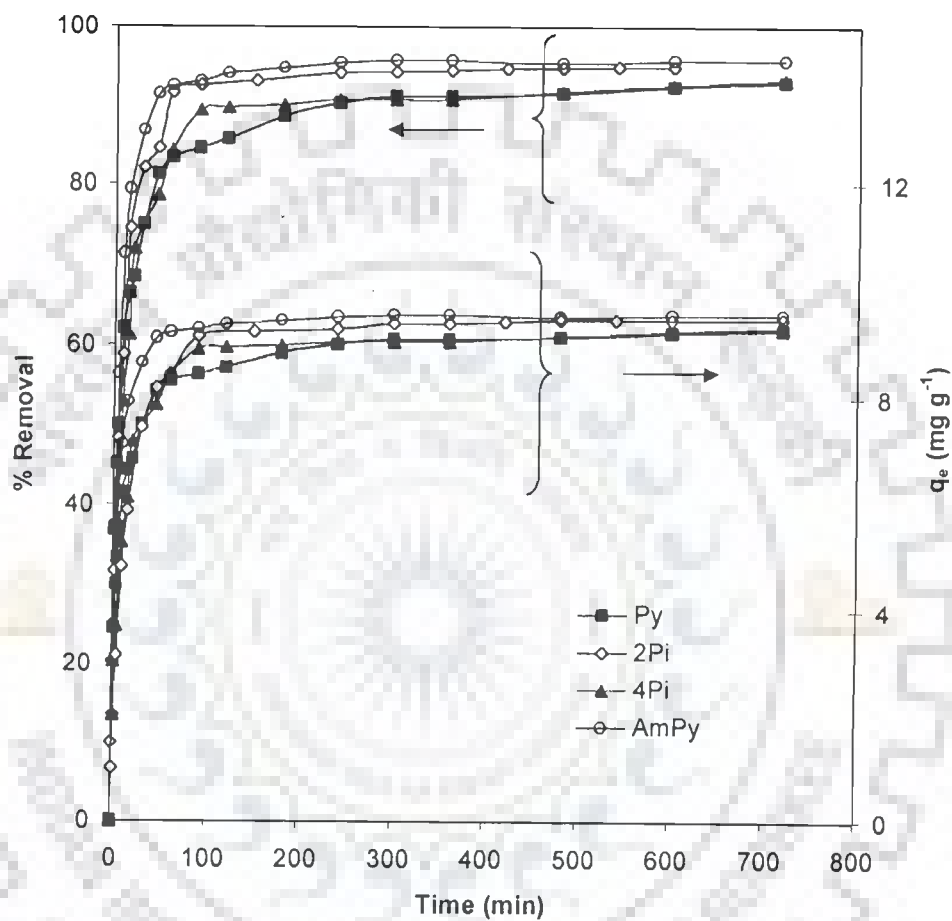
Fig. 6.3.12 **Effect of contact time on the removal of Py (C_0 = 300 mg dm^{-3} m = 50 g dm^{-3}), 2Pi, 4Pi (C_0 = 100 mg dm^{-3}, m = 10 g dm^{-3}) and AmPy (C_0 = 100 mg dm^{-3}, m = 20 g dm^{-3}) (T= 303 K, pH = (6-7)) by GAC.**

6.3.5 Effect of Temperature

Temperature has a pronounced effect on the adsorption capacity of the adsorbents. Figs. 6.3.13 - 6.3.15 show the experimental adsorption isotherms, q_e versus C_e plots for the adsorption of Py onto BFA, RHA, and GAC, respectively, at different temperatures ranging from 293-323 K. It is found that the sorption of Py increases with an increase in temperature. Similar trends were observed for the sorption of 2Pi, 4Pi and AmPy on all the adsorbents. See Appendix A for the adsorption isotherm plots for Pi and AmPy and the adsorbents – BFA, RHA and GAC.

Since sorption is an exothermic process, it would be expected that an increase in temperature would result in a decrease in the sorption capacity of the adsorbent. However, if the adsorption process is controlled by the diffusion process (intraparticle transport-pore diffusion), the sorption capacity will increase with an increase in temperature due to endothermicity of the diffusion process. This results in the enhancement in the sorptive capacity of the adsorbents. The increase in adsorption capacity with temperature indicates that the mobility of the Py and its derivatives increases with a rise in temperature. It can also be said that reaction of adsorbates and surface functional groups is enhanced by increased temperature reaction. This trend suggests that a chemisorption reaction or an activated adsorption between adsorbates and functional groups on adsorbent surface takes place with Py and its derivatives by all the adsorbents. Increase in temperature will also increase the amount adsorbed at equilibrium for a chemisorption reaction. There are various possible interaction effects between different species in solution, and in particular, potential interactions on the surface depending on the adsorption mechanism. Factors that affect the preference for an adsorbate may be related to the characteristics of the binding sites (e.g. functional groups, structure, surface properties, etc.), the properties of the adsorbates (e.g. concentration, ionic size, ionic weight, ionic charge, molecular structure, ionic nature or standard redox potential, etc.) and the solution chemistry (e.g. pH, ionic strength, etc.). The micro- and meso-pore size distribution of an adsorbent and the shape of the pores coupled with the ionic size of the adsorbate play important roles in the sorption uptake of the adsorbate. The efficacy of various adsorbents for the removal of Py and its derivatives and the q_e values for a particular C_0 were found to be in order of 2Pi > 4Pi > Py > AmPy.
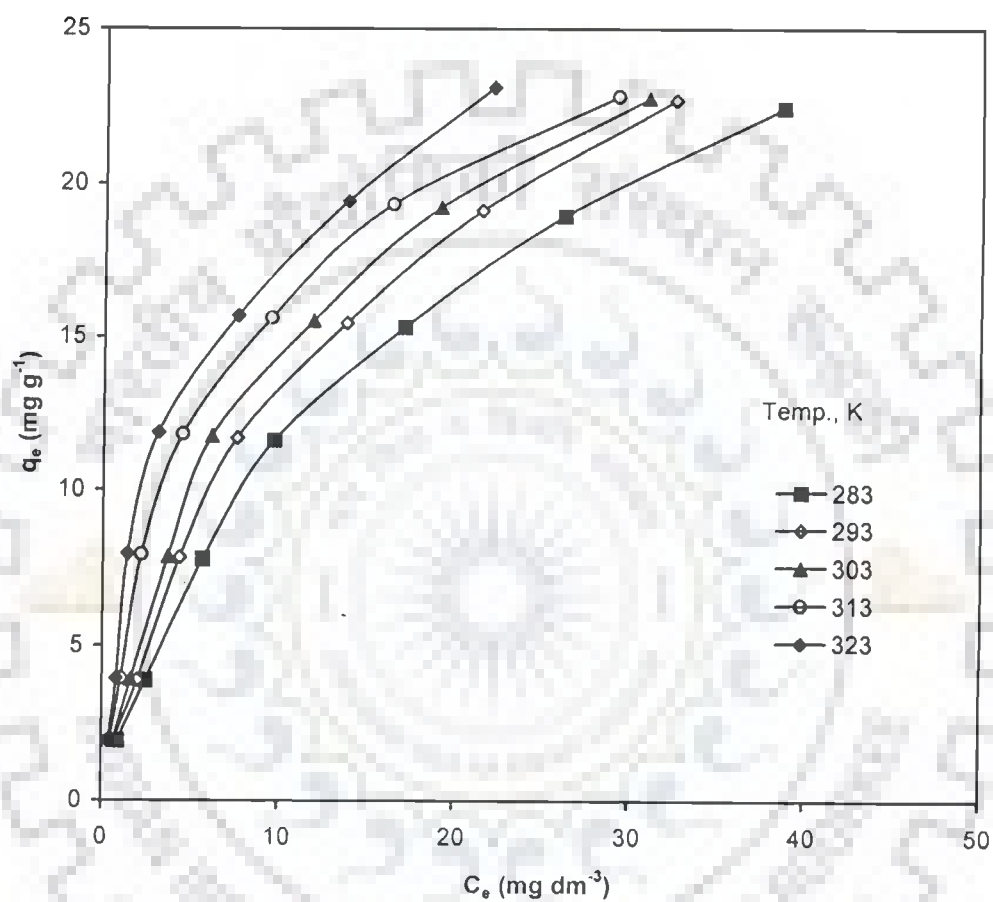
Fig. 6.3.13. Equilibrium adsorption isotherms at different temperatures for adsorption of Py onto BFA. ($pH_0 = 6.0$, $C_0 = 50\text{-}600$ mg dm^{-3}, $m = 25$ g dm^{-3}).
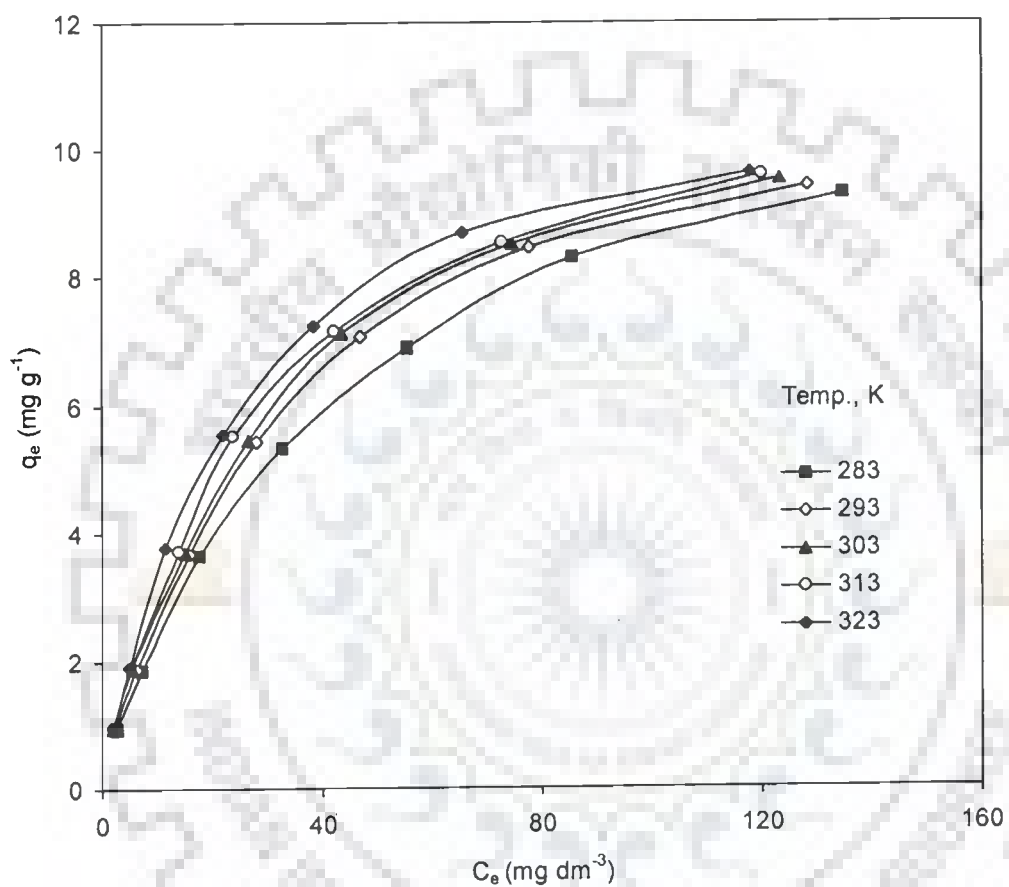
Fig. 6.3.14. Equilibrium adsorption isotherms at different temperatures for adsorption of Py onto RHA. (pH_0 = 6.0, C_0 = 50-600 mg dm^{-3}, m = 50 g dm^{-3})
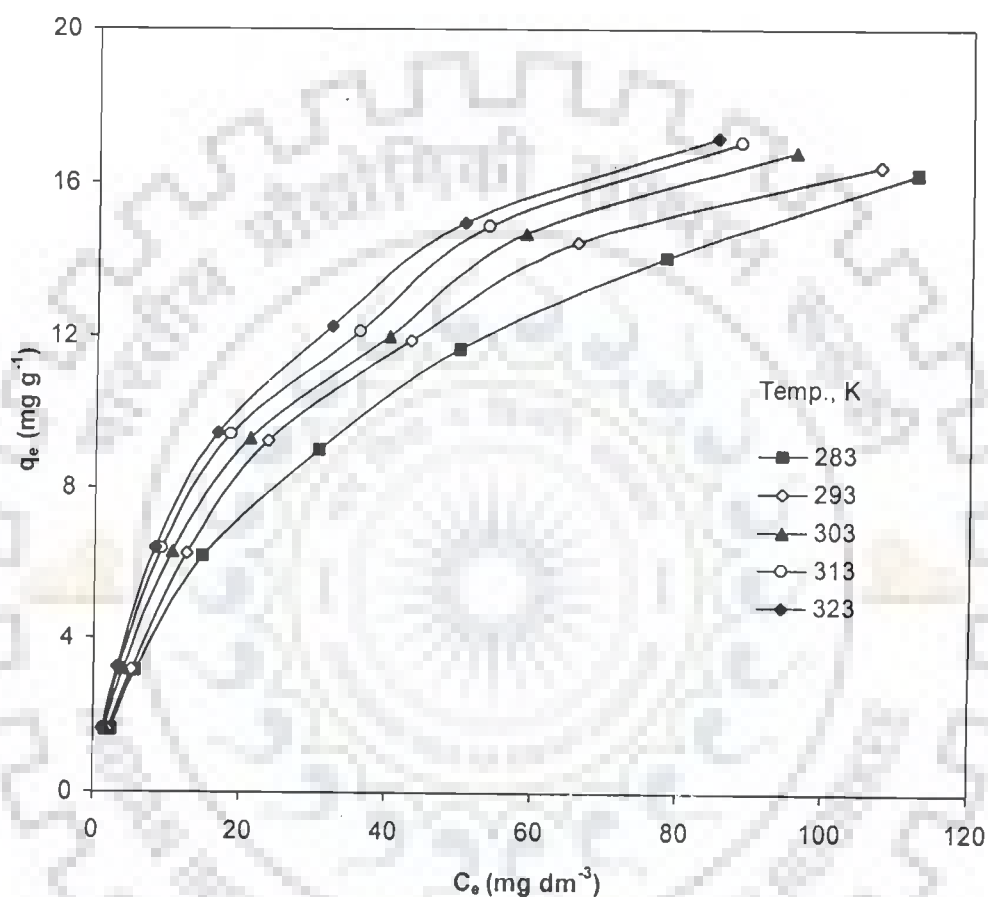
Fig. 6.3.15. Equilibrium adsorption isotherms at different temperatures for adsorption of Py onto GAC. ($pH_0 = 6.0$, $C_0 = 50\text{-}600$ mg dm^{-3}, $m = 30$ g dm^{-3}).

6.3.6 Adsorption Kinetic Study

Pseudo-first-order, pseudo-second-order and intraparticle diffusion models are the frequently used models, for the kinetic study. In addition to these models, the other kinetic models viz. Elovich, Bangham and modified Freundlich have been used in the present study to investigate the adsorption process of Py, 2Pi, 4Pi and AmPy onto BFA, RHA and GAC. The effect of significant parameters on the kinetics viz. adsorbent dose, initial concentration, temperature and agitation speed were studied for all the adsorbent-adsorbate system.

6.3.6.1 Pseudo-first-order model

In Chapter III, a simple sorption kinetics has been presented by Eq. (3.2.3), assuming a non-dissociative molecular adsorption of adsorbates onto adsorbents. It is represented as:

$$\log(q_e - q_t) = \log q_e - \frac{k_f}{2.303} t \qquad (6.3.1)$$

This equation is, however, valid only for the initial period of adsorption. Various investigators have erroneously fitted this equation to the adsorbate uptake data for later periods, ignoring the data of the initial period for the model fitting. The values of the pseudo-first-order adsorption rate constant (k_f) (Tables 6.3.1 - 6.3.3) were determined from Eq. (6.3.1) by plotting $\log(q_e - q_t)$ against t for Py, 2Pi, 4Pi and AmPy onto BFA, RHA and GAC. Experimental results did not follow first-order kinetics given by Eq. (6.3.1) as there was difference in two important aspects:(i) $k_f(q_e - q_t)$ does not represent the number of available sites, and (ii) $\log q_e$ was not equal to the intercept of the plot of $\log(q_e - q_t)$ against t.

6.3.6.2 Pseudo-second-order model

The pseudo-second-order model can be represented in the following form (Ho and McKay, 1999):

$$q_t = \frac{k_s q_e^2 t}{1 + k_s q_e t}$$

(6.3.2)

This equation has been solved by using non linear technique using Microsoft Excel's solver-add-in function constants k_S and q_e were obtained. Fig. 6.3.16 shows a representative plot of q_t versus t (experimental and calculated) for adsorption of Py and its derivatives on BFA (for Py $C_0 = 300$ mg dm^{-3} and 2Pi, 4Pi and AmPy $C_0 = 100$ mg dm^{-3} at 30 ^{0}C and at pH_0 6.0) at their respective dosage. The best-fit values of h, q_e and k_S along with the correlation coefficients for the pseudo-first-order and pseudo-second-order models for all the adsorbate-adsorbent systems are given in Tables 6.3.1-6.3.3. The $q_{e,exp}$ and the $q_{e,cal}$ values for the pseudo-first-order model and pseudo-second-order models are also shown in Tables 6.3.1-6.3.3. The $q_{e,exp}$ and the $q_{e,cal}$ values from the pseudo-second-order kinetic model are very close to each other. The calculated correlation coefficients are equal to unity for pseudo-second-order kinetics than that for the pseudo first-order kinetic model. Therefore, the sorption can be approximated more appropriately by pseudo-second-order kinetic model than the other kinetic models for the adsorption of, 2Pi, 4Pi and AmPy onto BFA, RHA and GAC.
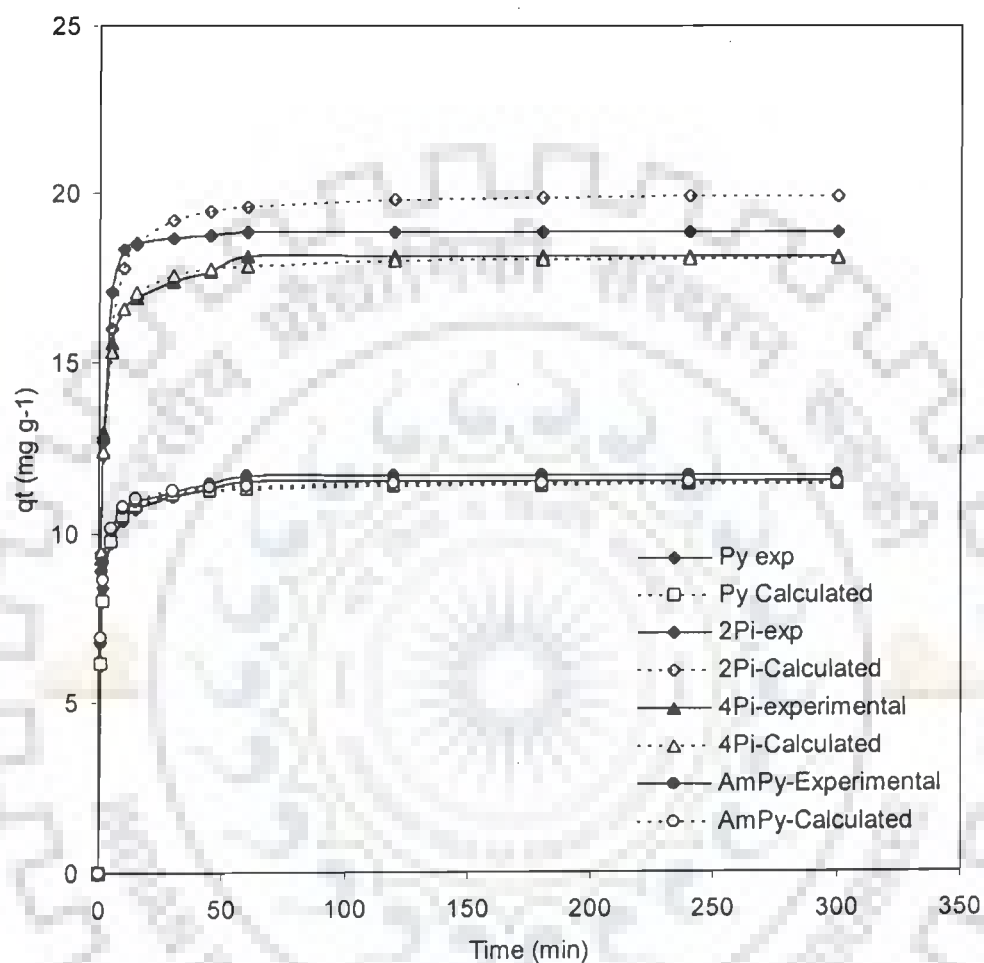
Fig. 6.3.16. Time versus q_t (**Experimental and Calculated**) plot for the removal of Py, 2Pi, 4Pi and AmPy by BFA. $T = 303$ K, $C_0 = 100$ mg/l, $m = 8, 5, 5,$ and 10 g dm^{-3} respectively.

Table 6.3.1. Kinetic parameters for the removal of Py, 2Pi, 4Pi and AmPy by BFA a) Effect of Adsorbent Dose.

Models	Py			2Pi			4Pi			AmPy		
Pseudo-first-order												
Constants	Dose (g dm^{-3})			Dose (g dm^{-3})			Dose (g dm^{-3})			Dose (g dm^{-3})		
	6	8	10	2	5	10	2	5	10	6	8	10
$q_{e,exp}$ (mg g^{-1})	15	11.64	9.5	36.5	18.9	9.8	32.5	18.2	9.4	15.3	11.8	9.7
$q_{e,calc}$ (mg g^{-1})	7.39	3.46	1.97	0.18	0.22	0.16	0.10	0.12	0.10	0.12	0.12	0.10
k_f (min^{-1})	0.22	0.16	0.15	18.45	3.60	1.44	15.43	4.57	0.87	4.73	2.68	1.73
R^2	0.93	0.94	0.91	0.94	0.78	0.73	0.90	0.80	0.52	0.85	0.83	0.78
Pseudo-second-order												
$q_{e,calc}$ (mg g^{-1})	14.98	11.48	9.45	35.98	20.02	10.05	29.82	18.14	9.60	15.06	11.53	9.38
h (mg g^{-1} min^{-1})	11.22	13.57	16.07	12.95	16.03	15.15	8.89	19.74	27.65	13.61	17.28	22.00
k_s (g mg^{-1} min^{-1})	0.05	0.10	0.18	0.01	0.04	0.15	0.01	0.06	0.30	0.06	0.13	0.25
R^2	1.00	1.00	1.00	1.00	1.00	1.00	1.00	1.00	1.00	1.00	1.00	1.00
Intra particle diffusion												
k_{int1} (mg g^{-1} min$^{-1/2}$)	4.01	2.75	2.03	8.71	6.08	2.53	9.57	4.85	1.60	4.08	2.51	1.68
C_1 (mg g^{-1})	2.89	3.81	4.15	4.11	3.66	3.68	1.77	5.11	5.64	3.60	4.79	5.14
R^2	0.91	0.89	0.80	0.98	0.99	0.88	0.95	0.92	0.75	0.84	0.82	0.86
k_{int2} (mg g^{-1} min$^{-1/2}$)	0.44	0.24	0.13	1.26	0.10	0.07	1.62	0.32	0.01	0.37	0.20	0.15
C_2 (mg g^{-1})	11.71	9.72	8.43	27.12	18.09	9.22	19.66	15.63	9.23	12.37	10.14	8.45
R^2	0.96	0.98	0.98	0.90	0.95	0.98	0.99	0.99	0.85	0.99	1.00	0.99
Elovich												
β (g mg^{-1})	0.51	0.84	1.31	0.16	0.46	1.24	0.21	0.53	2.07	0.56	0.97	1.57
α (mg g^{-1} min^{-1})	77.84	488.11	4780.04	57.31	455.91	4593.36	65.11	662.72	4467153.27	216.13	2082.99	53385.02
t_0 (min)	0.03	0.00	0.00	0.11	0.00	0.00	0.07	0.00	0.00	0.01	0.00	0.00
R^2	0.94	0.90	0.82	0.96	0.81	0.75	0.96	0.87	0.66	0.89	0.86	0.85
Bangham												
α	0.36	0.30	0.26	0.37	0.35	0.31	0.32	0.29	0.17	0.33	0.27	4.25
k_0 (mg^{-1}dm^{-3})	11.37	11.85	10.70	18.88	19.39	13.48	17.05	18.32	17.39	13.33	13.90	14.27
R^2	0.95	0.94	0.89	0.95	0.85	0.86	0.92	0.90	0.73	0.91	0.92	0.93
Modified Freundlich												
m	5.35	7.47	10.02	9.75	6.61	3.85	4.15	7.22	16.95	6.17	9.00	12.77
k (dm^{3}g^{-1} min^{-1})	0.08	0.07	0.07	0.07	0.11	0.14	0.13	0.11	0.08	0.08	0.08	0.07
R^2	0.87	0.84	0.77	0.71	0.77	0.92	0.89	0.81	0.64	0.81	0.81	0.82

Table 6.3.2. Kinetic parameters for the removal of Py, 2Pi, 4Pi and AmPy by BFA b) Effect of Initial Concentration.

Models	Py			2Pi			4Pi			AmPy		
Pseudo-first-order												
Constants	Concentration (mg dm^{-3})			Concentration (mg dm^{-3})			Concentration (mg dm^{-3})			Concentration (mg dm^{-3})		
	50	100	200	50	100	200	50	100	200	50	100	200
$q_{e,exp}$ (mg g^{-1})	6.02	11.6	20.4	9.73	18.9	33.4	9.3	18.2	31.9	5.95	11.8	22.4
$q_{e,calc}$ (mg g^{-1})	2.39	4.97	10.75	0.13	0.18	0.14	0.12	0.12	0.15	0.12	0.12	0.13
k_f (min^{-1})	0.23	0.25	0.26	1.83	3.59	10.36	2.13	4.57	10.67	1.17	2.69	6.28
R^2	0.87	0.84	0.80	0.68	0.71	0.90	0.76	0.80	0.90	0.83	0.83	0.89
Pseudo-second-order												
$q_{e,calc}$ (mg g^{-1})	5.89	11.48	19.84	10.06	20.02	31.70	9.20	18.14	31.17	5.83	11.53	21.63
h (mg g^{-1} min^{-1})	8.67	13.18	23.62	12.14	16.03	40.20	12.70	19.74	29.15	12.41	17.28	29.01
k_s (g mg^{-1} min^{-1})	0.25	0.10	0.06	0.12	0.04	0.04	0.15	0.06	0.03	0.37	0.13	0.06
R^2	1.00	1.00	1.00	1.00	1.00	1.00	1.00	1.00	1.00	1.00	1.00	1.00
Intra particle diffusion												
k_{int1} (mg g^{-1} min$^{-1/2}$)	1.10	2.75	4.05	2.77	6.08	6.08	2.14	4.85	7.36	0.94	2.51	4.51
C_1 (mg g^{-1})	2.61	3.81	7.88	2.81	3.66	12.64	3.37	5.11	8.73	3.20	4.79	8.55
R^2	0.91	0.89	0.84	0.98	0.99	0.95	0.97	0.92	0.96	0.86	0.82	0.93
k_{int2} (mg g^{-1} min$^{-1/2}$)	0.13	0.24	0.54	0.08	0.10	0.76	0.13	0.32	0.72	0.07	0.20	0.47
C_2 (mg g^{-1})	5.00	9.72	16.23	9.12	18.09	27.46	8.24	15.63	26.41	5.36	10.14	18.75
R^2	0.96	0.98	0.98	0.96	0.95	0.99	0.99	0.99	0.98	0.91	1.00	0.98
Elovich												
β (g mg^{-1})	0.51	0.84	1.31	1.04	0.46	0.28	1.13	0.53	0.26	2.29	0.97	0.44
α (mg g^{-1} min^{-1})	77.84	488.11	4780.04	719.20	455.24	807.10	829.41	663.77	340.38	8985.96	2082.99	1050.85
t_0 (min)	0.03	0.00	0.00	0.00	0.00	0.00	0.00	0.00	0.01	0.00	0.00	0.00
R^2	0.94	0.90	0.93	0.81	0.81	0.96	0.88	0.87	0.94	0.90	0.86	0.94
Bangham												
α	0.36	0.30	0.26	0.35	0.35	0.26	0.28	0.29	0.28	0.25	0.27	0.27
k_0 (mg^{-1} dm^{-3})	0.00	0.00	0.00	22.65	19.39	15.36	20.86	18.32	13.09	16.56	13.90	11.43
R^2	0.99	0.94	0.93	0.89	0.85	0.96	0.92	0.90	0.94	0.95	0.92	0.96
Modified Freundlich												
m	5.35	7.47	10.02	7.89	6.61	7.08	8.31	7.22	6.04	11.47	9.00	7.73
k (dm^3 g^{-1} min^{-1})	0.08	0.07	0.07	0.07	0.11	0.20	0.06	0.11	0.18	0.09	0.08	0.07
R^2	0.91	0.84	0.88	0.78	0.77	0.93	0.84	0.81	0.89	0.86	0.81	0.89

Table 6.3.3. Kinetic parameters for the removal of Py, 2Pi, 4Pi and AmPy by BFA c) Effect of Temperature.

Models	Py			2Pi			4Pi			AmPy		
Pseudo-first-order												
Constants	Temperature, K			Temperature, K			Temperature, K			Temperature, K		
	273	303	313	273	303	313	273	303	313	273	303	313
$q_{e,exp}$ (mg g^{-1})	11.2	11.64	11.9	18.72	18.9	19.22	17.5	18.2	18.6	11.2	11.8	11.93
$q_{e,calc}$ (mg g^{-1})	5.29	4.97	5.38	0.15	0.18	0.19	0.14	0.12	0.13	0.11	0.12	0.15
k_f (min^{-1})	0.25	0.25	0.25	6.66	3.59	3.26	5.24	4.57	3.58	3.81	2.69	2.25
R^2	0.82	0.84	0.82	0.86	0.71	0.75	0.89	0.80	0.76	0.90	0.83	0.89
Pseudo-second-order												
$q_{e,calc}$ (mg g^{-1})	11.10	11.50	11.70	18.60	20.11	19.12	17.00	18.14	'18.83	10.41	11.53	11.78
h (mg g^{-1} min^{-1})	12.32	13.23	15.06	13.84	24.26	12.47	20.23	19.74	24.82	11.92	17.42	18.08
k_s(g mg^{-1} min^{-1})	0.10	0.10	0.11	0.04	0.06	0.03	0.07	0.06	0.07	0.11	0.13	0.20
R^2	1.00	1.00	1.00	1.00	1.00	1.00	1.00	1.00	1.00	1.00	1.00	1.00
Intra particle diffusion												
k_{int1}(mg g^{-1} min$^{-1/2}$)	2.79	2.75	2.79	4.56	6.08	5.59	3.96	4.85	4.61	2.68	2.64	2.04
C_1(mg g^{-1})	3.30	3.81	4.02	4.03	3.66	5.46	5.54	5.11	6.82	2.96	4.47	6.27
R^2	0.89	0.89	0.87	0.99	0.99	0.99	0.97	0.92	0.79	0.96	0.75	0.75
k_{int2} (mg g^{-1} min$^{-1/2}$)	0.24	0.24	0.26	0.41	0.10	0.09	0.38	0.32	0.22	0.34	0.20	0.16
C_2 (mg g^{-1})	9.30	9.72	9.82	15.66	18.09	18.53	14.58	15.63	16.80	8.51	10.14	10.76
R^2	0.99	0.98	0.99	0.91	0.95	0.95	0.94	0.99	0.98	1.00	1.00	0.95
Elovich												
β (g mg^{-1})	0.83	0.84	0.85	0.39	0.46	0.52	0.52	0.53	0.61	0.78	0.95	1.17
α (mg g^{-1} min^{-1})	316.01	488.11	628.09	101.29	455.24	1429.40	391.74	663.77	3586.94	152.07	1706.29	25165.98
t_0 (min)	0.00	0.00	0.00	0.03	0.00	0.00	0.00	0.00	0.00	0.01	0.00	0.00
R^2	0.90	0.90	0.89	0.94	0.81	0.80	0.93	0.87	0.79	0.94	0.83	0.85
Bangham												
α	0.29	0.30	0.31	0.40	0.35	0.34	0.26	0.29	0.28	0.30	0.27	0.25
k_0(mg^{-1}dm^{-3})	0.00	0.00	0.00	14.05	19.39	22.85	22.66	18.32	16.31	9.54	13.57	16.91
R^2	0.92	0.94	0.94	0.96	0.85	0.86	0.85	0.90	0.95	0.96	0.89	0.93
Modified Freundlich												
m	7.01	7.47	7.72	5.25	6.61	7.89	6.88	7.22	8.84	6.52	8.87	11.86
k (dm^{3}g^{-1} min^{-1})	0.07	0.07	0.07	0.10	0.11	0.13	0.10	0.11	0.12	0.06	0.08	0.09
R^2	0.84	0.84	0.83	0.90	0.77	0.77	0.89	0.81	0.73	0.90	0.77	0.80

Table 6.3.4. Kinetic parameters for the removal of Py, 2Pi, 4Pi and AmPy by BFA d) Effect of Shaking Speed.

Models	Py			2Pi			4Pi			AmPy		
Pseudo-first-order												
Constants	RPM			RPM			RPM			RPM		
	100	150	200	100	150	200	100	150	200	100	150	200
$q_{e,exp}$ (mg g^{-1})	11.47	11.64	11.7	17.9	18.9	19.2	18.13	18.2	18.3	11.3	11..8	12.03
$q_{e,calc}$ (mg g^{-1})	7.46	4.97	4.24	0.18	0.18	0.16	0.16	0.12	0.16	0.13	0.12	0.10
k_f (min^{-1})	0.28	0.25	0.25	9.00	3.59	3.72	7.22	4.57	3.87	5.07	2.69	2.04
R^2	0.87	0.84	0.85	0.95	0.71	0.69	0.87	0.80	0.84	0.90	0.83	0.89
Pseudo-second-order												
$q_{e,calc}$ (mg g^{-1})	11.74	11.68	11.54	18.00	20.02	20.14	18.35	18.14	18.51.	11.36	11.53	11.43
h (mg g^{-1} min^{-1})	6.89	10.62	17.31	9.72	17.64	20.29	6.73	19.74	23.98	5.16	17.42	45.73
k_s (g mg^{-1} min^{-1})	0.05	0.08	0.13	0.03	0.04	0.05	0.02	0.06	0.07	0.04	0.13	0.35
R^2	1.00	1.00	1.00	1.00	1.00	1.00	1.00	1.00	1.00	1.00	1.00	1.00
Intra particle diffusion												
k_{int1} (mg g^{-1} min$^{-1/2}$)	3.92	2.75	2.43	4.88	6.08	5.97	5.48	4.85	4.60	3.52	2.51	1.08
C_1 (mg g^{-1})	0.21	3.81	4.86	1.33	3.66	4.19	0.56	5.11	6.43	0.40	4.79	8.31
R^2	0.99	0.89	0.85	1.00	0.99	0.98	0.96	0.92	0.95	0.97	0.82	0.98
k_{int2} (mg g^{-1} min$^{-1/2}$)	0.30	0.24	0.20	0.62	0.10	0.13	0.42	0.32	0.22	0.39	0.20	0.18
C_2 (mg g^{-1})	9.16	9.72	10.10	13.40	18.09	18.13	14.26	15.63	16.61	8.30	10.14	10.61
R^2	0.96	0.98	1.00	0.89	0.95	0.93	0.97	0.99	0.99	0.98	1.00	0.99
Elovich Equation												
β (g mg^{-1})	0.57	0.84	0.97	0.34	0.46	0.47	0.35	0.53	0.59	0.56	0.97	1.59
α (mg g^{-1} min^{-1})	30.52	488.11	2028.69	29.89	455.24	591.05	35.38	663.77	2315.81	22.43	2082.99	2299723.66
t_0 (min)	0.06	0.00	0.00	0.10	0.00	0.00	0.08	0.00	0.00	0.08	0.00	0.00
R^2	0.91	0.90	0.88	0.96	0.81	0.81	0.92	0.81	0.84	0.95	0.86	0.97
Bangham Equation												
α	0.43	0.30	0.27	0.45	0.35	0.36	0.43	0.29	0.26	0.44	0.27	0.20
k_0 (mg^{-1}dm^{-3})	7.10	11.85	13.77	9.61	19.39	20.25	9.88	18.32	21.50	6.28	13.90	19.89
R^2	0.93	0.94	0.93	0.97	0.85	0.87	0.92	0.90	0.89	0.95	0.92	0.99
Modified Freundlich Equation												
m	7.01	7.47	9.03	6.89	6.61	3.90	3.94	7.22	8.56	4.00	9.00	16.95
k (dm^{3}g^{-1} min^{-1})	0.05	0.07	0.08	0.12	0.11	0.07	0.07	0.11	0.12	0.05	0.08	0.10
R^2	0.85	0.84	0.83	0.77	0.77	0.92	0.85	0.81	0.80	0.87	0.81	0.96

Table 6.3.5. Kinetic parameters for the removal of Py, 2Pi, 4Pi and AmPy by RHA a) Effect of Adsorbent dose.

Models	Py			2Pi			4Pi			AmPy		
Pseudo-first-order												
Constants	Dose (g dm^{-3})			Dose (g dm^{-3})			Dose (g dm^{-3})			Dose (g dm^{-3})		
	20	30	40	10	20	30	10	20	30	20	30	40
	4.1	2.9	2.3	8.32	4.5	3.2	7.3	4.4	3.1	4.4	3.03	2.37
$q_{e,calc}$ (mg g^{-1})	0.23	0.22	0.15	0.13	0.12	0.08	0.11	0.11	0.08	0.10	0.09	0.08
k_f (min^{-1})	1.97	0.94	0.54	3.71	1.17	0.53	2.80	1.22	0.59	1.80	0.94	0.60
R^2	0.83	0.86	0.80	0.91	0.80	0.59	0.88	0.81	0.71	0.88	0.82	0.74
Pseudo-second-order												
$q_{e,calc}$ (mg g^{-1})	4.08	2.88	2.24	7.88	4.45	3.14	6.89	4.24	3.06	4.06	2.91	2.34
h (mg g^{-1} min^{-1})	3.83	4.40	5.62	5.58	5.54	6.21	5.70	5.39	7.48	3.30	3.39	3.56
k_s (g mg^{-1} min^{-1})	0.23	0.53	1.12	0.09	0.28	0.63	0.12	0.30	0.80	0.20	0.40	0.65
R^2	1.00	1.00	1.00	1.00	1.00	1.00	1.00	1.00	1.00	1.00	1.00	1.00
Intra particle diffusion												
k_{int1} (mg g^{-1} min$^{-1/2}$)	1.04	0.64	0.37	1.81	1.04	0.61	1.80	0.97	0.49	1.02	0.73	0.53
C_1 (mg g^{-1})	1.07	1.18	1.29	1.64	1.54	1.55	1.47	1.51	1.69	0.93	0.94	0.94
R^2	0.92	0.82	0.78	0.96	0.95	0.88	0.97	0.91	0.83	0.94	0.88	0.84
k_{int2} (mg g^{-1} min$^{-1/2}$)	0.10	0.05	0.03	0.29	0.07	0.02	0.23	0.09	0.04	0.15	0.08	0.04
C_2 (mg g^{-1})	3.36	2.51	2.03	6.10	3.94	2.94	5.47	3.67	2.77	3.15	2.41	2.04
R^2	0.98	1.00	0.98	0.98	0.92	0.82	1.00	0.98	0.94	0.99	1.00	1.00
Elovich Equation												
β (g mg^{-1})	2.09	3.96	7.13	0.82	2.18	4.56	1.05	2.25	4.91	1.73	3.19	4.84
α (mg g^{-1} min^{-1})	62.21	614.35	34436.41	23.56	212.91	9161.27	40.25	185.61	16138.96	21.31	104.18	487.84
t_0 (min)	0.01	0.00	0.00	0.05	0.00	0.00	0.02	0.00	0.00	0.03	0.00	0.00
R^2	0.92	0.85	0.83	0.97	0.90	0.80	0.96	0.91	0.86	0.97	0.90	0.85
Bangham Equation												
α	0.27	0.22	0.18	0.36	0.27	0.22	0.28	0.26	0.20	0.34	0.28	0.28
k_0 (mg^{-1} dm^{-3})	3.56	3.38	3.40	2.59	4.67	6.88	5.10	4.36	4.43	3.06	2.95	2.86
R^2	0.92	0.88	0.88	0.97	0.92	0.86	0.94	0.93	0.91	0.97	0.93	0.92
Modified Freundlich Equation												
m	6.35	9.15	13.77	4.61	7.62	11.92	5.34	7.54	12.74	5.24	7.28	9.12
k (dm^3 g^{-1} min^{-1})	0.02	0.02	0.02	0.04	0.03	0.02	0.04	0.03	0.02	0.02	0.02	0.02
R^2	0.86	0.79	0.79	0.93	0.85	0.77	0.91	0.86	0.83	0.92	0.84	0.79

Table 6.3.6. Kinetic parameters for the removal of Py, 2Pi, 4Pi and AmPy by RFA b) Effect of Initial Concentration .

Models	Py			2Pi			4Pi			AmPy		
Pseudo-first-order												
Constants	Concentration (mg dm^{-3})			Concentration (mg dm^{-3})			Concentration (mg dm^{-3})			Concentration (mg dm^{-3})		
	50	100	200	50	100	200	50	100	200	50	100	200
	1.56	2.9	5.2	2.3	4.5	8.3	2.5	4.4	8.2	1.6	3.03	5.6
$q_{e,calc}$ (mg g^{-1})	0.19	0.22	0.24	0.13	0.18	0.14	0.10	0.11	0.13	0.06	0.09	0.11
k_f (min^{-1})	0.45	0.94	1.57	1.83	3.59	10.36	0.86	1.22	2.24	0.52	0.94	2.14
R^2	0.91	0.86	0.92	0.68	0.71	0.90	0.85	0.81	0.85	0.78	0.82	0.94
Pseudo-second-order												
$q_{e,calc}$ (mg g^{-1})	1.52	2.88	5.10	2.30	4.46	7.80	2.30	4.25	7.96	1.50	2.91	5.13
h (mg g^{-1} min^{-1})	3.03	4.40	8.84	3.86	5.37	10.34	2.65	5.24	9.50	2.52	3.48	5.79
k_s (g mg^{-1} min^{-1})	1.31	0.53	0.34	0.73	0.27	0.17	0.50	0.29	0.15	1.12	0.41	0.22
R^2	1.00	1.00	1.00	1.00	1.00	1.00	1.00	1.00	1.00	1.00	1.00	1.00
Intra particle diffusion												
k_{int1} (mg g^{-1} min$^{-1/2}$)	0.23	0.64	0.90	0.49	1.04	1.69	0.51	0.97	1.72	0.31	0.73	1.12
C_1 (mg g^{-1})	0.84	1.18	2.51	1.02	1.54	2.97	0.81	1.51	2.95	0.68	0.94	1.80
R^2	0.84	0.82	0.87	0.86	0.95	0.92	0.89	0.91	0.88	0.84	0.88	0.86
k_{int2} (mg g^{-1} min$^{-1/2}$)	0.03	0.05	0.09	0.03	0.07	0.22	0.07	0.09	0.15	0.05	0.08	0.21
C_2 (mg g^{-1})	1.31	2.51	4.50	2.09	3.94	6.55	1.91	3.67	6.94	1.24	2.41	3.99
R^2	0.98	1.00	0.92	0.90	0.92	0.98	0.95	0.98	0.95	0.98	1.00	0.99
Elovich Equation												
β (g mg^{-1})	8.45	3.96	2.37	5.43	2.18	1.16	3.68	2.25	1.20	7.06	3.19	1.54
α (mg g^{-1} min^{-1})	1347.66	614.35	2088.57	1296.61	212.91	266.05	44.97	185.61	336.26	211.68	104.18	68.58
t_0 (min)	0.00	0.00	0.00	0.00	0.00	0.00	0.01	0.00	0.00	0.00	0.00	0.01
R^2	0.94	0.85	0.91	0.83	0.90	0.95	0.95	0.91	0.91	0.92	0.90	0.97
Bangham Equation												
α	0.24	0.22	0.18	0.23	0.27	0.24	0.37	0.26	0.24	0.29	0.28	0.28
k_0 (mg^{-1} dm^{-3})	0.69	0.64	0.56	6.00	4.67	3.88	4.35	4.36	3.97	3.54	2.95	2.30
R^2	0.97	0.88	0.91	0.88	0.92	0.95	0.98	0.93	0.91	0.94	0.93	0.97
Modified Freundlich Equation												
m	11.00	9.15	10.06	10.18	7.62	7.36	6.73	7.54	7.51	8.91	7.28	6.35
k (dm^3 g^{-1} min^{-1})	0.01	0.02	0.04	0.02	0.03	0.05	0.01	0.03	0.05	0.01	0.02	0.03
R^2	0.90	0.79	0.87	0.79	0.85	0.91	0.90	0.86	0.86	0.87	0.84	0.92

Table 6.3.7. Kinetic parameters for the removal of Py, 2Pi, 4Pi and AmPy by RHA c) Effect of Temperature.

Models	Py			2Pi			4Pi			AmPy		
Pseudo-first-order												
Constants	Temperature, K			Temperature, K			Temperature, K			Temperature, K		
	273	303	313	273	303	313	273	303	313	273	303	313
	2.8	2.9	3	4.33	4.5	4.6	4.2	4.4	4.5	2.94	3.03	3.12
$q_{e,calc}$ (mg g^{-1})	0.22	0.22	0.25	0.13	0.12	0.14	0.10	0.11	0.10	0.09	0.09	0.09
k_f (min^{-1})	0.97	0.94	5.38	1.51	1.17	1.09	1.23	1.22	1.08	0.95	0.94	0.59
R^2	0.93	0.86	0.82	0.91	0.80	0.81	0.82	0.81	0.79	0.78	0.81	0.85
Pseudo-second-order												
$q_{e,calc}$ (mg g^{-1})	2.82	2.86	3.02	4.20	4.46	4.58	4.06	4.25	4.35	2.85	2.91	2.94
h (mg g^{-1} min^{-1})	2.86	4.34	5.19	4.59	5.57	5.87	4.95	5.24	7.19	2.92	3.48	4.32
k_s (g mg^{-1} min^{-1})	0.36	0.53	0.57	0.26	0.28	0.28	0.30	0.29	0.38	0.36	0.41	0.50
R^2	1.00	1.00	1.00	1.00	1.00	1.00	1.00	1.00	1.00	1.00	1.00	1.00
Intra particle diffusion												
k_{int1} (mg g^{-1} min$^{-1/2}$)	0.74	0.64	0.65	1.00	1.11	1.13	0.95	0.97	0.86	0.82	0.78	0.68
C_1 (mg g^{-1})	0.77	1.18	1.36	1.25	1.37	1.47	1.39	1.51	1.98	0.63	0.84	1.11
R^2	0.87	0.82	0.76	0.86	0.90	0.86	0.92	0.91	0.91	0.83	0.81	0.80
k_{int2} (mg g^{-1} min$^{-1/2}$)	0.05	0.05	0.04	0.12	0.07	0.06	0.09	0.09	0.07	0.07	0.08	0.09
C_2 (mg g^{-1})	2.42	2.51	2.73	3.47	3.94	4.09	3.46	3.67	3.87	2.35	2.41	2.45
R^2	0.96	1.00	0.96	0.91	0.92	0.83	1.00	0.98	0.99	0.99	1.00	1.00
Elovich												
β (g mg^{-1})	3.25	3.96	0.85	1.95	2.13	2.21	2.30	2.25	2.59	2.99	3.12	3.29
α (mg g^{-1} min^{-1})	73.23	614.35	628.09	57.69	172.19	288.23	149.84	185.61	938.86	47.00	86.09	173.28
t_0 (min)	0.00	0.00	0.00	0.01	0.00	0.00	0.00	0.00	0.00	0.01	0.00	0.00
R^2	0.87	0.85	0.77	0.93	0.87	0.84	0.92	0.91	0.91	0.87	0.87	0.90
Bangham												
α	0.27	0.22	0.21	0.30	0.28	0.28	0.25	0.26	0.23	0.29	0.29	0.29
k_0 (mg^{-1}dm^{-3})	1.88	0.00	0.00	3.76	4.55	4.93	4.04	4.36	5.23	2.57	2.88	3.18
R^2	0.88	0.88	0.82	0.94	0.90	0.88	0.92	0.93	0.93	0.88	0.90	0.93
Modified Freundlich												
m	6.83	9.15	10.67	6.42	7.47	7.96	7.36	7.54	9.33	6.46	7.15	8.01
k (dm^{3}g^{-1} min^{-1})	0.02	0.02	0.02	0.02	0.03	0.03	0.03	0.03	0.03	0.02	0.02	0.02
R^2	0.81	0.79	0.72	0.88	0.82	0.79	0.87	0.86	0.87	0.79	0.80	0.84

Table 6.3.8. Kinetic parameters for the removal of Py, 2Pi, 4Pi and AmPy by RHA d) Effect of Shaking Speed.

Models	Py			2Pi			4Pi			AmPy		
Pseudo-first-order												
Constants	RPM			RPM			RPM			RPM		
	100	150	200	100	150	200	100	150	200	100	150	200
	2.82	2.9	2.97	4.4	4.5	4.6	4.2	4.4	4.5	2.95	3.03	3.07
$q_{e,calc}$ (mg g^{-1})	0.23	0.22	0.20	0.15	0.12	0.11	0.13	0.11	0.10	0.11	0.09	0.09
k_f (min^{-1})	1.33	0.94	0.84	1.97	1.17	1.19	1.47	1.22	1.17	1.27	0.94	0.85
R^2	0.88	0.86	0.85	0.88	0.80	0.77	0.83	0.81	0.83	0.86	0.82	0.81
Pseudo-second-order												
$q_{e,calc}$ (mg g^{-1})	2.81	2.87	2.92	4.60	4.45	4.64	4.18	4.25	4.31	2.88	2.91	2.95
h (mg g^{-1} min^{-1})	2.21	3.31	3.61	2.11	4.83	4.72	2.99	3.99	4.44	1.50	2.34	2.83
k_s (g mg^{-1} min^{-1})	0.28	0.53	0.60	0.10	0.28	0.22	0.19	0.29	0.39	0.22	0.41	0.53
R^2	1.00	1.00	1.00	1.00	1.00	1.00	1.00	1.00	1.00	1.00	1.00	1.00
Intra particle diffusion												
k_{int1} (mg g^{-1} min$^{-1/2}$)	0.80	0.64	0.61	1.44	1.04	1.27	1.12	0.97	0.83	0.79	0.73	0.64
C_1 (mg g^{-1})	0.49	1.18	1.34	0.00	1.54	1.21	0.84	1.51	1.99	0.39	0.94	1.23
R^2	1.00	0.82	0.77	1.00	0.95	0.86	1.00	0.91	0.90	0.99	0.88	0.89
k_{int2} (mg g^{-1} min$^{-1/2}$)	0.06	0.05	0.05	0.13	0.07	0.07	0.09	0.09	0.09	0.09	0.08	0.07
C_2 (mg g^{-1})	2.34	2.51	2.57	3.46	3.94	4.00	3.53	3.67	3.78	2.25	2.41	2.53
R^2	1.00	1.00	1.00	0.91	0.92	0.98	0.98	0.98	0.99	0.98	1.00	1.00
Elovich Equation												
β (g mg^{-1})	2.72	3.96	4.26	1.37	2.18	2.05	1.82	2.25	2.52	2.31	3.19	3.62
α (mg g^{-1} min^{-1})	20.08	614.35	1735.92	7.80	212.91	152.83	29.70	185.61	727.92	8.75	104.18	395.45
t_0 (min)	0.02	0.00	0.00	0.09	0.00	0.00	0.02	0.00	0.00	0.05	0.00	0.00
R^2	0.92	0.85	0.83	0.93	0.90	0.84	0.92	0.91	0.93	0.95	0.90	0.91
Bangham Equation												
α	0.32	0.22	0.21	0.44	0.27	0.30	0.32	0.26	0.24	0.38	0.28	0.26
k_0 (mg^{-1}dm^{-3})	2.20	3.38	3.73	2.39	4.67	4.61	3.29	4.36	5.12	1.87	2.95	3.45
R^2	0.92	0.88	0.87	0.93	0.92	0.88	0.93	0.93	0.95	0.96	0.93	0.94
Modified Freundlich Equation												
m	5.51	9.15	10.22	3.84	7.62	7.01	5.53	7.54	9.12	4.58	7.28	8.79
k (dm^{3}g^{-1} min^{-1})	0.01	0.02	0.02	0.02	0.03	0.03	0.02	0.03	0.03	0.01	0.02	0.02
R^2	0.87	0.79	0.77	0.87	0.85	0.77	0.88	0.86	0.89	0.90	0.84	0.86

Table 6.3.9. Kinetic parameters for the removal of Py, 2Pi, 4Pi and AmPy by GAC a) Effect of Adsorbent Dose .

Models	Py			2Pi			4Pi			AmPy		
Pseudo-first-order												
Constants	Dose (g dm^{-3})			Dose (g dm^{-3})			Dose (g dm^{-3})			Dose (g dm^{-3})		
	10	20	30	5	10	20	5	10	20	10	20	30
	8.75	4.65	3.3	15.03	8.7	4.9	11.7	8.5	4.7	9.1	4.8	3.3
$q_{e,calc}$ (mg g^{-1})	0.28	0.26	0.25	0.11	0.13	0.13	0.13	0.12	0.16	0.11	0.12	0.13
k_f (min^{-1})	13.05	4.88	2.56	13.37	7.31	3.31	9.40	6.41	3.00	6.78	2.81	1.75
R^2	0.83	0.87	0.92	1.00	1.00	0.96	0.99	0.97	0.97	0.98	0.93	0.93
Pseudo-second-order												
$q_{e,calc}$ (mg g^{-1})	9.60	5.02	3.67	13.95	7.53	4.81	10.62	8.42	5.16	7.38	4.59	3.20
h (mg g^{-1} min^{-1})	1.20	0.96	0.81	1.95	1.70	1.16	2.26	1.42	1.07	2.18	1.69	1.54
k_s (g mg^{-1} min^{-1})	0.01	0.04	0.06	0.01	0.03	0.05	0.02	0.02	0.04	0.04	0.08	0.15
R^2	1.00	1.00	1.00	0.99	0.99	1.00	1.00	1.00	1.00	0.99	1.00	1.00
Intra particle diffusion												
k_{int} (mg g^{-1} min$^{-1/2}$)	1.14	0.54	0.34	2.01	1.09	0.55	1.42	1.03	0.51	1.05	0.48	0.30
C (mg g^{-1})	0.89	0.95	0.98	0.36	0.91	1.12	1.66	1.17	1.31	1.36	1.48	1.28
R^2	0.92	0.85	0.78	0.98	0.96	0.89	0.95	0.93	0.82	0.97	0.87	0.83
Elovich Equation												
β (g mg^{-1})	0.50	1.02	1.56	0.30	0.54	1.03	0.41	0.56	1.08	0.56	1.15	1.81
α (mg g^{-1} min^{-1})	2.95	2.28	2.43	3.87	3.05	2.78	4.70	3.25	3.23	3.84	4.22	4.76
t_0 (min)	0.67	0.43	0.26	0.87	0.61	0.35	0.52	0.55	0.29	0.47	0.21	0.12
R^2	0.99	0.97	0.95	0.97	0.97	0.99	0.99	0.99	0.97	0.98	0.99	0.98
Bangham Equation												
α	0.70	0.65	0.65	0.67	0.62	0.66	0.51	0.62	0.61	0.58	0.56	0.57
k_0 (mg^{-1} dm^{-3})	1.54	1.18	0.11	2.16	1.83	1.37	2.81	1.81	1.48	2.27	1.84	1.55
R^2	0.99	0.98	0.97	1.00	0.99	1.00	0.99	0.99	0.96	0.99	0.99	1.00
Modified Freundlich Equation												
m	2.00	2.40	2.73	1.89	2.31	2.67	2.40	2.23	2.67	2.60	3.21	3.77
k (dm^3 g^{-1} min^{-1})	0.01	0.01	0.01	0.02	0.02	0.01	0.02	0.02	0.01	0.02	0.02	0.01
R^2	0.95	0.92	0.86	0.99	0.99	0.94	0.89	0.96	0.87	0.99	0.94	0.92

Table 6.3.10. Kinetic parameters for the removal of Py, 2Pi, 4Pi and AmPy by GAC b) Effect of Initial Concentration

Models	Py			2Pi			4Pi			AmPy		
Pseudo-first-order												
Constants	Concentration (mg dm^{-3})			Concentration (mg dm^{-3})			Concentration (mg dm^{-3})			Concentration (mg dm^{-3})		
	50	100	200	50	100	200	50	100	200	50	100	200
	2.44	4.65	8.34	4.5	8.7	16	4.8	8.5	15.8	2.43	4.8	9.2
$q_{e,calc}$ (mg g^{-1})	0.27	0.30	0.27	0.13	0.13	0.14	0.12	0.12	0.12	0.12	0.12	0.15
k_f (min^{-1})	2.40	5.91	10.95	3.31	7.31	14.51	3.31	6.41	12.51	1.41	2.81	6.72
R^2	0.88	0.82	0.82	1.00	1.00	1.00	0.98	0.97	0.98	0.93	0.93	0.99
Pseudo-second-order												
$q_{e,calc}$ (mg g^{-1})	2.68	5.02	12.04	3.77	7.53	13.56	4.33	8.42	16.61	2.30	4.60	8.65
h (mg g^{-1} min^{-1})	0.57	0.96	0.87	0.09	1.70	0.93	1.12	1.42	2.21	1.06	1.48	2.32
k_s (g mg^{-1} min^{-1})	0.08	0.04	0.01	0.04	0.03	0.01	0.06	0.02	0.01	0.20	0.07	0.03
R^2	1.00	1.00	0.99	1.00	0.99	0.99	1.00	1.00	1.00	1.00	1.00	1.00
Intra particle diffusion												
k_{int} (mg g^{-1} min$^{-1/2}$)	0.27	0.54	1.08	0.50	1.09	2.11	0.53	1.03	1.99	0.24	0.48	1.05
C (mg g^{-1})	0.66	0.95	1.02	0.94	0.91	0.90	1.02	1.17	1.71	0.85	1.48	1.96
R^2	0.83	0.85	0.86	0.95	0.96	0.97	0.92	0.93	0.94	0.87	0.87	0.92
Elovich Equation												
β (g mg^{-1})	2.04	1.02	0.52	1.16	0.54	0.28	1.08	0.56	0.29	2.35	1.15	0.54
α (mg g^{-1} min^{-1})	1.58	2.28	2.90	2.50	3.05	4.74	2.60	3.25	5.37	2.76	4.22	4.96
t_0 (min)	0.31	0.43	0.67	0.34	0.61	0.74	0.36	0.55	0.64	0.15	0.21	0.37
R^2	0.97	0.97	0.98	0.99	0.97	0.96	0.99	0.99	1.00	0.99	0.99	1.00
Bangham Equation												
α	0.68	0.65	0.75	0.54	0.62	0.63	0.60	0.62	0.65	0.56	0.56	0.60
k_0 (mg^{-1} dm^{-3})	0.27	0.22	0.08	2.75	1.83	1.45	2.75	1.81	1.43	2.12	1.23	1.32
R^2	0.98	0.98	0.94	1.00	0.99	0.99	1.00	0.99	0.98	1.00	0.99	0.99
Modified Freundlich Equation												
m	2.63	2.40	1.77	2.86	2.31	2.14	2.75	2.23	2.02	3.57	3.21	2.66
k (dm^3 g^{-1} min^{-1})	0.01	0.01	0.01	0.01	0.02	0.03	0.02	0.02	0.01	0.01	0.02	0.02
R^2	0.89	0.92	0.88	0.98	0.99	0.99	0.97	0.96	0.94	0.95	0.94	0.95

Table 6.3.11. Kinetic parameters for the removal of of Py, 2Pi, 4Pi and AmPy by GAC c) Effect of Temperature.

Models	Py			2Pi			4Pi			AmPy		
Pseudo-first-order												
Constants	Temperature, K			Temperature, K			Temperature, K			Temperature, K		
	273	303	313	273	303	313	273	303	313	273	303	313
	4.5	4.65	4.7	8.4	8.7	9	8	8.5	8.9	4.6	4.8	4.95
$q_{e,calc}$ (mg g^{-1})	0.28	0.26	0.30	0.11	0.13	0.14	0.12	0.12	0.12	0.13	0.12	0.12
k_f (min^{-1})	6.13	5.04	5.04	7.43	7.35	1.09	6.47	6.43	6.03	3.21	2.82	2.57
R^2	0.84	0.87	0.89	1.00	1.00	0.81	0.98	0.97	0.97	0.98	0.93	0.93
Pseudo-second-order												
$q_{e,calc}$ (mg g^{-1})	5.24	6.08	5.06	7.28	7.53	7.36	8.36	8.42	7.91	4.35	4.60	4.58
h (mg g^{-1} min^{-1})	0.55	0.74	1.03	1.06	1.70	2.17	1.40	1.42	2.50	1.23	1.69	2.52
k_s (g mg^{-1} min^{-1})	0.02	0.02	0.04	0.02	0.03	0.04	0.02	0.02	0.04	0.07	0.08	0.12
R^2	1.00	1.00	1.00	0.99	1.00	1.00	1.00	1.00	1.00	1.00	1.00	1.00
Intra particle diffusion												
k_{int} (mg g^{-1} min$^{-1/2}$)	0.57	0.57	0.55	1.11	1.10	1.05	1.02	1.04	0.97	0.51	0.49	0.44
C (mg g^{-1})	0.45	0.77	1.05	0.23	0.85	1.59	0.74	1.13	2.03	1.06	1.47	1.92
R^2	0.90	0.84	0.80	0.98	0.96	0.96	0.94	0.92	0.92	0.90	0.86	0.85
Elovich Equation												
β (g mg^{-1})	0.99	0.96	0.98	0.52	0.52	0.54	0.55	0.53	0.57	1.07	1.11	1.22
α (mg g^{-1} min^{-1})	1.44	1.89	2.40	2.03	2.72	3.91	2.38	2.92	4.76	2.43	3.68	6.86
t_0 (min)	0.70	0.55	0.42	0.95	0.71	0.47	0.77	0.64	0.37	0.38	0.25	0.12
R^2	0.99	0.97	0.96	0.98	0.99	0.99	1.00	1.00	1.00	0.99	0.98	0.98
Bangham Equation												
α	0.75	0.74	0.69	0.71	0.65	0.59	0.55	0.65	0.55	0.60	0.58	0.55
k_0 (mg^{-1} dm^{-3})	0.67	0.87	1.15	1.16	0.84	1.18	2.69	1.68	2.69	1.33	1.72	2.27
R^2	0.97	0.95	0.96	1.00	1.00	1.00	0.99	0.98	0.99	0.99	0.99	0.99
Modified Freundlich Equation												
m	1.83	1.98	2.27	1.89	2.22	2.65	1.95	2.16	2.81	2.70	3.12	3.88
k (dm^3 g^{-1} min^{-1})	0.02	0.01	0.01	0.01	0.02	0.02	0.01	0.01	0.02	0.01	0.01	0.02
R^2	0.91	0.88	0.88	0.98	0.98	0.98	0.93	0.94	0.96	0.94	0.92	0.92

Table 6.3.12 Kinetic parameters for the removal of Py, 2Pi, 4Pi and AmPy by GAC d) Effect of Shaking Speed.

Models	Py			2Pi			4Pi			AmPy		
Pseudo-first-order												
Constants	RPM			RPM			RPM			RPM		
	100	150	200	100	150	200	100	150	200	100	150	200
	4.4	4.65	4.7	8.3	8.9	9	8.1	8.5	8.9	4.5	4.8	4.9
$q_{e,calc}$ (mg g^{-1})	0.28	0.26	0.27	0.13	0.13	0.12	0.11	0.12	0.12	0.14	0.12	0.13
k_f (min^{-1})	6.50	5.04	4.81	7.62	7.31	6.62	6.56	6.41	6.54	3.70	2.81	2.43
R^2	0.84	0.87	0.88	1.00	1.00	0.99	0.99	0.97	0.98	0.99	0.93	0.94
Pseudo-second-order												
$q_{e,calc}$ (mg g^{-1})	5.25	5.49	5.36	7.76	7.53	7.56	7.32	8.42	8.06	4.80	4.59	4.40
h (mg g^{-1} min^{-1})	0.58	1.00	0.86	1.20	1.70	2.29	1.07	1.42	1.95	0.69	1.69	2.71
k_s(g mg^{-1} min^{-1})	0.02	0.03	0.03	0.02	0.03	0.04	0.02	0.02	0.03	0.03	0.08	0.14
R^2	1.00	1.00	1.00	0.99	0.99	1.00	0.99	1.00	1.00	1.00	1.00	1.00
Intra particle diffusion												
k_{int}(mg g^{-1} min$^{-1/2}$)	0.58	0.56	0.55	1.12	1.09	1.02	1.01	1.03	1.04	0.58	0.48	0.42
C(mg g^{-1})	0.37	0.83	1.08	0.27	0.91	1.70	0.73	1.17	1.60	0.53	1.48	1.98
R^2	0.93	0.84	0.83	0.98	0.96	0.95	0.97	0.93	0.94	0.92	0.87	0.88
Elovich Equation												
β (g mg^{-1})	0.99	0.98	1.00	0.53	0.54	0.57	0.58	0.56	0.56	0.99	1.15	1.33
α (mg g^{-1} min^{-1})	1.37	2.01	2.52	2.23	3.05	4.54	2.62	3.25	4.19	1.60	4.22	9.38
t_0 (min)	0.74	0.51	0.40	0.84	0.61	0.39	0.66	0.55	0.43	0.63	0.21	0.08
R^2	0.99	0.97	0.97	0.98	0.97	0.99	0.99	0.99	0.99	0.99	0.99	0.99
Bangham Equation												
α	0.74	0.70	0.67	0.70	0.62	0.56	0.62	0.62	0.58	0.70	0.56	0.48
k_0 (mg^{-1}dm^{-3})	0.67	1.00	1.25	1.21	1.83	2.58	1.51	1.81	2.36	0.85	1.84	2.60
R^2	0.98	0.97	0.98	1.00	0.99	1.00	1.00	0.99	1.00	0.99	0.99	0.99
Modified Freundlich Equation												
m	1.86	2.16	2.43	1.90	2.31	2.76	2.14	2.23	2.58	2.09	3.21	4.27
k (dm^{3}g^{-1} min^{-1})	0.01	0.01	0.01	0.01	0.02	0.02	0.01	0.02	0.02	0.01	0.02	0.02
R^2	0.94	0.91	0.91	0.98	0.99	0.99	0.98	0.96	0.97	0.96	0.94	0.96

6.3.6.3 Intra-particle Diffusion model

The adsorbate transport from the solution phase to the surface of the adsorbent particles occurs in several steps, as discussed in Chapter III. The overall adsorption process may be controlled either by one or more steps, e.g. film or external diffusion, pore diffusion, surface diffusion and adsorption on the pore surface, or a combination of more than one step. Generally, a process is diffusion controlled if its rate is dependent upon the rate at which components diffuse towards one another. The possibility of intra-particle diffusion was explored by using the intra-particle diffusion model (Weber and Morris, 1963).

$$q_t = k_{int} t^{0.5} + C \tag{6.3.7}$$

where, k_{int} is the intra-particle diffusion rate constant (mg g^{-1} min$^{0.5}$) and C (mg g^{-1}) is a constant that gives idea about the thickness of the boundary layer, i.e., larger the value of C the greater is the boundary layer effect (Kannan and Sundaram, 2001). If the Weber-Morris plot of q_t versus $t^{0.5}$ satisfies the linear relationship with the experimental data, then the sorption process is found be controlled by intra-particle diffusion only. However, if the data exhibit multi-linear plots, then two or more steps influence the sorption process. The mathematical dependence of fractional uptake of adsorbate on $t^{0.5}$ is obtained if the sorption process is considered to be influenced by diffusion in the cylindrical (or spherical) and convective diffusion in the adsorbate solution. It is assumed that the external resistance to mass transfer surrounding the particles is significant only in the early stages of adsorption. This is represented by the first sharper portion. The second linear portion is the gradual adsorption stage with intra-particle diffusion dominating.

Fig. 6.3.17 shows a representative q_t versus $t^{0.5}$ plot for Py, 2Pi, 4Pi and AmPy onto BFA for $C_0 = 100$ mg dm^{-3} at 303 K and pH_0 6.0. In the figure, the data points are related by two straight lines- the first straight portion depicting macro-pore diffusion and the second representing meso-pore diffusion. These show only the pore diffusion data.
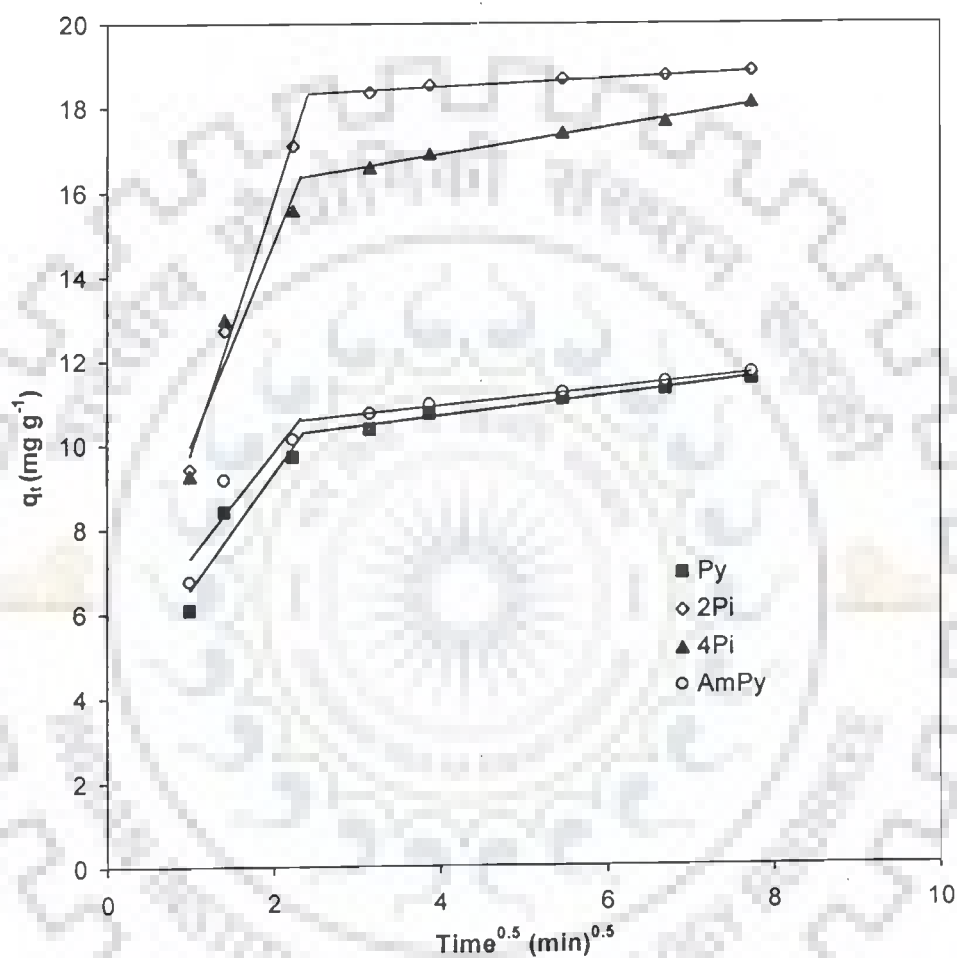
Fig. 6.3.17. Weber and Morris intra-particle diffusion plot for the removal of Py, 2Pi, 4Pi and AmPy by BFA. $T = 303$ K, $C_0 = 100$ mg/l, $m = 8$, 5, 5 and 8 g dm^{-3}.

158

Extrapolation of the linear portions of the plots back to the y-axis gives the intercepts, which provide the measure of the boundary layer thickness. If the intercept is large, the boundary layer effect will also be large. The deviation of straight lines from the origin (Fig. 6.3.17) may be due to difference in rate of mass transfer in the initial and final stages of adsorption. Further, such deviation of straight line from the origin indicates that the pore diffusion is not the sole rate-controlling step. The adsorption data for q versus $t^{0.5}$ plot show curvature for the initial period, usually attributed to boundary layer diffusion effects or external mass transfer effects (Crank, 1965; Mckay et al., 1980). The slope of the Weber-Morris plots - q_t versus $t^{0.5}$ - are defined as a rate parameter, characteristic of the rate of adsorption in the region where intra-particle diffusion is rate controlling. Similar plots were obtained for other adsorbate-adsorbent systems. The values of rate parameters are given in Tables 6.3.1-6.3.12.

6.3.6.4 The Elovich equation

The Elovich equation is given as follows (Cheung et al. 2000, Onal 2006):

$$\frac{dq_t}{dt} = \alpha e^{-\beta q_t} \tag{6.3.8}$$

where, α is the initial rate (mg g^{-1} min^{-1}) because (dq_t/d_t) approaches α when q_t approaches zero, and the parameter β (g mg^{-1}) is related to the extent of surface coverage and activation energy for chemisorptions (Teng and Hsieh, 1999).

For $q_t = 0$ at $t = 0$, equation can be integrated as:

$$q_t = \frac{1}{\beta} \ln(t + t_0) - \frac{1}{\beta} \ln(t_0) \tag{6.3.9}$$

where $t_0 = 1/\alpha\beta$. If t is much larger than t_0. Equation 6.3.9 can be simplified as:

$$q_t = \frac{1}{\beta} \ln(\alpha\beta) + \frac{1}{\beta} \ln t \tag{6.3.10}$$

The constants of Elovich equation are determined from the plot of $\ln t$ Vs q_t. All the constants of Elovich for all the adsorbate-adsorbent system are given in Table 6.3.1-Table 6.3.12.

6.3.6.5 Bangham's equation

Bangham's equation can be used to check the whether pore-diffusion is the only rate-controlling step or not in the adsorption system (Aharoni et al., 1979).

$$\log\log\left(\frac{C_0}{C_0 - q_t m}\right) = \log\left(\frac{k_{0B}m}{2.303V}\right) + \alpha\log(t) \tag{6.3.11}$$

where, α (<1) and k_{0B} are constants.

If the experimental data are represented by Eq. (6.3.11), then it is an indication that the adsorption kinetics is limited by the pore diffusion. Fig. 6.3.18 shows a representative plot of $\log\log(C_O/(C_O-q_t m))$ versus $\log(t)$ plot for Py, 2Pi, 4Pi and AmPy adsorption onto RHA for $C_0 = 100$ mg dm^{-3} at 303 K and at pH_0 6.0. However, the plot (Fig. 6.3.18) according to above equation did not yield linear curves and the values of R^2 are far from one. This shows that the diffusion of Py, 2Pi, 4Pi and AmPy into the pores of adsorbent is not the only rate-controlling step (Tutem et al., 1998). Similarly, it was found that pore diffusion was not the only rate-controlling step in diffusion of Py, 2Pi, 4Pi and AmPy onto other adsorbents. Values of the Bangham parameters and the correlation coefficients are given in Tables 6.3.1 through Table 6.3.12.

6.3.6.6 Modified Freundlich equation

The modified Freundlich equation was originally developed by Kuo and Lotse (1973). It is given as follows:

$$q_t = kC_0 t^{1/m} \tag{6.3.12}$$

where q_t is the amount adsorbed (mg g^{-1}) at any time t, k the apparent adsorption rate constant (dm^3 (g min)$^{-1}$), C$_0$ the initial concentration (mg dm^{-3}), t the contact time (min) and m is the Kuo-Lotse constant. Linear form of modified Freundlich equation is given as:

$$\ln q_t = \ln(kC_0) + \frac{1}{m}\ln t \tag{6.3.13}$$

The constants can be determined from the plot of $\ln q_t$ vs $\ln_t$ which are shown in Tables 6.3.1 through Table 6.3.12 for all the adsorbate-adsorbent systems.
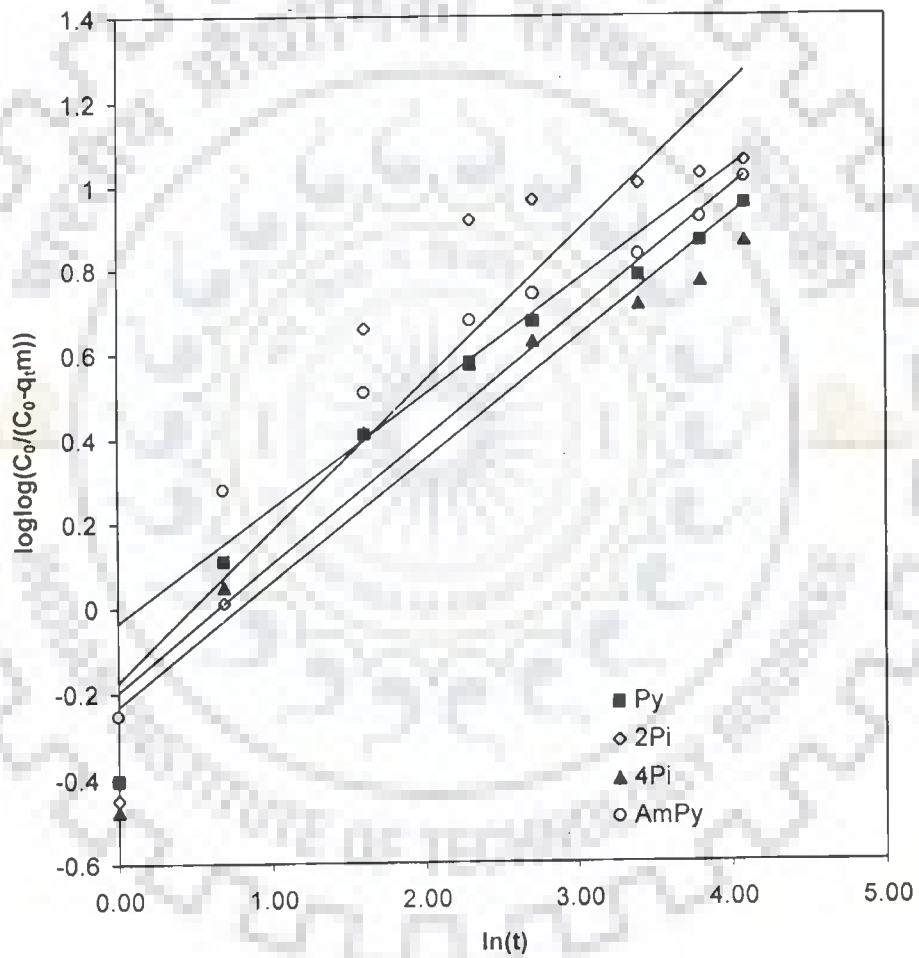
Fig. 6.3.18. Bangham plot for the removal of Py, 2Pi, 4Pi and AmPy by BFA. T = 303 K, C_0 = 100 mg/l, m = 8, 5, 5 and 8 g dm^{-3}.

6.3.7 Determination of Diffusivity

Kinetic data could be treated by simplified form of Vermeulen's approximation (Vermeulen, 1953) to the model given by Boyd et al. (1947), as discussed in Chapter III, for the calculation of effective particle diffusivity of adsorbates onto BFA, RHA and GAC.

$$F(t) = \left[1 - \exp\left(\frac{-\pi^2 D_e t}{R_a^2} \right) \right]^{1/2} \qquad (6.3.14)$$

Thus, the slope of the plot of $\ln\left[1/(1 - F^2(t)) \right]$ versus t gives D_e. Table 6.3.13 presents the values of effective diffusion coefficient (D_e) as calculated from Eq. (6.3.14). Average value of D_e are found to be 4.09, 3.89 and 24.5 x 10^{-10} $m^2 s^{-1}$ for Py, 3.44, 3.22 and 18.72 x 10^{-10} $m^2 s^{-1}$ for 2Pi, 2.9, 2.9 and 17.69 x 10^{-10} $m^2 s^{-1}$ for 4Pi and 2.98, 2.37 and 21.59 x 10^{-10} $m^2 s^{-1}$ for that of AmPy for adsorption onto BFA, RHA and GAC, respectively. This shows that Py have highest overall pore diffusion rate.

Table 6.3.13. Comparison of effective pore diffusivities of Py, 2Pi, 4Pi and AmPy for BFA, RHA and GAC systems.

	D_e ($m^2 s^{-1}$) x 10^{10}			
BFA				
C_o (mg dm^{-3})	Py	2Pi	4Pi	AmPy
50	3.95	3.38	2.86	3.12
100	4.13	4.12	2.88	2.9
200	4.18	2.82	2.95	2.91
Average	4.09	3.44	2.90	2.98
RHA				
C_o (mg dm^{-3})	Py	2Pi	4Pi	AmPy
50	3.59	3.21	2.43	2.00
100	3.74	3.38	2.93	2.51
200	4.34	3.06	3.33	2.59
Average	3.89	3.22	2.9	2.37
GAC				
C_o (mg dm^{-3})	Py	2Pi	4Pi	AmPy
50	27.53	19.33	18.56	21.34
100	24.70	18.39	17.50	20.81
200	21.26	18.43	17.00	22.61
Average	24.50	18.72	17.69	21.59

6.3.8 Adsorption Equilibrium Study

The experimental equilibrium adsorption data of Py, 2Pi, 4Pi and AmPy adsorption onto BFA, RHA and GAC have been tested by using the two-parameter Freundlich, Langmuir, and Temkin isotherm equations and the three parameter Redlich-Peterson (R-P), Toth and Radke-Prausnitz equations. As discussed in Chapter III, following equations represents these isotherms:

Freundlich $\qquad q_e = K_F C_e^{1/n}$ $\qquad\qquad\qquad$ (6.3.15)

Langmuir $\qquad q_e = \dfrac{q_m K_L C_e}{1 + K_L C_e}$ $\qquad\qquad\qquad$ (6.3.16)

Temkin $\qquad q_e = B_T \ln K_T + B_T \ln C_e$ $\qquad\qquad\qquad$ (6.3.17)

Redlich-Peterson $\qquad q_e = \dfrac{K_R C_e}{1 + a_R C_e^{\beta}}$ $\qquad\qquad\qquad$ (6.3.18)

Toth $\qquad q_e = \dfrac{q_e^{\infty} C_e}{\left[1/K_{th} + C_e^{Th} \right]^{1/Th}}$ $\qquad\qquad\qquad$ (6.3.19)

Radke-Prausnitz $\qquad q_e = \dfrac{K_{RP} k_{RP} C_e}{1 + K_{RP} C_e^{P}}$ $\qquad\qquad\qquad$ (6.3.20)

The Freundlich isotherm is valid for a heterogeneous adsorbent surface with a non-uniform distribution of heat of adsorption over the surface. The Langmuir isotherm, however, assumes that the sorption takes place at specific homogeneous sites within the adsorbent. The Redlich-Peterson, Toth and Radke-Prausnitz isotherms can, however be applied in homogenous as well as heterogeneous systems.

Non-linear regression analysis was carried out using the Solver-Add-in function of Excel (Office, 2003) to find out the isotherm parameters by fitting the experimental data.

Two different error functions of non-linear regression basin were employed in this study to find out the most suitable kinetic and isotherm models to represent the experimental data. The hybrid fractional error function (HYBRID) [Porter et al., 1999]

163

and the Marquardt's percent standard deviation (MPSD) error function [Marquardt, 1963] and Chi-square ($\chi 2$) [Ho, 2004] have been used previously by a number of researchers in the field. These error functions are given as

$$HYBRID = \frac{100}{n-p} \sum_{i=1}^{n} \left[\frac{(q_{e,\exp} - q_{e,calc})^2}{q_{e,\exp}} \right]_i \qquad (6.3.21)$$

$$MPSD = 100 \sqrt{\frac{1}{n-p} \sum_{i=1}^{n} \left(\frac{(q_{e,\exp} - q_{e,calc})}{q_{e,\exp}} \right)_i^2} \qquad (6.3.22)$$

$$\chi^2 = \sum \frac{(q_{e,\exp} - q_{e,calc})^2}{q_{e,calc}} \qquad (6.3.23)$$

where, n is number of data points, P is number of unknown parameters, $q_{e,exp}$ is the experimental adsorption capacity (mg g^{-1}) and $q_{e,calc}$ is the adsorption capacity calculated by isotherm model (mg g^{-1}).

HYBRID was developed to improve the fit of the square of errors function at low concentration values. The MPSD is similar in some respects to a geometric mean error distribution modified according to the number of degrees of freedom of the system. Chi-square ($\chi 2$) is the sum of the squares of the differences between the experimental data and data obtained by calculating from models, with each squared difference divided by the corresponding data obtained by calculating from models.

The parameters of the isotherm, and the correlation coefficient, R^2 for the fitting of the experimental data are listed in Tables 6.3.14 to 6.3.16. By comparing the results of the values for the error functions (Tables 6.3.17 to 6.3.19) and correlation coefficients (Tables 6.3.14 to 6.3.16), it is found that the Redlich-Peterson, Toth and Radke-Prausnitz isotherms generally represent the equilibrium sorption of Py and its derivatives at all temperatures onto BFA, RHA and GAC. Whereas, Langmuir isotherm best represent the equilibrium sorption data in some of the adsorbate-adsorbent systems.

K_F and $1/n$ indicate the adsorption capacity and adsorption intensity, respectively. Higher the value of $1/n$, the higher will be the affinity between the adsorbate and the adsorbent, and the heterogeneity of the adsorbent sites. The $1/n$ value indicates the relative distribution of energy sites and depends on the nature and strength of the adsorption process; for example, $1/n = 0.66$ refers to the fact that 66% of the active adsorption sites have equal energy level. It is found from Tables 6.3.14 to 6.3.16 that the BFA, RHA and GAC show greater heterogeneity for Py than that for other adsorbates. Since $1/n < 1$, all the adsorbates are favourably adsorbed by BFA, RHA and GAC. BFA generally showed greater heterogeneity than RHA and GAC for Py. The surface heterogeneity is due to the existence of crystal edges, type of cations, surface charges, and the degree of crystallinity of the surface. The net effect of these factors is temperature dependent. The Freundlich isotherm does not predict the saturation of the adsorbent surface by the adsorbate.

The q_m is the monolayer saturation at equilibrium, whereas, K_L corresponds to the concentration at which the amount of adorbates bound to the adsorbent is equal to $q_m/2$. This indicates the affinity of the adsorbates to bind with the adsorbents. A high K_L value indicates a higher affinity. The data in Tables 6.3.14 to 6.3.16 also indicate that the q_m value for 2Pi and 4Pi was higher than that of Py and AmPy. The values of K_L increased with an increase in temperature confirming endothermic nature of overall sorption process for all adsorbate-adsorbent systems.

Table 6.3.14. Isotherm parameters for the adsorption of Py and its derivatives onto BFA at different temperatures.

Model Constants	Langmuir			Freundlich			Temkin			Redlich-Peterson				Toth Isotherm				Radke-Prausnitz			
	K_L	q_m	R^2	K_F	$1/n$	R^2	B	K_T	R^2	a_R	K_R	β	R^2	Th	q_e^{inf}	K_{Th}	R^2	P	K_{RP}	k_{RP}	R^2
Py																					
283 K	0.06	31.06	0.99	2.26	0.66	0.99	5.56	1.03	0.95	0.51	3.20	0.58	0.99	0.62	51.46	0.16	0.99	0.77	0.19	12.71	1.00
293 K	0.08	30.67	0.99	2.70	0.65	0.99	5.52	1.33	0.95	0.69	4.43	0.57	0.98	0.67	44.33	0.17	0.99	0.79	0.22	14.06	0.98
303 K	0.10	29.76	1.00	2.99	0.64	0.98	5.56	1.51	0.97	0.28	3.63	0.75	0.99	0.70	40.71	0.19	1.00	0.81	0.24	14.90	1.00
313 K	0.17	27.10	1.00	3.94	0.58	0.96	5.18	2.40	0.98	0.17	4.61	1.00	0.99	0.72	33.54	0.28	0.99	0.91	0.25	19.72	1.00
323 K	0.23	26.95	0.99	4.74	0.57	0.93	5.17	3.24	0.99	1.11	10.19	0.61	0.89	0.81	30.27	0.31	0.99	0.91	0.34	20.16	0.99
2Pi																					
283 K	0.03	60.98	0.99	6.50	0.39	0.98	10.32	0.60	0.96	4.36	31.92	0.63	0.99	0.28	162.5	0.59	0.99	0.77	0.26	15.77	1.00
293 K	0.05	60.24	0.99	9.14	0.34	0.98	9.44	1.28	0.99	0.43	8.96	0.82	1.00	0.30	116.9	0.77	1.00	0.80	0.46	18.83	1.00
303 K	0.07	59.88	1.00	11.59	0.30	0.98	8.59	2.76	0.99	0.71	16.75	0.84	1.00	0.30	100.3	1.00	1.00	0.86	0.38	27.03	1.00
313 K	0.11	59.52	1.00	15.51	0.25	0.97	7.29	10.26	0.99	2.09	52.85	0.85	1.00	0.31	82.93	1.48	1.00	0.88	0.77	30.03	1.00
323 K	0.17	60.61	1.00	23.60	0.17	0.96	5.17	300.8	0.96	23.58	769.7	0.90	1.00	0.33	68.19	3.05	1.00	0.94	0.45	43.67	1.00
4Pi																					
283 K	0.05	52.08	1.00	7.74	0.34	0.94	8.87	1.06	0.99	0.10	3.71	0.94	1.00	0.57	61.52	0.28	1.00	0.83	0.57	18.59	1.00
293 K	0.05	54.35	1.00	8.43	0.34	0.94	8.99	1.13	1.00	0.16	4.95	0.90	1.00	0.59	62.72	0.29	1.00	0.85	0.37	22.08	1.00
303 K	0.06	57.14	1.00	9.21	0.33	0.94	9.29	1.33	1.00	0.21	6.17	0.89	1.00	0.60	65.28	0.29	1.00	0.88	0.24	27.93	1.00
313 K	0.07	59.17	1.00	10.47	0.32	0.94	9.16	1.86	1.00	0.21	7.94	0.93	1.00	0.60	66.31	0.34	1.00	0.90	0.23	32.47	1.00
323 K	0.07	60.61	1.00	11.21	0.31	0.95	9.16	2.25	1.00	0.36	11.04	0.88	1.00	0.63	66.43	0.32	1.00	0.91	0.21	36.10	1.00
AmPy																					
283 K	0.04	44.25	1.00	4.34	0.43	0.96	8.09	0.56	1.00	0.08	2.21	0.92	1.00	0.57	56.78	0.20	1.00	0.84	0.15	17.73	1.00
293 K	0.04	47.17	1.00	4.96	0.42	0.96	8.47	0.69	1.00	0.12	2.98	0.89	0.99	0.60	58.01	0.20	1.00	0.84	0.17	19.31	1.00
303 K	0.05	50.25	0.99	5.62	0.42	0.97	8.76	0.87	0.99	0.21	4.30	0.84	0.99	0.62	60.18	0.20	1.00	0.84	0.18	21.10	1.00
313 K	0.05	52.36	0.99	6.06	0.42	0.97	9.02	0.99	0.99	0.27	5.32	0.82	0.99	0.63	61.88	0.21	1.00	0.84	0.20	22.42	1.00
323 K	0.06	53.76	0.99	6.56	0.52	0.97	9.13	1.16	0.99	0.34	6.62	0.81	1.00	0.64	62.72	0.22	1.00	0.86	0.20	24.94	1.00

Table 6.3.15. Isotherm parameters for the adsorption of Py and its derivatives onto RHA at different temperatures.

Model Constants	Langmuir			Freundlich			Temkin			Redlich-Peterson				Toth Isotherm				Radke-Prausnitz			
	K_L	q_m	R^2	K_F	$1/n$	R^2	B	K_T	R^2	a_R	K_R	β	R^2	Th	q_e^{inf}	K_{Th}	R^2	P	K_{RP}	k_{RP}	R^2
Py																					
283 K	0.03	11.72	0.99	0.59	0.60	0.98	2.22	0.40	0.97	0.26	0.54	0.65	0.99	0.87	12.79	22.54	1.00	0.86	0.06	5.85	1.00
293 K	0.03	11.70	1.00	0.66	0.59	0.98	2.24	0.47	0.97	0.25	0.60	0.67	0.99	0.87	12.69	19.62	1.00	0.93	0.05	8.32	1.00
303 K	0.04	11.66	1.00	0.71	0.58	0.98	2.22	0.52	0.97	0.25	0.66	0.68	0.99	0.88	12.54	18.16	1.00	0.95	0.05	8.97	1.00
313 K	0.04	11.63	0.99	0.74	0.58	0.97	2.23	0.55	0.97	0.21	0.65	0.72	0.99	0.88	12.43	17.31	1.00	0.97	0.05	9.93	1.00
323 K	0.04	11.59	1.00	0.78	0.58	0.96	2.27	0.59	0.98	0.18	0.65	0.73	0.99	0.89	12.35	15.90	1.00	0.98	0.05	10.76	1.00
2Pi																					
283 K	0.02	16.81	0.99	1.19	0.46	0.99	3.11	0.31	0.97	0.35	0.95	0.69	1.00	0.28	60.35	0.43	1.00	0.70	0.30	2.88	1.00
293 K	0.02	16.75	0.99	1.40	0.43	0.99	3.03	0.41	0.98	0.37	1.16	0.71	1.00	0.30	46.14	0.45	1.00	0.72	0.33	3.31	1.00
303 K	0.03	16.69	0.99	1.65	0.41	0.98	2.94	0.55	0.99	0.32	1.30	0.76	1.00	0.33	36.56	0.47	1.00	0.75	0.32	4.02	1.00
313 K	0.03	16.64	0.99	1.76	0.40	0.97	2.94	0.61	0.99	0.38	1.49	0.74	1.00	0.34	34.55	0.48	1.00	0.80	0.23	5.25	1.00
323 K	0.05	16.58	1.00	2.09	0.38	0.97	2.82	0.90	0.99	0.41	1.97	0.78	1.00	0.35	30.46	0.56	1.00	0.85	0.20	7.05	1.00
4Pi																					
283 K	0.03	17.33	0.99	1.55	0.43	0.99	3.16	0.47	0.99	0.15	0.91	0.82	1.00	0.45	27.66	0.28	1.00	0.74	0.37	3.80	1.00
293 K	0.03	17.57	0.99	1.64	0.43	0.98	3.17	0.51	0.99	0.18	1.03	0.81	1.00	0.46	27.25	0.28	1.00	0.75	0.34	4.14	1.00
303 K	0.05	17.79	0.99	1.79	0.41	0.98	3.12	0.61	0.99	0.36	1.55	0.75	1.00	0.46	26.66	0.30	1.00	0.76	0.33	4.52	1.00
313 K	0.04	17.89	0.99	1.91	0.41	0.98	3.10	0.70	0.99	0.44	1.85	0.74	1.00	0.46	26.23	0.32	1.00	0.78	0.30	5.13	1.00
323 K	0.04	18.15	0.99	2.09	0.40	0.98	3.08	0.84	0.99	0.44	2.09	0.76	1.00	0.48	25.34	0.33	1.00	0.79	0.32	5.53	1.00
AmPy																					
283 K	0.03	9.67	1.00	0.88	0.42	0.96	1.83	0.38	1.00	0.07	0.35	0.89	1.00	0.64	11.63	0.13	1.00	0.86	0.10	4.11	1.00
293 K	0.03	10.70	1.00	0.92	0.44	0.96	2.02	0.39	1.00	0.14	0.48	0.80	0.99	0.67	12.64	0.11	1.00	0.86	0.09	4.86	1.00
303 K	0.03	11.61	0.99	1.05	0.43	0.97	2.12	0.48	0.99	0.13	0.58	0.84	1.00	0.69	13.37	0.11	1.00	0.88	0.08	5.69	1.00
313 K	0.03	12.33	0.99	1.12	0.44	0.97	2.26	0.52	1.00	0.10	0.61	0.89	1.00	0.74	13.74	0.10	1.00	0.88	0.09	6.17	1.00
323 K	0.04	12.95	0.99	1.22	0.44	0.97	2.34	0.60	0.99	0.19	0.84	0.81	1.00	0.75	14.29	0.10	1.00	0.89	0.09	6.96	1.00

Table 6.3.16. Isotherm parameters for the adsorption of Py and its derivatives onto GAC at different temperatures.

Model	Langmuir			Freundlich			Temkin			Redlich-Peterson				Toth Isotherm				Radke-Prausnitz			
Constants	K_L	q_m	R^2	K_F	$1/n$	R^2	B	K_T	R^2	a_R	K_R	β	R^2	Th	q_e^{inf}	K_{Th}	R^2	P	K_{RP}	k_{RP}	R^2
Py																					
283 K	0.03	20.49	0.99	1.06	0.60	0.99	3.85	0.45	0.97	0.15	0.85	0.73	1.00	0.56	34.79	7.57	1.00	0.75	0.14	6.15	1.00
293 K	0.04	20.41	1.00	1.22	0.59	0.98	3.87	0.54	0.97	0.22	1.11	0.70	0.99	0.57	33.13	6.76	1.00	0.77	0.16	6.67	1.00
303 K	0.04	20.37	0.99	1.41	0.58	0.98	3.82	0.67	0.97	0.23	1.33	0.73	1.00	0.58	31.47	6.04	1.00	0.80	0.15	7.93	1.00
313 K	0.05	20.33	0.99	1.59	0.56	0.98	3.78	0.80	0.97	0.39	1.82	0.67	1.00	0.58	30.36	5.41	1.00	0.81	0.16	8.45	1.00
323 K	0.06	20.28	0.99	1.70	0.56	0.98	3.78	0.89	0.97	0.31	1.82	0.72	1.00	0.60	28.95	5.30	1.00	0.82	0.17	9.07	1.00
2Pi																					
283 K	0.01	42.55	0.97	1.87	0.54	1.00	8.02	0.22	0.95	0.34	1.57	0.62	1.00	0.29	209.37	0.29	1.00	0.570	0.60	3.53	1.00
293 K	0.02	42.19	0.98	2.09	0.53	0.99	7.99	0.25	0.96	0.27	1.59	0.65	1.00	0.31	172.42	0.30	1.00	0.623	0.38	4.87	1.00
303 K	0.02	42.02	0.98	2.31	0.51	0.99	7.90	0.29	0.97	0.23	1.67	0.69	1.00	0.34	131.18	0.29	1.00	0.669	0.28	6.38	1.00
313 K	0.02	41.84	0.99	2.57	0.51	0.98	7.69	0.35	0.98	0.20	1.75	0.72	1.00	0.39	97.40	0.26	1.00	0.765	0.14	11.21	1.00
323 K	0.03	41.67	0.99	2.98	0.48	0.98	7.77	0.41	0.98	0.24	2.23	0.73	1.00	0.41	83.76	0.28	1.00	0.761	0.19	11.30	1.00
4Pi																					
283 K	0.02	38.61	0.98	2.52	0.48	0.99	7.16	0.33	0.97	0.25	1.80	0.71	1.00	0.30	130.48	0.37	1.00	0.60	1.34	3.82	1.00
293 K	0.02	39.22	0.98	2.75	0.47	0.98	7.14	0.37	0.97	0.41	2.52	0.68	0.99	0.35	98.31	0.34	1.00	0.60	1.39	4.08	1.00
303 K	0.02	40.49	0.98	3.02	0.46	1.00	7.22	0.43	0.96	0.73	3.88	0.64	1.00	0.40	80.17	0.29	1.00	0.61	1.21	4.58	1.00
313 K	0.03	41.32	0.97	3.28	0.46	0.98	7.29	0.49	0.96	0.67	4.04	0.66	1.00	0.40	79.24	0.31	1.00	0.62	1.26	4.91	1.00
323 K	0.03	41.49	0.97	3.80	0.44	1.00	7.09	0.64	0.96	1.06	6.39	0.65	1.00	0.41	73.29	0.34	1.00	0.63	1.82	5.27	1.00
AmPy																					
283 K	0.02	23.04	0.98	1.47	0.50	0.99	4.19	0.40	0.96	0.50	1.58	0.64	1.00	0.25	132.12	0.44	1.00	0.65	0.43	3.39	1.00
293 K	0.03	24.51	0.98	1.78	0.50	0.99	4.44	0.53	0.97	0.29	1.60	0.72	1.00	0.32	75.97	0.37	1.00	0.66	0.48	4.11	1.00
303 K	0.04	25.13	0.98	2.22	0.48	0.97	4.49	0.74	0.97	0.37	2.27	0.72	0.96	0.41	49.13	0.33	0.99	0.67	0.61	4.70	1.00
313 K	0.06	25.71	0.99	2.89	0.46	0.98	4.40	1.23	0.97	0.49	3.66	0.75	1.00	0.44	42.13	0.39	1.00	0.70	0.83	5.80	1.00
323 K	0.07	27.62	0.99	2.94	0.50	0.95	5.03	1.13	0.99	0.68	4.23	0.67	0.95	0.46	47.30	0.35	0.99	0.77	0.36	9.23	1.00

Table 6.3.17. Error analyses functions for adsorption of Py and its derivatives onto BFA.

Temperature(K)/ Isotherms	Py			2Pi			4Pi			AmPy		
	HYBRID	MPSD	χ2	HYBRID	MPSD	χ2	HYBRID	MPSD	χ2	HYBRID	MPSD	χ2
Langmuir												
283	0.84	15.56	0.14	5.60	26.20	7.55	3.77	9.77	0.76	4.01	12.45	1.03
293	0.55	17.77	0.18	-3.40	19.63	4.25	6.60	14.90	1.87	4.89	14.79	1.59
303	0.71	11.65	0.08	3.78	24.94	6.75	8.05	18.03	3.40	6.78	19.17	2.69
313	0.98	11.80	0.15	9.54	31.49	12.59	10.24	22.88	5.86	6.84	20.82	3.20
323	1.23	22.54	0.58	10.35	39.38	33.89	12.19	26.79	8.63	7.53	21.93	3.41
Freundlich												
283	-0.38	23.42	0.65	-0.62	9.50	1.40	-1.79	17.89	4.27	-1.05	16.22	2.32
293	-0.76	26.87	0.82	-12.84	16.40	1.94	-1.16	16.83	3.86	-1.29	17.32	2.59
303	-1.20	34.25	1.46	-9.84	16.44	1.74	-1.58	18.24	4.02	-1.06	16.24	2.35
313	-2.07	45.40	2.45	-11.42	20.48	2.04	-1.49	17.77	3.90	-1.26	16.11	2.56
323	-3.13	48.44	2.88	-24.36	37.92	5.66	-1.29	16.91	3.55	-57.01	60.36	46.70
Temkin												
283	12.90	44.72	-11.42	2.53	28.98	7.21	-6.69	9.86	0.61	1.46	6.23	0.17
293	12.32	97.55	-10.15	-15.18	18.33	2.73	-0.77	3.25	0.13	1.58	6.27	0.23
303	11.38	77.21	-24.11	-12.76	16.42	2.07	-1.05	5.08	0.17	2.65	10.48	0.64
313	9.25	56.75	7.03	-17.08	24.70	3.14	-0.73	4.08	0.13	3.19	13.35	1.06
323	4.71	37.49	1.13	-38.30	58.26	13.05	-0.21	3.37	0.15	4.09	17.05	1.68
Redlich-Peterrson												
283	-0.30	11.76	0.18	-0.11	10.65	1.22	0.37	1.55	0.03	-0.44	4.59	0.22
293	-0.43	16.99	0.28	-18.85	20.24	2.33	0.04	0.88	0.01	-0.69	6.05	0.26
303	-0.22	11.63	0.22	-15.87	18.90	1.98	-0.29	5.54	0.25	-0.32	6.23	0.25
313	-0.53	14.69	0.16	-21.03	28.07	3.05	-1.10	6.60	0.53	-0.97	6.99	0.33
323	-3.20	42.54	1.89	-53.67	75.99	15.46	-0.50	5.79	0.36	-0.13	4.36	0.17
Toth												
283	-0.04	5.97	0.06	-0.25	12.86	0.93	-0.78	5.51	0.14	-0.43	4.91	0.11
293	0.03	8.40	0.10	-16.93	17.65	1.71	0.06	2.60	0.04	0.45	6.63	0.25
303	-0.34	5.62	0.10	-9.36	13.76	1.00	0.38	6.65	0.36	1.40	8.22	0.46
313	-0.69	8.06	0.17	-17.99	22.44	2.34	1.52	7.49	0.56	1.52	9.83	0.65
323	-0.30	13.29	0.55	-43.79	52.90	12.03	3.54	11.13	1.15	1.96	9.98	0.62
Radke-Prausnitz												
283	-2.06	6.62	0.07	2.21	17.47	1.66	-0.16	1.62	0.03	-0.75	4.80	0.18
293	0.04	8.61	0.11	-15.96	15.96	1.61	-0.19	0.94	0.01	-0.94	6.78	0.34
303	-0.80	6.24	0.11	-8.65	10.31	1.18	-0.81	5.83	0.33	-0.65	6.29	0.25
313	-0.20	12.80	0.12	-9.59	10.89	1.23	-0.80	5.59	0.32	-0.50	7.18	0.36
323	-0.20	12.80	0.52	6.24	36.03	15.27	-0.51	6.06	0.41	0.06	5.50	0.32

Table 6.3.18. Error analyses functions for adsorption of Py and its derivatives onto RHA.

Temperature(K)/	Py			2Pi			4Pi			AmPy		
Isotherms	HYBRID	MPSD	$\chi 2$	HYBRID	MPSD	$\chi 2$	HYBRID	MPSD	$\chi 2$	HYBRID	MPSD	$\chi 2$
Langmuir												
283	2.10	9.19	0.06	4.15	18.01	0.73	5.45	15.59	0.58	3.15	9.07	0.13
293	1.31	9.04	0.06	5.77	19.25	0.86	5.20	16.22	0.64	4.22	11.00	0.20
303	0.27	9.54	0.09	6.30	20.45	1.02	-21.02	24.62	2.48	4.64	14.70	0.36
313	1.57	8.00	0.05	5.47	17.36	0.72	6.32	20.42	1.03	4.75	13.80	0.33
323	0.11	4.24	0.02	6.39	19.10	0.84	8.08	22.24	1.27	5.21	16.57	0.46
Freundlich												
283	-0.84	11.84	0.42	-0.17	6.74	0.16	-0.91	12.43	0.55	-1.35	15.60	0.50
293	-0.77	13.91	0.61	-0.59	7.82	0.22	-0.70	12.36	0.56	-0.95	15.57	0.51
303	-0.97	13.74	0.60	-0.32	9.57	0.31	-0.67	10.56	0.45	-0.69	13.17	0.40
313	-0.97	15.27	0.71	-0.63	12.40	0.56	-0.40	10.58	0.48	-0.91	15.08	0.54
323	-1.71	18.62	0.98	-0.76	12.92	0.75	-0.72	11.31	0.53	-1.01	13.55	0.51
Temkin												
283	8.90	43.50	8.56	3.84	20.24	0.91	2.68	12.23	0.29	0.24	1.81	0.00
293	8.49	43.35	7.62	3.55	18.43	0.73	2.68	12.83	0.32	0.95	4.30	0.02
303	8.47	41.65	5.56	3.02	14.95	0.47	3.37	17.06	0.61	2.32	10.79	0.15
313	-0.86	35.81	1.72	2.23	10.88	0.22	3.44	17.79	0.66	2.27	9.53	0.11
323	6.75	34.25	1.83	2.08	12.85	0.29	3.32	16.46	0.57	3.38	15.18	0.33
Redlich-Peterrson												
283	-0.38	6.60	0.10	-0.28	1.82	0.01	-0.06	1.89	0.02	-0.61	3.36	0.02
293	-0.43	8.26	0.17	0.11	0.75	0.00	-0.29	1.81	0.02	0.09	5.73	0.05
303	-0.21	7.17	0.14	-7.83	6.87	0.22	-0.10	2.21	0.02	-0.29	2.45	0.02
313	0.07	7.11	0.13	0.35	3.72	0.05	0.11	2.39	0.02	-0.29	4.40	0.05
323	-0.45	8.69	0.22	0.13	3.73	0.05	0.25	1.65	0.01	-0.20	3.67	0.03
Toth												
283	0.35	8.13	0.04	0.08	2.08	0.01	0.31	3.25	0.03	0.29	4.49	0.02
293	0.17	8.44	0.05	0.28	1.30	0.00	0.48	2.98	0.03	0.11	5.09	0.04
303	0.55	8.77	0.06	0.26	2.75	0.02	0.37	3.70	0.04	1.80	6.56	0.07
313	0.34	7.07	0.04	-0.98	4.74	0.04	0.36	3.76	0.03	1.22	6.88	0.08
323	-0.47	4.18	0.02	-0.23	3.48	0.04	0.23	4.30	0.05	2.69	10.23	0.15
Radke-Prausnitz												
283	1.02	6.60	0.06	0.03	1.90	0.01	-0.01	1.99	0.02	-0.75	6.48	0.09
293	2.10	9.00	0.15	-0.06	0.74	0.00	0.01	1.85	0.02	-0.84	5.91	0.06
303	-24.40	24.97	0.42	-0.55	1.91	0.01	0.04	2.20	0.02	-0.18	2.28	0.02
313	0.99	6.50	0.08	-0.14	2.21	0.02	0.04	2.33	0.02	-0.52	3.83	0.02
323	1.05	5.12	0.05	0.17	3.60	0.04	0.04	1.62	0.01	0.01	4.31	0.05

Table 6.3.19. Error analyses functions for adsorption of Py and its derivatives onto GAC.

Temperature (K)/ Isotherms	Py			2Pi			4Pi			AmPy		
	HYBRID	MPSD	χ^2	HYBRID	MPSD	χ^2	HYBRID	MPSD	χ^2	HYBRID	MPSD	χ^2
Langmuir												
283	0.41	7.85	0.16	0.90	15.00	1.25	3.47	16.73	1.48	4.24	19.13	0.96
293	-0.10	7.67	0.10	2.07	14.68	1.19	5.97	19.74	1.99	5.39	18.79	1.02
303	1.42	9.13	0.17	-3.30	14.00	1.31	6.33	21.85	2.52	5.63	20.34	1.63
313	1.44	10.27	0.22	2.79	11.51	0.66	5.32	22.37	2.78	7.08	22.08	1.54
323	1.41	9.69	0.18	3.74	13.79	0.89	8.32	25.80	3.88	4.73	16.03	1.12
Freundlich												
283	-0.48	11.17	0.47	-0.13	5.20	0.16	-0.17	8.05	0.41	-0.32	6.66	0.20
293	-0.73	13.29	0.86	-0.53	7.33	0.33	0.00	6.79	0.31	-0.30	9.53	0.32
303	-0.75	12.63	0.70	-8.03	10.82	1.29	-0.34	5.53	0.24	-1.29	16.83	0.70
313	-0.63	12.76	0.73	-0.80	11.28	1.10	-0.30	6.19	0.26	-0.89	12.47	0.69
323	-1.08	13.92	0.90	-0.72	11.22	1.24	0.01	5.74	0.25	-2.42	22.72	1.65
Temkin												
283	9.32	38.38	6.21	6.02	30.21	5.70	4.73	22.48	2.54	6.70	32.45	3.81
293	9.25	42.95	13.69	5.65	26.56	3.91	5.06	25.21	3.46	6.95	29.39	2.87
303	9.35	40.38	8.72	5.38	26.19	3.73	5.72	29.12	5.30	4.54	17.44	0.98
313	9.51	41.23	10.38	5.08	18.68	1.61	5.69	28.46	5.06	7.38	29.42	3.05
323	9.38	40.78	9.41	4.81	24.04	2.81	5.97	30.32	6.22	3.39	11.54	0.47
Redlich-Peterrson												
283	-0.17	1.76	0.01	-0.25	1.66	0.02	0.07	2.16	0.05	0.02	2.68	0.03
293	-0.47	6.01	0.13	-0.18	2.77	0.03	-0.23	1.52	0.03	0.01	3.90	0.05
303	-0.01	3.25	0.04	0.06	1.37	0.01	0.38	1.15	0.01	-1.45	12.45	0.27
313	-0.08	4.82	0.10	0.15	2.36	0.05	0.02	1.64	0.03	-0.08	2.51	0.04
323	-0.24	4.17	0.07	0.03	3.12	0.06	0.18	1.88	0.03	-2.09	17.76	0.65
Toth												
283	-0.26	1.82	0.01	-0.90	2.45	0.05	-0.52	3.19	0.06	-0.67	2.89	0.02
293	-0.18	4.72	0.05	0.50	3.43	0.05	-0.62	3.19	0.10	-0.12	4.41	0.04
303	-0.14	2.59	0.02	-1.17	2.19	0.02	0.00	5.87	0.21	-0.19	12.85	0.34
313	0.18	3.12	0.03	-0.27	3.41	0.04	0.01	6.17	0.27	0.05	4.54	0.11
323	-0.25	2.99	0.02	-0.35	2.88	0.05	0.86	8.14	0.39	-0.91	16.40	0.40
Radke-Prausnitz												
283	0.01	1.52	0.01	0.05	1.86	0.04	0.05	2.37	0.07	0.07	3.03	0.03
293	0.86	5.51	0.07	0.07	4.04	0.16	-0.02	1.59	0.03	-0.08	4.40	0.08
303	0.22	3.01	0.03	0.20	3.03	0.10	0.05	1.12	0.01	-1.07	12.30	0.38
313	0.29	3.47	0.04	-0.04	0.72	0.00	0.02	1.72	0.04	-0.04	2.67	0.05
323	0.36	3.73	0.04	0.35	3.45	0.06	-0.01	1.94	0.04	-2.74	15.33	0.81

6.3.9 Estimation of Thermodynamic Parameters

As discussed in Chapter III, The Gibbs free energy change of the adsorption process is related to the adsorption equilibrium constant by the classical Van't Hoff equation:

$$\Delta G^0_{ads} = -RT \ln K_{ads} \tag{6.3.24}$$

The Gibbs free energy change is also related to the change in entropy and heat of adsorption at a constant temperature as given by the equation:

$$\Delta G^0_{ads} = \Delta H^0 - T\Delta S^0 \tag{6.3.25}$$

The above two equations give,

$$\ln K_{ads} = \frac{-\Delta G^0_{ads}}{RT} = \frac{\Delta S^0}{R} - \frac{\Delta H^0}{R}\frac{1}{T} \tag{6.3.26}$$

where, ΔG^0_{ads} is the free energy change (kJ mol^{-1}), ΔH^0 is the change in enthalpy (kJ mol^{-1}), ΔS^0 is the entropy change (kJ mol^{-1} K^{-1}), K_{ads} is the equilibrium constant of interaction between the adsorbate and the BFA surface, T is the absolute temperature (K) and R is the universal gas constant (8.314 J mol^{-1} K^{-1}). Thus ΔH^0 can be determined by the slope of the linear Van't Hoff plot i.e. as $\ln(K_{ads})$ versus $(1/T)$, using the equation:

$$\Delta H^0 = \left[R\frac{d\ln K}{d(1/T)} \right] \tag{6.3.27}$$

This ΔH^0 corresponds to the isosteric heat of adsorption ($\Delta H_{st,0}$) with zero surface coverage (i.e. $q_e = 0$) (Suzuki, 1990). K_{ad} at $q_e = 0$ was obtained from the intercept of the $\ln(q_e/C_e)$ versus q_e plot (Khan and Singh, 1987). Figs. 6.3.19 shows the Van't Hoff's plot for $\ln(q_e/C_e)$ Vs q_e, from which ΔH^0 and ΔS^0 values have been estimated (Table 6.3.20 to Table 6.3.22).

172

Table 6.3.20. Thermodynamic parameters for the sorption of Py, 2Pi, 4Pi and AmPy onto BFA

Compounds	ΔG^0_{ads} (kJ mol^{-1})					ΔH^0 (kJ mol^{-1})	ΔS^0 (kJ mol^{-1} K^{-1})
	283 K	293 K	303 K	313 K	323 K		
Py	-17.99	-19.47	-20.96	-22.44	-23.92	23.98	0.15
2Pi	-18.27	-22.77	-27.26	-31.76	-36.25	108.96	0.45
4Pi	-20.79	-22.21	-23.63	-25.05	-26.46	19.32	0.14
AmPy	-19.00	-20.22	-21.44	-22.66	-23.88	15.54	0.12

Table 6.3.21. Thermodynamic parameters for the sorption of Py, 2Pi, 4Pi and AmPy onto RHA.

Compounds	ΔG^0_{ads} (kJ mol^{-1})					ΔH^0 (kJ mol^{-1})	ΔS^0 (kJ mol^{-1} K^{-1})
	283 K	293 K	303 K	313 K	323 K		
Py	-14.19	-14.97	-15.76	-16.55	-17.33	8.03	0.08
2Pi	-15.11	-16.39	-17.66	-18.93	-20.21	20.97	0.13
4Pi	-16.21	-17.19	-18.17	-19.15	-20.14	11.61	0.10
AmPy	-14.46	-15.43	-16.39	-17.36	-18.32	12.84	0.10

Table 6.3.22. Thermodynamic parameters for the sorption of Py, 2Pi, 4Pi and AmPy onto GAC.

Compounds	ΔG^0_{ads} (kJ mol^{-1})					ΔH^0 (kJ mol^{-1})	ΔS^0 (kJ mol^{-1} K^{-1})
	283 K	293 K	303 K	313 K	323 K		
Py	-15.66	-16.72	-17.78	-18.84	-19.90	14.39	0.11
2Pi	-15.92	-16.98	-18.03	-19.08	-20.14	13.90	0.11
4Pi	-16.91	-17.96	-19.02	-20.08	-21.14	13.04	0.11
AmPy	-16.02	-17.51	-18.99	-20.48	-21.97	26.08	0.15

173
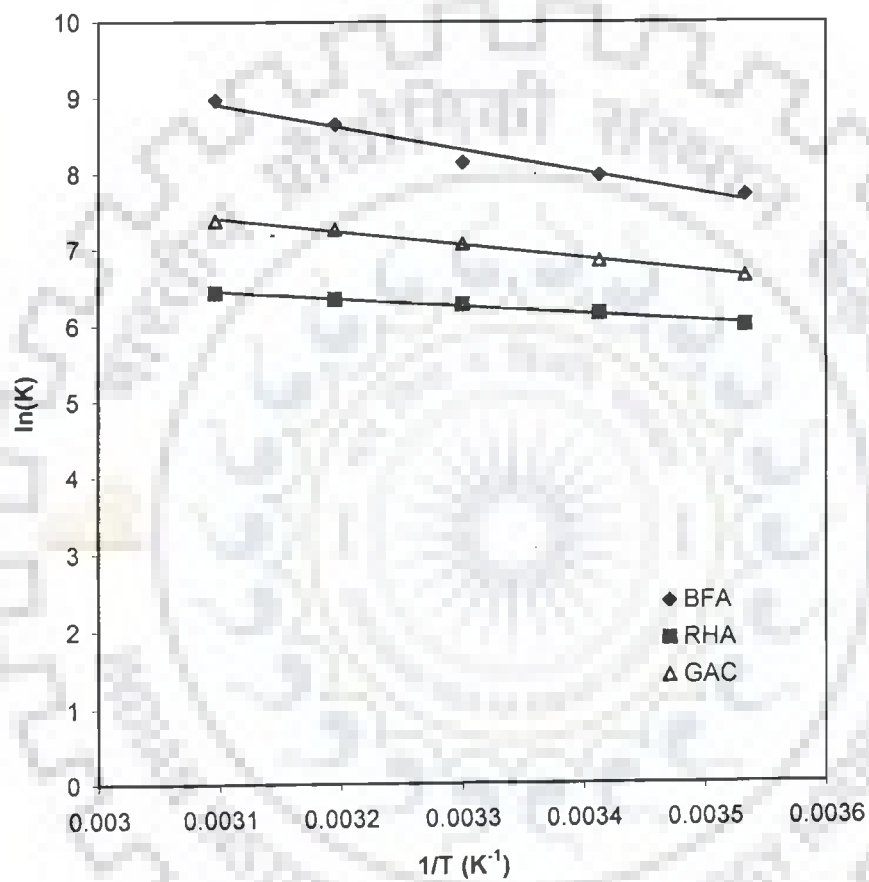
Fig. 6.3.19. Van't Hoff plot for the adsorption of Py onto BFA, RHA and GAC.

For significant adsorption to occur, the free energy change of adsorption, ΔG_{ads}^0, must be negative. The thermodynamic relation between ΔG_{ads}^0, ΔH^0 and ΔS^0 suggests that either (i) ΔH^0 is positive and ΔS^0 is positive and that the value of $T\Delta S$ is much larger than ΔH^0, or (ii) ΔH^0 is negative and ΔS^0 is positive or that the value of ΔH^0 is more than $T\Delta S$. The adsorption of Py, 2Pi, 4Pi and 3-aminoyridine onto BFA, RHA and GAC is endothermic in nature, giving a positive value of ΔH^0. Hence, ΔS^0 has to be positive and that the positive value of $T\Delta S$ has to be larger than ΔH^0. The positive ΔH^0 value confirms the endothermic nature of the overall-sorption process. The adsorption process in the solid-liquid system is a combination of two processes: (a) the desorption of the solvent (water) molecules previously adsorbed, and (b) the adsorption of the adsorbate species. The adsorbates have to displace more than one water molecule for their adsorption and this results in the endothermicity of the adsorption process. Therefore, ΔH^0 will be positive. The positive value of ΔS^0 suggests increased randomness at the solid-solution interface with some structural changes in the adsorbate and adsorbent and an affinity of the BFA, RHA and GAC towards Py, 2Pi, 4Pi and 3-aminoyridine (Ho and Ofomaja, 2005). Also, positive ΔS^0 value corresponds to an increase in the degree of freedom of the adsorbed species (Raymon, 1998). ΔG_{ads}^0 values are negative indicating that the sorption process led to a decrease in Gibbs free energy. Negative ΔG_{ads}^0 indicates the feasibility and spontaneity of the adsorption process.

6.3.10 Isosteric Heat of Adsorption

Apparent isosteric heat of adsorption ($\Delta H_{st,a}$) at constant surface coverage (by considering the range of q_e values obtained in each experiment. e.g. for Py adsorption on BFA q_e =4, 8, 12, 16, 20 mg g^{-1}) is calculated using Clausius-Clapeyron equation (Young and Crowell, 1962).

$$\frac{d \ln C_e}{dT} = \frac{-\Delta H_{st,a}}{RT^2} \tag{6.3.28}$$

or $\quad \Delta H_{st,a} = R \left. \dfrac{d \ln C_e}{d(1/T)} \right|_{q_e}$ $\hfill$ (6.3.29)

For this purpose, the equilibrium concentration (C_e) at a constant equilibrium amount of adsorbed solute, q_e, is obtained from the adsorption isotherm data at different temperatures. $\Delta H_{st,a}$ is calculated from the slope of the $\ln C_e$ versus ($1/T$) plot for different q_e of Py, 2Pi, 4Pi and AmPy onto BFA, RHA and GAC. The isosters corresponding to different equilibrium adsorption uptake of Py by BFA is shown in Fig. 6.3.20. Similar isosters were obtained for other systems as well. The linear regression correlation coefficients of the isosters and the corresponding isosteric enthalpies for all the adsorbate and adsorbent systems are presented in Table 6.3.23.

The results shown in Table 6.3.23 suggest that Eq. (6.3.28) represents the experimental data very well. The variation of $\Delta H_{st,a}$ for the adsorption of Py and 2Pi with the surface loading is presented in Fig. 6.3.21. The $\Delta H_{st,a}$ is high at very low coverage and decreases steadily with q_e indicating that the BFA, RHA and GAC have energetically heterogeneous surfaces. The dependence of heat of adsorption with surface coverage is usually observed to display the adsorbent-adsorbate interaction followed by the adsorbate-adsorbate interaction. The adsorbent-adsorbate interaction takes place initially at lower q_e values resulting in high heats of adsorption. On the other hand, adsorbate-adsorbate interaction occurs with an increase in the surface coverage. The variation in $\Delta H_{st,a}$ with surface loading can also be attributed to the possibility of having lateral interactions between adsorbed solute. Similar trends were obtained for the adsorption of 2Pi onto BFA, RHA and GAC. The increase in $\Delta H_{st,a}$ is observed in the system, adsorption of 4Pi and AmPy onto BFA, RHA and GAC. The increase in the $\Delta H_{st,a}$ values for 4Pi and AmPy with surface loadings may be attributed to interactions of 4Pi and AmPy molecules with the adsorbents. Similar results were reported by Liu and Ren [2006] and Srivastava et al. [2006b]. The positive values of isosteric heat of adsorption for all the adsorbate-adsorbent systems shows that the sorption of Py, 2Pi, 4Pi and AmPy by BFA, RHA and GAC is an endothermic process.
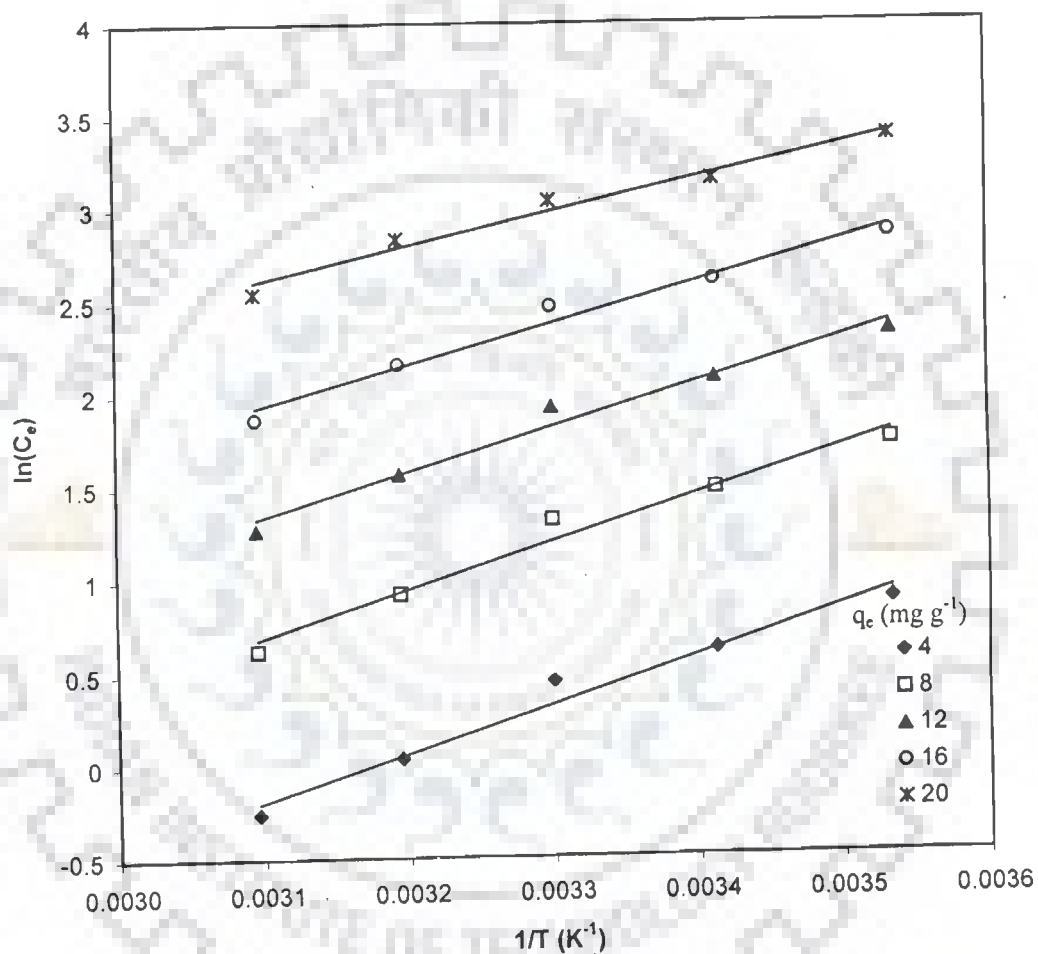
Fig. 6.3.20. Adsorption isosters for determining isosteric heat of adsorption for Py-BFA system.
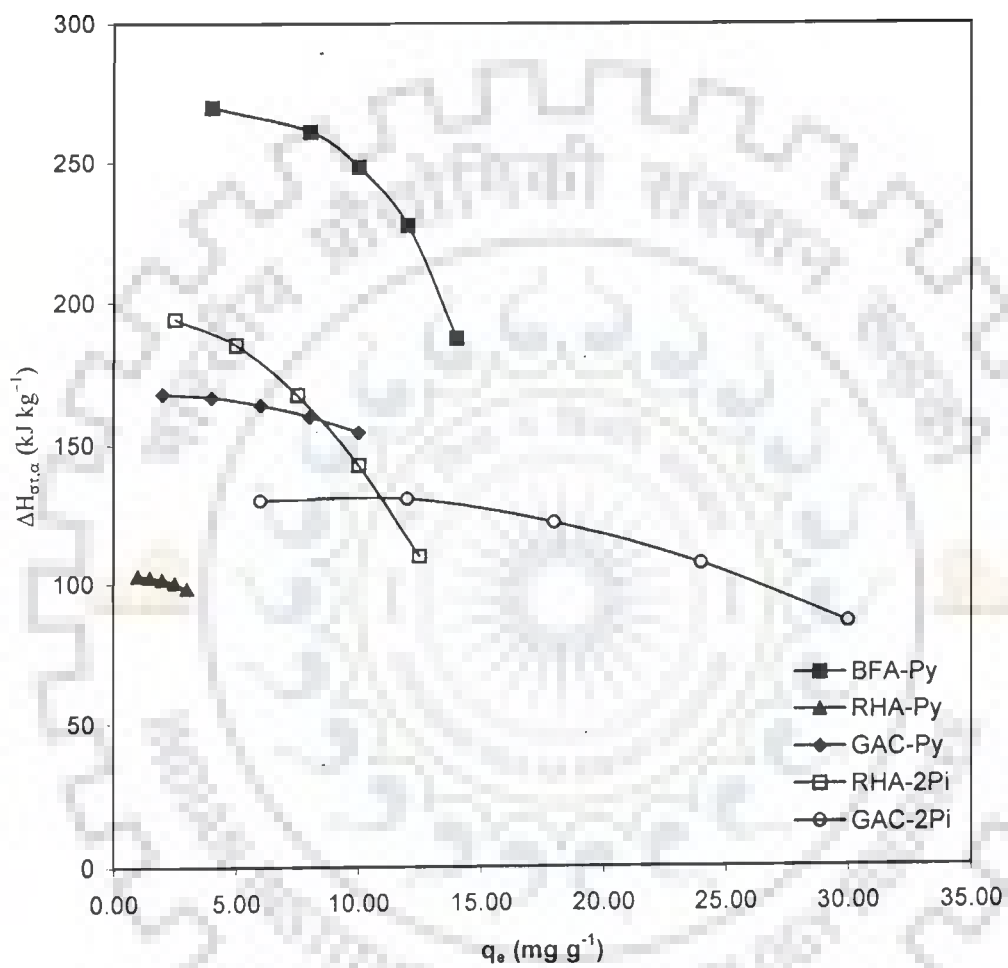
Fig. 6.3.21. Variation of $\Delta H_{st,a}$ with respect to surface loading of the Py and 2Pi for adsorption onto BFA..

Table 6.3.23. Isosteric enthalpy of Py and its derivatives onto BFA, RHA and GAC.

BFA	Py					2Pi				
q_e (mg g^{-1})	4.00	8.00	10.00	12.00	14.00	10.00	20.00	30.00	40.00	50.00
$\Delta H_{st, a}$ (kJ kg^{-1})	269.92	261.27	248.47	227.66	187.63	378.03	376.86	374.87	370.91	359.25
	4Pi					AmPy				
q_e (mg g^{-1})	10.00	20.00	30.00	40.00	50.00	8.00	16.00	24.00	32.00	40.00
$\Delta H_{st, a}$ (kJ kg^{-1})	147.78	169.58	195.03	232.32	307.55	142.41	154.13	173.49	211.91	330.71
RHA										
	Py					2Pi				
q_e (mg g^{-1})	1.00	1.50	2.00	2.50	3.00	2.50	5.00	7.50	10.00	12.50
$\Delta H_{st, a}$ (kJ kg^{-1})	103.14	102.59	101.80	100.59	98.51	194.28	185.26	167.74	142.94	109.97
	4Pi					AmPy				
q_e (mg g^{-1})	3.00	6.00	9.00	12.00	15.00	1.50	3.00	4.50	6.00	7.50
$\Delta H_{st, a}$ (kJ kg^{-1})	83.38	86.15	90.82	100.39	131.21	121.21	149.59	179.33	215.05	263.51
GAC										
	Py					2Pi				
q_e (mg g^{-1})	2.00	4.00	6.00	8.00	10.00	6.00	12.00	18.00	24.00	30.00
$\Delta H_{st, a}$ (kJ kg^{-1})	168.10	166.94	164.22	160.14	154.57	130.19	130.85	122.24	107.24	86.24
	4Pi					AmPy				
q_e (mg g^{-1})	6.00	12.00	18.00	24.00	30.00	4.00	8.00	12.00	16.00	20.00
$\Delta H_{st, a}$ (kJ kg^{-1})	123.66	134.83	135.34	128.45	114.30	276.04	304.28	311.99	306.24	287.85

6.4 BATCH ADSORPTION STUDY USING TAGUCHI'S DESIGN OF EXPERIMENTAL METHODOLOGY

In this section, the results of Taguchi's method for optimizing the design of experiments will be discussed. The effect of individual process parameters and their interactions on the selected response/quality characteristics will also be discussed. The mean or the average values and S/N ratio of the quality/response characteristics for each parameter at different levels have been calculated from experimental data. For the graphical representation of the change in value of quality characteristic and that of S/N ratio with the variation in process parameters, the response curves have been plotted. These response curves have been used for examining the parametric effects on the response characteristics. The analysis of variance (ANOVA) for raw data and S/N data has been performed to identify the significant parameters and to quantify their effect on the response characteristics. The most favorable conditions (optimal settings) of process parameters in terms of mean response of characteristics have been established by analyzing response curves and the ANOVA tables.

6.4.1 Experiment Results of Single, Binary and Ternary Batch Study

In single batch system, the removal of Py, 2Pi, 4Pi and AmPy was studied individually. The main parameters studied in single batch adsorption study are: initial concentrations ($C_{0,i}$), adsorbent dosage (m), temperature (T) and contact time (t). Similarly the removal of Py, 2Pi, 4Pi was studied in the binary system in three combinations of i) Py and 2Pi ii) Py and 4Pi and iii) 2Pi and 4Pi. The main parameters studied in binary systems were $C_{0,i}$, m and t. Similarly the removal of Py, 2Pi, 4Pi was studied simultaneously. The main parameters studied are, $C_{0,i}$, T, initial pH (pH_0), m and contact time t. The parameters and OA are selected so as to have the equal DOF of Taguchi array and the total DOF of the experiment [Roy, 1990]. Experiments were conducted according to the test conditions specified by L₉ OA (Table 4.4.4, Chapter IV) for single and binary system and L₂₇ OA (Table 4.4.5, Chapter IV) for ternary system.

Table 6.4.1. Experimental q_{tot} values for adsorption of Py, 2Pi, 4Pi and AmPy onto BFA using Taguchi design of experiment.

Trial No.	Py				2Pi				4Pi				AmPy			
	q_{tot} (mg g^{-1})			S/N Ratio (dB)	q_{tot} (mg g^{-1})			S/N Ratio (dB)	q_{tot} (mg g^{-1})			S/N Ratio (dB)	q_{tot} (mg g^{-1})			S/N Ratio (dB)
	R_1	R_2	R_3		R_1	R_2	R_3		R_1	R_2	R_3		R_1	R_2	R_3	
1	7.87	7.86	7.89	17.92	11.76	11.77	11.78	21.41	12.01	12.02	12.00	21.59	7.95	8.30	8.30	18.25
2	11.45	11.47	11.51	21.20	18.73	18.69	18.66	25.43	19.10	19.07	19.15	25.62	11.73	12.43	12.43	21.71
3	28.68	28.81	28.63	29.16	34.38	33.38	34.50	30.65	53.83	72.77	54.50	35.37	26.83	27.58	27.00	28.67
4	5.61	5.60	5.62	14.98	3.92	3.89	4.31	12.09	9.13	9.17	9.15	19.23	5.81	6.21	6.21	15.66
5	16.99	16.95	17.00	24.60	23.94	24.00	23.91	27.58	28.42	28.45	28.38	29.07	16.50	18.54	18.54	25.00
6	11.91	11.91	11.90	21.52	17.47	17.44	17.43	24.83	17.55	17.54	17.58	24.89	11.44	12.40	12.40	21.62
7	3.82	3.79	3.83	11.63	5.85	5.87	5.88	15.37	5.76	5.79	5.83	15.26	3.96	4.15	4.15	12.21
8	19.98	19.89	19.90	25.99	25.13	24.25	25.63	27.95	34.77	34.85	34.98	30.85	19.40	24.48	24.47	26.99
9	10.94	10.98	10.88	20.77	17.31	17.16	17.29	24.74	22.52	22.43	22.37	27.02	11.12	12.37	12.37	21.52
Total	117.25	117.26	117.16		158.48	156.44	159.36		203.08	222.08	203.93		114.74	126.45	125.86	
Mean	13.02				17.57				23.30				13.59			

Table 6.4.2. Experimental q_{tot} values for adsorption of Py, 2Pi, 4Pi and AmPy onto RHA using Taguchi design of experiment.

Trial No.	Py q_{tot} (mg g^{-1})			S/N Ratio (dB)	2Pi q_{tot} (mg g^{-1})			S/N Ratio (dB)	4Pi q_{tot} (mg g^{-1})			S/N Ratio (dB)	AmPy q_{tot} (mg g^{-1})			S/N Ratio (dB)
	R_1	R_2	R_3		R_1	R_2	R_3		R_1	R_2	R_3		R_1	R_2	R_3	
1	2.16	2.15	2.16	6.67	2.29	2.29	2.29	7.21	2.11	2.11	2.12	6.49	2.28	2.48	2.48	7.63
2	2.79	2.79	2.85	8.97	3.02	3.03	3.03	9.62	3.00	3.00	3.01	9.55	3.03	3.30	3.31	10.12
3	5.10	5.08	5.11	14.14	5.84	6.09	5.95	15.50	6.78	6.79	6.78	16.63	5.53	5.48	5.58	14.86
4	1.42	1.40	1.42	3.01	1.43	1.44	1.42	3.10	1.37	1.37	1.38	2.75	1.49	1.65	1.65	4.04
5	3.95	3.97	3.94	11.94	4.43	4.44	4.44	12.94	4.48	4.48	4.46	13.01	4.33	4.94	4.94	13.46
6	3.21	3.21	3.19	10.11	3.42	3.41	3.41	10.66	3.46	3.46	3.45	10.77	3.46	3.72	3.72	11.20
7	1.05	1.06	1.05	0.46	1.06	1.05	1.06	0.48	0.90	0.89	0.90	-0.94	1.14	1.24	1.24	1.60
8	3.88	3.90	3.93	11.82	4.27	4.26	4.29	12.61	4.42	4.42	4.40	12.89	4.16	4.92	4.92	13.30
9	1.98	1.96	1.98	5.90	2.09	2.09	2.10	6.42	2.05	2.07	2.07	6.29	2.14	2.47	2.47	7.39
Total	25.53	25.52	25.63		27.85	28.09	27.99		28.57	28.59	28.57		27.57	30.20	30.31	
Mean		2.84				3.11				3.18				3.26		

Table 6.4.3. Experimental q_{tot} **value1s for adsorption of Py, 2Pi, 4Pi and AmPy onto GAC using Taguchi design of experiment.**

Trial No.	Py				2Pi				4Pi				AmPy			
	q_{tot} (mg g^{-1})			S/N Ratio (dB)	q_{tot} (mg g^{-1})			S/N Ratio (dB)	q_{tot} (mg g^{-1})			S/N Ratio (dB)	q_{tot} (mg g^{-1})			S/N Ratio (dB)
	R_1	R_2	R_3		R_1	R_2	R_3		R_1	R_2	R_3		R_1	R_2	R_3	
1	3.21	3.21	3.20	10.13	6.28	6.28	6.26	15.95	6.34	6.33	6.36	16.05	3.24	3.33	3.32	10.36
2	4.61	4.59	4.62	13.26	8.58	8.57	8.61	18.67	8.91	8.88	8.93	18.99	4.80	4.98	4.98	13.84
3	11.62	11.60	11.63	21.30	17.80	18.35	18.10	25.14	19.80	29.01	19.53	26.74	12.57	12.70	12.37	21.97
4	2.38	2.39	2.37	7.53	4.63	4.64	4.65	13.33	4.47	4.45	4.50	13.02	2.39	2.49	2.49	7.80
5	6.91	6.93	6.92	16.80	13.07	13.08	13.05	22.32	13.46	13.42	13.48	22.58	7.12	7.47	7.46	17.32
6	4.82	4.82	4.83	13.66	8.89	8.90	8.91	18.99	9.41	9.44	9.40	19.48	4.82	4.98	4.98	13.85
7	1.59	1.59	1.59	4.03	3.16	3.15	3.16	9.99	3.11	3.09	3.12	9.84	1.62	1.66	1.66	4.33
8	7.86	7.82	7.86	17.89	14.16	14.13	14.25	23.03	16.26	16.30	16.22	24.22	8.27	9.84	9.84	19.30
9	4.12	4.15	4.13	12.32	7.42	7.38	7.46	17.40	8.28	8.22	8.33	18.36	4.35	4.93	4.94	13.47
Total	47.11	47.11	47.14		83.97	84.48	84.45		90.05	99.15	89.87		49.18	52.38	52.05	
Mean		5.24				9.37				10.34				5.69		

Table 6.4.4. Experimental q_{tot} values for adsorption of Py, 2Pi and 4Pi in binary system onto BFA, RHA and GAC by using Taguchi design of experiment.

Py-2Pi												
Trial No.	BFA			S/N Ratio (dB)	RHA			S/N Ratio (dB)	GAC			S/N Ratio (dB)
	q_{tot} (mg g^{-1})				q_{tot} (mg g^{-1})				q_{tot} (mg g^{-1})			
	R_1	R_2	R_3		R_1	R_2	R_3		R_1	R_2	R_3	
1	24.70	24.69	24.76	27.86	5.87	5.87	5.86	15.37	10.94	10.94	10.92	20.77
2	8.21	8.20	8.21	18.28	2.41	2.41	2.40	7.63	3.16	3.17	3.15	9.99
3	8.00	8.00	7.98	18.06	2.39	2.38	2.39	7.55	3.19	3.19	3.20	10.09
4	6.20	6.19	6.20	15.84	1.64	1.63	1.65	4.30	2.45	2.44	2.45	7.77
5	27.47	27.46	27.41	28.77	5.57	5.56	5.57	14.91	11.20	10.94	11.48	20.99
6	20.56	20.56	20.50	26.25	5.46	5.46	5.44	14.73	8.17	7.92	8.05	18.11
7	8.26	8.26	8.25	18.34	2.46	2.46	2.45	7.81	3.28	3.28	3.27	10.30
8	6.11	6.10	6.11	15.72	1.62	1.61	1.62	4.19	2.39	2.38	2.39	7.56
9	0.00	0.00	0.00	0.00	0.00	0.00	0.00	0.00	0.00	0.00	0.00	0.00
Total	109.51	109.47	109.42		27.41	27.38	27.38		44.77	44.26	44.91	
Mean		12.16				3.04				4.96		
Py-4Pi												
1	28.11	28.22	28.05	28.98	6.28	6.30	6.27	15.96	11.28	11.28	11.28	21.04
2	8.08	8.06	8.04	18.13	2.45	2.46	2.45	7.79	3.28	3.28	3.28	10.31
3	8.19	8.19	8.19	18.26	2.40	2.41	2.40	7.62	3.24	3.24	3.24	10.22
4	6.25	6.25	6.24	15.91	1.67	1.66	1.66	4.43	2.50	2.50	2.50	7.96
5	27.71	27.82	27.10	28.80	6.15	6.16	6.14	15.77	11.06	11.06	11.06	20.87
6	22.09	22.08	22.07	26.88	5.95	5.96	5.95	15.49	9.13	9.13	9.13	19.21
7	8.33	8.33	8.32	18.41	2.49	2.48	2.48	7.91	3.33	3.33	3.33	10.45
8	6.15	6.15	6.16	15.78	1.63	1.63	1.62	4.22	2.14	2.14	2.14	6.61
9	0.00	0.00	0.00	0.00	0.00	0.00	0.00	0.00	0.00	0.00	0.00	0.00
Total	114.91	115.10	114.17		29.01	29.05	28.98		45.95	45.95	45.95	
Mean		12.75				3.22				5.11		
2Pi-4Pi												
1	40.88	38.85	42.92	32.21	6.51	6.40	6.50	16.22	17.58	17.63	17.58	24.91
2	12.23	12.22	12.21	21.74	2.48	2.48	2.47	7.87	5.66	5.71	5.62	15.06
3	12.25	12.22	12.24	21.75	2.47	2.47	2.48	7.86	5.97	5.99	5.95	15.52
4	9.98	9.98	9.97	19.98	1.67	1.67	1.66	4.43	4.40	4.42	4.44	12.91
5	38.46	37.40	37.33	31.53	6.28	6.28	6.31	15.97	18.39	18.27	18.51	25.29
6	30.85	31.09	30.68	29.79	6.07	6.10	6.06	15.67	14.85	14.77	15.26	23.49
7	12.31	12.30	12.30	21.80	2.49	2.48	2.49	7.92	6.11	6.07	6.08	15.69
8	9.80	9.79	9.78	19.82	1.67	1.67	1.66	4.43	4.62	4.66	4.60	13.31
9	0.00	0.00	0.00	0.00	0.00	0.00	0.00	0.00	0.00	0.00	0.00	0.00
Total	166.76	163.85	167.43		29.63	29.54	29.64		77.59	77.51	78.04	
Mean		18.45				3.29				8.63		

Table 6.4.5. Experimental q_{tot} values for ternary adsorption of Py, 2Pi and 4Pi onto BFA, RHA and GAC.

Trial No.	BFA q_{tot} (mg g^{-1})			S/N Ratio (dB)	RHA q_{tot} (mg g^{-1})			S/N Ratio (dB)	GAC q_{tot} (mg g^{-1})			S/N Ratio (dB)
	R_1	R_2	R_3		R_1	R_2	R_3		R_1	R_2	R_3	
1	0.00	0.00	0.00	0.00	0.00	0.00	0.00	0.00	0.00	0.00	0.00	0.00
2	5.81	5.87	5.76	15.29	1.67	1.67	1.67	4.43	2.48	2.48	2.48	7.88
3	8.32	8.32	8.31	18.40	2.48	2.48	2.48	7.88	3.30	3.31	3.30	10.38
4	4.16	4.16	4.16	12.39	1.25	1.25	1.25	1.92	1.66	1.66	1.66	4.42
5	22.01	22.06	22.16	26.88	4.42	4.42	4.43	12.92	8.16	8.17	8.17	18.24
6	18.44	18.43	18.42	25.31	4.52	4.52	4.51	13.09	5.06	5.06	5.06	14.08
7	12.26	12.26	12.27	21.77	3.22	3.22	3.23	10.17	4.84	4.84	4.84	13.70
8	12.41	12.40	12.43	21.88	3.63	3.63	3.63	11.20	4.60	4.60	4.60	13.25
9	38.80	38.81	38.69	31.77	7.72	7.70	7.71	17.74	13.93	13.92	13.93	22.88
10	6.17	6.17	6.20	15.82	1.62	1.62	1.62	4.20	2.37	2.37	2.37	7.49
11	8.23	8.23	8.24	18.31	2.45	2.45	2.45	7.78	3.08	3.08	3.08	9.77
12	28.07	28.12	27.97	28.96	5.84	5.84	5.84	15.33	10.94	10.97	10.94	20.79
13	22.11	22.23	22.12	26.91	4.37	4.35	4.38	12.80	5.79	5.79	5.78	15.25
14	17.75	17.81	17.78	25.00	4.52	4.52	4.52	13.10	6.94	6.94	6.94	16.83
15	16.32	16.34	16.32	24.26	4.66	4.66	4.66	13.37	6.34	6.35	6.34	16.05
16	12.22	12.21	12.22	21.74	3.53	3.53	3.53	10.96	4.71	4.71	4.71	13.45
17	35.38	35.13	35.38	30.95	7.34	7.34	7.34	17.32	15.40	15.40	15.41	23.75
18	28.06	28.04	28.06	28.96	7.19	7.19	7.19	17.13	8.71	8.71	8.71	18.80
19	8.16	8.16	8.17	18.24	2.38	2.38	2.38	7.54	3.21	3.21	3.21	10.13
20	26.63	26.51	26.64	28.50	5.68	5.69	5.68	15.09	11.08	11.07	11.07	20.88
21	23.38	23.38	23.41	27.38	5.69	5.69	5.69	15.10	6.90	6.91	6.91	16.78
22	17.43	17.44	17.43	24.83	4.30	4.30	4.30	12.66	6.37	6.37	6.38	16.09
23	16.32	16.30	16.32	24.25	4.67	4.67	4.67	13.38	6.11	6.11	6.11	15.72
24	36.55	36.43	36.56	31.25	8.80	8.77	8.79	18.88	15.97	15.92	15.94	24.05
25	34.64	34.58	34.64	30.79	7.56	7.56	7.56	17.57	9.70	9.71	9.68	19.73
26	25.70	25.67	26.30	28.26	6.54	6.55	6.54	16.32	10.65	10.64	10.63	20.54
27	22.61	22.63	22.59	27.08	6.36	6.36	6.36	16.07	9.12	9.12	9.12	19.20
Total	507.94	507.67	508.54		122.41	122.37	122.39		187.42	187.40	187.38	
Mean		18.82				4.53				6.94		

The respective parameters in single, binary and ternary systems were varied at three levels (Table 4.4.1 to 4.4.3, Chapter-IV) to understand their effect on the selected response characteristics (amount adsorbed in mg of adsorbate per g of adsorbent (q_{tot})). Each experiment was repeated three times for each trial condition. The q_{tot} data for Py and its derivatives adsorption onto BFA, RHA and GAC are given in Table 6.4.1 to Table 6.4.5 for single, binary and ternary systems. It is found that the adsorption is strongly dependent on the parametric conditions used.

6.4.2 Effect of Process Parameters in Single Batch Adsorption System

The average or mean values of response characteristics q_{tot} and S/N ratio for each parameter at level 1, 2, and 3 are calculated from Table 6.4.1 to Table 6.4.5. The raw data for the average value of q_{tot} and S/N ratio for each parameter ($C_{0,i}$, m, T and t) at levels 1, 2, and 3 are given in Table 6.4.6 to 6.4.8 for Py, 2Pi, 4Pi and AmPy onto BFA, RHA, and GAC, respectively.

Table 6.4.9 summarizes the parameters that have highest influence on q_{tot} for the raw and S/N data. Individually at level stage with q_{tot} as the desired response characteristic. m (parameter B) has highest influence at level 1, and C_0 (parameter A) has highest influence at level 3, for adsorption of Py, 2Pi, 4Pi and AmPy onto BFA, RHA and GAC. An increase in adsorption with m can be attributed to the availability of greater surface area and more adsorption sites. The difference between level 2 and level 1 ($L_2 - L_1$) of each factor indicates the relative influence of the effect.

The larger the difference, the stronger is the influence. $C_{0,i}$ shows strong influence on q_{tot} as compared to other parameters. The removal increased with an increase in the adsorbate concentration as the resistance to the uptake of adsorbates from the solution decreases with an increase in the concentration.

Table 6.4.6. Average and main effects of q_{tot} values for BFA - raw and S/N data

Factors	Raw Data (Average Value)			Main Effects (Raw Data)		S/N Data (Average Value)			Main Effects (S/N Data)	
	L_1	L_2	L_3	L_2-L_1	L_3-L_2	L_1	L_2	L_3	L_2-L_1	L_3-L_2
Py										
A	6.78	13.09	19.20	6.31	6.11	8.87	21.70	25.09	12.83	3.39
B	19.85	11.36	7.87	-8.50	-3.49	18.38	20.26	17.02	1.88	-3.23
C	11.93	12.48	14.67	0.55	2.19	14.18	20.83	20.66	6.65	-0.16
D	11.44	14.06	13.57	2.62	-0.49	14.24	20.69	20.74	6.45	0.05
2Pi										
A	9.05	18.49	25.16	9.43	6.67	9.15	24.93	27.69	15.78	2.76
B	25.45	15.56	11.69	-9.89	-3.86	19.53	21.70	20.54	2.17	-1.16
C	17.66	15.49	19.55	-2.16	4.05	16.33	21.63	23.82	5.29	2.19
D	17.80	16.63	18.27	-1.17	1.64	16.76	21.39	23.63	4.63	2.25
4Pi										
A	12.46	21.99	35.45	9.53	13.45	11.49	26.02	29.78	14.53	3.76
B	39.22	18.89	11.79	-20.33	-7.10	22.07	24.64	20.58	2.57	-4.06
C	20.95	20.52	28.42	-0.43	7.90	16.89	24.99	25.42	8.10	0.43
D	19.70	27.17	23.02	7.47	-4.15	16.84	25.40	25.06	8.56	-0.34
AmPy										
A	7.37	14.39	19.03	7.02	4.64	9.29	22.32	25.10	13.03	2.78
B	20.62	12.04	8.12	-8.58	-3.93	18.55	20.79	17.36	2.24	-3.43
C	12.67	13.65	14.47	0.98	0.83	14.42	21.42	20.87	7.01	-0.56
D	12.08	13.80	14.91	1.72	1.11	14.45	20.86	21.40	6.42	0.54

Table 6.4.7. Average and main effects of , values for RHA - raw and S/N data

Factors	Raw Data (Average Value)			Main Effects (Raw Data)		S/N Data (Average Value)			Main Effects (S/N Data)	
	L_1	L_2	L_3	L_2-L_1	L_3-L_2	L_1	L_2	L_3	L_2-L_1	L_3-L_2
Py										
A	1.48	2.96	4.08	1.48	1.13	1.16	9.16	12.06	8.00	2.91
B	3.66	2.73	2.14	-0.93	-0.59	8.65	7.97	5.75	-0.68	-2.23
C	2.69	2.84	2.99	0.15	0.15	6.20	8.32	7.86	2.11	-0.46
D	2.66	2.89	2.97	0.23	0.08	6.36	7.94	8.07	1.58	0.13
2Pi										
A	1.53	3.20	4.60	1.67	1.40	1.19	9.81	13.03	8.62	3.22
B	4.11	2.96	2.25	-1.14	-0.71	9.37	8.55	6.12	-0.82	-2.44
C	2.94	3.04	3.35	0.10	0.31	6.71	8.79	8.53	2.08	-0.26
D	2.85	3.23	3.25	0.38	0.03	6.76	8.60	8.67	1.84	0.07
4Pi										
	L_1	L_2	L_3	L_2-L_1	L_3-L_2	L_1	L_2	L_3	L_2-L_1	L_3-L_2
A	1.44	3.18	4.90	1.73	1.73	0.60	9.65	13.47	9.04	3.82
B	4.42	2.95	2.15	-1.47	-0.80	9.84	8.44	5.44	-1.40	-3.00
C	2.88	3.08	3.56	0.20	0.48	6.50	8.80	8.42	2.30	-0.39
D	2.84	3.42	3.26	0.58	-0.16	6.77	8.62	8.32	1.85	-0.30
AmPy										
A	1.72	3.43	4.63	1.71	1.20	1.88	10.35	13.17	8.47	2.82
B	4.19	3.18	2.42	-1.00	-0.76	9.38	9.21	6.81	-0.18	-2.40
C	3.17	3.30	3.32	0.13	0.02	7.03	9.51	8.86	2.48	-0.65
D	3.07	3.18	3.54	0.11	0.35	7.11	8.84	9.45	1.74	0.61

Table 6.4.8. Average and main effects of q_{tot} values for GAC - raw and S/N data

Factors	Raw Data (Average Value)			Main Effects (Raw Data)		S/N Data (Average Value)			Main Effects (S/N Data)	
	L_1	L_2	L_3	L_2-L_1	L_3-L_2	L_1	L_2	L_3	L_2-L_1	L_3-L_2
Py										
A	2.70	5.22	7.79	2.52	2.57	3.85	13.76	17.26	9.91	3.49
B	7.87	4.63	3.21	-3.23	-1.43	13.07	12.53	9.28	-0.54	-3.25
C	4.75	5.02	5.94	0.26	0.92	8.98	13.03	12.87	4.05	-0.16
D	4.52	5.73	5.45	1.21	-0.28	8.98	12.98	12.91	4.01	-0.07
2Pi										
A	5.07	9.68	13.35	4.61	3.67	7.77	19.22	22.15	11.45	2.93
B	13.23	8.76	6.11	-4.46	-2.65	16.06	18.11	14.97	2.05	-3.14
C	8.92	9.24	9.94	0.32	0.70	12.76	18.45	17.93	5.69	-0.52
D	8.30	9.67	10.13	1.37	0.47	12.55	18.14	18.45	5.59	0.31
4Pi										
A	5.29	10.50	15.22	5.22	4.72	7.62	19.75	22.93	12.14	3.18
B	15.77	8.94	6.29	-6.83	-2.66	16.99	18.20	15.12	1.21	-3.07
C	9.36	10.05	11.60	0.69	1.55	12.88	18.91	18.52	6.03	-0.38
D	8.87	11.20	10.94	2.33	-0.26	12.82	18.60	18.88	5.78	0.28
AmPy										
A	2.95	5.85	8.27	2.90	2.43	4.04	14.50	17.71	10.46	3.21
B	8.87	4.91	3.29	-3.96	-1.62	13.76	12.99	9.51	-0.77	-3.47
C	5.13	5.57	6.37	0.44	0.80	9.23	13.65	13.38	4.42	-0.27
D	4.86	6.10	6.10	1.24	0.01	9.23	13.38	13.65	4.15	0.27

Table 6.4.9. Summary of parameters having highest influence on q_{tot} values for BFA, RHA and GAC.

Adsorbent	Raw Data (Average Value)			Main Effects (Raw Data)		S/N Data (Average Value)			Main Effects (S/N Data)	
	L_1	L_2	L_3	L_2-L_1	L_3-L_2	L_1	L_2	L_3	L_2-L_1	L_3-L_2
Py										
BFA	B	D	A	A	A	B	A	A	A	A
RHA	B	A	A	A	A	B	A	A	A	A
GAC	B	D	A	A	A	B	A	A	A	A
2Pi										
BFA	B	A	A	A	A	B	A	A	A	A
RHA	B	A	A	A	A	B	A	A	A	A
GAC	B	A	A	A	A	B	A	A	A	A
4Pi										
BFA	B	A	A	A	A	B	A	A	A	A
RHA	B	D	A	A	A	B	A	A	A	A
GAC	B	D	A	A	A	B	A	A	A	A
AmPy										
BFA	B	A	A	A	A	B	A	A	A	A
RHA	B	A	A	A	A	B	A	A	A	A
GAC	B	D	A	A	A	B	A	A	A	A

Factors	
A	Initial Concentration, C_0 (mg dm^{-3})
B	Adsorbent Dose, m (g dm^{-3})
C	Temperature, T (Kelvin, K)
D	Time, t (min)

6.4.3 Effect of Process Parameters for Binary Batch Adsorption System

The effect of individual parameters on the selected response characteristics (q_{tot}) are being reported in this section. The average or mean values of response characteristics (q_{tot}) and S/N ratio for each parameter ($C_{0,i}, C_{0,j}\ m$ and t) at level 1, 2, and 3 are calculated from Table 6.4.4.

The raw data for the average value of q_{tot} and S/N ratio for each parameter at levels 1, 2, and 3 are given in Tables 6.4.10 to 6.4.12 for Py-2Pi, Py-4Pi and 2Pi-4Pi onto BFA, RHA, and GAC, respectively.

Table 6.4.10. Average and main effects of q_{tot} values for BFA – raw and S/N data in binary system

Factors	Raw Data (Average Value)			Main Effects (Raw Data)		S/N Data (Average Value)			Main Effects (S/N Data)	
	L_1	L_2	L_3	L_2-L_1	L_3-L_2	L_1	L_2	L_3	L_2-L_1	L_3-L_2
Py-2Pi										
A	4.82	13.01	18.66	8.19	5.65	11.39	20.62	24.36	9.23	3.74
B	4.70	13.95	17.84	9.25	3.89	11.26	20.97	24.15	9.71	3.18
C	17.39	10.95	8.15	-6.44	-2.79	18.88	19.27	18.23	0.39	-1.04
D	9.58	12.97	13.94	3.39	0.97	14.85	20.59	20.94	5.74	0.36
Py-4Pi										
A	4.86	14.11	19.27	9.25	5.16	11.44	20.96	24.65	9.52	3.68
B	4.78	13.95	19.51	9.17	5.56	11.35	20.95	24.76	9.60	3.81
C	18.56	11.49	8.19	-7.06	-3.30	19.26	19.52	18.27	0.26	-1.26
D	10.05	14.19	14.01	4.14	-0.18	15.00	21.05	21.00	6.05	-0.05
2Pi-4Pi										
A	7.43	20.97	26.95	13.54	5.98	13.93	24.59	27.69	10.66	3.10
B	7.34	19.98	28.02	12.63	8.05	13.86	24.42	27.93	10.56	3.52
C	26.21	16.88	12.25	-9.33	-4.63	21.25	23.20	21.77	1.95	-1.43
D	14.37	21.03	19.94	6.67	-1.09	17.18	24.65	24.38	7.47	-0.26

Table 6.4.11. Average and main effects of q_{tot} values for RHA – raw and S/N data in binary system

Factors	Raw Data (Average Value)			Main Effects (Raw Data)		S/N Data (Average Value)			Main Effects (S/N Data)	
	L_1	L_2	L_3	L_2-L_1	L_3-L_2	L_1	L_2	L_3	L_2-L_1	L_3-L_2
Py-2Pi										
A	1.37	3.30	4.47	1.93	1.17	4.04	9.06	12.39	5.03	3.33
B	1.33	3.20	4.59	1.87	1.39	3.91	8.95	12.64	5.03	3.69
C	3.81	2.90	2.42	-0.91	-0.49	10.09	7.74	7.66	-2.35	-0.08
D	2.62	3.30	3.21	0.68	-0.08	7.45	9.07	8.97	1.62	-0.11
Py-4Pi										
A	1.38	3.45	4.83	2.07	1.38	4.11	9.33	12.96	5.21	3.64
B	1.34	3.42	4.91	2.08	1.49	3.95	9.33	13.12	5.38	3.79
C	4.14	3.08	2.45	-1.06	-0.63	10.58	8.05	7.77	-2.53	-0.27
D	2.80	3.45	3.42	0.65	-0.03	7.76	9.34	9.30	1.57	-0.04
2Pi-4Pi										
A	1.38	3.54	4.95	2.15	1.41	4.12	9.51	13.17	5.39	3.66
B	1.38	3.48	5.01	2.10	1.54	4.10	9.42	13.27	5.33	3.85
C	4.25	3.13	2.48	-1.12	-0.66	10.73	8.18	7.88	-2.55	-0.29
D	2.85	3.54	3.48	0.69	-0.06	7.85	9.50	9.44	1.66	-0.06

Table 6.4.12. Average and main effects of q_{tot} values for GAC – raw and S/N data in binary system

Factors	Raw Data (Average Value)			Main Effects (Raw Data)		S/N Data (Average Value)			Main Effects (S/N Data)	
	L_1	L_2	L_3	L_2-L_1	L_3-L_2	L_1	L_2	L_3	L_2-L_1	L_3-L_2
Py-2Pi										
A	1.91	5.49	7.48	3.59	1.99	6.03	12.77	16.39	6.75	3.62
B	1.86	5.60	7.42	3.74	1.81	5.88	12.92	16.40	7.03	3.48
C	7.38	4.29	3.21	-3.09	-1.08	13.92	11.15	10.13	-2.77	-1.02
D	3.74	5.52	5.62	1.79	0.10	9.37	12.88	12.95	3.51	0.07
Py-4Pi										
A	1.94	5.57	7.81	3.62	2.24	6.14	12.65	16.77	6.52	4.11
B	1.80	5.61	7.91	3.82	2.30	5.61	13.04	16.90	7.43	3.86
C	7.44	4.59	3.28	-2.86	-1.31	13.97	11.26	10.33	-2.71	-0.93
D	4.13	5.67	5.51	1.54	-0.16	9.84	13.07	12.65	3.24	-0.43
2Pi-4Pi										
A	3.50	9.30	13.11	5.79	3.81	9.53	17.76	21.43	8.22	3.68
B	3.53	9.49	12.88	5.96	3.39	9.61	17.75	21.36	8.15	3.61
C	12.00	8.00	5.91	-3.99	-2.10	16.73	16.57	15.42	-0.16	-1.15
D	6.87	9.33	9.70	2.46	0.37	12.85	17.78	18.10	4.93	0.32

Table 6.4.13 summarizes the parameters that have highest influence on the q_{tot} for the raw and S/N data for the removal of Py, 2Pi and 4Pi from aqueous solution by BFA, RHA and GAC. Individually at level stage with q_{tot} as the desired response characteristic, m (parameter C) has highest influence at level 1. Other parameters have highest influence at level 2, 3 for adsorption of Py, 2Pi, and 4Pi in binary systems onto BFA, RHA and GAC. An increase in adsorption with m can be attributed to the availability of greater surface area and more adsorption sites. The difference between level 2 and level 1 ($L_2 - L_1$) of each factor indicates the relative influence of the effect. The larger the difference, the stronger is the influence. $C_{0,i}$ show strong influence on q_{tot} as compared to other parameters. The solute removal increased with an increase in the adsorbate concentration as the resistance to the uptake of adsorbates from the solution decreases with the increase in concentration.

Table 6.4.13. Average and main effects of q_{tot} values for GAC – raw and S/N data in binary system

Adsorbent	Raw Data (Average Value)			Main Effects (Raw Data)		S/N Data (Average Value)			Main Effects (S/N Data)	
	L_1	L_2	L_3	L_2-L_1	L_3-L_2	L_1	L_2	L_3	L_2-L_1	L_3-L_2
Py-2Pi										
BFA	C	B	A	B	A	C	B	A	B	A
RHA	C	A	B	A	B	C	D	B	B	B
GAC	C	B	A	B	A	C	B	B	B	A
Py-4Pi										
BFA	C	D	B	A	B	C	D	B	B	B
RHA	C	A	B	B	B	C	D	B	B	B
GAC	C	D	B	B	B	C	D	B	B	A
2Pi-4Pi										
BFA	C	A	B	A	B	C	D	B	A	B
RHA	C	A	B	A	B	C	A	B	A	B
GAC	C	B	A	B	A	C	D	A	A	A

Factors	
A	Initial Concentration, $C_{0,1}$ (mg dm^{-3})
B	Initial Concentration, $C_{0,2}$ (mg dm^{-3})
C	Dose, m (mg dm^{-3})
D	Time, t (min)

6.4.4 Effect of Process Parameters in Ternary Batch Adsorption System

The effect of individual Py and its derivatives removal parameters ($C_{0,i}$, T, pH_0, m and t) on the selected response characteristics (q_{tot}) are being reported in this section. The interaction effect of concentration of one compound with respect to (w.r.t) other compound are also discussed. The average or mean values of response characteristics and S/N ratio for each parameter at level 1, 2, and 3 are calculated from Table 6.4.5. The raw data for the average value of q_{tot} and S/N ratio for each parameter at levels 1, 2, and 3 along with interactions at the assigned levels are given in Table 6.4.14. Table 6.4.15 summarizes the parameters that have highest influence on the q_{tot} for the raw and S/N data for the simultaneous removal of Py, 2Pi and 4Pi from aqueous solution by BFA, RHA and GAC. Individually at level stage with q_{tot} as the desired response characteristic, m (parameter F) has highest influence at level 1, pH_0 or T (parameter D or E) has highest influence at level 2, and $C_{0,2Pi}$ or $C_{0,4Pi}$ (parameters B or C) have highest influence at level 3. An increase in adsorption with m can be attributed to the availability of greater surface area and more adsorption sites. The difference between level 2 and level 1 ($L_2 - L_1$) of each factor indicates the relative influence of the effect. The larger the difference, the stronger is the influence. It can be seen from Table 6.4.25 that no single parameter has overriding influence on the removal of Py, 2Pi and 4Pi from aqueous solution by BFA, RHA and GAC. $C_{0,i}$ shows strong influence on q_{tot} as compared to other parameters. The removal increased with an increase in the adsorbate concentration as the resistance to the uptake of adsorbates from the solution decreases with an increase in the sorbate concentration.

Table 6.4.14. Average and main effects of q_{tot} values for BFA, RHA and GAC – raw and S/N data in ternary system

Factors	Raw Data (Average Value)			Main Effects (Raw Data)		S/N Data (Average Value)			Main Effects (S/N Data)	
	L_1	L_2	L_3	L_2-L_1	L_3-L_2	L_1	L_2	L_3	L_2-L_1	L_3-L_2
BFA										
A	13.58	19.37	23.50	5.78	4.14	19.30	24.55	26.73	5.25	2.18
B	12.75	19.02	24.68	6.27	5.66	18.99	24.56	27.02	5.58	2.46
C	13.02	18.93	24.49	5.91	5.56	19.16	24.37	27.04	5.20	2.67
D	17.28	20.10	19.07	2.81	-1.02	22.59	23.65	24.33	1.07	0.68
E	18.18	19.71	18.57	1.53	-1.14	22.64	23.65	24.28	1.01	0.62
F	27.12	17.25	12.08	-9.87	-5.16	26.22	23.62	20.73	-2.60	-2.90
G	18.26	18.79	19.40	0.53	0.62	22.60	24.31	23.66	1.70	-0.64
AxB	17.41	19.37	19.67	1.95	0.30	21.76	24.12	24.70	2.36	0.58
AxC	17.66	18.68	20.11	1.02	1.42	21.75	24.13	24.70	2.38	0.57
BxC	17.73	19.16	19.56	1.43	0.41	21.89	23.96	24.73	2.07	0.77
RHA										
A	3.21	4.61	5.77	1.40	1.16	8.82	12.44	14.73	3.63	2.29
B	3.09	4.61	5.90	1.52	1.29	8.59	12.46	14.94	3.86	2.49
C	3.14	4.55	5.91	1.41	1.37	8.65	12.39	14.96	3.75	2.56
D	4.26	4.69	4.65	0.42	-0.04	11.95	11.67	12.38	-0.28	0.71
E	4.45	4.69	4.45	0.24	-0.24	12.01	11.80	12.19	-0.21	0.38
F	5.75	4.36	3.49	-1.38	-0.87	14.18	11.80	10.01	-2.38	-1.79
G	4.37	4.48	4.75	0.12	0.26	11.87	12.24	11.89	0.36	-0.35
AxB	4.34	4.59	4.67	0.25	0.09	11.34	12.01	12.64	0.67	0.62
AxC	4.37	4.54	4.69	0.17	0.15	11.28	12.15	12.56	0.87	0.41
BxC	4.35	4.61	4.63	0.26	0.02	11.33	12.05	12.61	0.72	0.55
GAC										
A	4.89	7.14	8.79	2.25	1.64	11.65	15.80	18.13	4.15	2.33
B	4.82	6.93	9.07	2.11	2.14	11.57	15.64	18.37	4.07	2.73
C	4.29	7.61	8.92	3.32	1.31	11.14	16.32	18.11	5.18	1.79
D	6.54	7.21	7.08	0.68	-0.13	14.95	14.97	15.65	0.02	0.68
E	5.55	7.83	7.44	2.28	-0.39	13.71	15.66	16.20	1.95	0.53
F	10.11	6.04	4.68	-4.07	-1.35	18.40	14.69	12.49	-3.71	-2.20
G	6.68	7.00	7.14	0.31	0.15	14.87	15.61	15.09	0.74	-0.52
AxB	6.52	6.98	7.32	0.46	0.34	14.22	15.27	16.08	1.05	0.82
AxC	6.90	6.70	7.22	-0.20	0.52	14.41	15.36	15.80	0.95	0.43
BxC	6.78	6.97	7.07	0.18	0.10	14.37	15.27	15.94	0.90	0.67

Table 6.4.15. Summary of parameters having highest influence on q_{tot} values for BFA, RHA and GAC.

	Raw data, Average value			Main effects (Raw data)		S/N data, Average value			Main effects (S/N data)	
	L_1	L_2	L_3	L_2-L_1	L_3-L_2	L_1	L_2	L_3	L_2-L_1	L_3-L_2
BFA	F	D	B	B	B	F	B	C	B	C
RHA	F	E	C	B	C	F	B	C	B	C
ACC	F	E	B	C	B	F	C	B	C	B

Parameters		Units	Parameters		Units
A:	$C_0(Py)$	mg dm^{-3}	D:	Temp	(^{0}C)
B:	$C_0(2Pi)$	mg dm^{-3}	E:	pH$_0$	-
C:	$C_0(4Pi)$	mg dm^{-3}	F:	m	g dm^{-3}
			G:	Time	(min)

The response curves for the individual effects of adsorption parameters on the average value of q_{tot} and respective S/N ratio for the adsorption Py, 2Pi, 4Pi and AmPy onto BFA are given in Figs. 6.4.1 through 6.4.8 for single, binary and ternary sorbates-sorbent systems. For RHA and GAC, response curves for only ternary adsorption of Py, 2Pi and 4Pi are given in Fig. 6.4.9-6.4.10. An increase in the levels of factors such as T and t from 1 to 2 and from 2 to 3 has resulted in an increase in the q_{tot} values for all adsorbents. It has been shown in earlier sections that the adsorption of Py, 2Pi, 4Pi and AmPy from aqueous solution onto BFA, RHA and GAC is endothermic in nature due to the endothermicity of the pore-diffusion of molecules of py and its derivatives into meso and micro-pores of the adsorbents; and the chemisorptive nature of the adsorption process. This endothermicity manifests itself in the enhancement of the sorptive capacity of the adsorbents with an increase in T. Also the adsorption increases with t until equilibrium is reached between the solute molecules in the solution and the solid phases. During the initial stage of sorption, a large number of vacant surface sites are available for adsorption. As the sorption progresses, difficulty is encountered in occupying the vacant sites due to the repulsive forces between the solute molecules onto the solid surface and in the bulk solution phase. Besides, the adsorbates are adsorbed into the meso-pores that get almost saturated with adsorbate during the initial stage of adsorption. Thereafter, the molecules have to traverse farther and deeper into the pores encountering much larger resistance. This results in the slowing down of the adsorption during the later period of adsorption.

An increase in pH_0 has resulted in higher adsorption up to level 2 and subsequent increase resulted in the decrease in the desired characteristic (q_{tot}). As shown in earlier sections, the optimum pH_0 for the adsorption of Py, 2Pi, 4Pi and AmPy from aqueous solution onto BFA, RHA and GAC is 6.0 – 7.0. In case of m, an increase in m from level 1 to level 2 and subsequently to level 3 led to a decrease in the value of q_{tot}.
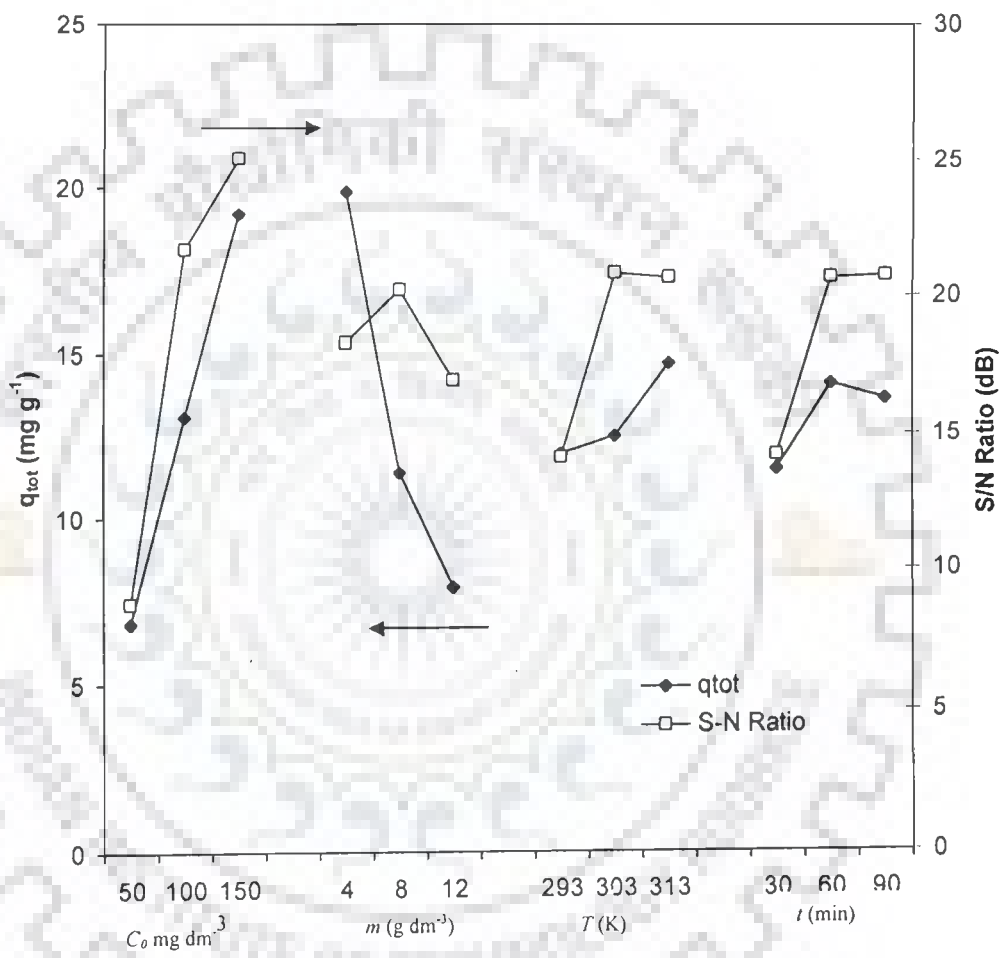
Fig. 6.4.1. **Effect of process parameters on** q_{tot} **and S/N ratio for adsorption of Py onto BFA.**
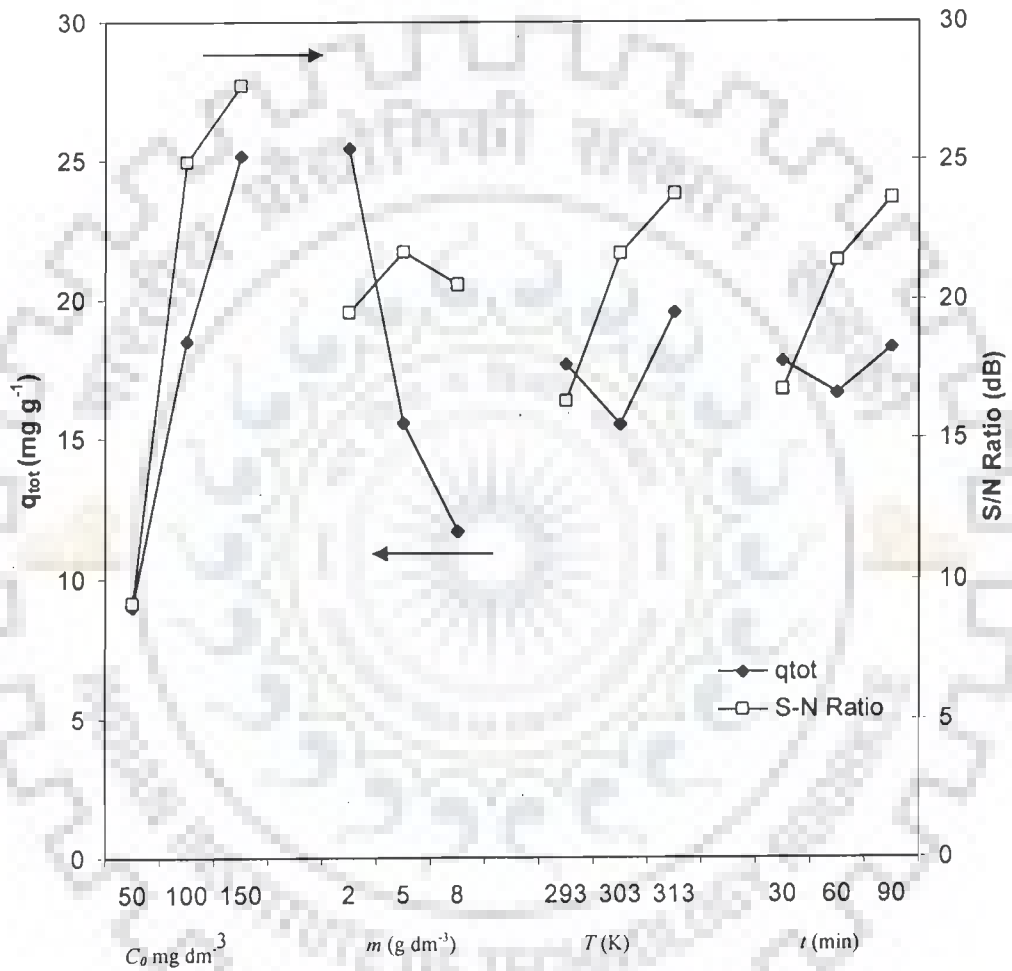
Fig. 6.4.2. Effect of process parameters on q_{tot} and S/N ratio for adsorption of 2Pi onto BFA.
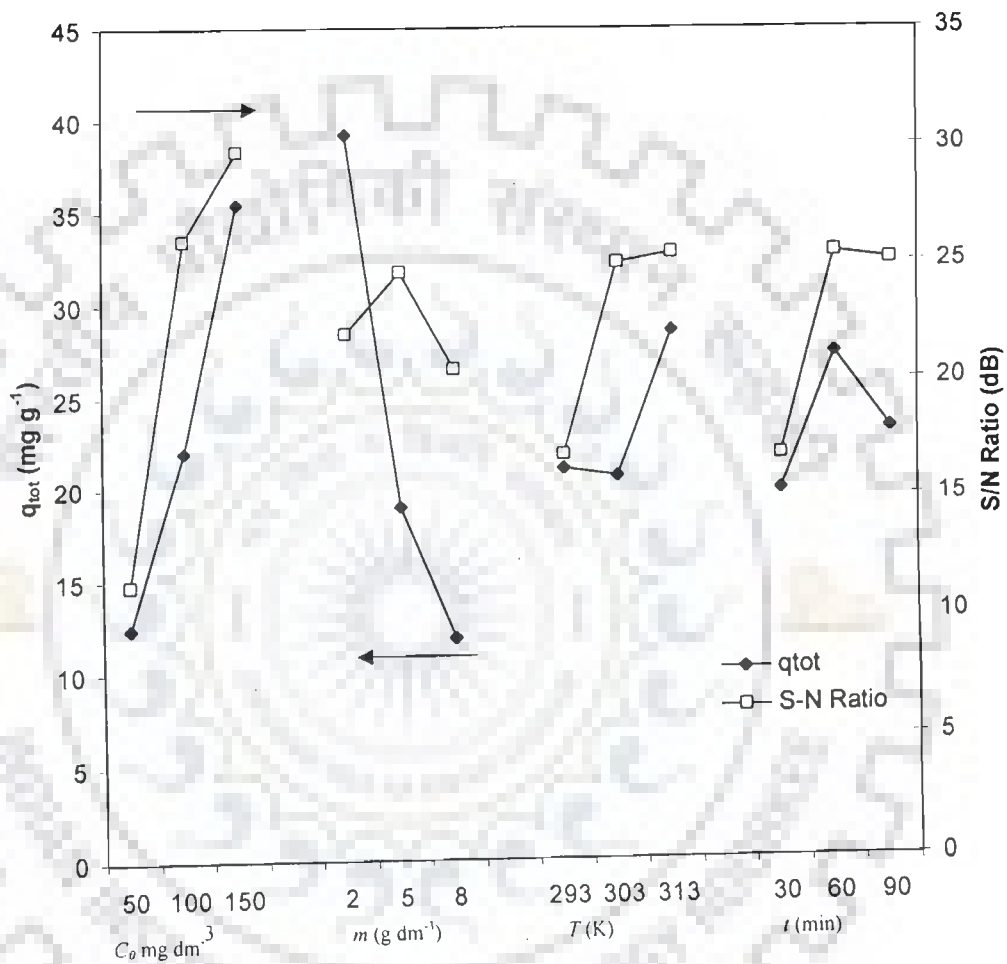
Fig. 6.4.3. **Effect of process parameters on** q_{tot} **and S/N ratio for adsorption of 4Pi onto BFA.**
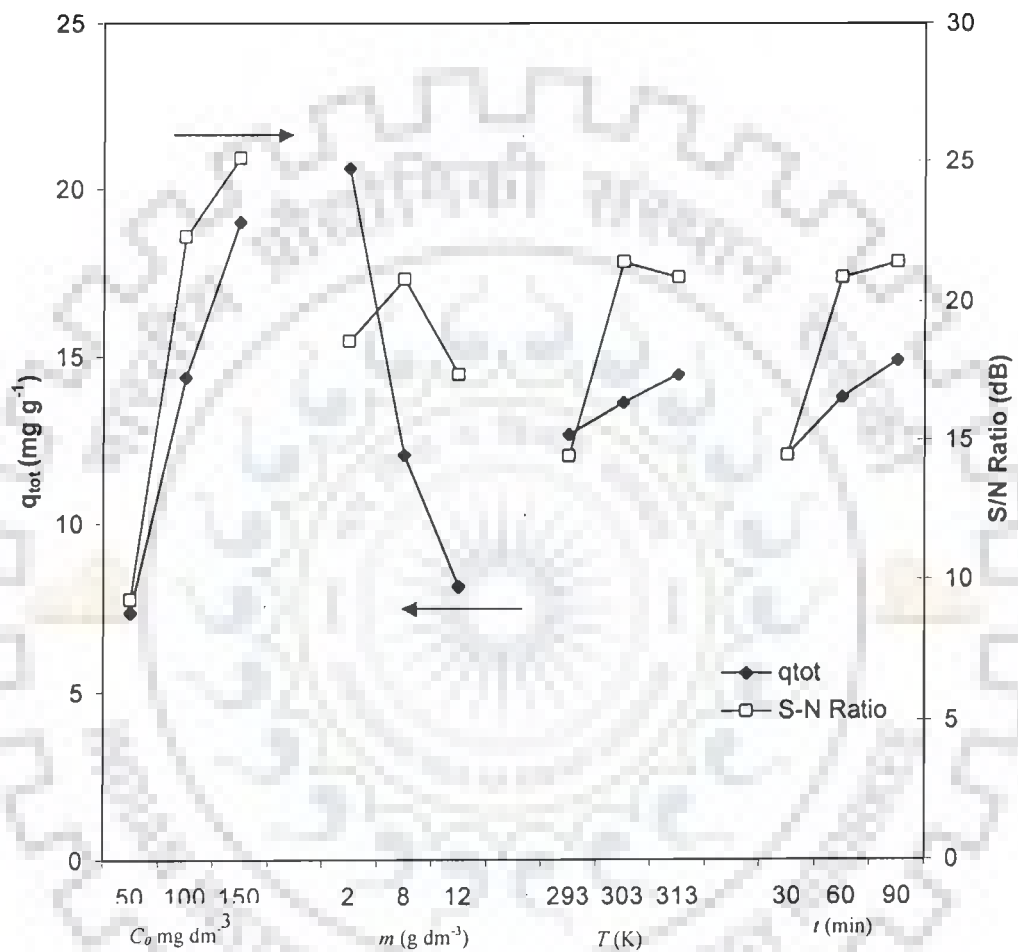
Fig. 6.4.4. Effect of process parameters on q_{tot} and S/N ratio for adsorption of AmPy onto BFA.
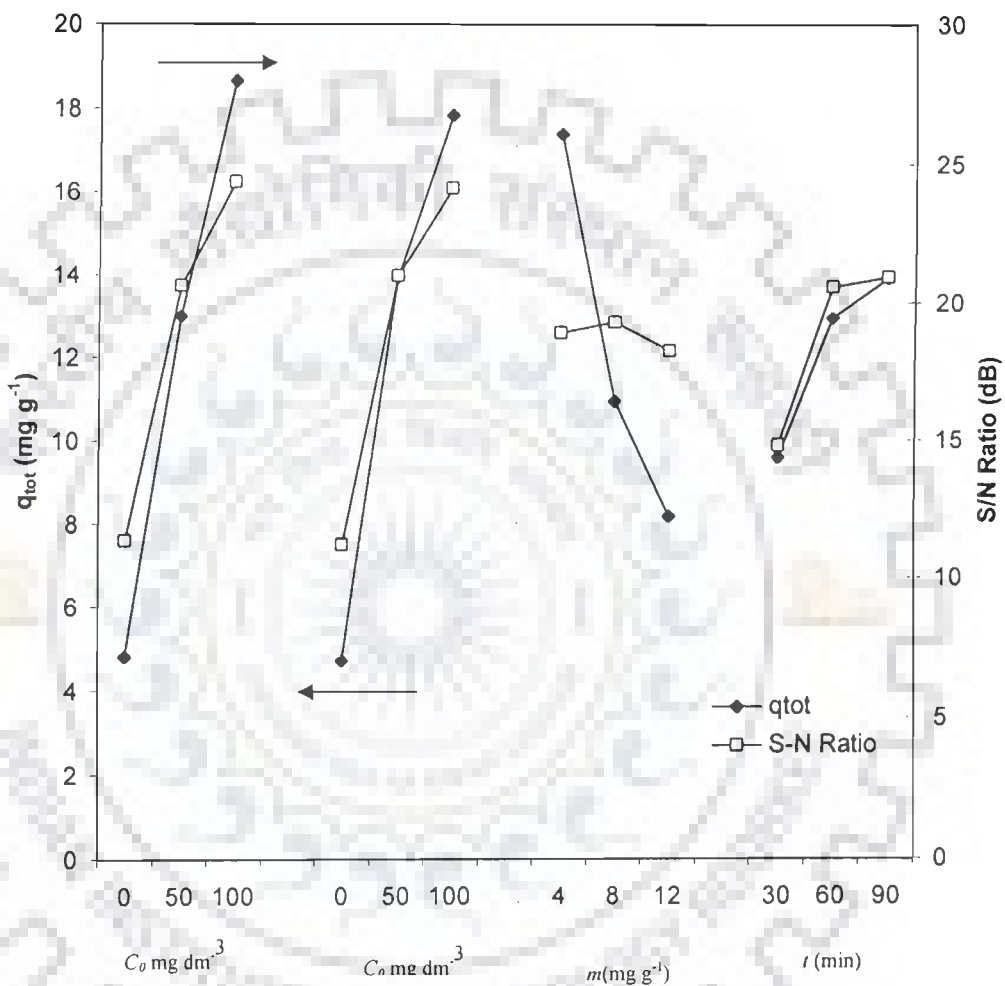
Fig. 6.4.5. Effect of process parameters on q_{tot} and S/N ratio for adsorption of Py and 2Pi in binary system onto BFA.
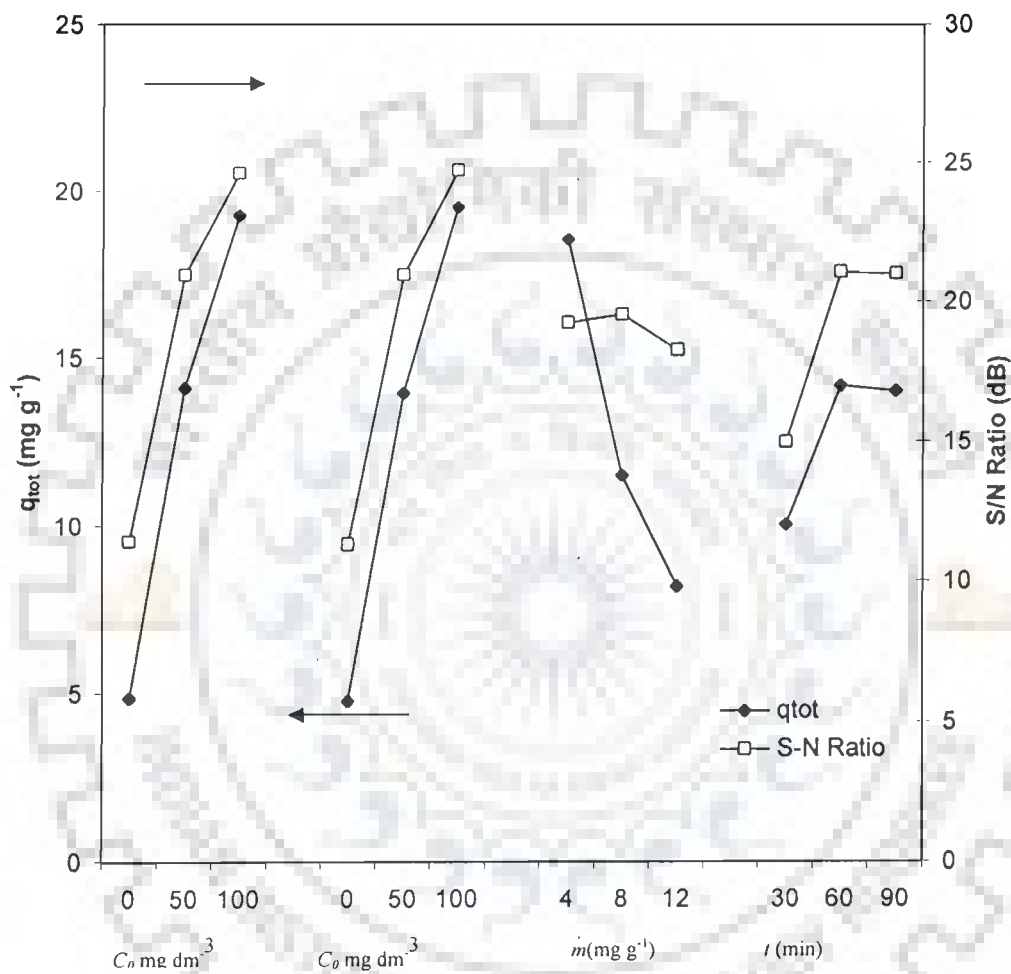
Fig. 6.4.6. Effect of process parameters on q_{tot} and S/N ratio for adsorption of Py and 4Pi in binary system onto BFA.
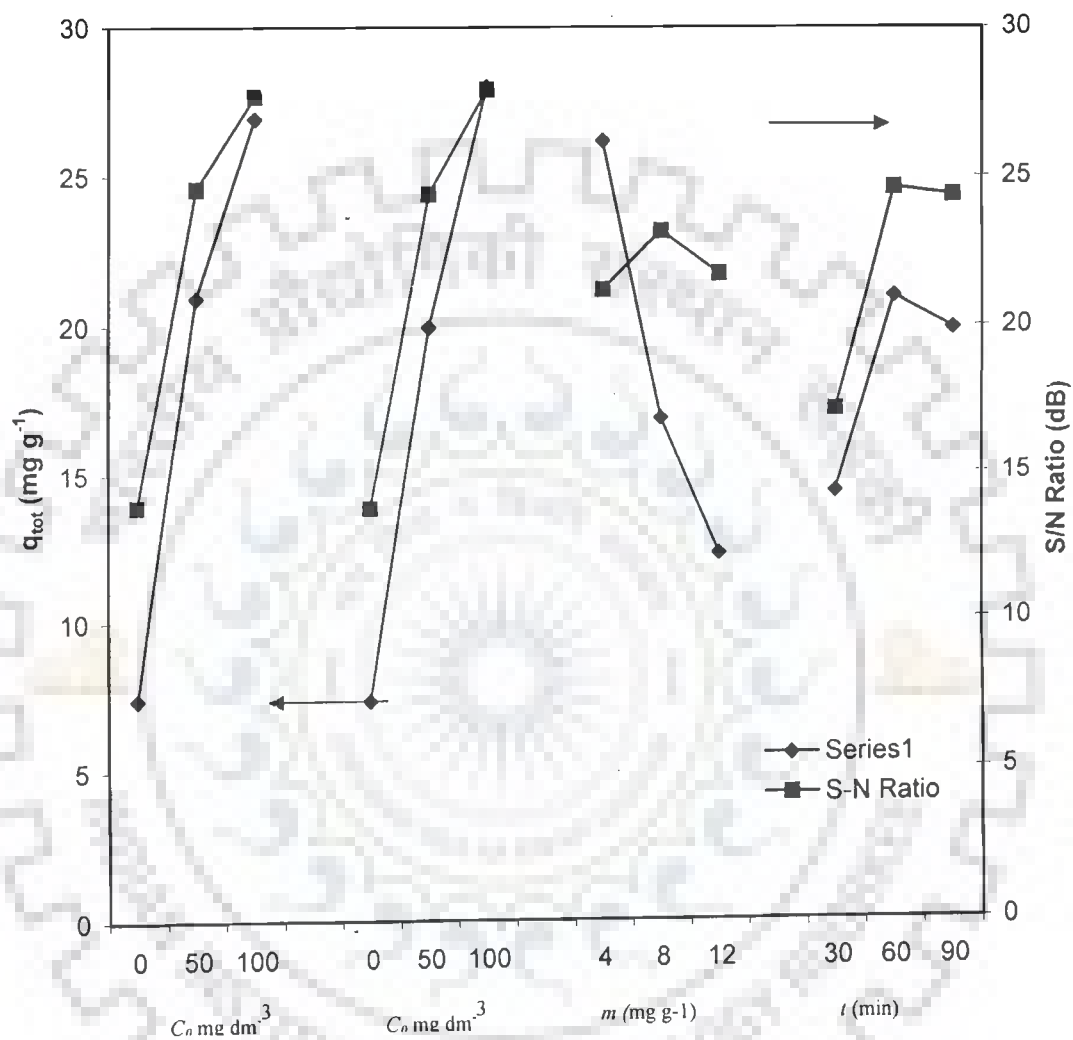
Fig. 6.4.7. Effect of process parameters on q_{tot} and S/N ratio for adsorption of 2Pi and 4Pi in binary system onto BFA.
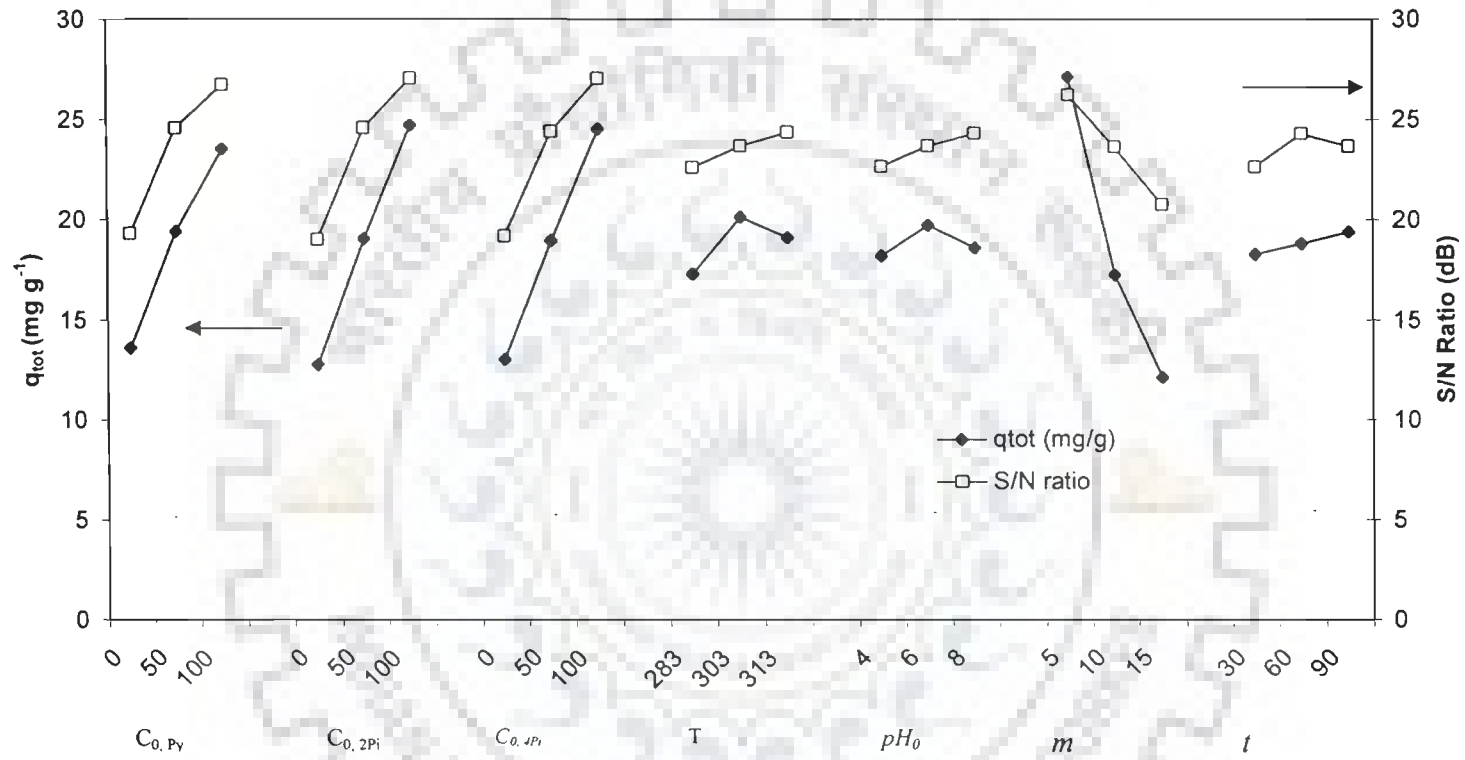
Fig. 6.4.8. Effect of process parameters on q_{tot} **and S/N ratio for multi-component adsorption of Py, 2Pi and 4Pi by BFA.**
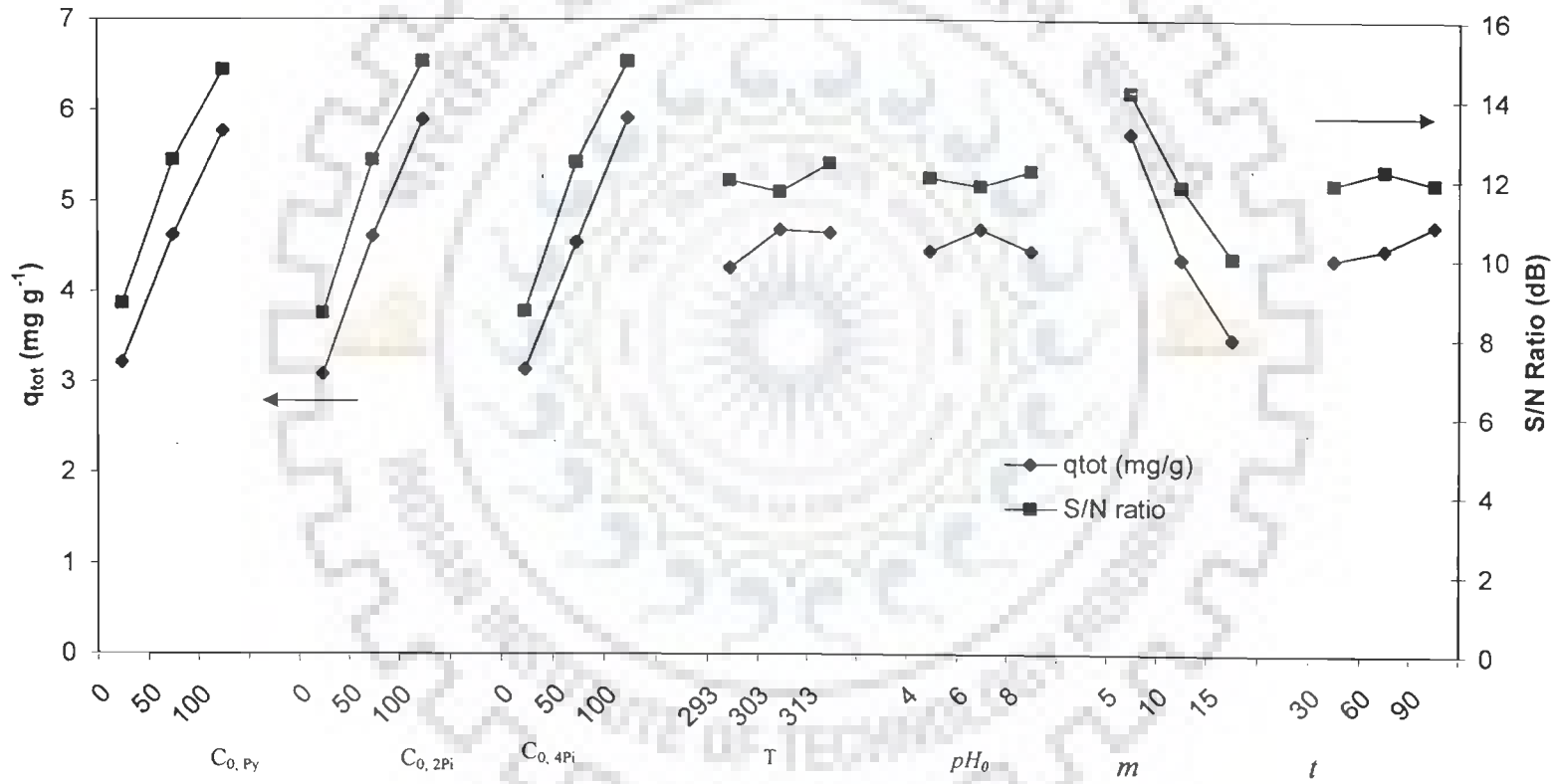
Fig. 6.4.9. Effect of process parameters on q_{tot} **and S/N ratio for multi-component adsorption of Py, 2Pi and 4Pi by RHA.**
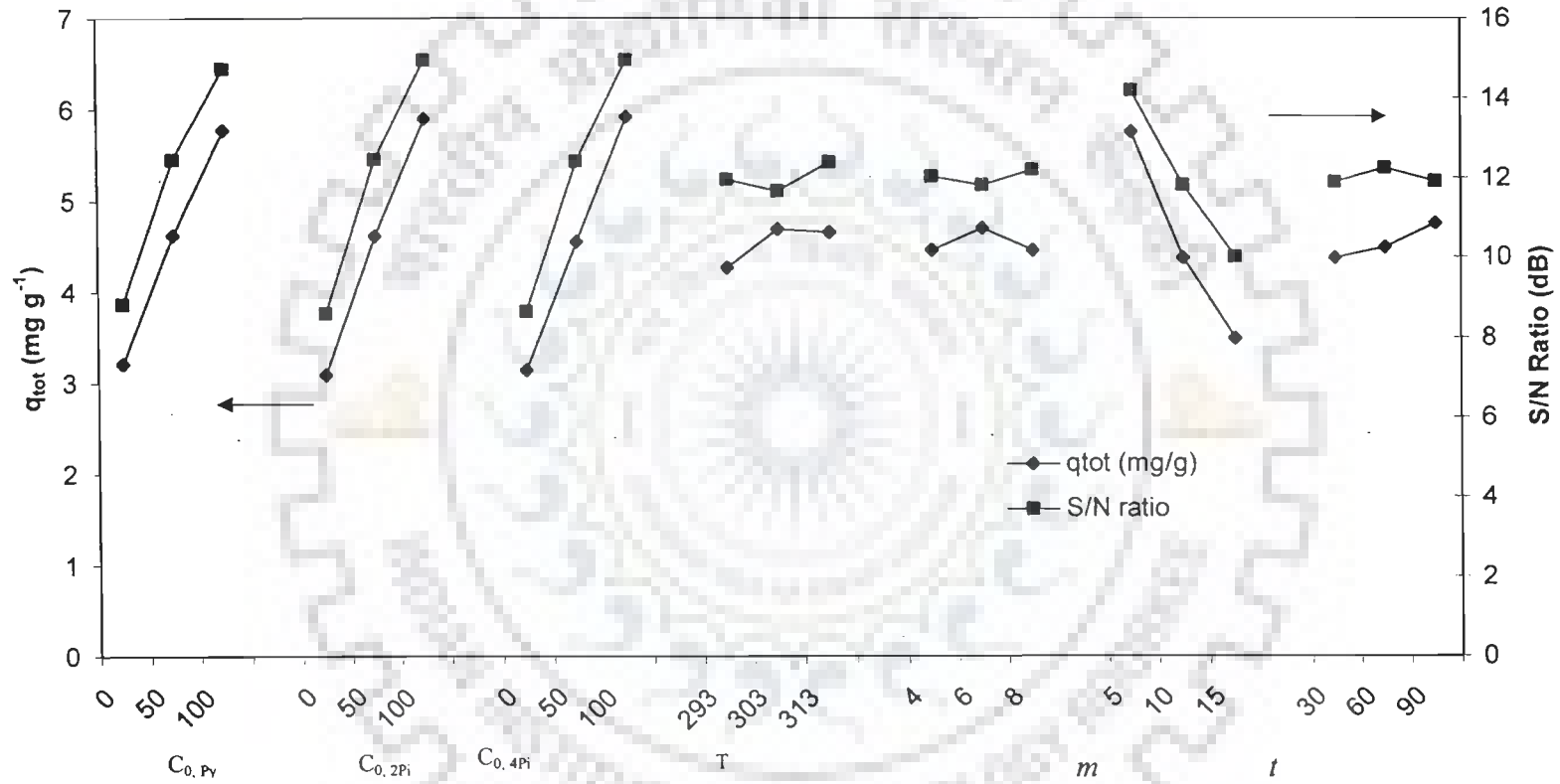
Fig. 6.4.10. Effect of process parameters on q_{tot} **and S/N ratio for multi-component adsorption of Py, 2Pi and 4Pi by GAC.**
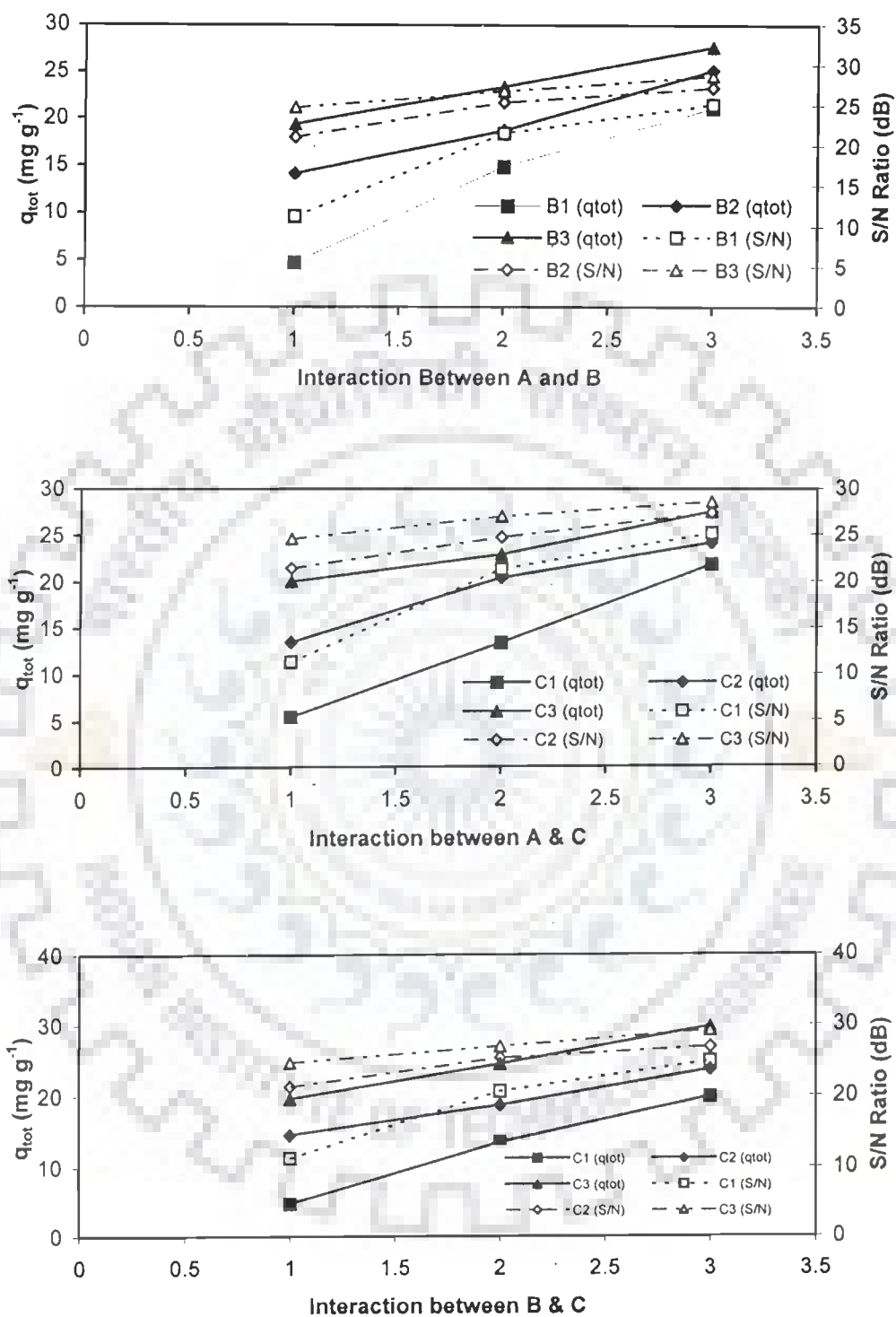
Fig. 6.4.11. The Interaction between parameters A, B, C at 3 levels on q_{tot} and S/N ratio for simultaneous adsorption of py, 2Pi and 4Pi by BFA.
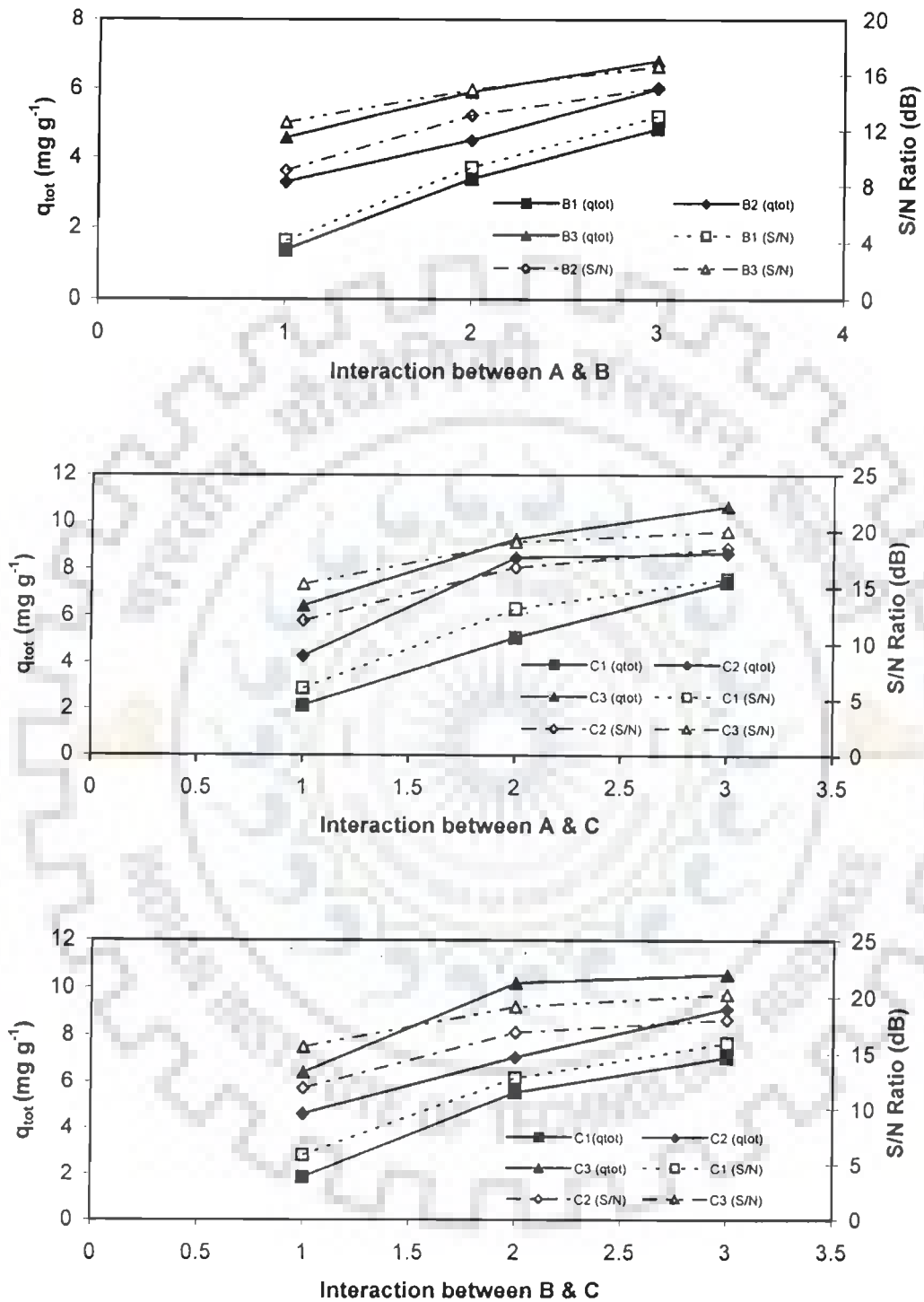
Fig. 6.4.12. The Interaction between parameters A, B, C at 3 levels on q_{tot} and S/N ratio for simultaneous adsorption of py, 2Pi and 4Pi by RHA.
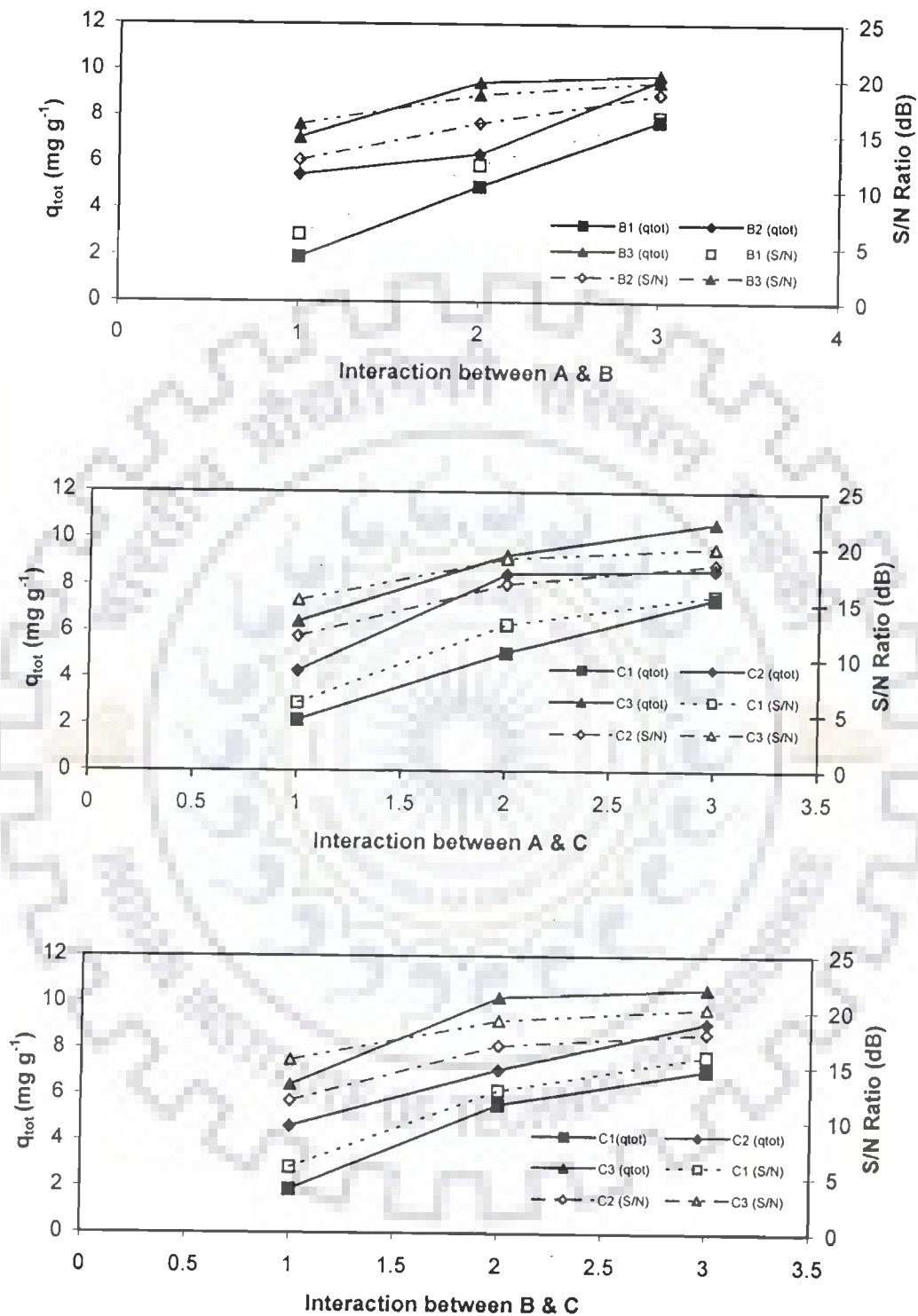
Fig. 6.4.13. The Interaction between parameters A, B, C at 3 levels on q_{tot} and S/N ratio for simultaneous adsorption of py, 2Pi and 4Pi by GAC.

Table 6.4.16. Summary of optimal level of various parameters on q_e values for the removal of Py, 2Pi, 4Pi and AmPy in single component system by BFA, RHA and GAC.

Adsorbent	Py				2Pi			
	Optimal Parameter level				Optimal Parameter level			
BFA	A_3	B_1	C_3	D_2	A_3	B_1	C_3	D_3
RHA	A_3	B_1	C_3	D_3	A_3	B_1	C_3	D_3
GAC	A_3	B_1	C_3	D_2	A_3	B_1	C_3	D_3
	4Pi				AmPy			
BFA	A_3	B_1	C_3	D_2	A_3	B_1	C_3	D_3
RHA	A_3	B_1	C_3	D_2	A_3	B_1	C_3	D_3
GAC	A_3	B_1	C_3	D_2	A_3	B_1	C_3	D_3

Table 6.5.17. Summary of optimal level of various parameters on q_{tot} values for the removal of Py, 2Pi, 4Pi in binary system by BFA, RHA and GAC.

Adsorbent	Py-2Pi				Py-4Pi				2Pi-4Pi			
	Optimal Parameter level				Optimal Parameter level				Optimal Parameter level			
BFA	A_3	B_3	C_1	D_3	A_3	B_3	C_1	D_2	A_3	B_3	C_1	D_2
RHA	A_3	B_3	C_1	D_2	A_3	B_3	C_1	D_2	A_3	B_3	C_1	D_2
GAC	A_3	B_3	C_1	D_3	A_3	B_3	C_1	D_2	A_3	B_3	C_1	D_3

Table 6.5.18. Summary of optimal level of various parameters on q_{tot} values for the removal of Py, 2Pi, 4Pi in ternary system by BFA, RHA and GAC.

Adsorbent	Optimal parameter level						
BFA	A_3	B_3	C_3	D_2	E2	F1	G3
RHA	A_3	B_3	C_3	D_2	E2	F1	G3
ACC	A_3	B_3	C_3	D_2	E2	F1	G3

Lataye et al. (2006) have shown that unit adsorption of Py decreases with an increase in m though the % removal increases due to the availability of greater surface area and more adsorption sites. An increase in $C_{0,i}$ generally increases the q_{tot} value as the resistance to the uptake of adsorbate from the solution decreases with an increase in $C_{0,i}$.

It can be noted from Table 6.4.14 that the interactions between initial concentrations of Py, 2Pi, 4Pi [(A x B), (A x C) or (B x C)] are significant in affecting the average value of q_{tot}. These interaction graphs are shown in Figs. 6.4.11- 6.4.13 for q_{tot} values alongwith the S/N ratios for the ternary adsorption system of Py and its derivatives onto BFA, RHA and GAC.

6.4.5   Selection of Optimal Levels

Since q_{tot} is 'higher the better' type quality characteristic, therefore, greater values of q_{tot} is considered optimal. Tables 6.4.16 - Table 6.4.18 summarize the optimal levels of various parameters obtained after examining the response curves (Figs. 6.4.1 through 6.4.10) of the average values of q_{tot} and S/N ratios for adsorption of Py, 2Pi, 4Pi and AmPy onto BFA, RHA and GAC in single, binary and ternary sorbate systems. Table 6.4.16 indicates that the 3rd levels of parameters A (C_0), 1st level of parameter B (m), 3rd level of parameter C and 2nd or 3rd level of parameter D (t) give higher average value of q_{tot} and S/N ratio.

Since the aim of the present work was to maximise the q, amount of Py and its derivatives with highest possible concentration of Py, 2Pi, 4Pi and AmPy, the third level of C_0 with less m to get maximum uptake q_e is used for further calculations.

Table 6.4.17 indicates that the 3rd levels of parameters A and B (C_0), 1st level of parameter C (m), 3rd/2nd level of parameter D give higher average values of q_{tot} and S/N ratios for different sorbate-sorebnt systems.

Table 6.4.18 indicates that 3rd levels of parameters A, B and C (C_0), 2nd level of parameter D (Temperature), 2nd level of parameter E (pH$_0$), 1st level of parameter F (adsorbent dose, m) and 3rd level of parameter G (Time) give higher average values of q_{tot} and S/N ratios. The above results confirms the earlier results of the present study, e.g. pH$_0$ 6. Since all the three compounds are present together in the ternary systems, the 3rd levels of parameters A, B and C ($C_{0,Py}$, $C_{0,2Pi}$ and $C_{0,4Pi}$) are used for further calculations.

Table 6.4.19. ANOVA of q_{tot} and S/N ratio data for single adsorption of Py, 2Pi, 4Pi by and AmPy BFA.

Factors	Raw Data						S/N Data					
	S	DOF	V	F	S`A	P	S	DOF	V	F	S`A	P
Py												
A	693.46	2	346.73	197.77	689.96	47.58	439.36	2	219.68	27.77	423.54	67.72
B	684.01	2	342.01	195.08	680.51	46.92	(15.82)	(2)	(7.91)	POOLED		
C	37.69	2	18.85	10.75	34.19	2.36	86.35	2	43.18	5.46	70.54	11.28
D	(35.03)	(2)	(17.52)	(9787.66)	(35.03)	(2.42)	83.86	2	41.93	5.30	68.04	10.88
Error	35.06	20	1.75	1.00	45.58	3.14	15.82	2	7.91	1.00	63.28	10.12
Total	1450.23	26	709.34		1450.23	100.00	625.39	8	312.70		625.39	100.00
2Pi												
A	1178.83	2	589.42	801.37	1177.36	54.18	600.17	2	300.08	84.78	593.09	77.04
B	905.40	2	452.70	615.48	903.92	41.60	(7.08)	(2)	(3.54)	POOLED		(0.92)
C	74.04	2	37.02	50.33	72.57	3.34	88.81	2	44.41	12.55	81.74	10.62
D	(12.85)	(2)	(6.43)	(62.22)	(12.64)	(0.59)	73.81	2	36.90	10.43	66.73	8.67
Error	14.71	20	0.74	1.00	19.12	0.88	7.08	2	3.54	1.00	28.32	3.68
Total	2172.98	26	1079.87		2172.98	100.00	769.87	8	384.93		769.87	100.00
4Pi												
A	2401.00	2	1200.50	49.69	2352.68	34.15	559.46	2	279.73	22.10	534.14	61.80
B	3650.37	2	1825.19	75.54	3602.05	52.28	(25.32)	(2)	(12.66)	POOLED		(2.93)
C	354.97	2	177.48	7.35	306.65	4.45	138.58	2	69.29	5.47	113.26	13.10
D	(252.30)	(2)	(126.15)	(9.83)	(226.65)	(3.66)	140.93	2	70.47	5.57	115.62	13.38
Error	483.21	20	24.16	1.00	628.17	9.12	25.32	2	12.66	1.00	101.28	11.72
Total	6889.55	26	3227.33		6889.55	100.00	864.29	8	432.15		864.29	100.00
AmPy												
A	619.88	2	309.94	104.85	613.97	42.93	427.30	2	213.65	23.52	409.13	65.32
B	736.58	2	368.29	124.59	730.67	51.08	(18.17)	(2)	(9.08)	POOLED		(2.90)
C	14.73	2	7.37	2.49	8.82	0.62	90.99	2	45.50	5.01	72.82	11.63
D	(36.69)	(2)	(18.35)	(14.73)	(34.20)	(2.57)	89.84	2	44.92	4.94	71.67	11.44
Error	59.12	20	2.96	1.00	76.86	5.37	18.17	2	9.08	1.00	72.68	11.60
Total	1430.32	26	688.56		1430.32	100.00	626.30	8	313.15		626.30	100.00

(S/S'A- Sum of the Squares, DOF – Degree of Freedom, V –Variance, F – Variance ratio, P - % Contribution)

Table 6.4.20. ANOVA of q_{tot} and S/N ratio data for single adsorption of Py, 2Pi, 4Pi by and 3APy by RHA.

Factors	Raw Data						S/N Data					
	S	DOF	V	F	S`A	P	S	DOF	V	F	S`A	P
Py												
A	30.67	2	15.34	785.77	30.63	72.83	191.40	2	95.70	35.16	185.96	85.25
B	10.54	2	5.27	270.04	10.50	24.97	13.87	2	6.93	2.55	8.42	3.86
C	(0.39)	(2)	(0.19)	(667.30)	(0.38)	(0.92)	7.41	2	3.70	1.36	1.96	0.90
D	0.46	2	0.23	11.72	0.42	1.00	(5.44)	(2)	(2.72)	POOLED		(2.50)
Error	0.39	20	0.02	1.00	0.51	1.21	5.44	2	2.72	1.00	21.78	9.98
Total	42.06	26	20.86		42.06	100.00	218.12	8	109.06		218.12	100.00
2Pi												
A	42.67	2	21.34	504.16	42.59	70.73	224.93	2	112.46	31.93	217.88	84.82
B	15.75	2	7.88	186.09	15.67	26.02	17.20	2	8.60	2.44	10.16	3.96
C	(0.81)	(2)	(0.41)	(225.85)	(0.81)	(1.35)	7.69	2	3.85	1.09	0.65	0.25
D	0.94	2	0.47	11.11	0.86	1.42	(7.04)	(2)	(3.52)	POOLED		(2.74)
Error	0.85	20	0.04	1.00	1.10	1.83	7.04	2	3.52	1.00	28.17	10.97
Total	60.21	26	29.73		60.21	100.00	256.87	8	128.43		256.87	100.00
4Pi												
A	53.87	2	26.94	244.81	53.65	65.84	261.99	2	131.00	44.39	256.09	83.33
B	23.79	2	11.89	108.10	23.57	28.92	30.32	2	15.16	5.14	24.42	7.94
C	(2.20)	2	1.10	23305.28	2.20	2.70	9.12	2	4.56	1.54	3.22	1.05
D	1.62	2	0.81	7.37	1.40	1.72	5.90	2	2.95	POOLED		1.92
Error	2.20	20	0.11	1.00	2.86	3.51	5.90	2	2.95	1.00	23.61	7.68
Total	81.48	26	39.75		81.48	100.00	307.33	8	153.67		307.33	100.00
AmPy												
A	38.61	2	19.30	395.90	38.51	70.28	207.04	2	103.52	23.26	198.14	83.15
B	14.14	2	7.07	145.04	14.05	25.63	12.41	2	6.20	1.39	3.51	1.47
C	0.12	2	0.06	1.26	0.02	0.22	9.94	2	4.97	1.12	1.04	0.44
D	1.07	2	0.53	10.96	0.97	1.77	8.90	2	4.45	POOLED		3.74
Error	0.98	20	0.05	1.00	1.27	2.31	8.90	2	4.45	1.00	35.61	14.94
Total	54.79	26	26.96		54.79	100.00	238.30	8	119.15		238.30	100.00

213

Table 6.4.21. ANOVA of q_{tot} and S/N ratio data for single adsorption of Py, 2Pi, 4Pi by and 3APy GAC.

Factors	Raw Data						S/N Data					
	S	DOF	V	F	S`A	P	S	DOF	V	F	S`A	P
Py												
A	116.35	2	58.17	167.22	115.65	49.61	289.99	2	145.00	11.49	264.75	69.97
B	102.52	2	51.26	147.35	101.83	43.68	25.24	2	12.62	POOLED		6.67
C	6.95	2	3.48	22080.14	6.95	2.98	31.58	2	15.79	1.25	6.34	1.68
D	7.28	2	3.64	10.46	6.58	2.82	31.55	2	15.78	1.25	6.31	1.67
Error	6.96	20	0.35	1.00	9.04	3.88	25.24	2	12.62	1.00	100.97	26.68
Total	233.10	26	113.42		233.10	100.00	378.37	8	189.18		378.37	100.00
2Pi												
A	309.69	2	154.85	607.42	309.18	54.83	346.35	2	173.18	22.77	331.14	67.98
B	232.75	2	116.38	456.51	232.24	41.19	15.21	2	7.61	POOLED		3.12
C	4.93	2	2.47	269.29	4.92	0.87	59.47	2	29.73	3.91	44.25	9.09
D	16.35	2	8.18	32.08	15.84	2.81	66.06	2	33.03	4.34	50.84	10.44
Error	5.10	20	0.25	1.00	6.63	1.18	15.21	2	7.61	1.00	60.86	12.49
Total	563.90	26	279.66		563.90	100.00	487.09	8	243.54		487.09	100.00
4Pi												
A	444.34	2	222.17	54.24	436.15	44.21	391.88	2	195.94	27.25	377.50	69.29
B	430.89	2	215.45	52.60	422.70	42.84	14.38	2	7.19	POOLED		2.64
C	23.62	2	11.81	3.65	17.15	2.39	68.40	2	34.20	4.76	54.02	9.92
D	29.43	2	14.72	3.59	21.24	2.15	70.11	2	35.06	4.87	55.73	10.23
Error	81.92	20	4.10	1.00	106.49	10.79	14.38	2	7.19	1.00	57.53	10.56
Total	986.59	26	456.43		986.59	100.00	544.78	8	272.39		544.78	100.00
AmPy												
A	128.01	2	64.00	139.16	127.09	43.14	306.50	2	153.25	10.00	275.86	67.15
B	148.16	2	74.08	161.07	147.24	49.98	30.64	2	15.32	POOLED		7.46
C	7.14	2	3.57	31.25	6.91	2.42	36.85	2	18.43	1.20	6.21	1.51
D	9.22	2	4.61	10.02	8.30	2.82	36.81	2	18.40	1.20	6.17	1.50
Error	9.20	20	0.46	1.00	11.96	4.06	30.64	2	15.32	1.00	122.57	29.84
Total	294.58	26	143.15		294.58	100.00	410.81	8	205.40		410.81	100.00

Table 6.4.22. ANOVA of q_{tot} and S/N ratio data for binary adsorption of Py, 2Pi and 4Pi by BFA.

Factors	Raw Data						S/N Data					
	S	DOF	V	F	S`A	P	S	DOF	V	F	S`A	P
Py-2Pi												
A	871.93	2	435.97	92.63	862.52	39.39	267.21	2	133.60	160.09	265.54	43.55
B	819.85	2	409.93	87.10	810.44	37.01	270.62	2	135.31	162.13	268.95	44.11
C	403.66	2	201.83	42.88	394.25	18.01	1.67	2	0.83			0.27
D	94.12	2	47.06	5882.52	94.12	4.30	70.24	2	35.12	42.08	68.57	11.25
Error	94.13	20	4.71	1.00	122.37	5.59	1.67	2	0.83	1.00	6.68	1.09
Total	2189.58	26	1052.43			100.00	609.74	8	304.87			100.00
Py-4Pi												
A	959.86	2	479.93	97.04	949.97	37.12	278.63	2	139.32	105.63	275.99	43.11
B	995.95	2	497.98	100.69	986.06	38.53	286.45	2	143.23	108.59	283.81	44.33
C	504.58	2	252.29	51.01	494.69	19.33	2.64	2	1.32			0.41
D	98.59	2	49.30	2766.51	98.56	3.85	72.55	2	36.27	27.50	69.91	10.92
Error	98.91	20	4.95	1.00	128.59	5.02	2.64	2	1.32	1.00	10.55	1.65
Total	2559.30	26	1235.14		2559.30	100.00	640.27	8	320.14		640.27	100.00
2Pi-4Pi												
A	1800.31	2	900.16	75.20	1776.37	36.22	312.79	2	156.40	51.20	306.69	40.96
B	1955.95	2	977.97	81.70	1932.01	39.39	322.11	2	161.06	52.73	316.00	42.20
C	909.02	2	454.51	37.97	885.08	18.05	6.11	2	3.05			0.82
D	230.18	2	115.09	224.81	229.16	4.69	107.76	2	53.88	17.64	101.65	13.58
Error	239.40	20	11.97	1.00	311.22	6.35	6.11	2	3.05	1.00	24.43	3.26
Total	4904.68	26	2344.61		4904.68	100.00	748.77	8	374.39		748.77	100.00

Table 6.4.23. ANOVA of q_{tot} and S/N ratio data for binary adsorption of Py, 2Pi and 4Pi by RHA.

Factors	Raw Data						S/N Data					
	S	DOF	V	F	S`A	P	S	DOF	V	F	S`A	P
Py-2Pi												
A	44.13	2	22.06	179.44	43.88	42.33	106.21	2	53.10	21.54	101.28	42.63
B	48.08	2	24.04	195.53	47.84	46.14	115.03	2	57.51	23.33	110.10	46.34
C	9.01	2	4.50	36.63	8.76	8.45	11.43	2	5.72	2.32	6.50	2.74
D	2.46	2	1.23	2924.16	2.46	2.37	4.93	2	2.46			2.07
Error	2.46	20	0.12	1.00	3.20	3.08	4.93	2	2.46	1.00	19.72	8.30
Total	103.68	26	50.73		103.68	100.00	237.60	8	118.80		237.60	100.00
Py-4Pi												
A	54.30	2	27.15	225.13	54.06	42.37	118.74	2	59.37	24.50	113.90	42.90
B	57.67	2	28.84	239.11	57.43	45.01	127.54	2	63.77	26.32	122.69	46.22
C	13.21	2	6.61	54.78	12.97	10.17	14.35	2	7.17	2.96	9.50	3.58
D	2.41	2	1.21	29211.25	2.41	1.89	4.85	2	2.42			1.83
Error	2.41	20	0.12	1.00	3.14	2.46	4.85	2	2.42	1.00	19.38	7.30
Total	127.60	26	62.72		127.60	100.00	265.47	8	132.74		265.47	100.00
2Pi-4Pi												
A	57.89	2	28.94	220.24	57.62	42.73	124.40	2	62.20	23.54	119.11	43.84
B	59.85	2	29.93	227.72	59.59	44.18	127.30	2	63.65	24.09	122.02	44.91
C	14.50	2	7.25	55.18	14.24	10.56	14.72	2	7.36	2.78	9.43	3.47
D	2.62	2	1.31	2584.44	2.62	1.94	5.29	2	2.64			1.95
Error	2.63	20	0.13	1.00	3.42	2.53	5.29	2	2.64	1.00	21.14	7.78
Total	134.87	26	66.25		134.87	100.00	271.70	8	135.85		271.70	100.00

216

Table 6.4.24. ANOVA of q_{tot} and S/N ratio data for binary adsorption of Py, 2Pi and 4Pi by GAC.

Factors	Raw Data						S/N Data					
	S	DOF	V	F	S`A	P	S	DOF	V	F	S`A	P
Py-2Pi												
A	143.73	2	71.87	70.11	141.68	36.04	166.18	2	83.09	7.19	143.06	37.00
B	144.58	2	72.29	70.53	142.53	36.26	172.16	2	86.08	7.45	149.04	38.55
C	84.29	2	42.14	41.12	82.24	20.92	23.12	2	11.56			5.98
D	20.32	2	10.16	56.70	20.30	5.17	25.16	2	12.58	1.09	2.04	0.53
Error	20.50	20	1.03	1.00	26.65	6.78	23.12	2	11.56	1.00	92.47	23.92
Total	393.11	26	187.33		393.11	100.00	386.61	8	193.31		386.61	100.00
Py+4Pi												
A	157.67	2	78.84	122.51	156.39	36.89	172.42	2	86.21	9.29	153.87	37.52
B	171.81	2	85.91	133.49	170.53	40.23	197.57	2	98.79	10.65	179.02	43.66
C	81.52	2	40.76	63.34	80.23	18.93	21.52	2	10.76	1.16	2.97	0.72
D	12.871	2	6.4353	7.83771	12.871	3.036	18.55	2	9.27			4.52
Error	12.87	20	0.64	1.00	16.73	3.95	18.55	2	9.27	1.00	74.20	18.09
Total	423.88	26	206.15		423.88	100.00	410.06	8	205.03		410.06	100.00
2Pi+4Pi												
A	420.77	2	210.39	98.49	416.50	40.09	222.75	2	111.38	72.48	219.68	44.35
B	403.17	2	201.59	94.37	398.90	38.39	217.58	2	108.79	70.80	214.51	43.31
C	172.30	2	86.15	40.33	168.03	16.17	3.07	2	1.54			0.62
D	42.54	2	21.27	2156.58	42.52	4.09	51.92	2	25.96	16.89	48.85	9.86
Error	42.72	20	2.14	1.00	55.54	5.35	3.07	2	1.54	1.00	12.29	2.48
Total	1038.96	26	500.26		1038.96	100.00	495.33	8	247.66		495.33	100.00

Table 6.4.25 ANOVA of q_{tot} and S/N ratio data for ternary adsorption of Py, 2Pi and 4Pi by BFA.

Parameter	Raw data					S/N data				
	S	DOF	V	P	F	S	DOF	V	P	F
A	1340.39	2	670.20	15.16	97548.39	262.62	2	131.31	20.28	21.46
B	1923.59	2	961.80	21.76	139991.05	305.15	2	152.58	23.56	24.94
C	1777.73	2	888.86	20.11	129375.84	288.82	2	144.41	22.30	23.60
D	109.62	2	54.81	1.24	7977.60	13.89	2	6.94	1.07	1.13
E	34.05	2	17.03	0.39	2478.20	12.24	2	6.12	0.94	1.00
F	3151.89	2	1575.95	35.65	229381.86	136.04	2	68.02	10.50	11.12
G	17.73	2	8.86	0.20	1290.16	(13.33)	(2)	(6.66)	POOLED	-
AxB	180.21	4	45.05	2.04	6557.59	92.24	4	23.06	7.12	3.77
AxC	203.88	4	50.97	2.31	7418.93	90.88	4	22.72	7.02	3.71
BxC	102.16	4	25.54	1.16	3717.37	80.07	4	20.02	6.18	3.27
Residual	0.37	54	0.01	0.20		0.00	2	6.12	0.94	
Model	8841.26	26	4299.07	99.80	625736.00	1295.26	26	575.72	99.06	94.09
Total	8841.63	80	4299.07	100.00		1295.26	26	587.95	100.00	

Table 6.4. 26. ANOVA of q_{tot} and S/N ratio data for ternary adsorption of Py, 2Pi and 4Pi by **RHA**.

Parameter	Raw data					S/N data				
	S	DOF	V	P	F	S	DOF	V	P	F
A	88.98	2	44.49	22.99	2438620.36	160.21	2	80.11	24.16	240.96
B	106.79	2	53.39	27.60	2926821.00	184.18	2	92.09	27.77	277.00
C	104.19	2	52.10	26.93	2855703.07	181.25	2	90.62	27.33	272.60
D	2.94	2	1.47	0.76	80543.02	2.30	2	1.15	0.35	3.46
E	1.03	2	0.51	0.27	28183.56	0.66	2	0.33	0.10	1.00
F	69.98	2	34.99	18.08	1917844.46	78.91	2	39.46	11.90	118.68
G	2.04	2	1.02	0.53	55936.15	(0.77)	(2)	(0.38)	POOLED	-
AxB	4.14	4	1.03	1.07	56709.92	18.32	4	4.58	2.76	13.78
AxC	3.94	4	0.99	1.02	54058.57	18.12	4	4.53	2.73	13.63
BxC	2.94	4	0.74	0.76	40312.11	18.48	4	4.62	2.79	13.90
Residual	0.00	54	0.00	0.27		0.00	0	0.33	0.10	
Model	386.97	26	190.73	99.73	10454731.21	663.20	26	317.54	99.90	955.16
Total	386.97	80	190.73	100.00		663.20	26	318.20	100.00	

Table 6.4.27. ANOVA of q_{tot} and S/N ratio data for ternary adsorption of Py, 2Pi and 4Pi by GAC.

Parameter	Raw data					S/N data				
	S	DOF	V	P	F	S	DOF	V	P	F
A	206.20	2	103.10	15.44	2796543.52	193.79	2	96.90	21.13	73.99
B	244.04	2	122.02	18.27	3309752.30	210.61	2	105.31	22.97	80.41
C	306.71	2	153.35	22.96	4159667.46	235.82	2	117.91	25.72	90.03
D	6.91	2	3.46	0.52	93734.62	2.87	2	1.44	0.31	1.10
E	80.44	2	40.22	6.02	1090968.82	30.91	2	15.46	3.37	11.80
F	430.30	2	215.15	32.21	5835944.79	160.62	2	80.31	17.52	61.32
G	2.99	2	1.49	0.22	40543.09	(2.62)	(2)	(1.31)	POOLED	-
AxB	36.65	4	9.16	2.74	248502.73	34.79	4	8.70	3.79	6.64
AxC	12.30	4	3.07	0.92	83380.80	20.45	4	5.11	2.23	3.90
BxC	9.27	4	2.32	0.69	62864.15	24.46	4	6.12	2.67	4.67
Residual	0.00	54	0.00	0.22		0.00	0	1.31	0.29	
Model	1335.80	26	653.35	99.78	17721901.27	916.97	26	437.25	99.71	333.86
Total	1335.80	80	653.35	100.00		916.97	26	439.86	100.00	

The contribution of individual factors is the key for the control to be enforced on the adsorption of various compounds onto BFA, RHA and GAC. In Taguchi's approach, analysis of variance (ANOVA) is used to analyze the results of the OA experiment and to determine how much variation has been contributed by each factor. ANOVA results for raw and S/N ratio data with desired response characteristic (q_{tot}) are given in Tables 6.4.19 - 6.4.27 for adsorption of Py, 2Pi, 4Pi and 3APy in single, binary and ternary systems onto BFA, RHA and GAC. From the calculated ratios (F), it can be inferred that all the factors and interactions considered in the experimental design with q_{tot} as the desired response characteristic are statistically significant at 95% confidence limit.

By studying the main effects of each of the factors, the general trends of the influence of the factors towards the adsorptive removal process can be characterized. The characteristics can be controlled in such a way that a lower or a higher value in a particular influencing factor produces the preferred result. Thus, the levels of factors to produce the best results can be predicted. The percentage contribution of each parameter on q_{tot} as desired response characteristic is shown in Fig. 6.4.14 -6.4.20. Tables 6.4.28 - 6.4.30 summarize the relative contribution of the highest influencing parameters on q_{tot} values and S/N ratios for the adsorption of Py, 2Pi, 4Pi and AmPy onto BFA, RHA and GAC for single, binary and ternary system, respectively.

Table 6.4.28. Summary of parameter having highest % contribution on q_{tot} value for the removal of Py and its derivatives in single component system for adsorption onto BFA, RHA and GAC.

Adsorbent	Raw Data		S/N Ration	
	Parameter	% Contribution	Parameter	% Contribution
Py				
BFA	A	47.58	A	67.72
RHA	A	72.83	A	85.25
GAC	A	49.61	A	69.97
2Pi				
BFA	A	54.18	A	77.04
RHA	A	70.73	A	84.82
GAC	A	54.83	A	67.98
4Pi				
BFA	B	52.28	A	61.80
RHA	A	65.84	A	83.33
GAC	A	44.21	A	69.29
AmPy				
BFA	B	51.08	A	65.32
RHA	A	70.28	A	83.15
GAC	B	49.98	A	67.15

Table 6.4.29. Summary of parameter having highest percent contribution to q_{tot} value for removal of Py and its derivatives in binary system for adsorption onto BFA, RHA and GAC.

Adsorbent	Raw Data		S/N Ration	
	Parameter	% Contribution	Parameter	% Contribution
Py-2Pi				
BFA	A	39.39	B	44.11
RHA	B	46.14	B	46.34
GAC	B	36.26	B	38.55
Py-4Pi				
BFA	B	38.53	B	44.33
RHA	B	45.01	B	46.22
GAC	B	40.23	B	43.66
2Pi-4Pi				
BFA	B	39.39	B	42.20
RHA	B	44.18	B	44.91
GAC	A	40.09	A	44.35

Table 6.4.30. Summary of parameter having highest percent contribution to q_{tot} value for removal of Py and its derivatives in tertiary system for adsorption onto BFA, RHA and GAC.

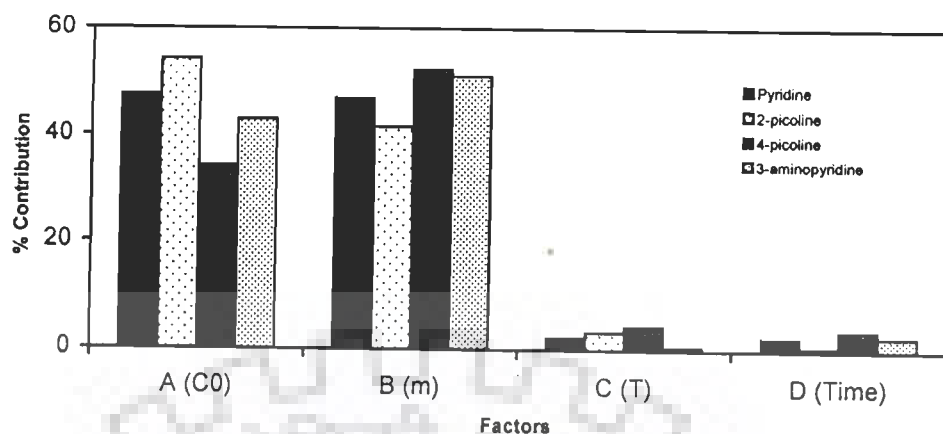|	Raw Data		S/N Data	
	Parameter	% Contribution	Parameter	% Contribution
BFA	B	21.76	B	23.56
RHA	B	27.60	B	27.77
ACC	C	22.96	C	25.72

Fig. 6.4.14.   Percent contribution of various parameters for q_{tot} for individual adsorption of Py, 2Pi, 4Pi and 3APy BFA.
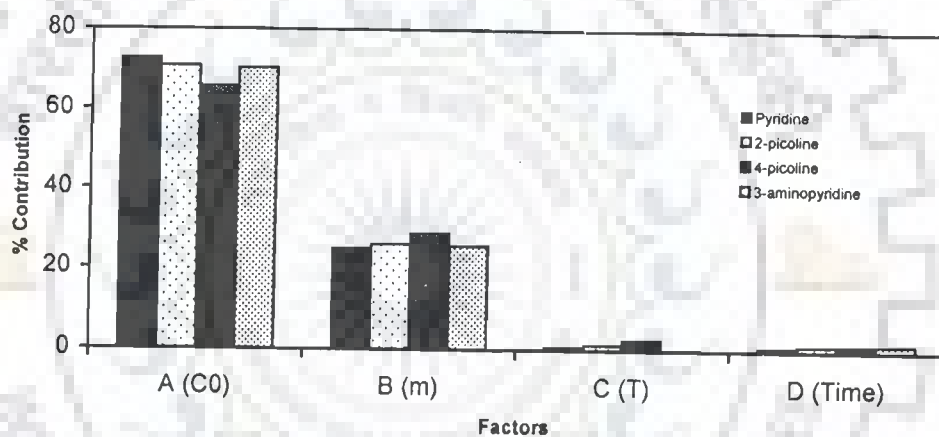

Fig. 6.4.15.   Percent contribution of various parameters for q_{tot} for individual adsorption of Py, 2Pi, 4Pi and 3APy RHA.

Fig. 6.4.16.   Percent contribution of various parameters for q_{tot} for individual adsorption of Py, 2Pi, 4Pi and 3APy GAC.

Fig. 6.4.17. Percent contribution of various parameters for q_{tot} for individual adsorption of Py, 2Pi, 4Pi and 3APy BFA.

Fig. 6.4.18. Percent contribution of various parameters for q_{tot} for individual adsorption of Py, 2Pi, 4Pi and 3APy RHA.
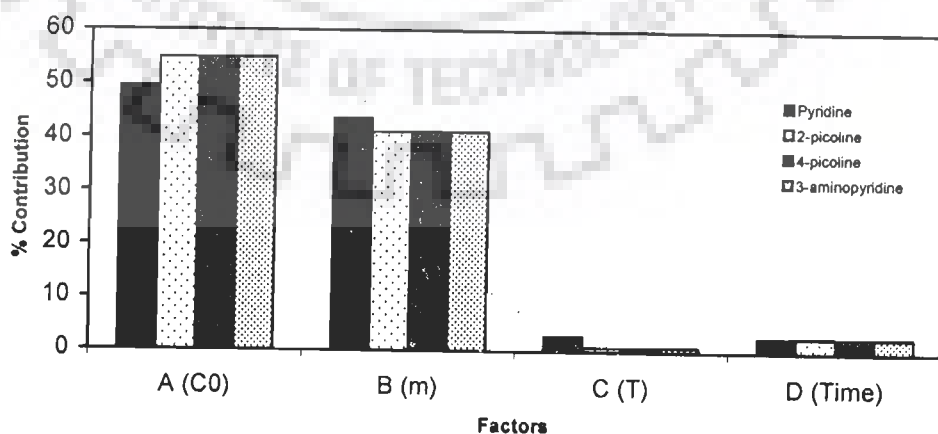

Fig. 6.4.19. Percent contribution of various parameters for q_{tot} for individual adsorption of Py, 2Pi, 4Pi and 3APy GAC.
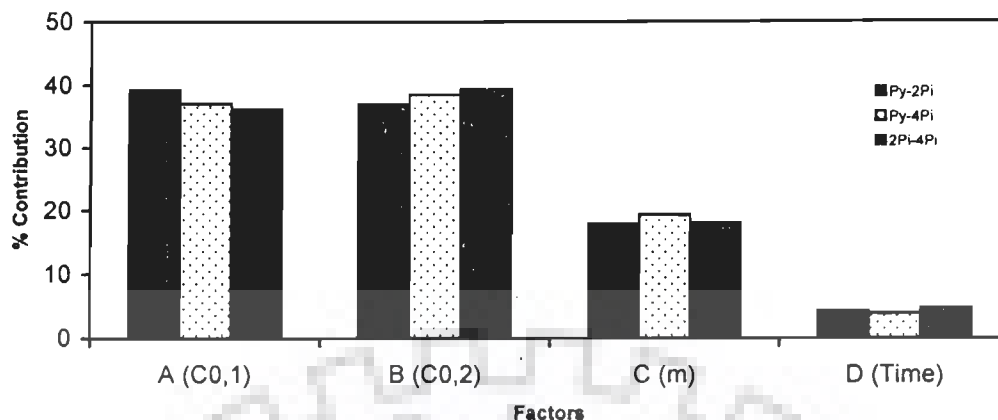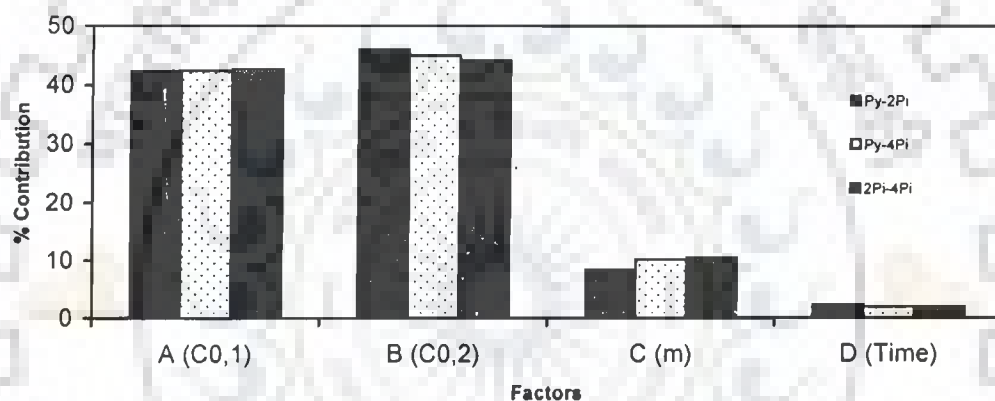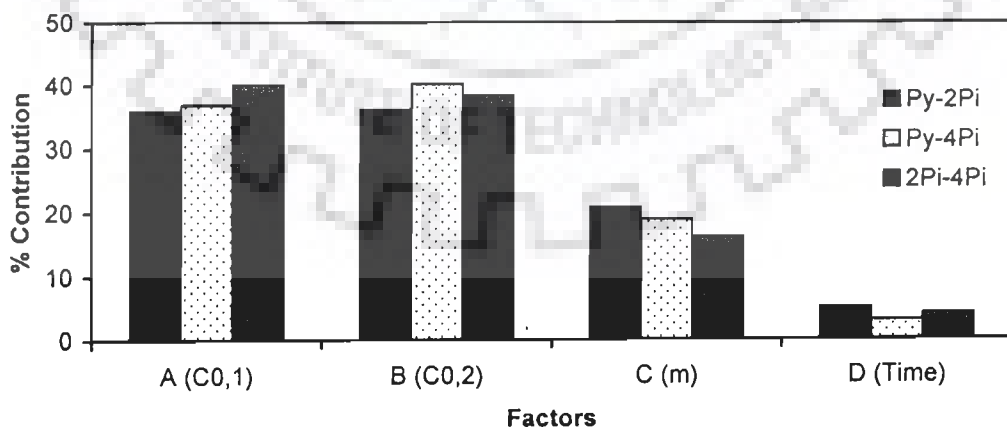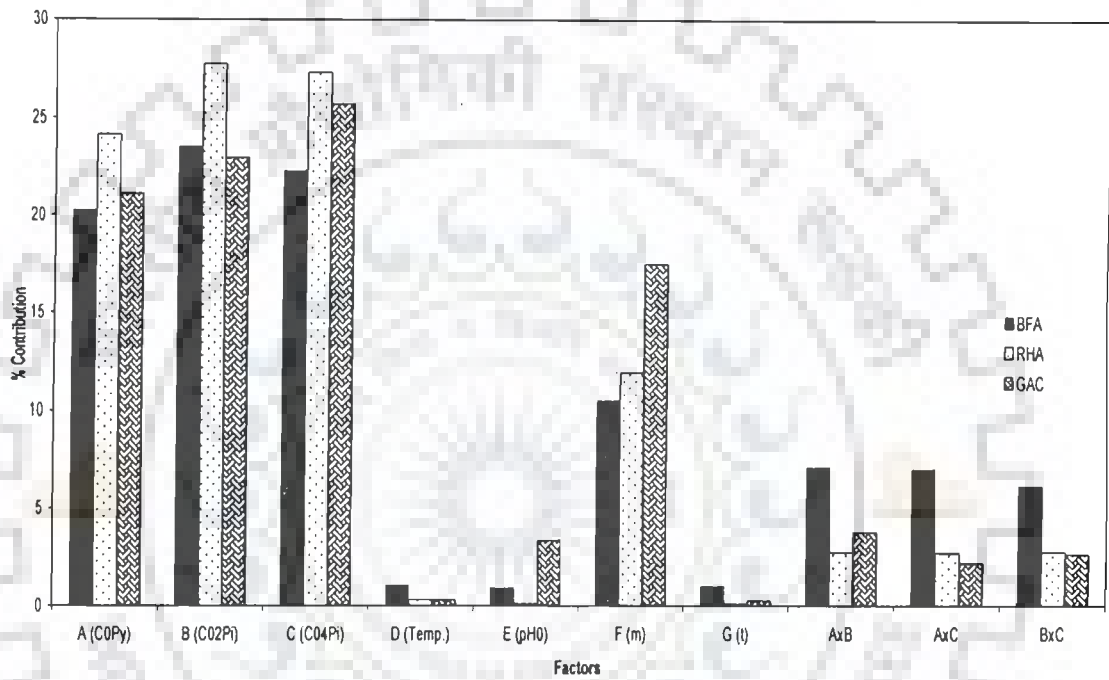
Fig. 6.4.20.   Percent contribution of various parameters for q_{tot} for multi-component adsorption of Py, 2Pi and 4Pi by BFA, RHA and GAC.

6.4.6 Estimation of Optimum Response Characteristics

In this section, the optimal values of the response characteristics (q_{tot}) along with their respective confidence intervals have been predicted. The results of the confirmation experiments conducted to validate the optimal results are also presented. The level of process parameters to be used for optimizing the q_{tot} value for the single, binary and ternary adsorption of Py, 2Pi, 4Pi and AmPy onto BFA, RHA and GAC has been discussed in the previous section. The Taguchi's approach for predicting the mean of response characteristic and the determination of confidence intervals for the predicted means have been presented in Chapter V.

The significant process parameters affecting the removal of Py by BFA and their optimal levels (as already selected) are: A3, B1, C3, D2

The average value (from Table 6.4.6) of q_{tot} (mg g^{-1}) at:

3rd level of concentration of Py ($\bar{A}_3$) = 19.20

1st level of adsorbent dose ($\bar{B}_1$) = 19.85

3rd level of Temperature ($\bar{C}_3$) = 14.67

2nd level of time ($\bar{D}_2$) = 14.06

The overall mean of q_{tot} ($\bar{T}_{BFA}$) = 13.02 (mg g^{-1})   (from Table 6.4.1)

The predicted optimum value of q_{tot} for BFA (μ_{BFA}) has been calculated as:

$$\mu_{BFA} = \bar{T}_{BFA} + (\bar{A}_3 - \bar{T}_{BFA}) + (\bar{B}_1 - \bar{T}_{BFA}) + (\bar{C}_3 - \bar{T}_{BFA}) + (\bar{D}_2 - \bar{T}_{BFA})$$

$$= 28.7 \text{ mg g}^{-1}$$

The 95 % confidence intervals for the mean of the population and three confirmation experiments (CI_{POP} and CI_{CE}) have been calculated by substituting the following values:

N = total number of results = 9 x 3 = 27; f_e (DOF error) = (26 – 8) = 18;

V_e (error variance) = 1.75 (recalculated from Table 6.4.19).

$$n_{eff} = \frac{N}{1 + [\text{Total DOF associated in the estimate of the mean}]}$$

$$= 3$$

$F_{0.05}(1, 18) = 4.414$ (Tabulated F-value)

$$CI_{POP} = \sqrt{\frac{F_\alpha(1, f_e) V_e}{n_{eff}}} = \pm 1.61$$

$$CI_{CE} = \sqrt{F_\alpha(1, f_e) \left[\frac{1}{n_{eff}} + \frac{1}{R} \right]} = \pm 1.69$$

The 95 % confidence intervals (CI_{POP} and CI_{CE}) of the predicted ranges of q_{tot} for BFA are as follows:

CI_{POP} : $27.09 < \mu_{BFA}$ (mg/g) < 30.31

CI_{CE} : $27.01 < \mu_{BFA}$ (mg/g) < 30.40

By adopting a similar procedure, predicted optimal q_{tot} values and confidence intervals (CI_{POP} and CI_{CE}) have been calculated and presented in Table 6.4.31 to 6.4.33, for adsorption of Py, 2Pi, 4Pi and AmPy onto BFA, RHA and GAC in single and multi-component systems.

6.4.7 Confirmation Experiments

Three confirmation experiments have been conducted for adsorption of Py, 2Pi, 4Pi and AmPy onto BFA, RHA and GAC in single and multicomponent systems at selected optimal levels of the process parameters. The average values of the characteristics are obtained and compared with the predicted values. The results are given in Tables 6.4.31- 6.4.33.

Table. 6.4.31. Predicted optimal q_{tot} values, confidence intervals and results of confirmation experiments for adsorption of Py, 2Pi, 4Pi and AmPy onto BFA, RHA and GAC.

Adsorbent	Optimal levels of process parameters	Predicted optimal values (mg g⁻¹)	Confidence intervals (95 %)	Average of Confirmation experiments (mg g⁻¹)
Py				
BFA	A_3, B_1, C_3, D_2	28.7	CI_{POP}:27.10< μ_{BFA} < 30.31 CI_{CE}: 27.01< μ_{BFA} < 30.40	28.63
RHA	A_3, B_1, C_3, D_2	5.17	CI_{POP}:5.01< μ_{RHA} < 5.34 CI_{CE}: 5.00< μ_{RHA} < 5.35	5.23
GAC	A_3, B_1, C_3, D_2	11.62	CI_{POP}:10.9< μ_{BFA} < 12.33 CI_{CE}:10.86< μ_{BFA} < 12.37	11.57
2Pi				
BFA	A_3, B_1, C_3, D_3	35.72	CI_{POP}:34.68< μ_{BFA} < 36.77 CI_{CE}: 34.63< μ_{BFA} < 36.82	35.69
RHA	A_3, B_1, C_3, D_3	5.99	CI_{POP}:5.74< μ_{BFA} < 6.24 CI_{CE}: 5.72< μ_{BFA} < 6.25	6.01
GAC	A_3, B_1, C_3, D_3	18.55	CI_{POP}:17.9< μ_{BFA} < 19.16 CI_{CE}: 17.91< μ_{BFA} < 19.20	18.73
4Pi				
BFA	A_3, B_1, C_3, D_2	60.37	CI_{POP}:54.40< μ_{BFA} < 66.33 CI_{CE}: 54.08< μ_{BFA} < 55.04	59.81
RHA	A_3, B_1, C_3, D_2	6.79	CI_{POP}:6.38< μ_{BFA} < 7.19 CI_{CE}: 6.36< μ_{BFA} < 7.21	6.68
GAC	A_3, B_1, C_3, D_2	22.78	CI_{POP}:22.33< μ_{BFA} < 25.24 CI_{CE}: 20.19< μ_{BFA} < 25.37	23.03
AmPy				
BFA	A_3, B_1, C_3, D_2	28.25	CI_{POP}:26.16< μ_{BFA} < 30.33 CI_{CE}: 26.05< μ_{BFA} < 30.40	27.98
RHA	A_3, B_1, C_3, D_3	5.89	CI_{POP}:6.2< μ_{BFA} <6.16 CI_{CE}: 5.61< μ_{BFA} < 6.17	5.98
GAC	A_3, B_1, C_3, D_3	12.55	CI_{POP}:11.73 < μ_{BFA} < 13.37 CI_{CE}: 11.68< μ_{BFA} < 13.42	12.78

Table. 6.4.32. Predicted optimal q_{tot} values, confidence intervals and results of confirmation experiments for adsorption of Py, 2Pi and 4Pi onto BFA, RHA and GAC in binary system.

Adsorbent	Optimal levels of process parameters	Predicted optimal values (mg g^{-1})	Confidence intervals (95 %)	Average of Confirmation experiments (mg g^{-1})
Py+2Pi				
BFA	A_3, B_3, C_1, D_3	31.34	$CI_{POP}: 28.70 < \mu_{BFA} < 33.97$	31.57
			$CI_{CE}: 28.56 < \mu_{BFA} < 34.11$	
RHA	A_3, B_3, C_1, D_2	7.04	$CI_{POP}: 6.61 < \mu_{RHA} < 7.46$	7.24
			$CI_{CE}: 6.59 < \mu_{RHA} < 7.48$	
GAC	A_3, B_1, C_3, D_2	13.02	$CI_{POP}: 11.79 < \mu_{GAC} < 14.25$	12.87
			$CI_{CE}: 11.73 < \mu_{GAC} < 14.32$	
Py+4Pi				
BFA	A_3, B_3, C_1, D_2	33.28	$CI_{POP}: 30.58 < \mu_{BFA} < 35.98$	33.56
			$CI_{CE}: 30.44 < \mu_{BFA} < 36.12$	
RHA	A_3, B_3, C_1, D_2	7.66	$CI_{POP}: 7.24 < \mu_{RHA} < 8.09$	7.91
			$CI_{CE}: 7.22 < \mu_{RHA} < 8.11$	
GAC	A_3, B_3, C_1, D_3	13.36	$CI_{POP}: 12.39 < \mu_{GAC} < 14.33$	13.69
			$CI_{CE}: 12.33 < \mu_{GAC} < 14.38$	
2Pi+ 4Pi				
BFA	A_3, B_3, C_1, D_2	46.87	$CI_{POP}: 42.67 < \mu_{BFA} < 51.06$	47.09
			$CI_{CE}: 42.44 < \mu_{BFA} < 51.29$	
RHA	A_3, B_3, C_1, D_2	7.81	$CI_{POP}: 7.37 < \mu_{RHA} < 8.25$	7.93
			$CI_{CE}: 7.35 < \mu_{RHA} < 8.28$	
GAC	A_3, B_3, C_1, D_2	21.78	$CI_{POP}: 20.01 < \mu_{GAC} < 23.55$	22.3
			$CI_{CE}: 19.91 < \mu_{GAC} < 23.65$	

Table. 6.4.33. Predicted optimal q_{tot} values, confidence intervals and results of confirmation experiments for adsorption of Py, 2Pi and 4Pi onto BFA, RHA and GAC in ternary system.

Adsorbent	Optimal levels of process parameters	Predicted optimal values (mg g^{-1})	Confidence intervals (95 %)	Average of Confirmation experiments (mg g^{-1})
BFA	A_3, B_3, C_3, D_2, E_2, F_1, G_3	46.1	CI$_{POP}$:45.44 < μ_{BFA} < 46.76 CI$_{CE}$: 45.41< μ_{BFA} < 46.80	46.39
RHA	A_3, B_3, C_3, D_2, E_2, F_1, G_3	10.26	CI$_{POP}$:10.04< μ_{RHA} < 10.48 CI$_{CE}$: 10.03< μ_{RHA} < 10.5	10.37
GAC	A_3, B_3, C_3, D_2, E_2, F_1, G_3	17.42	CI$_{POP}$:17.15< μ_{GAC} < 17.69 CI$_{CE}$:17.14< μ_{GAC} < 17.7	17.39

The results of the confirmation experiments are within 95% of CI_{CE} for respective adsorbents and adsorbates. It is to be pointed out that these optimal values are valid within the specified range of process parameters. Any extrapolation/ interpolation must be confirmed by conducting additional experiments.

6.5 MULTI-STAGE ADSORPTION

Multi-stage adsorption study was carried out for the removal of Py, 2Pi, 4Pi and AmPy from aqueous solution using BFA, RHA and GAC as adsorbents with the aim to bring down the final concentration of all the compounds below the maximum permissible concentration limit.

The supernatant obtained from the first stage (after agitating the effluent with respective adsorbents at optimum dosage) was again treated with fresh adsorbent at optimum dosage in the next stage and so on. The pH_0 of the solution was maintained at 6.0 in all the stages. C_0 was 100 mg dm^{-3} for each compound. The optimum dosage was 8 g dm^{-3} of BFA for Py and AmPy and 5 g dm^{-3} for 2Pi and 4Pi. The optimum

dosage of RHA was 30 g dm^{-3} for Py and AmPy and 20 g dm^{-3} for 2Pi and 4Pi. For GAC the optimum dosage was 20 g dm^{-3} of BFA for Py and AmPy and 10 g dm^{-3} for 2Pi and 4Pi.

The results for the removal of Py, 2Pi, 4Pi and AmPy from aqueous solution using BFA, RHA and GAC are shown in Table 6.5.1 and Figs. 6.5.1 - 6.5.3. Table 6.5.1 shows the final concentration (C_e) at the end of the treatment stage while Figs. 6.5.1 - 6.5.3 show the removal efficiencies for each stage of treatment by BFA, RHA and GAC, respectively. Table 6.5.2 shows the efficiencies of BFA, RHA and GAC.

It is found that the two-stage adsorption scheme with BFA, RHA and GAC shall be good to bring down the concentration of the given compounds in the aqueous solutions below the maximum concentration limit.

Table 6.5.1. **Multi-stage adsorption of Py, 2Pi, 4Pi and AmPy aqueous solution using BFA, RHA and GAC.**

Concentration (mg dm^{-3})	BFA				RHA				GAC			
	Py	2Pi	4Pi	AmPy	Py	2Pi	4Pi	AmPy	Py	2Pi	4Pi	AmPy
C_0	100	100	100	100	100	100	100	100	100	100	100	100
$C_{e,I}$	6.10	4.85	5.73	11.32	9.88	8.99	8.17	14.03	4.66	7.56	9.89	9.20
$C_{e,II}$	0.8	1.12	1.66	1.46	2.88	1.73	3.43	4.63	0.63	0.52	1.09	2.21
$C_{e,III}$	-	-	-	-	-	-	-	-	-	-	-	-

Table 6.5.2: **Removal efficiencies of BFA, RHA and GAC at various stages in multistage treatment**

BFA	Py	2Pi	4Pi	AmPy
Stage-I	93.90	95.15	94.27	88.68
Stage-II	86.89	76.98	71.07	87.12
RHA				
Stage-I	90.12	91.01	91.83	85.97
Stage-II	70.90	80.73	58.03	67.03
GAC				
Stage-I	95.35	92.44	90.11	90.80
Stage-II	86.57	93.17	89.02	76.00

Fig. 6.5.1. Removal efficiency of BFA at various stages in multistage treatment ($C_0 = 100$ mg dm^{-3}, T = 303 K, pH$_0$ = 6, t = 5 h)

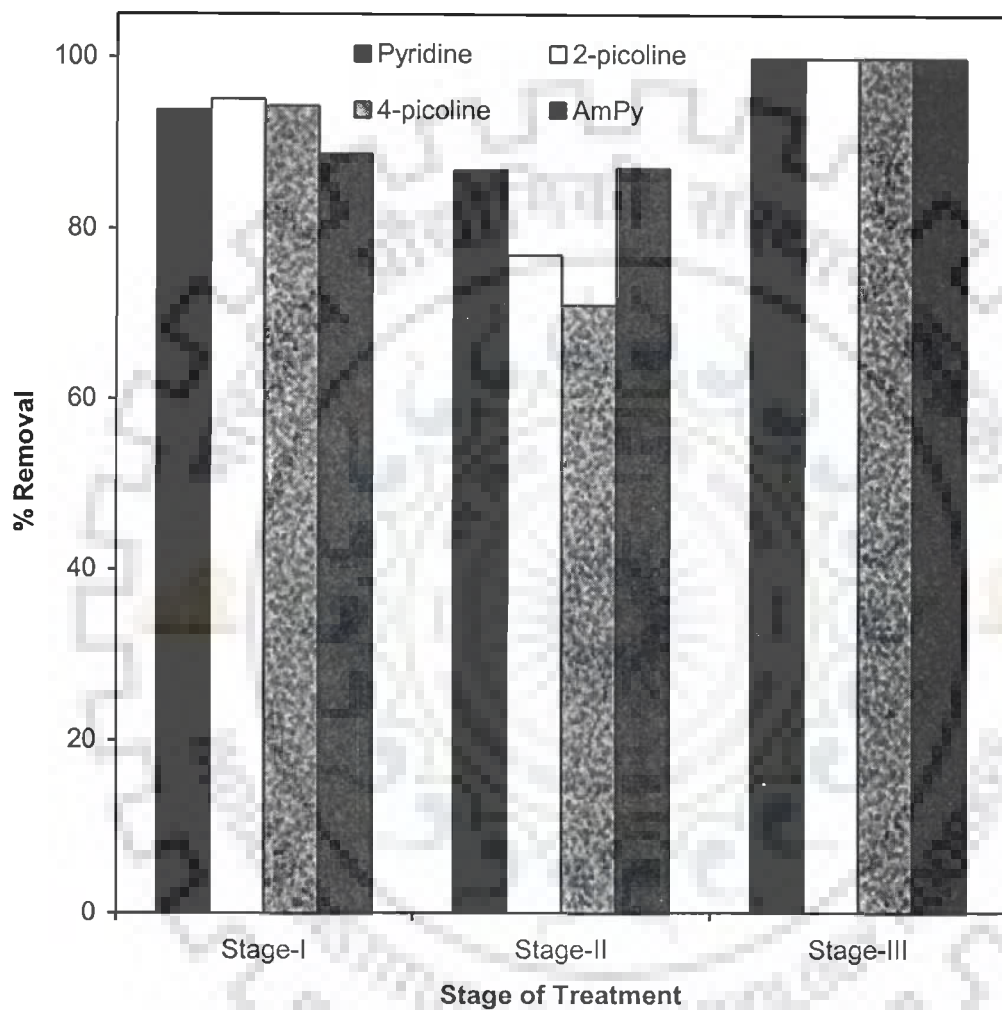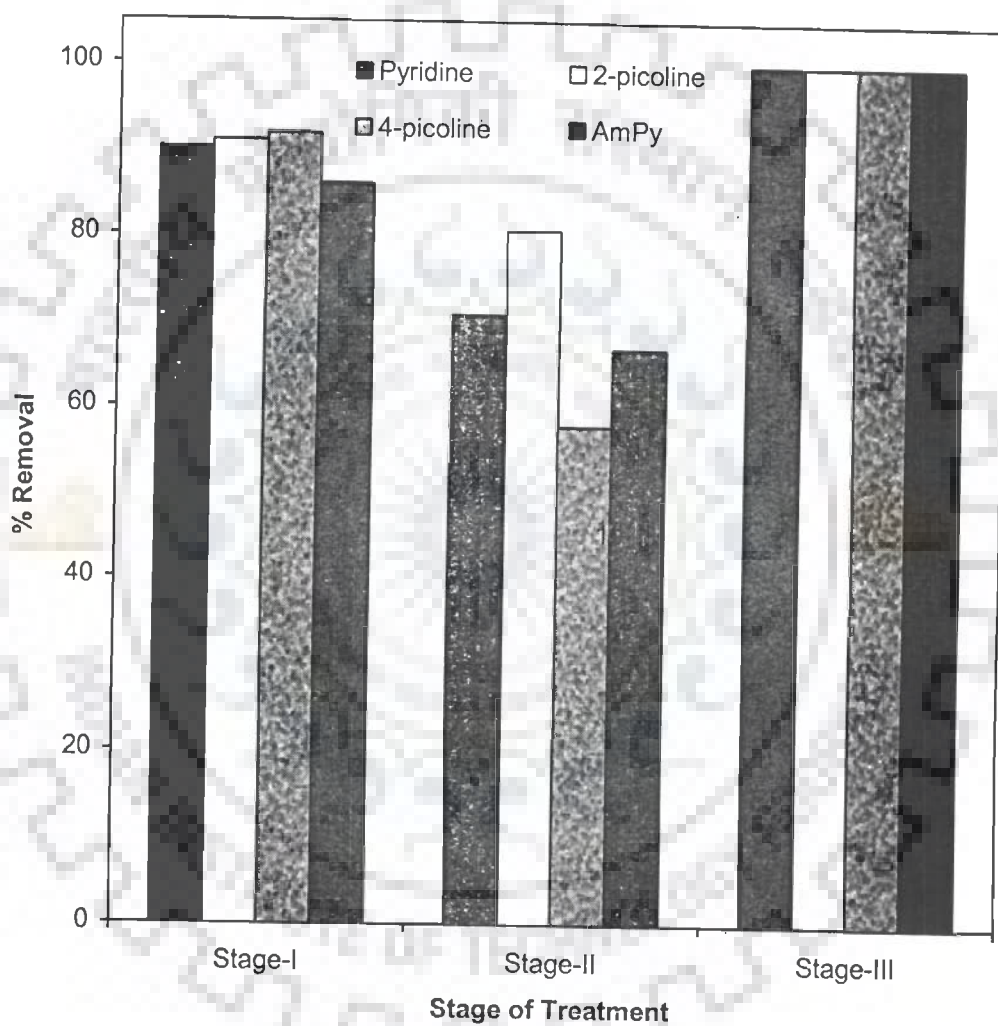**Fig 6.5.2. Removal efficiency of RHA at various stages in multistage treatment ($C_0 = 100$ mg dm^{-3}, T = 303 K, pH$_0$ = 6, t = 5 h)**

233
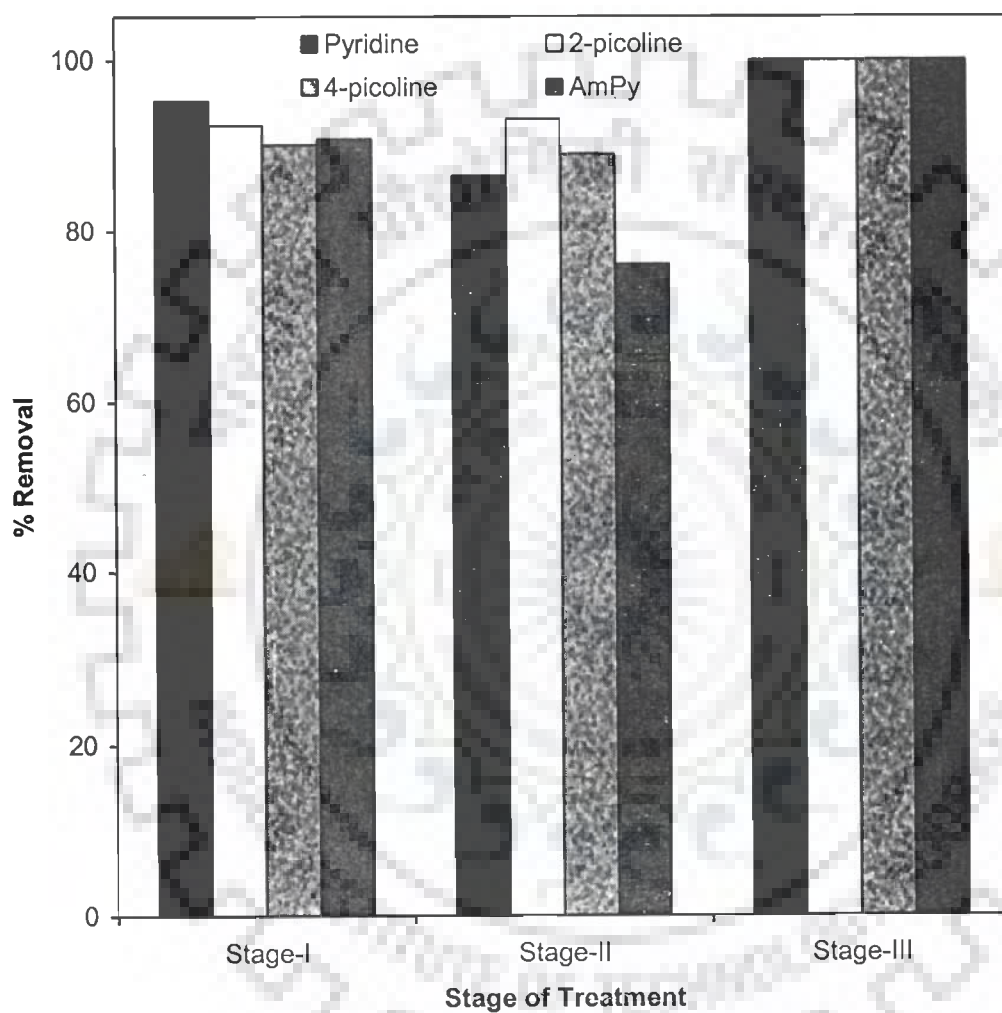
Fig. 6.5.3. Removal efficiency of GAC at various stages in multistage treatment ($C_0 = 100$ mg dm^{-3}, T = 303 K, pH$_0$ = 6, t = 5 h)

6.6   DESORPTION STUDY

The evaluation of the various desorbing (eluting) agents (solvents) for loaded/exhausted sorbents for the elution of sorbates was carried out under batch experimental conditions. The loaded adsorbents were obtained from the equilibrium adsorption study for a $C_0 = 100$ mg dm^{-3} of single components at $pH_0 = 6$, $T = 303$ K, $t = 5$ h and $m = 8$ g dm^{-3} for BFA, 30 g dm^{-3} for RHA and 20 g dm^{-3} for GAC. The adsorbents were filtered and dried in a dessicator for 48 h before being used for the desorption experiments. The desorption efficiencies of these solvents have been shown in Fig. 6.6.1 for Py, 2Pi, 4Pi and AmPy from loaded BFA, RHA and GAC, respectively.

Fig. 6.6.1 Desorption of Py, 2Pi, 4Pi and AmPy in water at different pH and various medium from BFA.

235

Table 6.6.1 to 6.6.3 show the desorption efficiencies of Py, 2Pi, 4Pi and AmPy from BFA, RHA and GAC at temperatures 288 K and 303 K. From the table it is seen that Py desorption efficiency of water at lower pH from BFA is 53.1% at 303 K temperature and it increases to 55% at 288 K. Similarly the desorption efficiency of 0.1 N H_2SO_4 for Py is 51.13% at normal temperature. It is observed that the efficiency of 0.1N $H_2SO_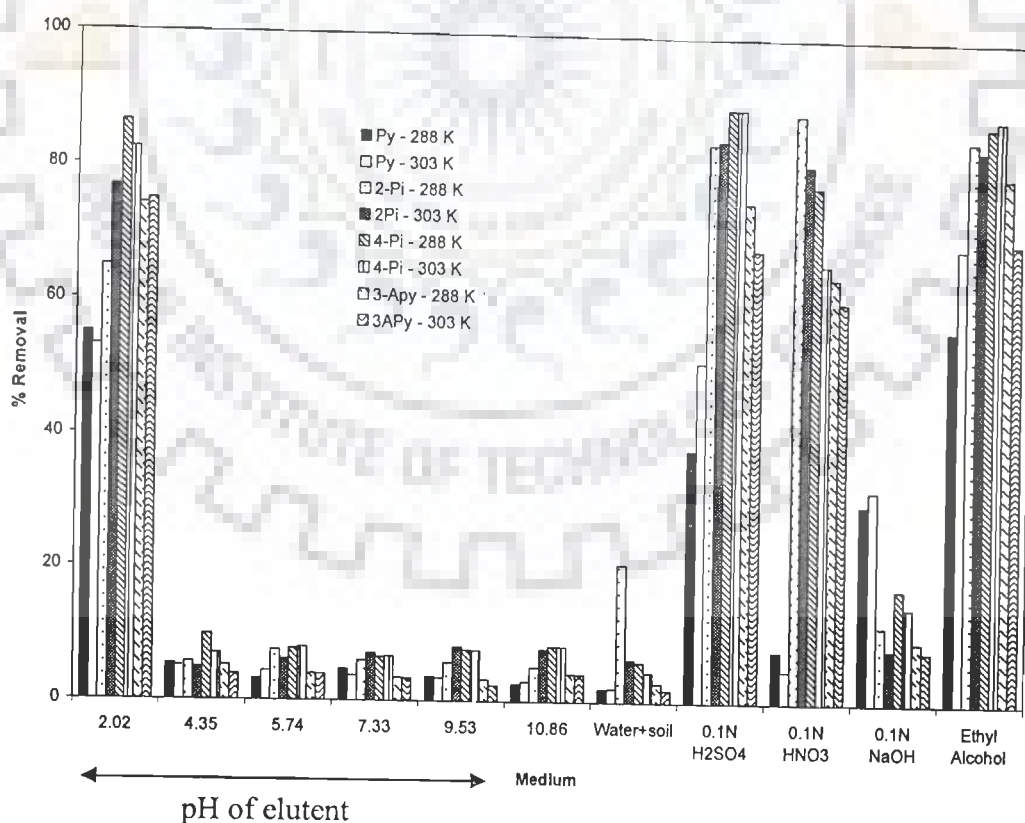4$ is more (about 90%) followed by 0.1N HNO_3 and acidic water. The maximum desorption efficiencies for Py, 2Pi, 4Pi and AmPy was 51, 84.5, 89, and 75% respectively for 0.1 N H2SO4 from BFA, 95, 86, 91 and 82% respectively from RHA and 93, 89, 91 and 88% respectively from GAC by H2SO4. The desorption efficiency is more in case of 0.1 N H2SO4 solution as compare to other acids in all the systems.

Table 6.6.1: **Desorption of Py, 2Pi, 4Pi and AmPy in water at different pH and various medium from BFA.**

Medium	% Desorption							
	Py		2Pi		4Pi		AmPy	
	288 K	303 K	288 K	303 K	288 K	303 K	288 K	303 K
Water at Different pH								
2.02	55.00	53.10	64.94	76.79	86.58	82.54	74.24	74.91
4.35	5.31	5.05	5.58	4.86	9.80	6.91	5.18	3.88
5.74	3.20	4.35	7.43	6.10	7.69	7.87	4.03	3.94
7.33	4.68	3.71	6.01	7.06	6.46	6.63	3.48	3.37
9.53	3.65	3.46	5.68	8.07	7.57	7.51	3.23	2.40
10.86	2.58	2.95	5.06	7.74	8.16	8.16	4.17	4.08
Water+soil	1.93	2.03	20.54	6.26	5.93	4.47	2.85	1.82
0.1N H_2SO_4	37.98	51.13	84.04	84.53	89.33	89.33	75.17	68.03
0.1N HNO_3	7.67	4.86	88.63	80.95	77.71	65.97	64.05	60.42
0.1N NaOH	29.75	32.02	11.52	8.06	17.08	14.39	9.21	7.76
Ethyl Alcohol	56.31	68.70	85.01	83.58	87.25	88.32	79.51	69.53

Table 6.6.2: Desorption of Py, 2Pi, 4Pi and AmPy in water at different pH and various medium from RHA.

Medium	% Desorption							
	Py		2Pi		4Pi		AmPy	
	288 K	303 K	288 K	303 K	288 K	303 K	288 K	303 K
Water at Different pH								
2.02	36.69	67.60	68.58	71.99	89.41	72.53	82.91	73.76
4.35	8.15	11.20	5.22	14.01	10.15	8.34	5.10	3.82
5.74	6.61	9.98	7.45	13.95	7.88	7.64	3.83	3.83
7.33	6.71	10.53	6.01	7.06	5.43	5.18	3.74	3.74
9.53	6.25	11.05	5.72	9.47	6.30	6.28	3.77	3.77
10.86	6.12	10.63	5.09	9.62	10.68	10.68	3.87	3.87
Water+soil	45.14	30.64	2.31	2.70	3.21	1.85	3.41	2.05
0.1N H_2SO_4	88.36	95.35	86.22	84.80	91.28	80.82	82.07	82.07
0.1N HNO_3	95.07	86.70	77.69	70.10	76.25	73.57	76.81	76.81
0.1N NaOH	7.57	12.15	7.88	5.69	11.95	8.02	4.78	4.03
Ethyl Alcohol	79.10	39.91	8596.00	84.57	90.32	82.31	83.14	84.32

Table 6.6.3: Desorption of Py, 2Pi, 4Pi and AmPy in water at different pH and various medium from GAC.

Medium	% Desorption							
	Py		2Pi		4Pi		AmPy	
	288 K	303 K	288 K	303 K	288 K	303 K	288 K	303 K
Water at Different pH								
2.02	37.21	69.89	87.42	81.82	85.49	89.95	86.21	81.90
4.35	2.76	9.01	9.11	7.53	6.85	5.14	6.60	6.67
5.74	2.54	9.55	8.90	9.13	5.34	5.22	3.09	2.40
7.33	2.61	9.17	7.76	6.01	4.60	4.47	2.57	2.34
9.53	2.68	9.16	9.83	11.30	4.28	3.17	3.05	2.36
10.86	2.56	8.97	8.05	16.56	5.52	5.40	3.11	2.42
Water+soil	1.64	3.01	4.70	12.54	3.78	2.41	1.90	1.28
0.1N H_2SO_4	73.98	93.09	89.19	88.90	91.17	90.06	88.10	51.32
0.1N HNO_3	62.30	12.52	83.72	83.13	80.12	79.98	82.51	82.51
0.1N NaOH	3.05	9.43	8.59	15.53	12.19	10.27	4.37	3.68
Ethyl Alcohol	72.42	51.63	90.21	89.51	92.36	92.15	87.95	82.31

6.7 ADSORPTION OF REAL WASTEWATER BY USING TAGUCHI'S DESIGN OF EXPERIMENTS

The Taguchi design of experimental methodology has been used for the treatment of real wastewater being discharged from a unit manufacturing pyridine and its derivatives. The sample wastewater was collected from the outlet after the recovery of ammonia in the pyridine/picoline production plant.

Table 6.7.1. Typical Characteristics Real Wastewater from Py and its derivative Manufacturing Industry

S. No.	Characteristics	Value (mg dm^{-3})
1	pH	11.59
2	Total Solids	11200
3	Total Volatile Solids	11160
4	Fixed Solids	40
5	COD	34800
6	BOD	5200
7	Pyridine	330.72
8	2-picoline	112.24
9	4-picoline	239.67
10	Aminopyridine	Not Detected

6.7.1 Experimental Results of Batch Study

The parameters were: m, pH_0, T and t. Each parameter was tested at three level (Table 6.7.2). Experiments were conducted according to the test conditions specified by L_9 OA (Table 4.4.4, Chapter IV). Each experiment was repeated three times for each trial condition. The q_{tot} data of Py, 2Pi and 4Pi adsorption onto BFA, RHA and GAC are given in Table 6.7.3.

Table 6.7.2: Parameters and their levels considered in the design for the removal of Py and its derivatives by BFA, RHA and GAC.

Factors	Parameters	Units	BFA			RHA			GAC		
			L_1	L_2	L_3	L_1	L_2	L_3	L_1	L_2	L_3
A	m	g dm^{-3}	10	25	40	40	50	60	20	30	40
B	pH_0	-	4	6	8	4	6	8	4	6	8
C	T	K	273	203	313	273	203	313	273	203	313
D	t	min	30	120	210	30	120	210	30	120	210

Table 6.7.3 Experimental q_{tot} values for adsorption of Py and its derivatives onto BFA, RHA and GAC from wastewater using Taguchi design of experiment.

Trial No.	BFA				RHA				GAC			
	Final $q_{e,tot}$ (mg g^{-1})			S/N Ratio (dB)	Final $q_{e,tot}$ (mg g^{-1})			S/N Ratio (dB)	Final $q_{e,tot}$ (mg g^{-1})			S/N Ratio (dB)
	R_1	R_2	R_3		R_1	R_2	R_3		R_1	R_2	R_3	
1	8.95	9.22	9.35	19.25	3.57	3.25	3.15	10.40	5.38	5.07	5.81	14.64
2	10.53	10.37	10.25	20.32	4.15	3.73	3.59	11.60	5.21	5.59	6.21	15.00
3	7.01	6.85	6.93	16.81	3.25	2.99	3.51	10.18	3.69	3.54	4.01	11.44
4	15.25	15.41	16.02	23.83	3.96	4.07	4.51	12.38	6.59	6.25	5.99	15.94
5	8.03	7.85	7.63	17.88	3.02	3.13	3.67	10.21	5.19	5.23	5.96	14.69
6	7.34	7.04	6.98	17.04	2.99	3.04	3.25	9.79	4.35	4.48	4.87	13.17
7	14.76	14.14	13.85	23.07	3.81	3.59	3.78	11.42	7.57	7.33	7.29	17.38
8	7.53	7.26	7.43	17.39	3.52	2.95	3.93	10.62	3.27	3.37	3.68	10.70
9	11.21	10.82	10.97	20.83	3.21	3.42	3.68	10.68	4.29	4.39	4.87	13.06
Total	90.61	88.95	89.41		31.48	30.17	33.07		45.54	45.27	48.69	
Avg.	9.96				3.51				5.17			

6.7.2 Effect of Process Parameters

The average or mean values of response characteristics q_{tot} and S/N ratio for each parameter at level 1, 2, and 3 are calculated from Table 6.7.3. The raw data for the average value of q_{tot} and S/N ratio for each parameter at levels 1, 2, and 3 are given in Table 6.7.4.

Table 6.7.5 summarizes the parameters that have highest influence on q_{tot} for the raw and S/N data. Individually at level stage with q_{tot} as the desired response characteristic, m (parameter A) has highest influence at level 1, and pH_0 (parameter B) has highest influence at level 2, for adsorption of Py, 2Pi, and 4Pi onto BFA, RHA and GAC.. The difference between level 2 and level 1 ($L_2 - L_1$) of each factor indicates the relative influence of the effect.

Table 6.7.4: Average and main effects of q_{tot} values for BFA RHA and GAC – raw and S/N data

Factors	Raw Data (Average Value)			Main Effects (Raw Data)		S/N Data (Average Value)			Main Effects (S/N Data)	
	L_1	L_2	L_3	L_2-L_1	L_3-L_2	L_1	L_2	L_3	L_2-L_1	L_3-L_2
BFA										
A	13.60	8.99	7.30	-4.62	-1.69	22.58	18.99	17.24	-3.59	-1.74
B	8.45	11.26	10.18	2.81	-1.08	18.34	20.68	19.79	2.34	-0.89
C	9.34	10.03	10.52	0.69	0.49	19.32	19.42	20.07	0.11	0.65
D	9.50	10.55	9.83	1.05	-0.72	19.40	19.96	19.44	0.57	-0.52
RHA										
A	3.78	3.54	3.20	-0.24	-0.33	11.50	10.87	10.06	-0.62	-0.81
B	3.38	3.76	3.38	0.37	-0.38	10.49	11.40	10.53	0.91	-0.86
C	3.34	3.58	3.60	0.24	0.02	10.43	10.93	11.06	0.50	0.13
D	3.45	3.58	3.49	0.13	-0.10	10.69	10.99	10.75	0.30	-0.24
GAC										
A	6.06	4.84	4.59	-1.22	-0.25	15.46	13.45	13.10	-2.01	-0.35
B	3.90	5.80	5.80	1.90	-0.01	11.73	15.21	15.06	3.48	-0.15
C	5.13	4.76	5.60	-0.37	0.84	14.13	13.27	14.61	-0.86	1.34
D	4.92	5.15	5.43	0.23	0.28	13.74	14.01	14.26	0.26	0.25

Table 6.7.5: **Summary of parameters having highest influence on q_{tot} values for the removal of Py and its derivatives by BFA, RHA and GAC.**

Factors	Raw Data (Average Value)			Main Effects (Raw Data)		S/N Data (Average Value)			Main Effects (S/N Data)	
	L_1	L_2	L_3	L_2-L_1	L_3-L_2	L_1	L_2	L_3	L_2-L_1	L_3-L_2
BFA	A	B	C	B	C	A	B	C	B	C
RHA	A	B	C	B	C	A	B	C	B	C
GAC	A	B	B	B	C	A	B	B	B	C

The response curves for the individual effects of adsorption parameters on the average value of q_{tot} and respective S/N ratio for the adsorption of Py and its derivatives onto BFA are given in Figs. 6.7.1 - 6.7.3 An increase in the levels of factors such as T and t from 1 to 2 and from 2 to 3 has resulted in an increase in the q_{tot} values for all adsorbents. The details have been already discussed in earlier section.
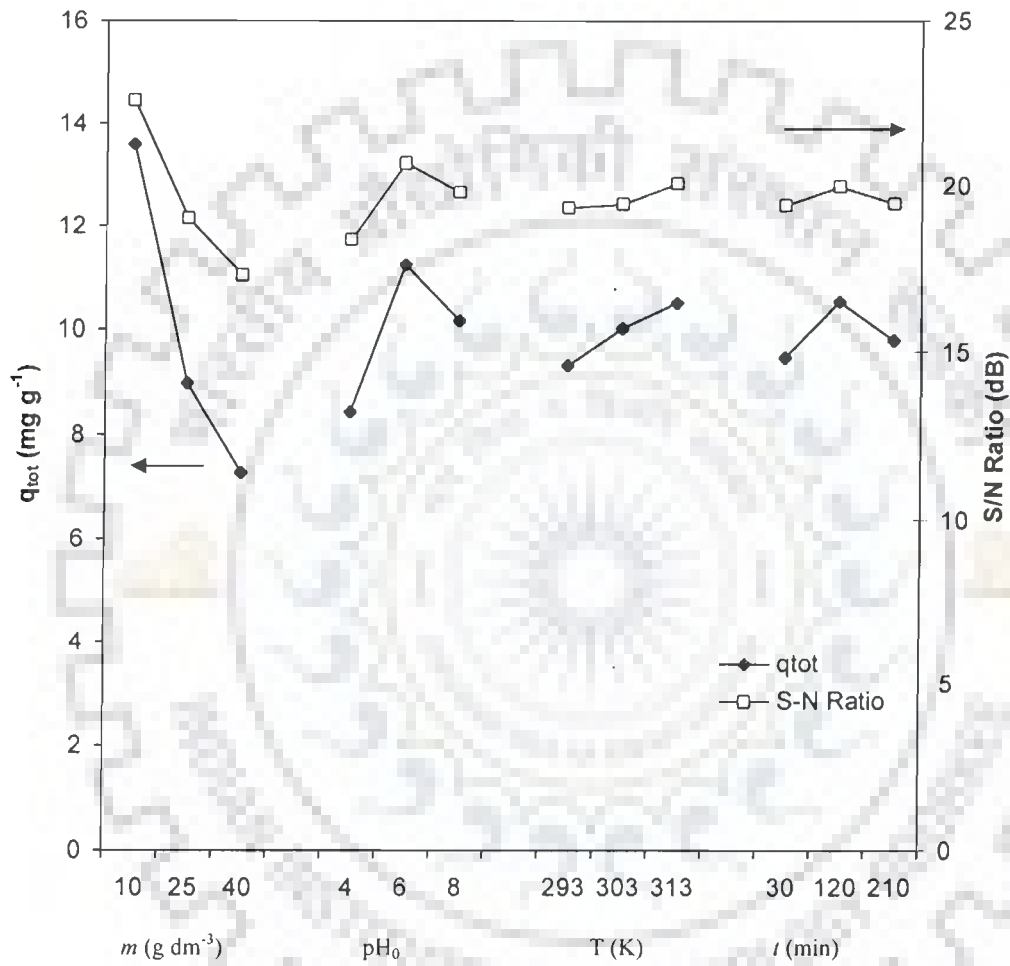
Fig. 6.7.1 **Effect of process parameters on q_{tot} and S/N ratio for adsorption of Py and its derivatives from real wastewater onto BFA.**
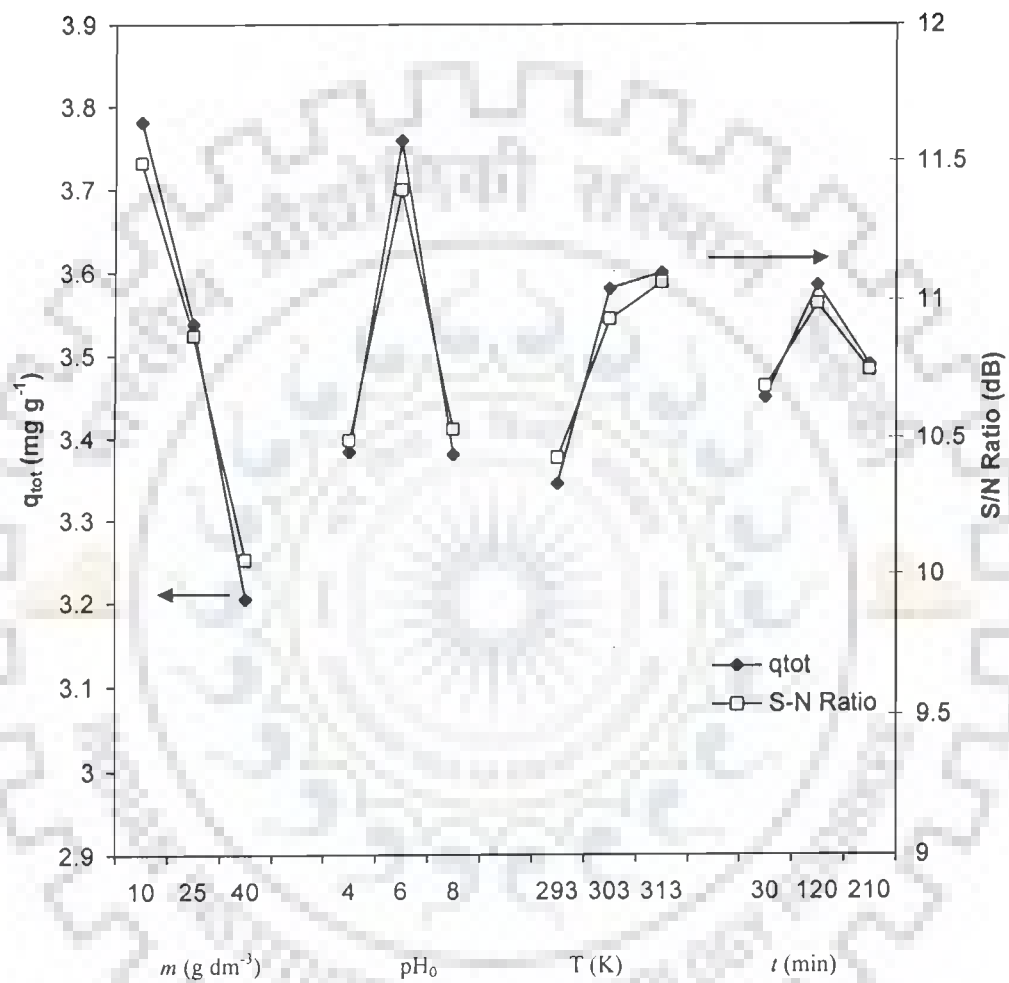
Fig. 6.7.2 **Effect of process parameters on** q_{tot} **and S/N ratio for adsorption of Py and its derivatives from real wastewater onto RHA.**
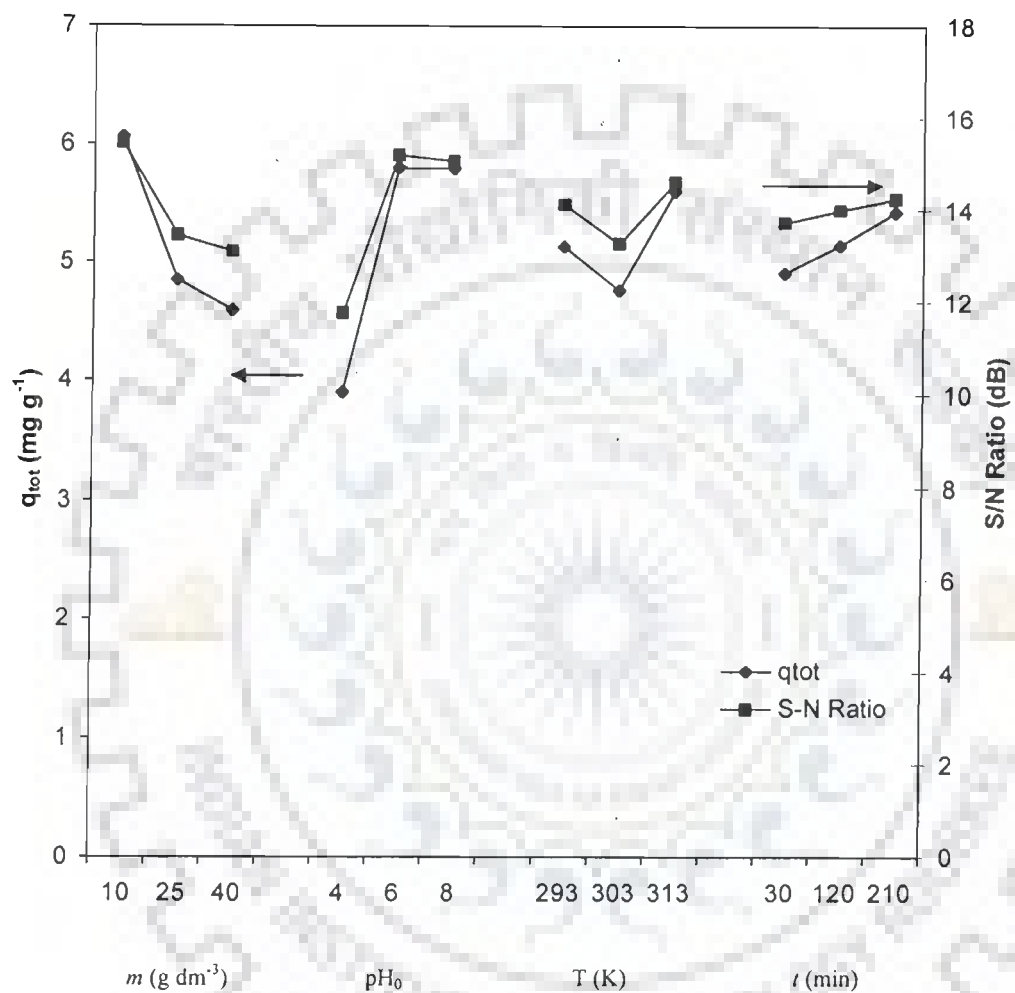
Fig. 6.7.3 **Effect of process parameters on q_{tot} and S/N ratio for adsorption of Py and its derivatives from real wastewater onto GAC.**

6.7.3   Selection of Optimal Levels

Since q_{tot} is 'higher the better' type quality characteristic, therefore, greater values, of q_{tot} is considered optimal. Table 6.7.6. summarizes the optimal level of various parameters obtained after examining the response curves (Figs. 6.7.1 through 6.4.3) of the average value of q_{tot} and S/N ratios for the adsorption of Py and its derivatives from wastewater onto BFA, RHA and GAC. Table 6.7.6 indicates that the 1st level of parameters A (m), 2nd level of parameter B (pH$_0$), 3rd level of parameter C (Temperature) and 2nd or 3rd level of parameter D (t) give higher average value of q_{tot} and S/N ratio. Table 6.7.7 shows the ANOVA for the removal of Py and its derivatives from real wastewater. Table 6.7.8 shows the contributions of the individual parameters on the removal.

Table 6.7.6: Summary of optimal level of various parameters on q_{tot} values for the removal of Py and its derivatives from real wastewater by adsorption onto BFA, RHA and GAC.

Adsorbent	Optimal Parameter Level			
BFA	A$_1$	B$_2$	C$_3$	D$_2$
RHA	A1	B$_2$	C$_3$	D$_2$
GAC	A1	B$_2$	C$_3$	D$_3$

Table 6.7.7. ANOVA of q_{tot} and S/N ratio data for adsorption of Py and its derivatives from real wastewater by BFA, RHA and GAC.

Factors	Raw Data						S/N Data					
	S	DOF	V	F	S`A	P	S	DOF	V	F	S`A	P
BFA												
A	191.85	2	95.93	300.16	191.21	79.38	44.33	2	22.17	74.68	43.74	80.61
B	36.29	2	18.15	56.78	35.66	14.80	8.34	2	4.17	0.15	7.75	14.28
C	6.35	2	3.17	9.93	5.71	2.37	0.99	2	0.50	1.67	0.40	0.73
D	(5.22)	(2)	(2.61)	(40.19)	(5.09)	(2.17)	0.59	(2)	(0.30)			(1.09)
Error	6.39	20	0.32	1.00	8.31	3.45	0.59	2	0.30	1.00	2.37	4.38
Total	240.89	26	117.57		240.89	100.00	54.26	8	**27.13**		54.26	100.00
RHA												
A	1.51	2	0.75	9.68	1.35	31.61	3.12	2.00	1.56	21.06	2.97	53.93
B	0.85	2	0.43	5.45	0.69	16.22	1.57	2.00	0.78	10.58	1.42	25.77
C	0.36	2	0.18	2.32	0.21	4.82	0.67	2.00	0.34	4.55	0.53	9.55
D	(0.09)	(2)	(0.04)	(0.52)	-	(2.00)	(0.15)	(2.00)	(0.07)			(2.69)
Error	1.56	20	0.08	1.00	2.03	47.35	0.15	2.00	0.07	1.00	0.59	10.75
Total	4.28	26	1.44		4.28	100.00	5.51	8.00	2.75		5.51	100.00
GAC												
A	11.16	2	5.58	35.72	10.85	27.75	9.72	2	4.86	24.42	9.32	25.83
B	21.60	2	10.80	69.13	21.29	54.45	23.20	2	11.60	58.29	22.80	63.19
C	3.21	2	1.61	10.27	2.90	7.41	2.77	2	1.38	6.95	2.37	6.56
D	(1.20)	(2)	(0.60)	(5.59)	(0.98)	(3.06)	(0.40)	(2)	(0.20)			(1.10)
Error	3.13	20	0.16	1.00	4.06	10.39	0.40	2	0.20	1.00	1.59	4.41
Total	39.10	26	18.14		39.10	100.00	36.09	8	18.04		36.09	100.00

Table 6.7.8: Summary of parameters having highest percent contribution to q_{tot} value for removal of Py and its derivatives from real wastewater by BFA, RHA and GAC.

Adsorbent	Raw Data		S/N Ratio	
	Parameter	% Contribution	Parameter	% Contribution
BFA	A	79.4	A	81
RHA	A	32	A	54
GAC	B	55	B	63

6.7.4 Estimation of Optimum Response Characteristics

The optimal values of the response characteristics (q_{tot}) along with their respective confidence intervals have been predicted. The results of the confirmation experiments conducted to validate the optimal results are also presented.

The significant process parameters affecting the combined % removal of Py and its derivatives in real wastewater by BFA and their optimal levels (as already selected) are: A_1, B_2, C_3, D_2.

The average value (from Table 6.7.3) of q_{tot} at:

1st level of factor A ($\bar{A}_1$) = 13.6

2nd level of factor B ($\bar{B}_2$) = 11.26

3rd level of factor C ($\bar{C}_3$) = 10.52

2nd level of time ($\bar{D}_2$) = 10.55

The overall mean of q_{tot} ($\bar{T}_{BFA}$) = 9.96   (from Table 6.7.2)

The predicted optimum value of q_{tot} for BFA (μ_{BFA}) has been calculated as:

$$\mu_{BFA} = \bar{T}_{BFA} + (\bar{A}_1 - \bar{T}_{BFA}) + (\bar{B}_2 - \bar{T}_{BFA}) + (\bar{C}_3 - \bar{T}_{BFA}) + (\bar{D}_2 - \bar{T}_{BFA})$$

$$= 16.06 \text{ mg g}^{-1}$$

The 95% confidence intervals for the mean of the population and three confirmation experiments (CI_{POP} and CI_{CE}) have been calculated by substituting the following values:

N = total number of results = 9 x 3 = 27; f_e (DOF error) = (26 – 8) = 18;

V_e (error variance) = 0.32 (recalculated from Table 6.7.6).

$$n_{eff} = \frac{N}{1 + [\text{Total DOF associated in the estimate of the mean}]}$$

$$= 3$$

$F_{0.05}$ (1, 18) = 4.414 (Tabulated F-value)

$$CI_{POP} = \sqrt{\frac{F_\alpha (1, f_e) V_e}{n_{eff}}} = \pm 0.686$$

$$CI_{CE} = \sqrt{F_\alpha (1, f_e) \left[\frac{1}{n_{eff}} + \frac{1}{R} \right]} = \pm 0.73$$

The 95 % confidence intervals (CI_{POP} and CI_{CE}) of the predicted ranges of q_{tot} for BFA are as follows:

CI_{POP} : $15.36 < \mu_{BFA} \text{ (mg/g)} < 16.74$

CI_{CE} : $15.33 < \mu_{BFA} \text{ (mg/g)} < 16.77$

By adopting a similar procedure, we can predict the optimal values of given confidence limit for other sorbent systems as well. The predicted optimal q_{tot} values and confidence intervals (CI_{POP} and CI_{CE}) are presented in Table 6.7.9 for combined adsorptive removal of Py and its derivatives onto BFA, RHA and GAC.

6.7.5 Confirmation Experiments

Three confirmation experiments have been conducted for the combined adsorption of Py and its derivatives from real wastewater onto BFA, RHA and GAC at selected optimal levels of the process parameters. The average values of the characteristics are obtained and compared with the predicted values. The results are

given in Table 6.7.9. Confirmation experiments are within 95% of CI_{CE} for respective adsorbents. It is to be pointed out that these optimal values are valid within the specified range of process parameters.

Table 6.7.9: Predicted optimal q_{tot} values, confidence intervals and results of confirmation experiments for adsorption of Py and its derivatives from wastewater onto BFA, RHA and GAC.

Adsorbent	Optimal levels of process parameters	Predicted optimal q_{tot} values (mg g^{-1})	Confidence Intervals (95%)	Average of Confirmation experiments q_{tot} (mg g^{-1})
BFA	$A_1B_2C_3D_2$	16.05	CI_{POP}:15.36 < μ_{BFA} < 16.74	15.53
			CI_{CE}:15.33 < μ_{BFA} < 16.77	
RHA	$A_1B_2C_3D_2$	4.2	CI_{POP}:3.86 < μ_{BFA} < 4.54	3.91
			CI_{CE}:3.84 < μ_{BFA} < 4.56	
GAC	$A_1B_2C_3D_3$	7.4	CI_{POP}:6.93 < μ_{BFA} < 7.88	7.21
			CI_{CE}:6.9 < μ_{BFA} < 7.91	

6.8 THERMAL OXIDATION OF THE SPENT ADSORBENTS

The spent adsorbents pose problem for the disposal and management therefore, it is necessary to have proper disposal and management of the spent adsorbents so as to provide safe environment. The use of low cost adsorbents for the treatment of various wastewaters generates large volumes of solid waste. These solid wastes have great potential for energy recovery. However, the separation of the adsorbents from the solvents by sedimentation, filtration, centrifugation, dewatering and drying is very important. These aspects are being studied separately in laboratory by other researchers and, therefore, will not be dealt with in this dissertation. The dried spent BFA, RHA

and GAC loaded by Py and its derivatives can be used directly or by making fire-briquettes in the furnace combustors/incinerators to recover energy value. The blank and loaded adsorbents were studied for their thermal degradation characteristics by thermogravimetric (TG) instrument.

The principal experimental variables which could affect the thermal degradation characteristics in air flow in a TGA are the pressure, the air (purge gas) flow rate, the heating rate, the weight of sample and the sample size fraction. In the present study, the operating pressure was kept slightly positive, the purge gas (air) flow rate was maintained at 200 ml min^{-1} and the heating rate was maintained at 100 K min^{-1}.

The thermo gravimetric analysis (TGA), differential thermal analysis (DTA) and differential thermal gravimetric (DTG) curves of the blank BFA is shown in Fig. 6.8.1. Rest of the figures of Py and 2Pi loaded BFA and blank and Py and 2Pi loaded, RHA and GAC for the highest possible heating rate of 100 K min^{-1} (for the instrument system) are shown in **Appendix-B**. The dried data obtained from these figures like, weight loss with temperature, enthalpy change, peak temperature etc. are shown in Tables 6.8.1-6.8.3.
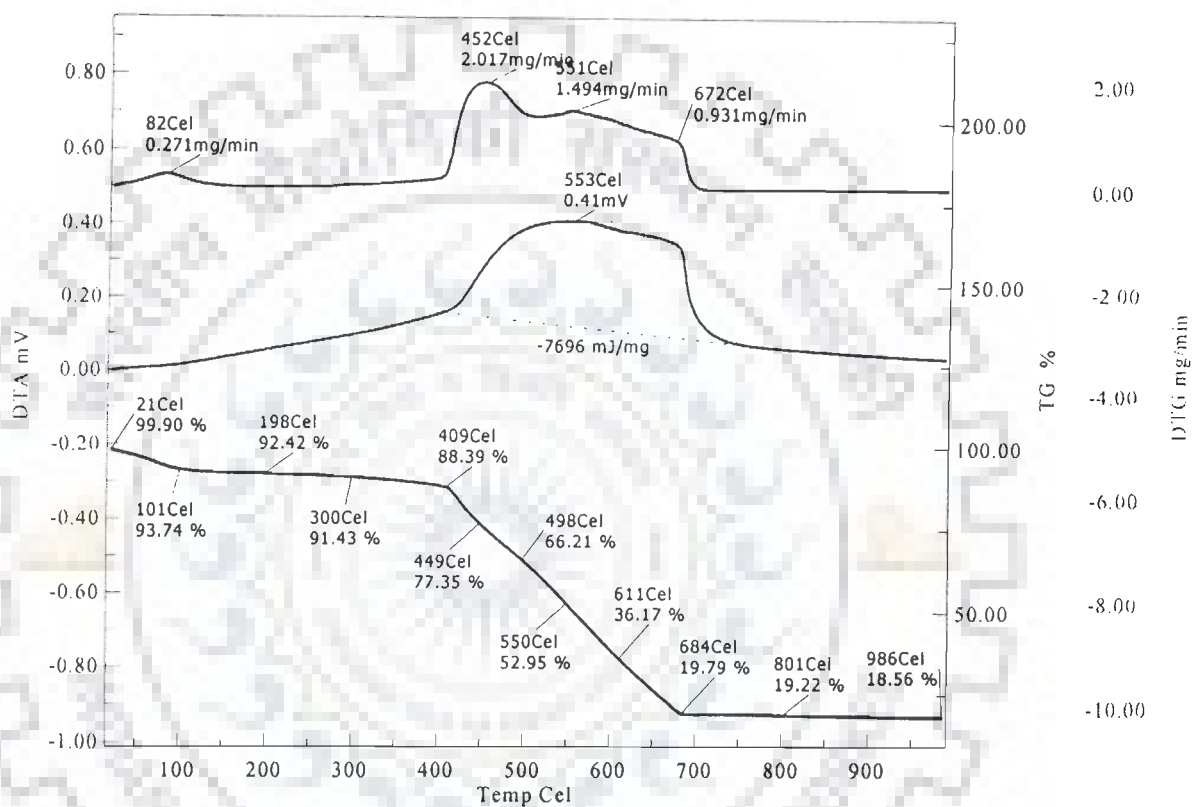
Fig. 6.8.1. Thermogravimetric analysis of BFA - blank

The TG traces for the blank and Py loaded BFA show that the loss of moisture and the evolution of some light weight molecules including water takes place (10-14% weight loss) from 21 °C to 409 °C. Higher temperature drying (> 100 °C) occurs due to loss of the surface tension bound water of the particles. A similar type of TG trace was obtained for RHA (Fig. B-3), in which moisture and light volatile components loss (~4 - 7% weight loss) takes place upto ~420 °C. TG trace for GAC, showed moisture and light volatile components weight loss (~9 - 12% weight loss) upto ~500 °C (Fig. B-4).

The rate of weight loss was found to increase between ~409 °C to 583 °C (11-70 % weight loss) for BFA, between 419 °C to 583 °C (4 -13 % weight loss) for RHA, and ~55 % weight loss between ~600 °C to 1000 °C for GAC. In these temperature ranges the blank and loaded adsorbents oxidize and lose their weight gradually.

Adsorbents do not show any endothermic transition between room temperature and 400 °C, indicating the lack of any crystalline or other phase change during the heating process [Ng et al., 2002]. The strong exothermic peak centered between 450-700 °C is due to the oxidative degradation of the sample. This broad peak as that observed from the first derivative loss curve (dTG), may be due to the combustion of carbon species. At higher temperatures (third zone), the samples present a gradual weight loss up to 950 °C. This weight loss has been reported to be associated in part with the evolution of CO_2 and CO.

The maximum rate of weight loss was obtained as 2.02 mg min^{-1} for blank BFA. RHA has lowest maximum rate of degradation (~1.17 mg min^{-1}). In the third stage of oxidation in the temperature span of ~680-980 °C for BFA and RHA, only ~1.5% weight loss was observed. At about 980 °C, the organics of the residue got oxidized, leaving the ash fraction in BFA and RHA. It may be noted that the ash content is very high for RHA followed by GAC and BFA. The nature of the TG curve

gives a clear indication that the three step degradation takes place for BFA and RHA whereas a two step degradation is observed for GAC.

The distribution of volatiles and oxidation products released during thermal degradation of all the blank and loaded adsorbents at 100 K min^{-1} heating rate is presented in Table 6.8.2. TGA and DTA curves were used to deduce drying and thermal degradation characteristics. The distribution of volatiles and oxidation products evolved in different temperature ranges show irregular pattern for all the residues. The weight loss because of the emanation of the volatiles and the oxidation products for the adsorbents is presented in Table 6.8.1.

The drying, pyrolysis and oxidation characteristics of the residues are presented in Table 6.8.3. No general trend has been observed in the increase or decrease of the volatilization of the adsorbents.

Table 6.8.1. Distribution of volatiles released during thermal degradation of blank and metal loaded adsorbents at an air flow rate of 100 K min^{-1}.

Adsorbent (Blank/ loaded)	Weight loss (%)				Total Volatile matter including moisture %
	<200 °C	200-400 °C	400-700 °C	>700 °C	
BFA	7.58	4.03	68.6	1.23	81.44
BFA-Py	6.4	3.05	77.03	1.32	87.8
BFA-2Pi	4.96	5.75	71.58	0.86	83.15
	<200 °C	200-400 °C	400-700 °C	>700 °C	
RHA	2.07	2.36	12.95	1.34	18.72
RHA-Py	2.31	2.01	15.78	1.02	21.12
RHA-2Pi	2.35	1.75	17.54	0.78	22.42
	<200 °C	200-400 °C	400-600 °C	>600 °C	
GAC	6.25	1.27	5.25	55.3	68.07
GAC-Py	3.73	1.14	4.97	52.89	62.73
GAC-2Pi	5.88	2.69	3.54	56.45	68.56

Table 6.8.2. Thermal degradation characteristics of blank and Py and its derivatives loaded adsorbents at an air flow rate of 100 K min^{-1}.

Adsorbent (Blank/loaded)	Drying Range	Moisture	Degradation Range	T_{max}	Max. Rate of Weight Loss (mg/min)
BFA	21-409	11.51	409-684	452	2.017
BFA-Py	24-476	14.7	476-681	491	0.863
BFA-2Pi	27-464	10.65	464-700	489	1.282
RHA	21-419	4.43	419-583	445	1.17
RHA-Py	26-450	5.04	450-629	549	0.917
RHA-2Pi	27-499	7.24	499-650	558	0.996
GAC	25-600	12.67	600-1000	620	1.771
GAC-Py	25-600	9.85	600-1000	615	1.407
GAC-2Pi	24-586	12.1	586-1000	722	1.625

The properties of DTA traces are presented in Table 6.8.3. The oxidation of the adsorbents shows exothermicity. This table also shows the temperature span of the exothermicity. Due to the higher heating rate of 100 K min^{-1}, no sharp peak of DTA traces are seen for any of the adsorbents.

Table 6.8.3. DTA for the blank and Py and its derivatives loaded adsorbents at an air flow rate of 100 K min^{-1}.

Adsorbent (Blank/loaded)	ΔH (MJ Kg^{-1})	$T_1 i$	$T_1 f$
BFA	-7696	409	684
BFA-Py	-7163	476	681
BFA-2Pi	-6940	464	700
RHA	-1641	419	583
RHA-Py	-1819	450	629
RHA-2Pi	-1866	401	650
GAC	-472	498	799
GAC-Py	-1871	500	1049
GAC-2Pi	253	24	300

6.9   DISPOSAL OF SPENT ADSORBENTS

The proximate and chemical analyses of the Py and its derivatives loaded BFA, RHA and GAC are given in Table 6.9.1. Table 6.2.1 shows the proximate and chemical analyses of blank adsorbents. It is seen from Table 6.9.1 that the Py and its derivatives loaded BFA has highest percentage of carbon content followed by GAC and RHA in that order. Comparison of carbon content of spent BFA (53-56%) with that of blank BFA (Table 6.2.1) (52.16%) shows increase in carbon content of BFA. This increase is due to loading of organic matters. Similar trends are observed for GAC and RHA also. Chemical analysis of ash of loaded adsorbents shows that RHA has highest SiO_2 content. Table 6.9.1 also shows that the heating value of the loaded BFA is comparable to that of GAC and RHA. The heating value of loaded RHA is lower because of its higher silica content. Slight increase in heating values may also inferred by comparing the heating values of blank and loaded adsorbents as given in Tables 6.2.1 and 6.9.1, respectively. For example, the heating values of blank and Py loaded BFA are 28.73 and 29.65 MJ kg^{-1}, respectively. Due to high energy content, blank and loaded BFA, RHA and GAC can become potential sources of energy for various industries requiring fuel for the production of heat. On thermal decomposition, these adsorbents also generate flammable gases such as light volatiles, carbon monoxide, hydrogen, and other organic vapours. These adsorbents can, therefore, be densified in the form of briquettes and could be pyrolyzed to convert them into smokeless fuel.

Table 6.9.1. Proximate and chemical analysis of Py, 2Pi, 4Pi and AmPy loaded BFA, RHA and GAC.

Characteristics	BFA				RHA				GAC			
	Py	2Pi	4Pi	AmPy	Py	2Pi	4Pi	AmPy	Py	2Pi	4Pi	AmPy
Proximate Analysis												
Moisture (%)	5.02	4.81	4.92	5.21	2.13	3.01	2.69	3.25	5.02	4.62	4.38	5.06
Volatile Matter (%)	14.35	13.98	14.02	14.63	6.89	6.39	6.34	6.57	3.52	3.13	3.94	3.67
Ash (%)	27.25	25.23	26.71	27.13	79.5	76.95	77.85	78.96	50.34	50.12	49.69	50.13
Fixed Carbon	53.38	55.98	54.35	53.03	11.48	13.65	13.12	11.22	41.12	42.13	41.99	41.14
Chemical Analysis of Ash												
Insoluble (%)	75.32	74.5	73.25	71.26	64.13	63.15	63.51	64.68	85.36	84.96	85.02	86.01
SiO_2 (%)	2.58	2.64	2.47	1.98	11.36	10.96	11.05	11.67	0.35	0.31	0.45	0.39
Fe_2O_3 & Al_2O_3 (%)	2.13	2.05	2.31	2.18	3.21	3.02	2.98	3.15	4.69	4.57	4.61	4.21
CaO (%)	13.95	12.36	14.35	13.95	17.21	16.85	16.89	17.35	1.68	1.58	1.67	1.49
MgO (%)	0.95	0.85	0.98	0.78	0.85	0.78	0.98	0.89	4.68	4.31	3.64	4.79
Others	5.07	7.6	6.64	9.85	3.24	5.24	4.59	2.26	3.24	4.27	4.61	3.11
Heating Value (MJ kg^{-1})	29.65	29.68	29.24	28.65	22.03	23.11	22.38	21.91	21.35	22.47	22.19	21.15

CONCLUSIONS AND RECOMMENDATIONS

7.1 CONCLUSIONS

From the present study, the following conclusions can be drawn:

1 The adsorbents, BFA and RHA are low density materials. The BFA and RHA have a fibrous structure with various types of mineral oxides. The pore size distribution results exhibited their predominantly mesoporous structure. The FTIR spectra of the adsorbents indicated the presence of various types of functional groups e.g. free and hydrogen bonded OH group, the silanol groups (Si-OH), CO group stretching from aldehydes and ketones on the surface of adsorbents. Thermogravimetric analysis exhibited the thermal stability of the adsorbents upto 400 °C.

2 XRD pattern showed the presence of Silica (SiO_2), Wollastonite ($CaSiO_3$), Aragonite ($CaCO_3$) and Akdalaite $[(Al_2O_3)_4.H_2O]$ in BFA, Cristobalite (SiO_2), Margaritasite $[(Cs,K,H_3O)_2(UO_2)2V_2O_8.(H_2O)]$ and Macedonite ($PbTiO_3$) in RHA, and Moganite (SiO_2), Akdalaite $[(Al_2O_3)_4.H_2O]$, Tamarugite $[NaAl(SO_4)_2.6H_2O]$ Fersilicate (FeSi) and Majorite $[Mg_3(Fe,Al,Si)_2(SiO_4)_3]$ as major components in GAC. Major pyridine compounds in Py and its derivatives loaded BFA, RHA and GAC were identified as pyridine 2,3-diacarboxylic acid or quinolinic acid ($C_7H_5NO_4$), pyridine 2,4-dicarboxylic acid hydrate ($C_7H_5NO_4.H_2O$) and pyridine 2, 5-diacarboxylic acid hydrate ($C_7H_5NO_4.H_2O$) zinc-picoline ($C_{20}H_{28}N_6S_2Zn$) and pyridine picrate ($C_{12}H_8N_4O_7$) at 2θ ~24.4° and 21°.

3 The point of zero charge (pH_{PZC}) of the BFA, RHA and GAC is 9.0, 10.15 and 9.25, respectively. The $pH_0 \approx 6$-7 is found to be the optimum for the individual removal of Py, 2Pi, 4Pi and AmPy from the aqueous solution by adsorption using BFA, RHA and GAC.

4   Optimum BFA, RHA and GAC dosages were found to be 8, 30 and 20 g dm^{-3}, for C_0 =100 mg dm^{-3} of Pyridine and AmPy, respectively, and 5, 10 and 10 g dm^{-3} of BFA, RHA and GAC, respectively, for that of 2Pi and 4Pi. 5 h could be taken as the equilibrium contact time for adsorption onto GAC and RHA whereas 6h have been found as the equilibration adsorption time for BFA.

5   The sorption kinetics could be represented by the pseudo-second-order kinetic model. The adsorption processes could be well described by a two-stage diffusion model.

6   Redlich-Peterson, Toth and Radke-Prausnitz isotherms generally well represent the equilibrium adsorption of Py, 2Pi, 4Pi and AmPy for the adsorption on BFA, RHA and GAC.

7   An increase in temperature induces a positive effect on the sorption process. The heat of adsorption (ΔH^0) and change in entropy (ΔS^0) for adsorption on BFA, RHA and GAC are found in the range of 23-108 kJ mol^{-1} and 0.12-0.15 kJ mol^{-1} K^{-1}; 8-21 kJ mol^{-1} and 0.1-0.13 kJ mol^{-1} K^{-1}; and 13-26 kJ mol^{-1} and 0.1-0.15 kJ mol^{-1} K^{-1}; respectively. The values of change in Gibbs free energy (ΔG^0_{ads}) were found in the range of 18-36 kJ mol^{-1}, 14-20 kJ mol^{-1} and 15-22 kJ mol^{-1} for BFA, RHA and GAC, respectively. The negative value of change in Gibbs free energy indicated the feasibility and spontaneity of adsorption on the adsorbents.

8   The positive isosteric heat of adsorption, the heat of adsorption (ΔH^0) and change in entropy (ΔS^0) for adsorption confirm the endothermic nature of adsorption for all systems.

9   The Taguchi's orthogonal array (OA) experimental design (DOE) methodology for optimizing the experiments was found to be very economical in the sorption studies for single and sorbate systems. This approach facilitated the understanding of the factors such as C_o, T, pH_0, m and t at three levels with a OA layout of L$_9$ (3^4) could be optimized with the 'bigger-is-better' as quality character with the 9 sets of experiments only.

10   For ternary 'bigger-is-better' systems at three levels with a OA layout of L_{27} (3^{13}) could be optimized with the 'bigger-is-better' as quality character with the 27 sets of experiments only.

11   The interactions between initial concentrations of Py, 2Pi and 4Pi [(A x B), (A x C) or (B x C)] is not much significant in affecting the average value of q_{tot}.

12   All the factors and the interactions considered in the experimental design with q_{tot} as the desired response characteristic are statistically significant at 95% confidence limit.

13   Three-stage treatment with BFA, RHA and GAC as adsorbents brings down the concentration of individual Py, 2Pi, 4Pi and AmPy (C_0 = 100 mg/l) upto zero. However two-stage treatment scheme shall be suitable for the removal of Py and its derivatives from waste waters to bring down their concentration to well below the maximum permissible limit for discharge into surface waters.

14   The use of the water at lower pH and mineral acids, viz., H_2SO_4, and HNO_3 showed higher recovery efficiencies ($\approx$ 90 %) of Py and its derivatives for BFA, RHA and GAC.

15   The analysis of the spent adsorbents for its specific energy shows that the spent adsorbents can be used as a fuel.

16   BFA has the maximum removal efficiency as compared to RHA and GAC. The order of efficiency of these adsorbents is BFA > GAC > RHA.

7.2   RECOMMENDATIONS

On the basis of the present studies, the following recommendations may be made for future studies:

1   BFA and RHA from different sources should be characterized for their physico-chemical parameters and surface characteristics and the protocol for adsorption studies should be standardized.

2 Column and scale-up studies should be conducted to evaluate the suitability of BFA and RHA as adsorbents for the removal of Py and its derivatives from wastewater.

3 RHA has maximum amount of silica and therefore, the ash obtained after the combustion/incineration of spent RHA which may be used to manufacture bricks for civil construction sector.

4 Taguchi's design of experimental methodology should be evaluated further for its application in effluent treatment experiments using adsorption process and the design of scaled-up adsorption systems.

REFERENCES

1. Abou-Mesalam M.M., Sorption kinetics of copper, zinc, cadmium and nickel ions on synthesized silico-antimonate· ion exchanger, Colloid Surface A: Physicochem. Eng. Aspects, 225, 85-94 (2003).

2. Akiyama M., Suzuki E., Onom Y., Direct synthesis of tetramethoxysilane from rice hull ash by reaction with dimethyl carbonate, Inorg. Chim. Acta, 207(2), 259-261 (1993).

3. Adam F., Chua J. H., The adsorption of palmytic acid on rice husk ash chemically modified with Al(III) ion using the sol–gel technique, J. Colloid Interf. Sci., 280, 55-61 (2004).

4. Aharoni C., Sideman S., Hoffer E., Adsorption of phosphate ions by colloid ion-coated alumina, J. Chem. Technol. Biotechnol., 29, 404-412 (1979).

5. Akita S., Takeuchi H., Sorption equilibria of pyridine derivatives in aqueous solution on porous resins and ion exchange resins. J. Chem. Eng. Jpn., 26, 237-241 (1993).

6. Allen S.J., Mckay G., Khader K.Y.H., Intraparticle diffusion of a basic dye during adsorption onto sphagnum peat, Environ. Pollut., 56, 39-42 (1989).

7. Ardizzone S., Høiland H., Lagioni C., Sivieri E. Pyridine and aniline adsorption from an apolar solvent: the role of the solid adsorbent, J. Electroanal. Chem., 447, 17–23 (1998).

8. Bailey G. W., White J. L., Rothberg T., Adsorption of organic herbicides by montmorillnite: rate of pH and chemical character of adsorbate, Soil Sci. Soc. Am. Proc., 32, 22-34 (1968).

9. Bailey S.E., Olin T.J., Bricka R.M., Adrian D.D. A review of potentially low cost sorbents for heavy metals, Water Res. 33, 2469-2479 (1999).

10. Baker R. A., Threshold odors of organic chemicals, J. Am. Water Works Ass., 55, 913-916 (1963).

11. Baker R.A., Luh M.D., Pyridine sorption from aqueous solution by montmorillonite and kaoline, Water Res., 5, 839-848 (1971).

12. Barker T.B., Eng. Quality by Design, Marcel Dekker, Inc., New York (1990).

13. Balistrieri, L.S., Murray, J.W., The surface chemistry of goethite (α-FeOOH) in major ion seawater, Am. J. Sci., 281(6), 788-806 (1981).

14. Barkakati P., Bordoloi D., Borthakur P.C., Paddy husk as raw material and fuel for making portland cement, Cement Concrete Res., 24(4), 613-620 (1994).

15. Barnes R.A., Properties and reactions of pyridine and its hydrogenated derivatives. In Pyridine and Its Derivatives, Part I, Chap. 1. p 57. Interscience, New York, (1960).

16. Barrado E., Vega M., Pardo R., Grande P., Del Valle J.L., Optimisation of a purification method for metal-containing wastewater by use of a Taguchi experimental design, Water Res., 30(10), 2309-2314 (1996).

17. Barret, E.P., Joyner, L.G., Halenda, P.P., The determination of pore volume and area distributions in porous substances: 1. Computations from nitrogen isotherms. J. Am. Chem. Soc., 73, 373–380 (1951).

18. Beg K., Sahai V., Gupta R., Statistical media optimization and alkaline protease production from *Bacillus mojaensis* in a bioreactor, Process Biochem., 39(2), 203-209 (2003).

19. Bludau H., Karge h. G., Niessen W., Sorption, sorption kinetics and diffusion of pyridine in zeolites, Micropor. Mesopor. Mat., 22, 297-308 (1998).

20. Boateng A.A., Skeete D.A., Incineration of rice hull for use as a cementitious material: the Guyana experience, Cement Concrete Res., 20, 795-802 (1990).

21. Boyd G.E., Adamson A.W., Meyers L.S., The exchange adsorption of ions from aqueous solution by organic zeolites II Kinetics, J. Am. Chem. Soc., 69, 2836-2848 (1947).

22. Brunauer S., P.H. Emmet, F. Teller, J. Am. Chem. Soc., 60, 309 (1938).

23. Byrne D.M., Taguchi S., The Taguchi approach to parameter design. Quality Progress, December, 19-26 (1987).

24. Cain R. B., Houghtont C., Wright K., A microbial Metabolism of the Pyridine Ring, metabolism of 2- and 3-hydroxypyridines by the maleamate pathway in *Achromobacter* sp., Biochem. J. 140, 293-300 (1974).

25. Carlos M. C., Adsorption of organic molecules from aqueous solutions on carbon materials, Carbon, 42, 83-94 (2004).

26. Chakraborty S., Basu J. K., De S., DasGupta S., Adsorption of reactive dyes from a textile effluent using sawdust as the adsorbent, Ind. Eng. Chem. Res. 45, 4732 - 4741 (2006).

27. Cheung C.W., Porter J.F., McKay G., Sorption kinetics for the removal of copper and zinc from effluents using bone char, Sep. and Purif. Technol. 19, 55-64 (2000).

28. Chidambara Raj C.B., Quen H.L., Advanced oxidation processes for wastewater treatment: Optimization of UV/H_2O_2 process through a statistical technique, Chem. Eng. Sci., 60, 5305 - 5311 (2005).

29. Cobb B. D., Clarkson J.M., A simple procedure for optimizing the polymerase chain reaction (PCR) using modified Taguchi methods, Nucleic Acids Res. 22, 3801-3805 (1994).

30. Crank J., The Mathematics of Diffusion, Oxford Clarendon Press, London, 1st ed, (1965).

31. Crittenden J.C. Berrigan J.K. Hand E.W., Design of rapid small-scale adsorption tests for a constant diffusivity, J. Water Pollut. Control Fed., 58, 312-319 (1986).

32. Davila-Jimenez M.M., Elizalde-Gonzalez M.P., Pelaez-Cid A.A., Adsorption interaction between natural adsorbents and textile dyes in aqueous solution, Colloid Surface A: Physicochem. Eng. Aspects, 254, 107-114 (2005).

33. Davis J.T., Rideal E. K., Electrostatic Phenomena. In *Interfacial Phenomena*, Chap. 2, Academic Press, New York, p. 95 (1963).

34. Dehnad K., Quality Control, Robust Design, and the Taguchi Method, Pacific Grove, California (1989).

35. Deshpande C.V., Pathic P.P., Kaul S.N., Swaminathan T., Activated carbon adsorption for the treatment of nitrochlorobenzene wastewater. Indian J. of Environl. Protection, 17, 14-18 (1996).

36. Diez P. R., Amalvy J. I., A density functional study of the adsorption of pyridine, 2-vinylpyridine, and 4-vinylpyridine onto a silica surface, J. Mol. Struc- Theochem, 634, 187–193 (2003).

37. Drillia P., Stamatelatou K., Lyberatos G., Fate and mobility of pharmaceuticals in solid matrices, Chemosphere, 60, 1034 –1044 (2005).

38. Ezzati A., Gorouhi E., Mohammadi T., Separation of water in oil emulsions using microfiltration, Desalination, 185, 371-382 (2005).

39. FAO Statistical Database, (2002) http://apps.fao.org.

40. Farmer V.C., Mortland M. M., An infrared study of the co-ordination of pyridine and water to exchangeable cations in montmorillonite and saporite. J. Chem. Soc. (Inogr.Phys. Theor.), 344-351 (1966).

41. Feng Q., Lin Q., Gong F., Sugita S., Shoya M., Adsorption of lead and mercury by rice husk ash, J. Colloid Interf. Sci., 278, 1-8, (2004).

42. Fogler H.S., Elements of Chemical Reaction Eng., Prentice-Hall PTR, 3, (1998).

43. Freundlich H.M.F., Over the adsorption in solution, J. Phys. Chem., 57, 385-471 (1906).

44. Fredrich M., Seidel A., Gelbin D., Kinetics of adsorption of phenol and indole from aqueous solutions on activated carbons, Chem. Eng. Process, 24, 33-38 (1989).

45. Gilchrist, T.L., Heterocyclic Chemistry, Pitmax Press, London, (1985).

46. Giles C.H., MacEwar T. H., Nakhwas S.N., Smith D., Studies in adsorption, part XI. A system of classification of solution adsorption isotherms, and its use in diagnosis of adsorption mechanisms and in measurement of specific surface area of solids. J. Chem. Soc, 3, 3973-3993 (1960).

47. Giles C.H., Smith D., Huiston A. A General treatment and classification of the solute adsorption isotherm. I. Theoretical. J. Colloid Interf. Sci. 47, 7655-7665 (1974).

48. Gilliland E.R., Baddur R.F., Perkinson G.P., Sladek K.S., Diffusion on surfaces, Ind. Eng. Chem. Fundam. 13, 95-99 (1974).

49. Han J. J., Yang T. H., Rhee J. S., Optimization of reaction variables for sucrose monoester production using lipase in a solvent free system by Taguchi's method, Biotechnol. Tech., 12, 295-299 (1998).

50. Hara N., Noma H., Honma S., Sarejprasong S. Uparisajkui S., Suitability of rice husk ash obtained by fluidized-bed combustion for blended cement, 9th International Conference on the Chemistry of Cement, 3, 72-78(1992).

51. Hasley G.D. Jr., Taylor H.S., The adsorption of hydrogen on tungsten powders, J. Chem. Phys., 15, 624 (1947).

52. Helfferich F., Ion exchange, New York: McGraw-Hill (1962).

53. Ho Y.S., Mckay G., The kinetics of sorption of divalent metal ions onto sphagnum mass peat, Water Res. 34(3), 735-742 (2000).

54. Ho Y.S., Mckay G., Kinetic model for lead(II) sorption onto peat, Adsorp. Sci. Technol. 16(4) 243-255 (1998).

55. Ho Y.S., Mckay G., Pseudo-second order model for sorption processes, Process Biochem. 34 (5) 415-465 (1999).

56. Ho Y. S. Selection of optimum isotherm, Carbon, 42, 2115-2116 (2004).

57. Ho Y. S., Ofomaja A.E., Kinetics and thermodynamics of lead ion sorption on palm kernel fibre from aqueous solution. Process Biochem., 40, 3455-3461 (2005).

58. Ho Y. S. Second-order kinetic model for the sorption of cadmium on to tree fern: A comparison of linear and non-linear methods, water research, 40, 119-125 (2006).

59. Ho Y. S., Ofomaja A.E., Biosorption thermodynamics of cadmium on coconut copra meal as biosorbent, Biochem. Eng. J., 30, 117-123 (2006a).

60. Ho Y. S., Ofomaja A.E. Kinetic studies of Copper ion adsorption on palm kernel fibre, J. Hazard. Mater., B137, 1796-1802 (2006b).

61. Ho Y.S., McKay G., Pseudo-second order model for sorption processes. Process Biochemistry, 34, 451–465 (1999).

62. Houghton C., Cain R. B., Microbial metabolism of the pyridine ring, formation of pyridinediols (dihydroxypyridines) as intermediates in the degradation of pyridine compounds by micro-organisms, Biochem. J., 130, 879-893 (1972).

63. Hu J.Y., Ong S.L., Ng W.J., Liu W., Use of a sequencing batch reactor for Nitrogen and Phosphorus removal from municipal wastewater, J. Environ. Eng., 131(5), 734-744 (2005).

64. Iniesta J., Michaud P. A., Panizza M., Comninellis Ch. Electrochemical oxidation of 3-methylpyridine at a boron-doped diamond electrode: application to electroorganic synthesis and wastewater treatment, Electrochemistry Communications, 3, 346-351 (2001).

65. IS 1350 (part I), Methods of Test for Coal and Coke, Proximate Analysis, Bureau of Indian Standards, Manak Bhawan, New Delhi, India (1984).

66. IS 2720 (part-4), Methods for test for soils: Part 4. Grain Size Analysis (Second revision), Bureau of Indian Standards, Manak Bhawan, New Delhi, India (1985).

67. IS 355, Methods for the determination of Chemical Composition of Ash of Coal and Coke, Bureau of Indian Standards, Manak Bhawan, New Delhi, India, (1984).

68. IUPAC Manual of Symbols and Terminology of Colloid Surface, Butterworths, London, 1 (1982).

69. James J., Rao M.S., Reactivity of rice husk ash, Cement Concrete Res., 16, 296-302 (1986a).

70. James J., Rao M.S., Reaction product of lime and silica from rice husk ash, Cement Concrete Res., 16, 67-73 (1986b).

71. Jeney C., Dobay O., Lengyel A., Adam E., Nasz I., Taguchi optimization of ELISA procedures, J. Immun. Method, 223, 137-146 (1999).

72. Jori A., Calamari D., Cattabeni F., Domenico F., Galli C., Galli E., Silano v., Ecotoxicological profile of pyridine working party on ecotoxicological profiles of chemicals. Ecotox. Environ. Safety, 7, 251-275 (1983).

73. Joseph J., Piganatiells J. R., An overview of the strategy and tactics of Taguchi, IIE Trans, 20, 247-253 (1988).

74. Kalapathy U.A., Proctor A., Shultz J., A simple method for production of pure silica from rice hull ash, Bioresource Tech., 73, 257-262 (2000a).

75. Kalapathy U.A., Proctor A., Shultz .J., Production and properties of flexible sodium silicate films from rice hull ash, Bioresource Tech., l73, 99-106(2000b).

76. Kamath S.R., Proctor A., Silica gel from rice hull ash: preparation and characterization, Cereal Chem., 75, 484-487 (1998).

77. Kannan N., Sundaram M. M., Kinetics and mechanism of removal of methylene blue by adsorption on various carbons - a comparative study, Dyes Pigments, 51(1), 25-40 (2001).

78. Khan A. A., Singh R. P., Adsorption thermodynamics of carbofuran on Sn (IV) arsenosilicate in H^+, Na^+ and Ca^{2+} forms. Colloid Surface, 24, 33-42 (1987).

79. Kim Y., Kim C., Choi I., Rengraj S., Yi J., Arsenic removal using mesoporous alumina prepared via a templating method. Environ. Sci. Technol., 38, 924–931 (2004).

80. Kirk R. E., Othmer D. F., Encyclopedia of chemical technology, 3rd ed., John Wiley Science, New York, 15, 454-480 (1982).

81. Kirk R. E., Othmer D. F., Pyridine and pyridine derivatives. In Encyclopedia of Chemical Technology, 2nd ed., 16, 780-806 (1968).

82. Kirk R. E., Othmer D. F., Pyridine and pyridine derivatives. In Encyclopedia of Chemical Technology 4th ed., John Wiley Science, New York, 20, 641-679 (1996).

83. Koul V.K., Gupta A.K., Uptake of sodium chloride by mixture of weakly acidic and weakly basic ion exchange resins: equilibrium and kinetic studies, Chem. Eng. Sci., 59, 1423 – 435 (2004).

84. Kumar R., Mishra I.M., Mall I.D., Treatment of pyridine bearing wastewater using activated carbon, Research and Industry, 40, 33-37 (1995).

85. Kuo S., Lotse E. G., Kinetics of phosphate adsorption and desorption by hematite and gibbsite., Soil Sci. Soc. Am. J., 116, 400–406 (1973).

86. Lagergren S., About the theory of so called adsorption of soluble substances, Ksver Veterskapsakad Handl, 24, 1-6 (1898).

87. Langmuir I., The adsorption of gases on plane surfaces of glass, mica and platinum, J. Am. Chem. Soc., 40, 1361-1403 (1918).

88. Lataye D.H., Mishra I.M., Mall I.D. Removal of pyridine from aqueous solution by adsorption on bagasse fly ash, Ind. Eng. Chem. Res., 45(11), 3934-3943 (2006).

89. Lataye D.H., Mishra I.M., Mall I.D., Adsorptive removal of pyridine and its derivatives by using cheap adsorbents. National seminar on "Technology for Sustainable- Development-Perspective and Strategies" Institute of Technology, Guru Ghasidas University, Bilaspur (Chhattisgarh), January 6-7, (2007a).

90. Lataye D. H., Mishra, I. M., Mall, I.D., Adsorptive removal of pyridine from aqueous solution by rice husk ash. All India Seminar on "Energy and Environmental Issues Related to Chemical Industry", Organised by The Institution of Engineers (India) U.P. State Centre, Lucknow in association with Harcourt Butler Technological Institute, Kanpur, U.P. on 10th and 11th March, (2007b).

91. Lataye D. H., Mishra, I. M., Mall, I.D., Removal of pyridine from aqueous solution by adsorption on commercial grade granular activated carbon (GAC). National Conference on "Emerging Technology and Developments in Civil Engineering" Organised by Department of Civil Engineering, Govt. College of Engineering, Amravati on 22nd-23rd March, (2007c).

92. Lataye D.H., Mishra I.M., Mall I.D., Adsorption of 2-picoline onto bagasse fly ash from aqueous solution, Chem. Eng. J., doi:10.1016/j.cej.2007.05.043, (2007d).

93. Lataye D.H., Mishra I.M., Mall I.D., Pyridine sorption from aqueous solution by rice husk ash (RHA) and granular activated carbon (GAC), J. Hazrd. Mater., Communicated (2007e).

94. Lataye D.H., Mishra I.M., Mall I.D., Adsorption of α-picoline onto rice husk ash and granular activated carbon from aqueous solution: equilibrium and thermodynamic study, Sep. Purif. Technol., Communicated (2007f).

95. Lee S.T., Rhee S.K., Lee G. M., Biodegradation of pyridine by freely suspended and immobilized *Pimelobacter* sp. Appl. Microbiol. Biotechnol. 41, 652-657 (1994).

96. Lee J. J., Rhee S.-K, Lee S.T., Degradation of 3-methylpyridine and 3-ethylpyridine by *Gordonia nitida* LE31, Appl. Environ. Microb., 67(9), 4342–4345 (2001).

97. Lewis R. J. SR., Sax's Dangerous Properties of Industrial Materials; Eleventh edition, John Wiley & Sons: Hoboken, New Jersey, 3106 (2004).

98. Liu B., Yang Y., Ren Q., Parallel pore and surface diffusion of levulinic acid in basic polymeric adsorbents Journal of Chromatography A, 1132, 190–200 (2006).

99. Luh M. D., Baker R.A., Sorption and desorption of pyridine-clay in aqueous solution, Water Res. 5, 849-859 (1971).

100. Lust E, Janes A., Miidla P., Lust K., Adsorption of pyridine on the (111), (001) and (011) faces of bismuth. J. Electroanal. Chem., 425, 25-37 (1997).

101. Lyberatos G., Personal communication (2006).

102. Mall I.D., Mishra N., Mishra I.M. Removal of organic matter from sugar mill effluent using bagasse fly ash and activated carbon, Res. Indus., 39(6), 115-119 (1994).

103. Mall I.D., Upadhyay S.N., Sharma Y.C., A review on economical treatment of wastewaters, effluents by adsorption. Int. J. Environ. Studies, 51, 77–124, (1996).

104. Mall I.D., Tewari S., Singh N., Mishra I.M., Utilisation of bagasse fly ash and carbon waste from fertiliser plant for treatment of Py and 3-picoline bearing wastewater. Proceeding of the Eighteenth International Conference on Solid Waste Technology and Management held at Philadelphia, PA, USA, March 23-26, (2003).

105. Mall I.D., Srivastava V.C., Agarwal N.K., Mishra I.M., Adsorptive removal of malachite green dye from aqueous solution by bagasse fly ash and activated

carbon-kinetic study and equilibrium isotherm analyses. Colloid Surface A. 264, 17–28 (2005 a).

106. Mall I.D., Srivastava V.C., Agarwal N.K, Mishra I.M., Removal of Congo red from aqueous solution by bagasse fly ash and activated carbon: Kinetic study and equilibrium isotherm analyses. Chemosphere, 61, 492-501 (2005 b).

107. Mane V.S., Mall I.D., Srivastava V.C., Kinetic and equilibrium isotherm studies for the adsorptive removal of brilliant green dye from aqueous solution by rice husk ash. J. Environ. Manag. (2006) doi:10.1016/j.jenvman.2006.06.024.

108. Marquardt D. W., An algorithm for least-squares estimation of nonlinear parameters, J. Soc. Ind. Appl. Math., 11, 431-441 (1963).

109. Martin C., Martin I., Rives V., An FT-IR study of the adsorption of pyridine, formic acid and acetic acid on magnesia and molybdena-magnesia, Journal of Molecular Catalysis, 73, 51-63 (1992).

110. McKay G, Otterburn M. S., Sweeney A. G., The removal of colour from effluent using various adsorbents- III Silica: Rate processes, Water Res., 14, 15-20 (1980).

111. Merck W., Fritz W., Schlunder E.U., Competitive adsorption of two dissolved organics onto activated carbon-II: Adsorption kinetics in batch reactors, Chem. Eng. Sci., 36, 743-757 (1980).

112. Mitra A., Fundamentals of Quality Control and Improvement, Pearson Educational Asia, Delhi (1998).

113. Mohammadi T., Moheb A., Sadrzadeh M., Razmi A., Separation of copper ions by electrodialysis using Taguchi experimental design, Desalination, 169, 21-31 (2004).

114. Mohan D., Singh K.P., Sinha S., Gosh D., Removal of pyridine from aqueous solution using low cost activated carbons derived from agricultural waste materials, Carbon, 42, 2409-2421 (2004).

115. Mohan D., Singh K.P., Sinha S., Gosh D., Removal of pyridine derivatives from aqueous solution by activated carbon developed from agricultural waste materials, Carbon, 43, 1680-1693 (2005).

116. Mohan S. V., Sistla S., Guru R. K., Prasad K. K., Kumar C. S., Ramakrishna S.V., Sarma P.N. Microbial degradation of pyridine using *Pseudomonas* sp. and isolation of plasmid responsible for degradation, Waste Manage. 23, 167–171 (2003).

117. Moustafa S.F., Morsi M.B., Almel-Din A., Formation of silicon carbide from rice hulls, Can. Metall. Quart, 36(5), 355-358 (1997).

118. Nakbanpote W., Thiraveetyan P., Kalambaheti C., Preconcentration of gold by rice husk ash, Mineral Eng., 13 (4), 391-400 (2000).

119. Ng J.C.Y., Cheung W.H., McKay G., Equilibrium studies of the sorption of Cu (II) ions chitosan, J. Colloid Interf. Sci., 255, 64-74 (2002).

120. Niu J., Conway B. E., Development of techniques for purification of wastewaters: removal of pyridine from aqueous solution by adsorption at high-area C-cloth electrodes using in situ optical spectrometry, J. Electroanal. Chem. 521, 16-28. (2002).

121. O'Loughlin E. J., Sims G. K., Trainal S. J., Biodegradation of 2-methyl, 2-ethyl, and 2-hydroxypyridine by an *Arthrobacter* sp. isolated from subsurface sediment, Biodegradation, 10, 93–104, (1999).

122. Onal Y., Kinetics of adsorption of dyes from aqueous solution using activated carbon prepared from waste apricot. J. Hazard. Mater., B137, 1719-1728 (2006).

123. Ozacar M., Sengil I.A., Adsorption of metal complex dyes from aqueous solutions by pine sawdust. Biresource Technol., 96 (7), 791-795, (2005).

124. Padoley K.V., Rajvaidya A.S., Subbarao T.V., Pandey R.A., Biodegradation of pyridine in a completely mixed activated sludge process, Bioresource Technol., 97, 1225–1236 (2006).

125. Pejov L., Skapin T., Adsorption of pyridine on the Lewis acid sites of microcrystalline c-alumina: a quantum chemical cluster model study, Chem. Phys. Lett., 400, 453–461 (2004).

126. Pereira W. E., Rostad C. E., Garbarino J. R., Hult M. F., Groundwater contamination by organic bases derived from coal-tar wastes, Environ. Toxicol. Chem., 2, 283-294 (1983).

127. Phadke M.S., Dehnad K., Optimization of product and process design for quality and cost, Qual. Reliab. Eng. Int., 4, 159-169 (1988).

128. Phadke M.S., Quality Eng. Using Robust Design, Prentice Hall, Englewood Cliffs, New Jersey (1989).

129. Porter J. F., McKay G., Choy K. H., The prediction of sorption from a binary mixture of acidic dyes using single- and mixed isotherm variants of the ideal adsorbed solute theory, Chem. Eng. Sci., 54, 5863-85 (1999).

130. Prasad K.K., Mohan S.V., Rao R.S., Pati B.R., Sarma P.N., Laccase production by *Pleurotus ostreatus* 1804: Optimization of submerged culture conditions by Taguchi DOE methodology, Biochem. Eng. J., 24, 17-26 (2005).

131. Prieto O., Fermoso J., Nunez Y., del Valle J.L., Irusta R., Decolouration of textile dyes in wastewaters by photocatalysis with TiO_2, Solar Energy, 79, 376-383 (2005).

132. Proctor A., Palaniappan S., Soy oil lutein adsorption by rice hull ash, J. Am. Oil Chemists' Soc., 66(11), 1618-1621 (1989).

133. Proctor A., Clark P.K., Parker C.A., Rice hull ash adsorbent performance under commercial soy oil bleaching conditions, J. Am. Oil Chemists' Soc., 72(4), 459-462 (1995).

134. Radke C. J., Prausnitz J. M., Thermodynamics of multisolute adsorption from dilute liquid solutions, AIChE J., 18, 761 (1972).

135. Radovic L.R., Moreno-Castilla C., Rivera-Utrilla J., Carbon materials as adsorbents in aqueous solutions. In: Radovic, L.R. editor. Chemistry and physics of carbon, vol. 27. New York: Marcel Dekker, (2000).

136. Radovic L.R., Silva I.F., Ume J.I., Menedez J.A., Leon L.Y., Scaroni A.W., An experimental and theoretical study of the adsorption of aromatics possessing electron-withdrawing and electron-donating functional groups by chemically modified activated carbons, Carbon, 35(9), 1339-1348 (1997).

137. Rao R.S., Prakasham R.S., Prasad K.K., Rajesham S., Sarma P.N., Rao L.V. Xylitol production by *Candida* sp.: parameter optimization using Taguchi approach, Process Biochem., 39, 951-956 (2004).

138. Raymon C., Chemistry: Thermodynamic, McGraw-Hill, Boston, 737 (1998).

139. Ricordel S., Taha S., Cisse I., Dorange G., Heavy metals removal by adsorption onto peanut husks carbon: characterization, kinetic study and modeling, Sep. Purif. Technol., 24, 389-401 (2001).

140. Redlich O., Peterson D.L., A useful adsorption isotherm. J. Phys. Chem., 63, 1024–1026 (1959).

141. Reichenberg D., Properties of ion-exchange resin in relation to their structure. III. Kinetics of exchange, J. Am. Chem. Soc., 75, 589 (1953).

142. Rhee S.K., Lee G. M., Lee S. T., Influence of a supplementary carbon source on biodegradation of pyridine by freely suspended and immobilized *Pimelobacter* sp., Appl. Microbiol. Biotechnol., 44, 816-822 (1996).

143. Rhee S.K., Lee G. M., Yoon J.H., Park Y.H., Bae H.S., Lee S.T., Anaerobic and Aerobic Degradation of Pyridine by a Newly Isolated Denitrifying Bacterium, Applied and Environmental Microbiology, 63(7), 2578–2585 (1997).

144. Ricordel S., Taha S., Cisse I., Dorange G., Heavy metals removal by adsorption onto peanut husks carbon: characterization, kinetic study and modeling, Sep. Purif. Technol., 24, 389-401 (2001).

145. Rogers J. E., Riley R. G., Li S. W., O'malley M. L., Thomas B. L., Microbial transformation of alkylpyridines in groundwater, Water Air Soil Poll., 24, 443-454 (1985).

146. Roy R.K., A primer on the Taguchi method, Society of Manufacturing Engineers, Michigan (1990).

147. Roy R.K., Design of Experiments Using the Taguchi Approach: 16 Steps to Product and Process Improvement, John Wiley & Sons, New York (2001).

148. Ross P.J., Taguchi techniques for quality Eng., McGraw Hill, New York (1996).

149. Ross P.J., Taguchi Techniques for Quality Eng., McGraw Hill, New York (1988).

150. Sabah E., Celik M.S., Interaction of pyridine derivatives with sepiolite. J. Colloid Interf. Sci., 251, 33-38 (2002).

151. Salas J., Alvarez M., Veras J., Rice husk and fly ash concrete blocks, Int. J. Cement Composites Lightweight Concrete, 9(3), 177-182 (1987).

152. Sandhya S., Urn T.S., Stynarayana S., Kaul S.N. Biodegradation of pyridine from pharmaceutical wastewater, Int. J. Environ. Stud., 5, 1097–1104 (2002).

153. Seidel A., Carl P.S., The concentration dependance of surface diffusion for adsorption on energetically heterogeneous adsorbents, Chem. Eng. Sci., 44, 189-194 (1989).

154. Sen T. K., Mahajan S.P., Khilar K. C., Adsorption of Cu^{2+} and Ni^{2+} on iron oxide and kaolin and its importance on Ni^{2+} transport in porous media. Colloid Surface A, 211, 91-102 (2002).

155. Shukla A., Zhang Y.H., Dubey P., Margrave J.L., Shukla S.S., The role of sawdust in the removal of unwanted materials from water, J of Hazard. Mater., B95 (1-2), 137-152 (2002).

156. Shukla, O. P. Microbial decomposition of pyridine. Indian J. Exp. Biol. 11, 463-465 (1973).

157. Sims G. K., Sommers L. E., Konopka A., Degradation of pyridine by micrococcus luteus isolated from soil, Appl. Environ. Microb., 51(5), 963-968 (1986).

158. Singh V.K., Tiwari P.N., Removal and recovery of chromium(VI) from industrial waste water J. Chem. Technol. Biotechnol, 69, 376-382 (1997).

159. Skelland A. H. P., Diffusional Mass Transfer, Wiley, New York (1974).

160. Smith J.M., Kinetics of Adsorption, Ch.2 In Adsorption from Aqueous Solution Advances in Chemistry, Amirican Cjhemical Society Washington DC, (1968).

161. Sreenivas Rao R., Prakasham R. S., Krishna Prasad K., Rajesham S., Sarma P. N., Venkateswar Rao L., Xylitol production by *Candida* sp.: parameter optimization using Taguchi approach, Process Biochem, 39, 951-956 (2003).

162. Srivastava V.C., Mall I.D., Mishra I.M., Treatment of pulp and paper mill wastewaters with polyaluminium chloride and bagasse fly ash. Colloid Surfaces A, 260, 17 – 28 (2005).

163. Srivastava V. C., Mall I. D., Mishra I. M., Characterization of mesoporous rice husk ash (RHA) and adsorption kinetics of metal ions from aqueous solution onto RHA, J., Hazard. Mater., B134, 257-267 (2006a).

164. Srivastava V.C. Swamy M.M., Mall I.D., Prasad B., Mishra I.M., Adsorptive removal of phenol by bagasse fly ash and activated carbon: Equilibrium, kinetics and thermodynamics, Colloid Surface A, 272, 89–104 (2006b).

165. Srivastava V.C., Mall I.D., Mishra I. M., Multi-component adsorption study of metal ions onto bagasse fly ash using Taguchi's Design of Experimental Methodology. Ind. Eng. Chem. Res, (Accepted, 2007).

166. Stern M., Heinzle E., Kut O. M., Hungerbuhler K., Removal of substituted pyridines by combined ozonation/fluidiaed bed biofilm treatment, Water Sci. Technol., 34(4), 329-335 (1997).

167. Sudo Y., Misic D.M, Suzuki M., Concentration dependence of effective surface diffusion coefficient in aqueous phase adsorption on activated carbon, Chem. Eng. Sci., 33, 1287-1290 (1978).

168. Suzuki M., Fujii T., Concentration dependence of surface diffusion coefficient of propionic acid in activated carbon particles, AIChE J., 28, 380-385 (1982).

169. Suzuki M. Adsorption Engineering, Kodansha-Elsevier, Tokyo, 1990.

170. Swamy M.M., Mall I.D., Prasad B, Mishra I.M., Resorcinol removal from aqueous solution by bagasse fly ash and activated carbon. Inst. Eng. (India) J. Environ. 77(2), 49-54 (1997).

171. Swamy M.M., Mall I.D., Prasad B., Mishra I.M. Sorption characteristics of o-cresol on bagasse fly ash and activated carbon. Ind. J Environ. Health, 40(1), 67-78 (1998).

172. Tadjeddine A., Le Rille A., Pluchery O., HeH bert P., Zheng W.Q., Marin T., Adsorption of pyridine on gold, studied by difference frequency generation

(DFG) using the CLIO-FEL Nuclear Instruments and Methods in Physics Research A, 429, 481-484 (1999).

173. Taguchi G., Introduction to Quality Eng., Quality Resources, New York (1986).

174. Taguchi G., Wu Y., Off-line Quality Control, Central Japan Quality Control Association, Nagaya, Japan (1979).

175. Temkin M.I., Pyzhev V., Kinetics of ammonia synthesis on promoted iron catalysts, Acta Physiochim. URSS, 12, 327–356 (1940).

176. Teng H., Hsieh C., Activation energy for oxygen chemisorption on carbon at low temperatures, Ind. Eng. Chem. Res. 38, 292-297 (1999).

177. Theng B. K. G. *The Chemistry of Clay-organic Reactions*, Hilger, London (1974).

178. Tien C., Adsorption Calculations and Modeling, Butterworth-Heinemann, 1994.

179. Tong L., Wang C., Chen C., Dynamic multiple responses by ideal solution analysis, Eur. J. Operat. Res., 156, 433-444 (2004).

180. Torng C.C., Chou C. Y. Liu H.R., Applying quality engineering technique to improve wastewater treatment, J. Ind. Technol., 15(1), 1-7 (1998).

181. Toth J. State equations of the solid gas interface layer, Acta. Chem. Acad. Hung., 69, 311-328 (1971).

182. Tutem E., Apak R., Unal C.F., Adsorptive removal of chlorophenols from water by bituminous shale, Water Res., 32, 2315-2324 (1998).

183. Tuts R., Rice husk ash cement project in Kenya, BASIN News, 7, 17-21 (1994).

184. Uma B., Sandhya S., Pyridine degradation and heterocyclic nitrification by Bacillus coagulance, Can. J. Microbiol., 43, 595-598 (1997).

185. Uma B., Sandhya S., Kinetics of pyridine degradation along with toluene and methylene chloride with Bacillus sp. in packed bed reactor, Bioprocess Eng. 18, 303-305 (1998).

186. Usmani T.H., Ahmed T.W., Ahmed S.Z., Yousufzai A.H.K., Activated carbon from rice husk. Part-I. Activated agent selection, Pakistan J. Sci. Ind., 36(6-7), 236-239 (1993).

276

187. Vermeulen T., Theory for irreversible and constant pattern solid diffusion, Ind. Eng. Chem., Res. 45(8), 1664-1670 (1953).

188. Viraraghavan T., Alfaro F.M., Adsorption of phenol from wastewater by peat, fly ash and bentonite, J. Hazard. Mater., 57, 59-70 (1998).

189. Watson G. K., Houghtont C. Cain R. B., Microbial metabolism of the pyridine ring the hydroxylation of 4-hydroxypyridine to pyridine-3, 4-diol (3, 4-dihydroxypyridine) by 4-hydroxypyridine-3-hydroxylase, Biochem. J. 140, 265-276 (1974).

190. Watson G. K., Cain R. B., Microbial metabolism of the pyridine ring, metabolic pathways of pyridine biodegradation by soil bacteria Biochem. J. 146, 157-172 (1975).

191. Weber J. B., Molecular structure and pH effects on the adsorption of 1, 3, 5-triazine compounds on montmorillonite clay, Am. Miner. 51, 1657-1690 (1966).

192. Weber W.J. Jr., Morris J.C. Kinetics of adsorption on carbon from solution, J Sanit. Engg. Div. ASCE, 89 (SA2), 31-59 (1963).

193. Weber W.J. Jr., Physical Chemical Processes for water Quality Control, Wiley Interscience, New York, (1972)

194. Yates, F.S. Pyridine and their benzo derivatives: (vi) applications in: A.R.Katritzky, C.W. Rees Eds., Comprehensive Heterocyclic Chemistry: The Structure, Reaction, Synthesis and uses of Heterocyclic compounds, Vol. 2, Part 2 A, Chapter 2.09, Pergamon Press, Oxford, 511-524, (1984).

195. Young D.M., Crowell A. D., Physical Adsorption of Gases, Butterworths, London, 1962.

196. Yu L.J., Shukla S.S., Dorris K.L., Shukla A., Margrave J.L., Adsorption of chromium from aqueous solutions by maple sawdust J. Hazard. Mater., 100 (1-3), 53-63, (2003).

197. Zaki M.I., Hussein G.A.M., Mansour S.A.A., El-ammawy H.A., Adsorption and surface reactions of pyridine on pure and doped ceria catalysts as studied by infrared spectroscopy, J. Molecular Catalysis, 51, 209 – 220 (1989).

198. Zawadzki J., An infrared study of acid sites on carbons by pyridine adsorption, Carbon, 26(5), 327-633 (1988).

199. Zhao H., Xu S., Zhong J., Bao X., Kinetic study on the photo-catalytic degradation of pyridine in TiO_2 suspension systems, Catalysis Today, 93-95, 857-861 (2004).

200. Zhao X. S., Lu (Max) G.Q., Millar G.J., Advances in mesoporous molecular sieve MCM-41, Ind. Eng. Chem. Res., *35*, 2075-2090 (1996).

201. Zhu S., Bell P.R.F., Greenfield P.F., Adsorption of pyridine onto spent rundle oil shale in dilute aqueous solution. Water Res, 22(10), 1331–1337 (1988).

Web Reference

202. http://www.jubl.net/msds
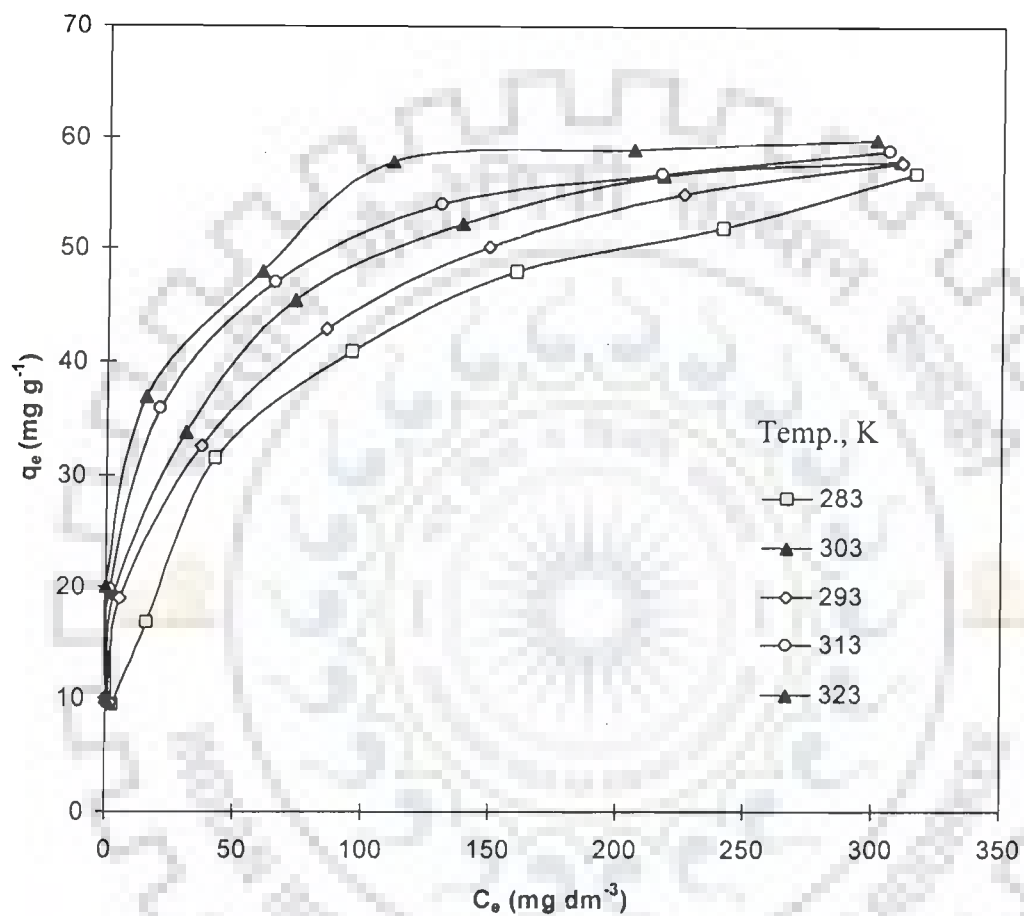
Fig. A-1. Equilibrium adsorption isotherms at different temperatures for adsorption of 2Pi onto BFA. ($pH_0 = 6.0$, $C_0 = 50\text{-}600$ mg dm^{-3}, $m = 5$ g dm^{-3}).
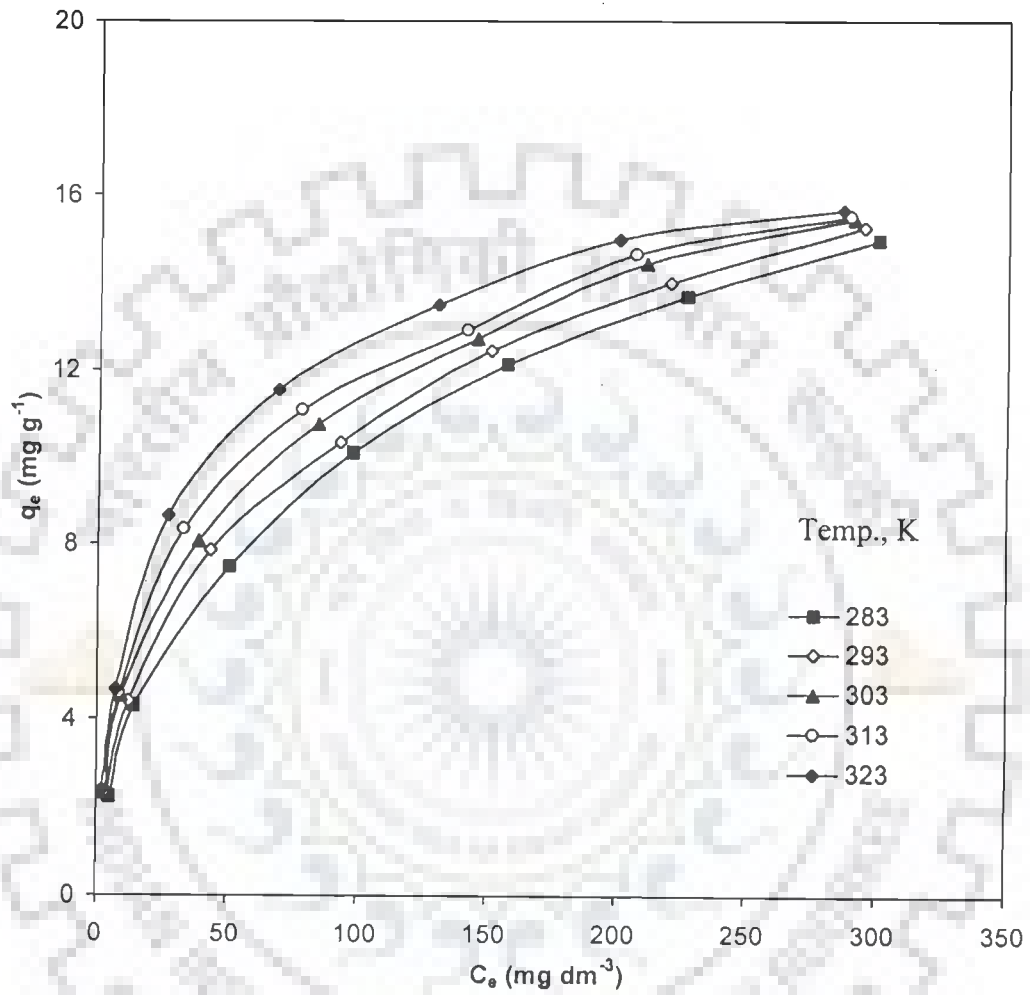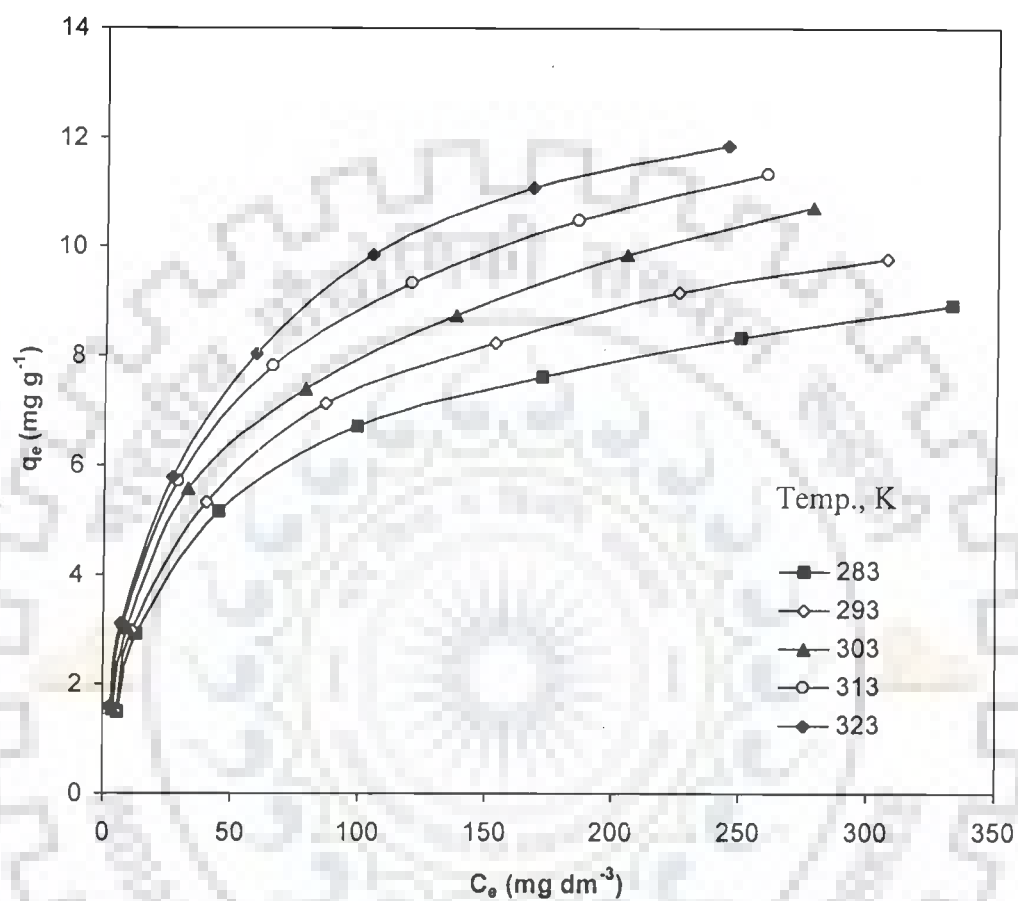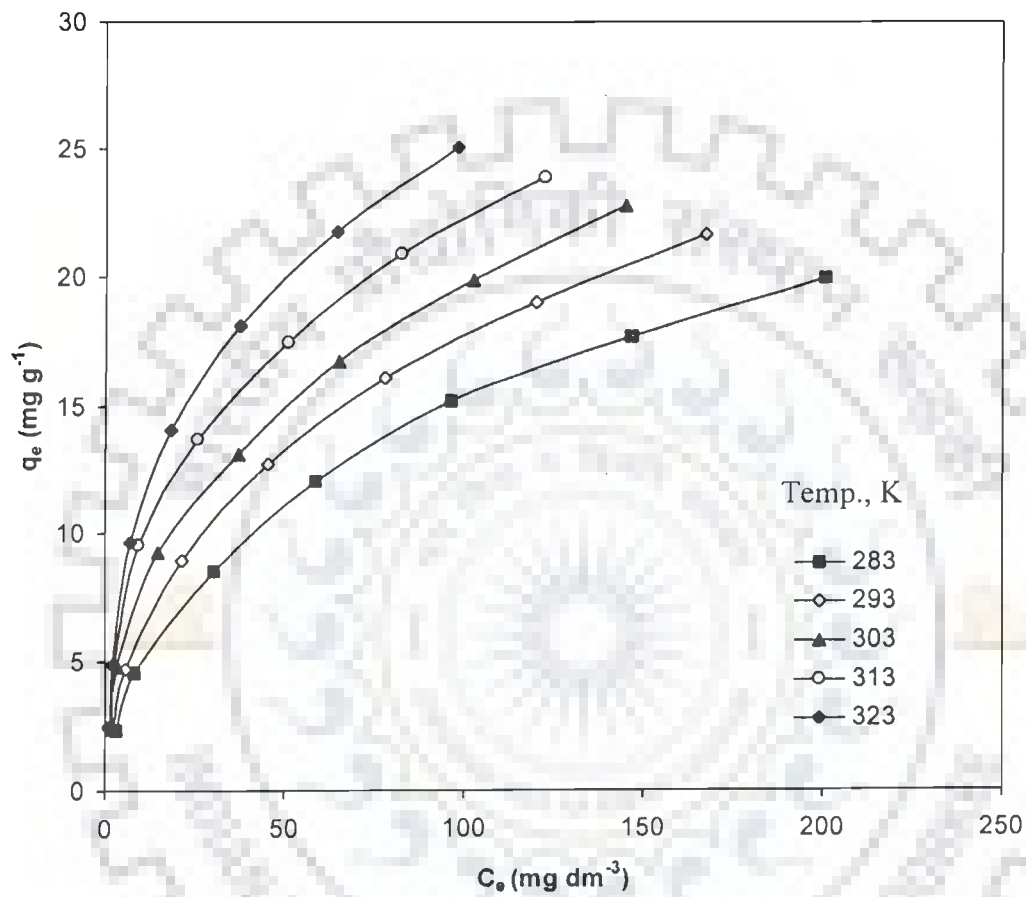
Fig. A-2. Equilibrium adsorption isotherms at different temperatures for adsorption of 2Pi onto RHA. ($pH_0 = 6.0$, $C_0 = 50\text{-}600$ mg dm^{-3}, $m = 20$ g dm^{-3}).
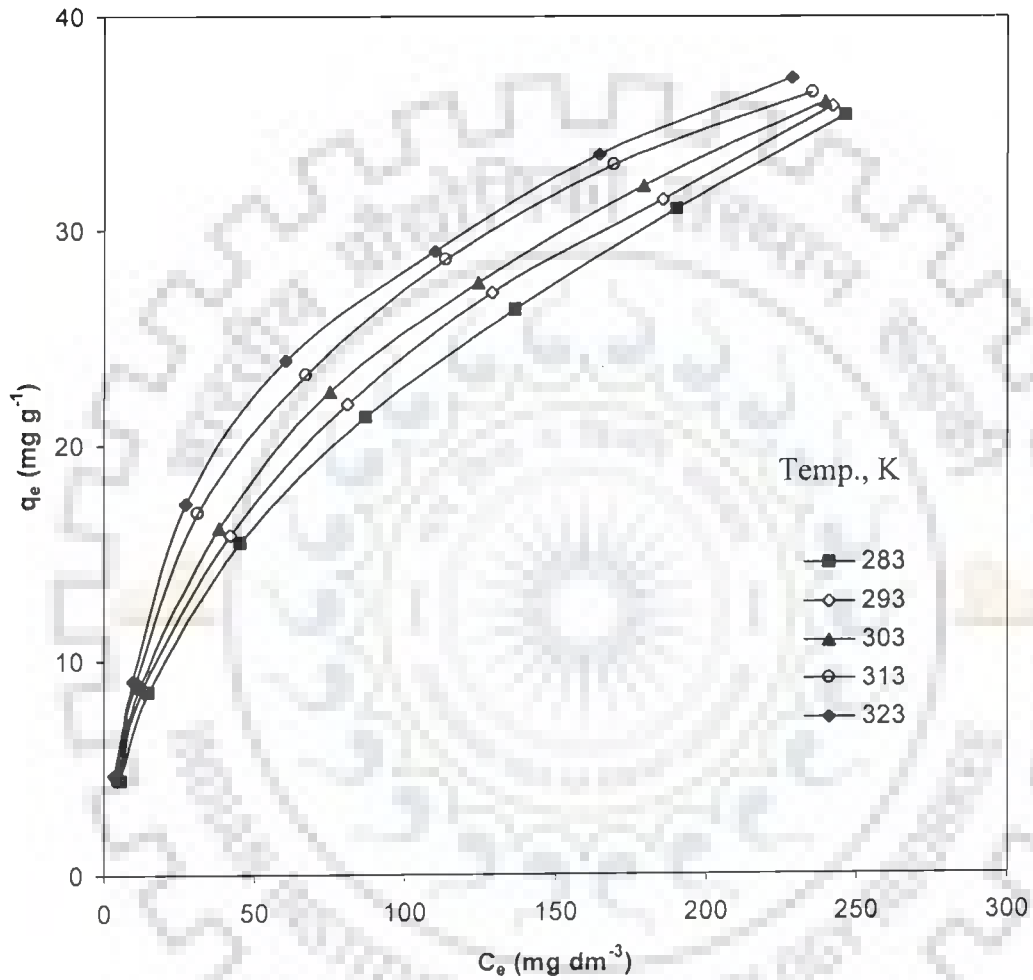
Fig. A-3. Equilibrium adsorption isotherms at different temperatures for adsorption of 2Pi onto GAC. ($pH_0 = 6.0$, $C_0 = 50\text{-}600$ mg dm^{-3}, $m = 10$ g dm^{-3}).
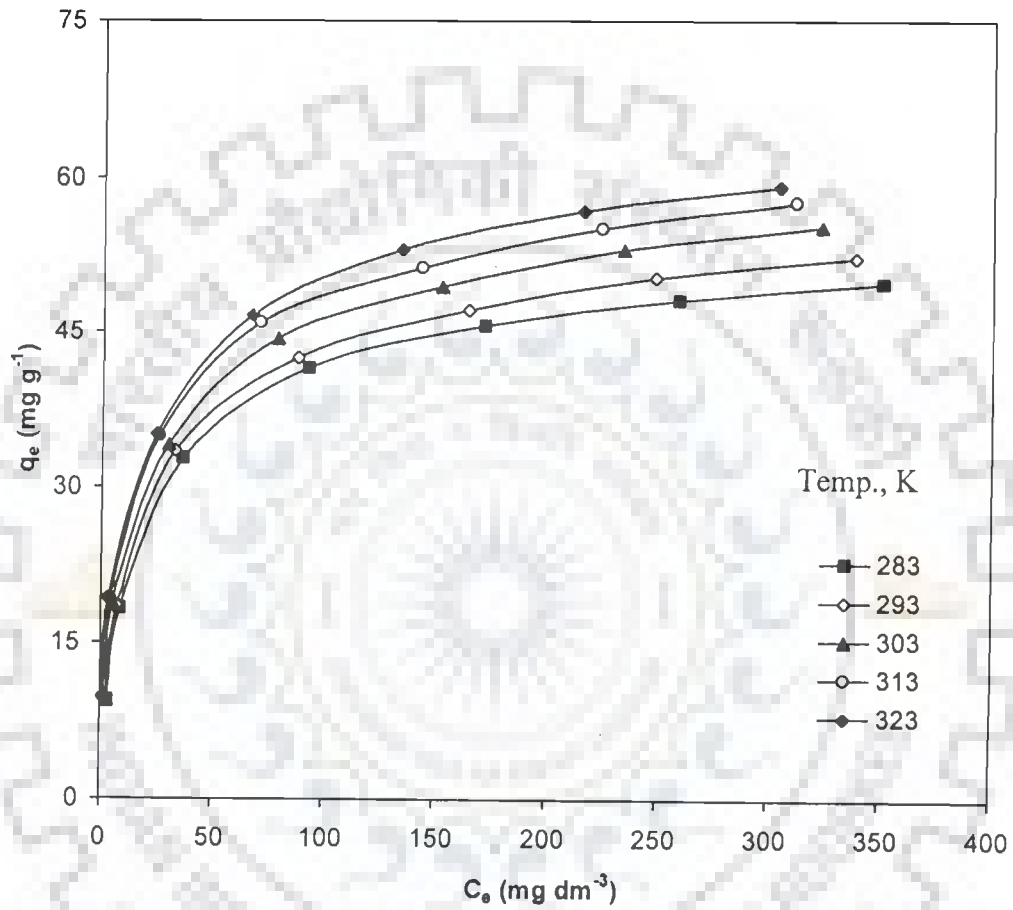
Fig. A-4. **Equilibrium adsorption isotherms at different temperatures for adsorption of 4Pi onto BFA.** ($pH_0 = 6.0$, $C_0 = 50\text{-}600$ mg dm^{-3}, $m = 5$ g dm^{-3}).
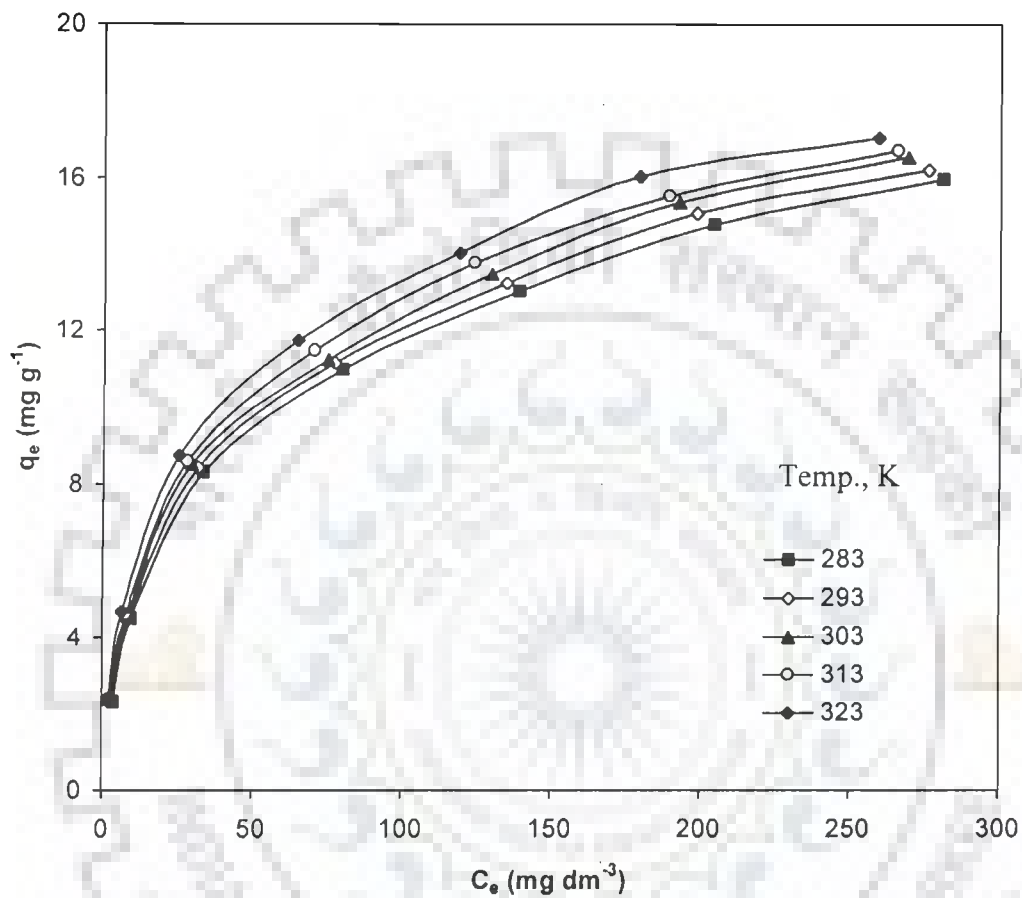
Fig. A-5. Equilibrium adsorption isotherms at different temperatures for adsorption of 4Pi onto RHA. ($pH_0 = 6.0$, $C_0 = 50\text{-}600$ mg dm^{-3}, $m = 20$ g dm^{-3}).
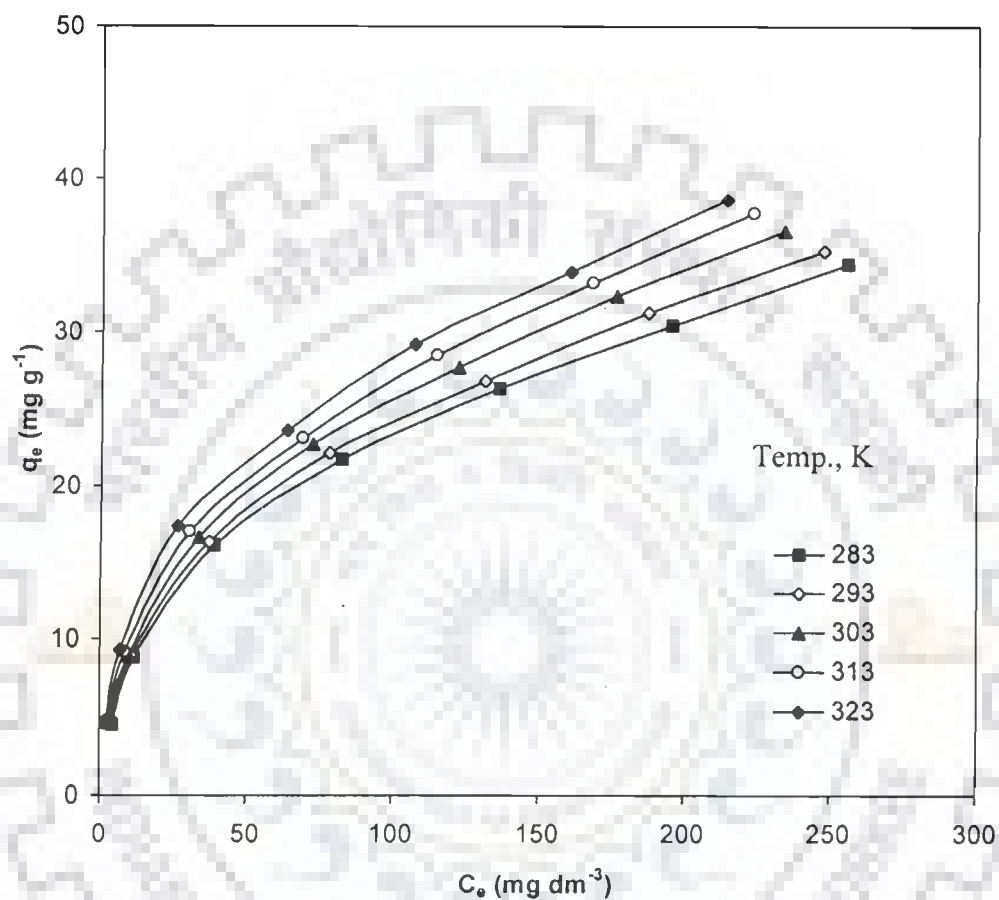
Fig. A-6. **Equilibrium adsorption isotherms at different temperatures for adsorption of 4Pi onto GAC.** (pH_0 = 6.0, C_0 = 50-600 mg dm^{-3}, m = 10 g dm^{-3}).
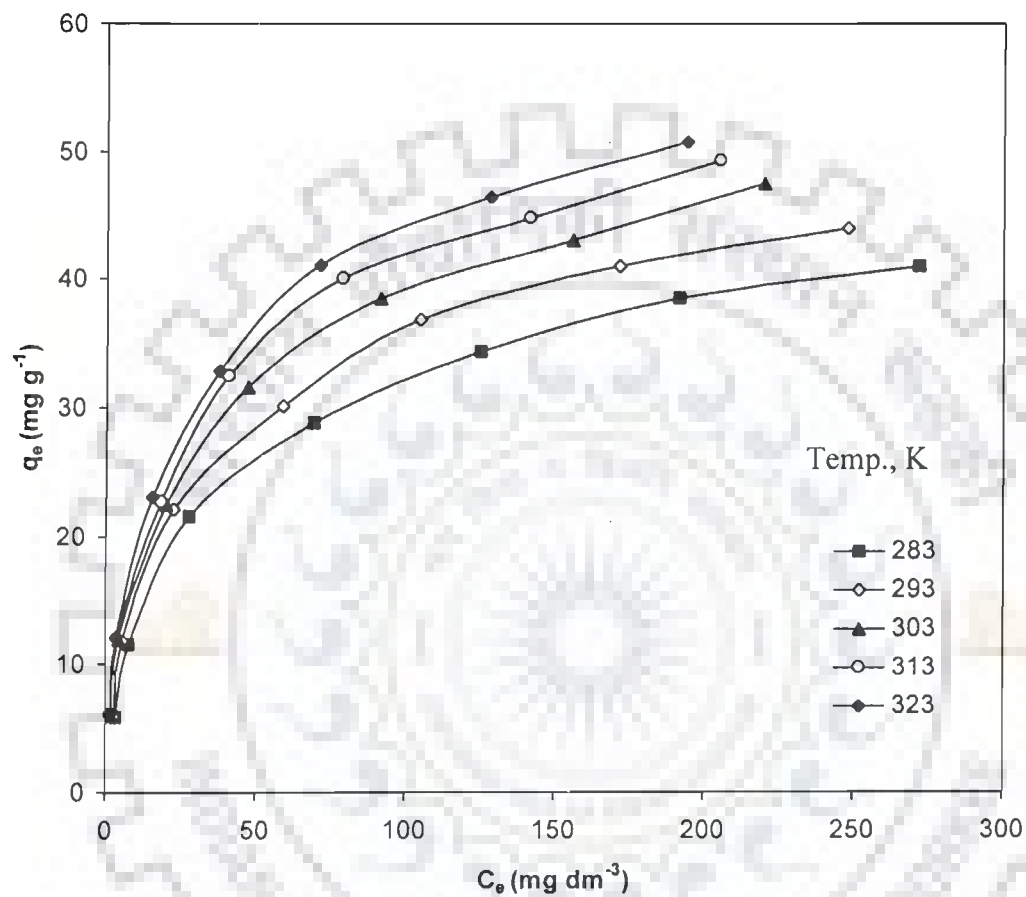
Fig. A-7. Equilibrium adsorption isotherms at different temperatures for adsorption of AmPy onto BFA. ($pH_0 = 6.0$, $C_0 = 50\text{-}600$ mg dm^{-3}, $m = 8$ g dm^{-3}).

Fig. A-8. Equilibrium adsorption isotherms at different temperatures for adsorption of AmPy onto RHA. ($pH_0 = 6.0$, $C_0 = 50\text{-}600$ mg dm^{-3}, $m = 30$ g dm^{-3}).

Fig. A-9. Equilibrium adsorption isotherms at different temperatures for adsorption of AmPy onto GAC. (pH_0 = 6.0, C_0 = 50-600 mg dm^{-3}, m = 20 g dm^{-3}).
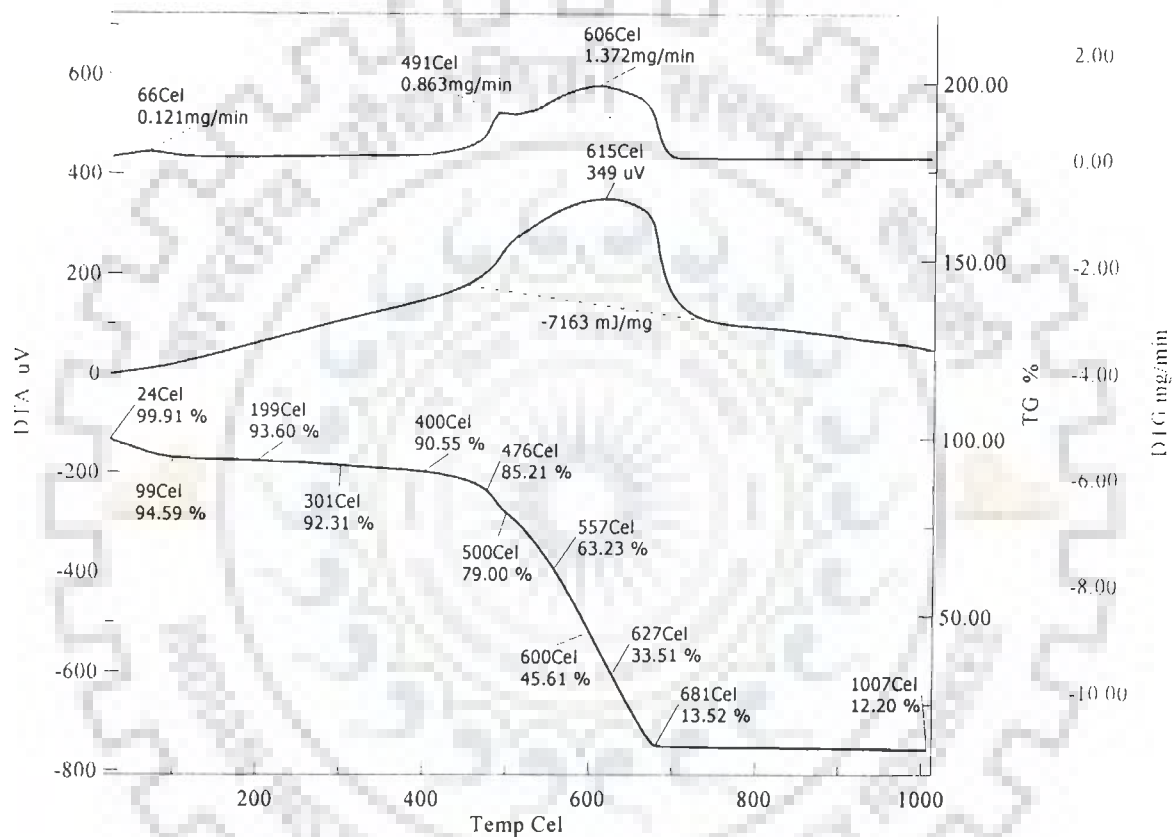
Fig. B-1. Thermogravimetric analysis of BFA loaded with pyridine
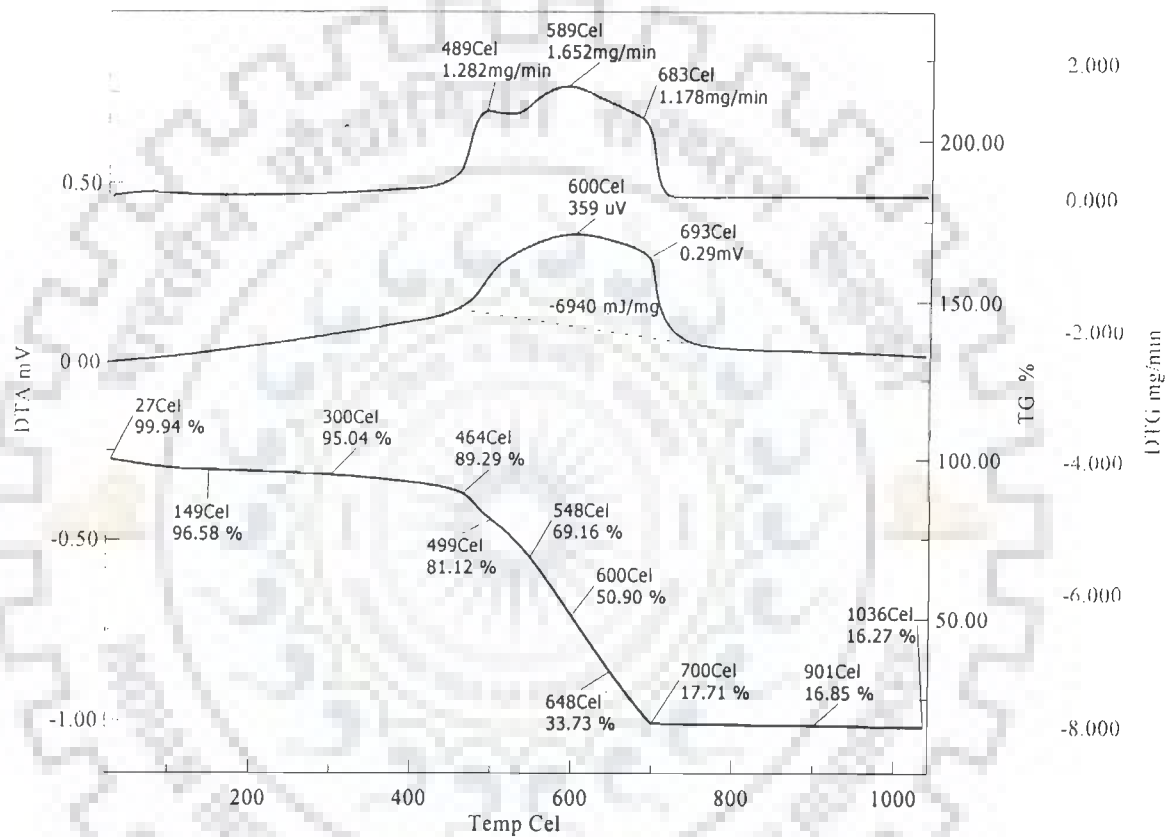
Fig. B-2. Thermogravimetric analysis of BFA loaded with 2-picoline
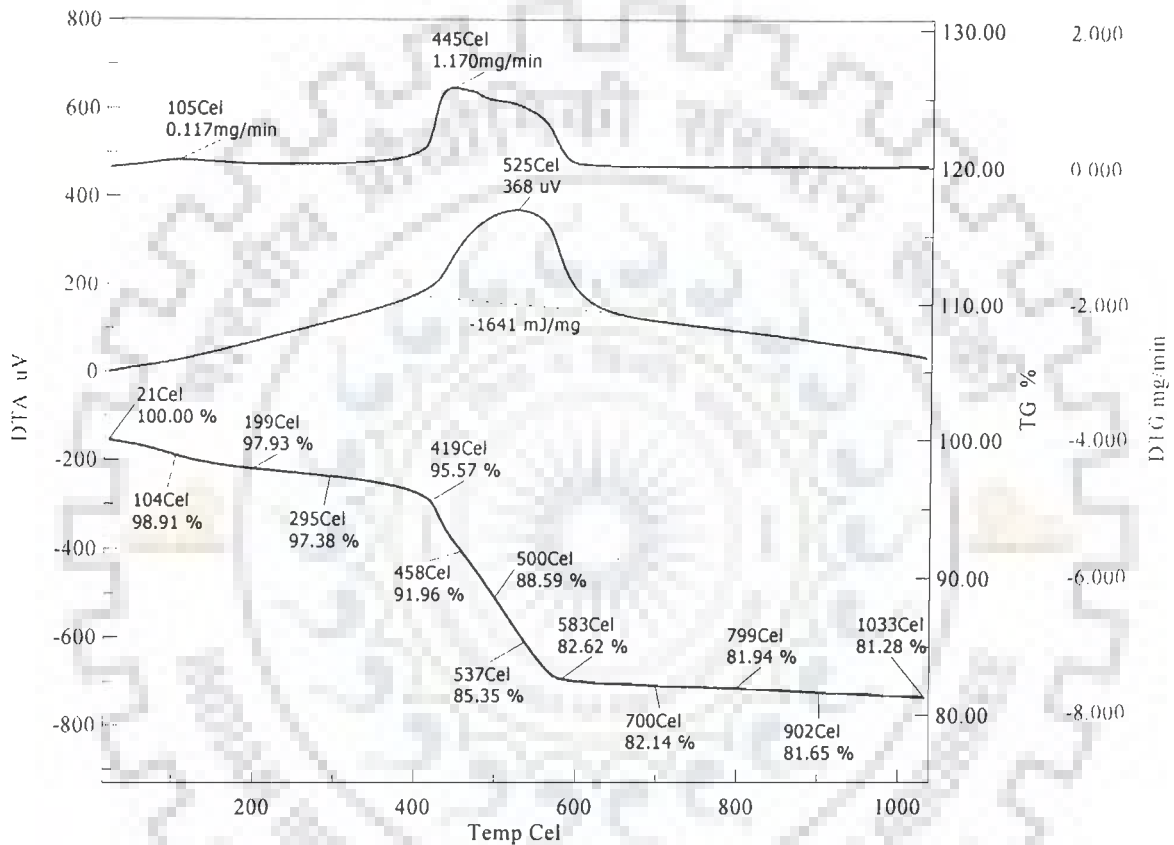
Fig. B-3. hermogravimetric analysis of RHA-Blank
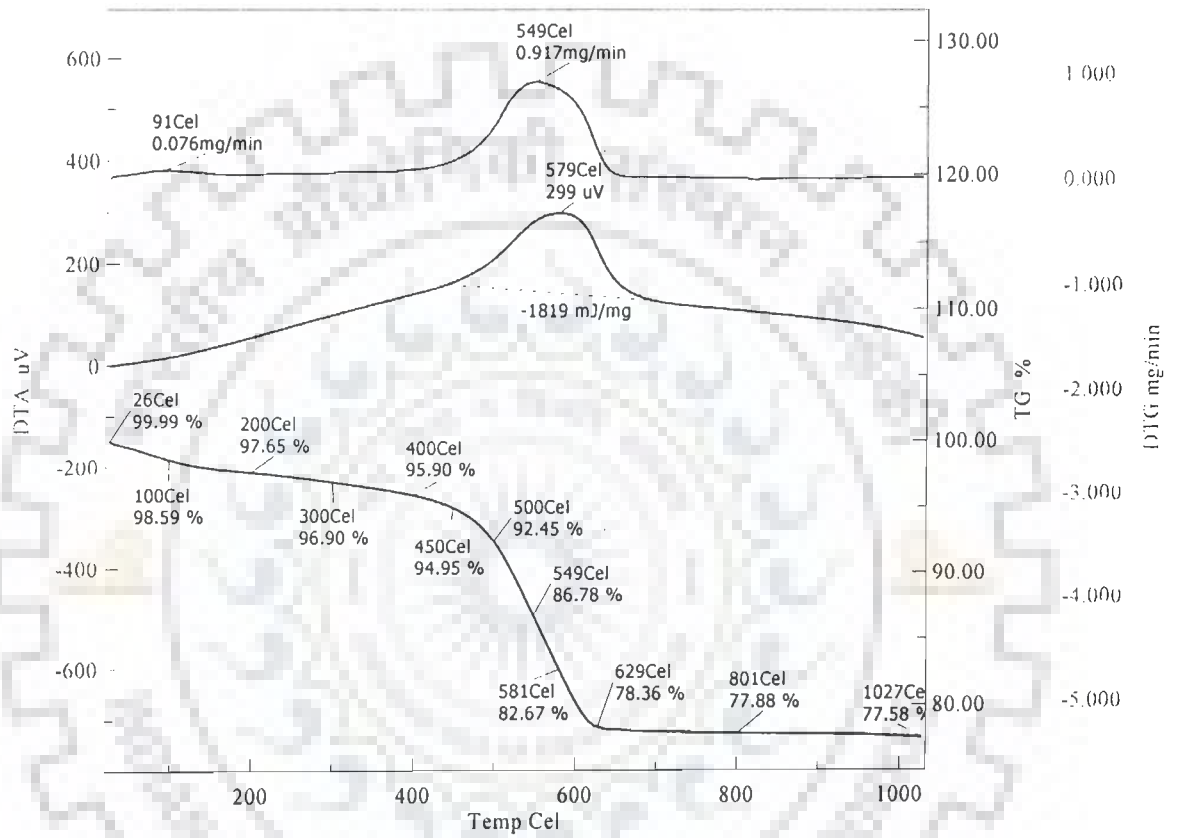
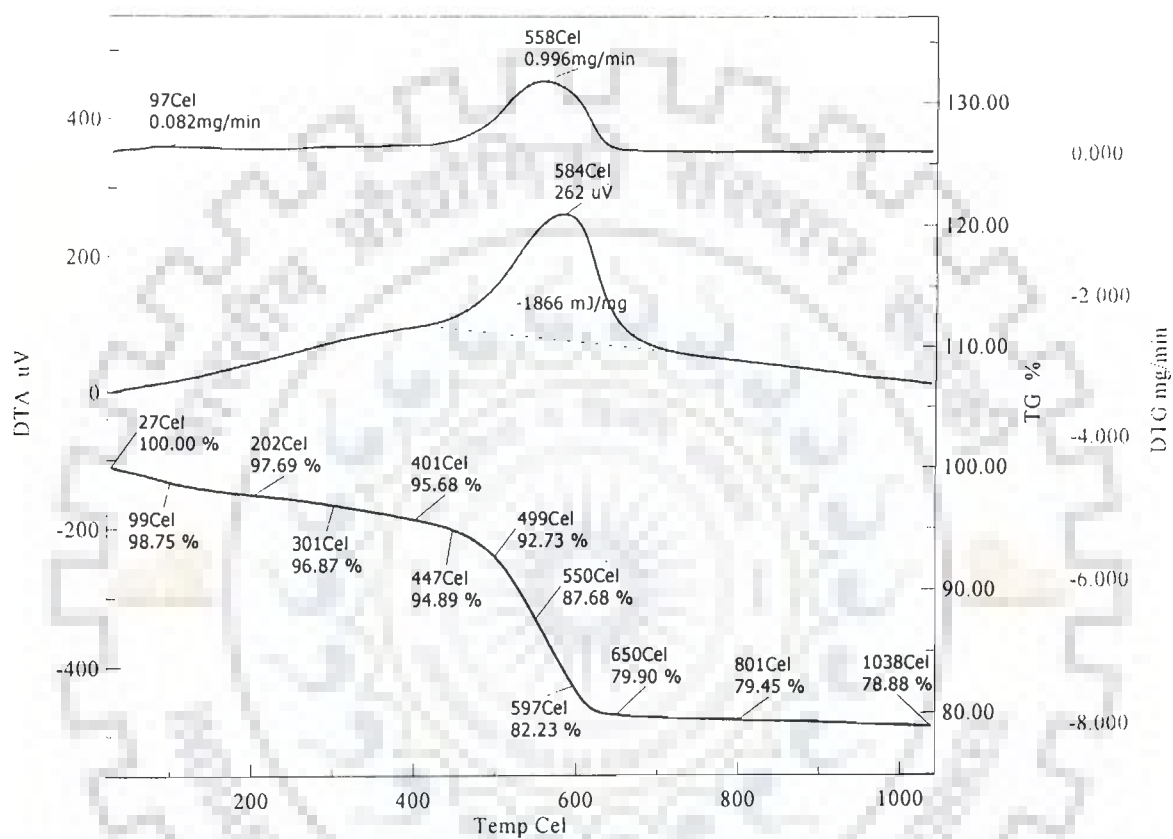**Fig. B-4. Thermogravimetric analysis of RHA loaded with pyridine**

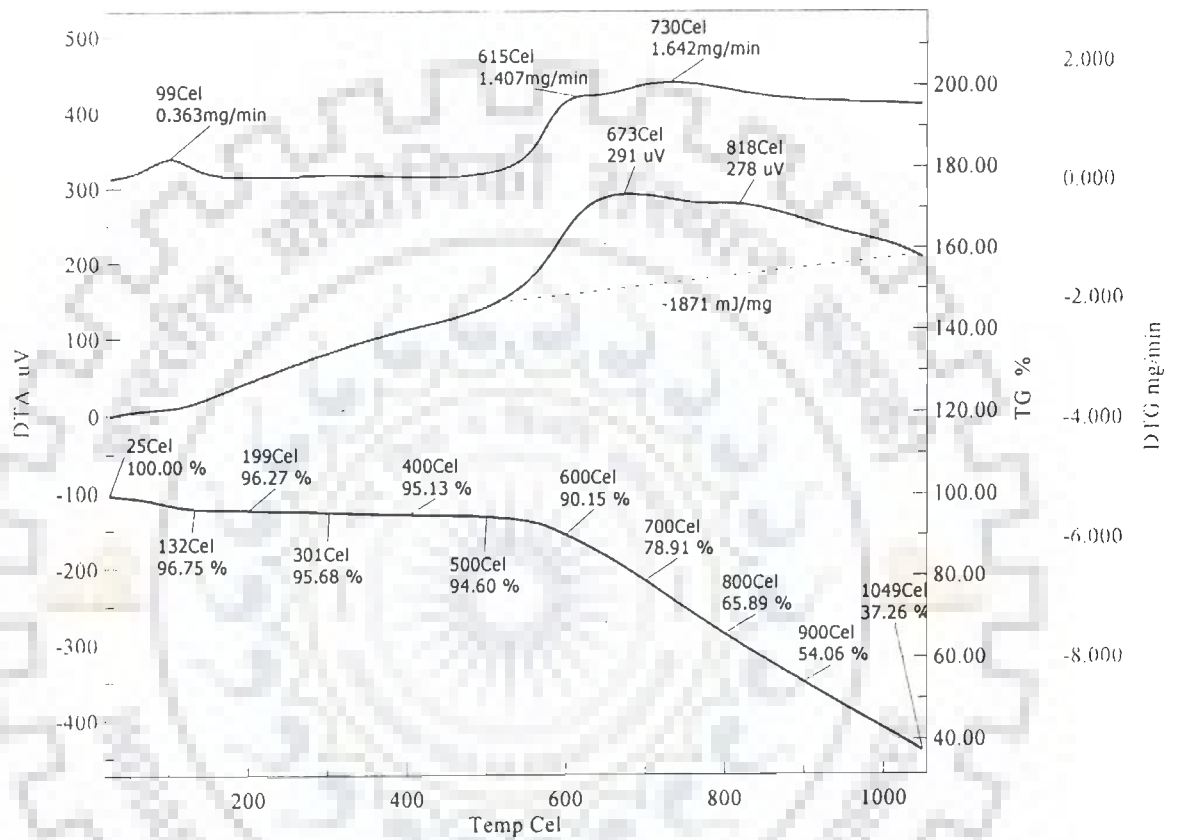**Fig. B-5. Thermogravimetric analysis of RHA loaded with 2-picoline**

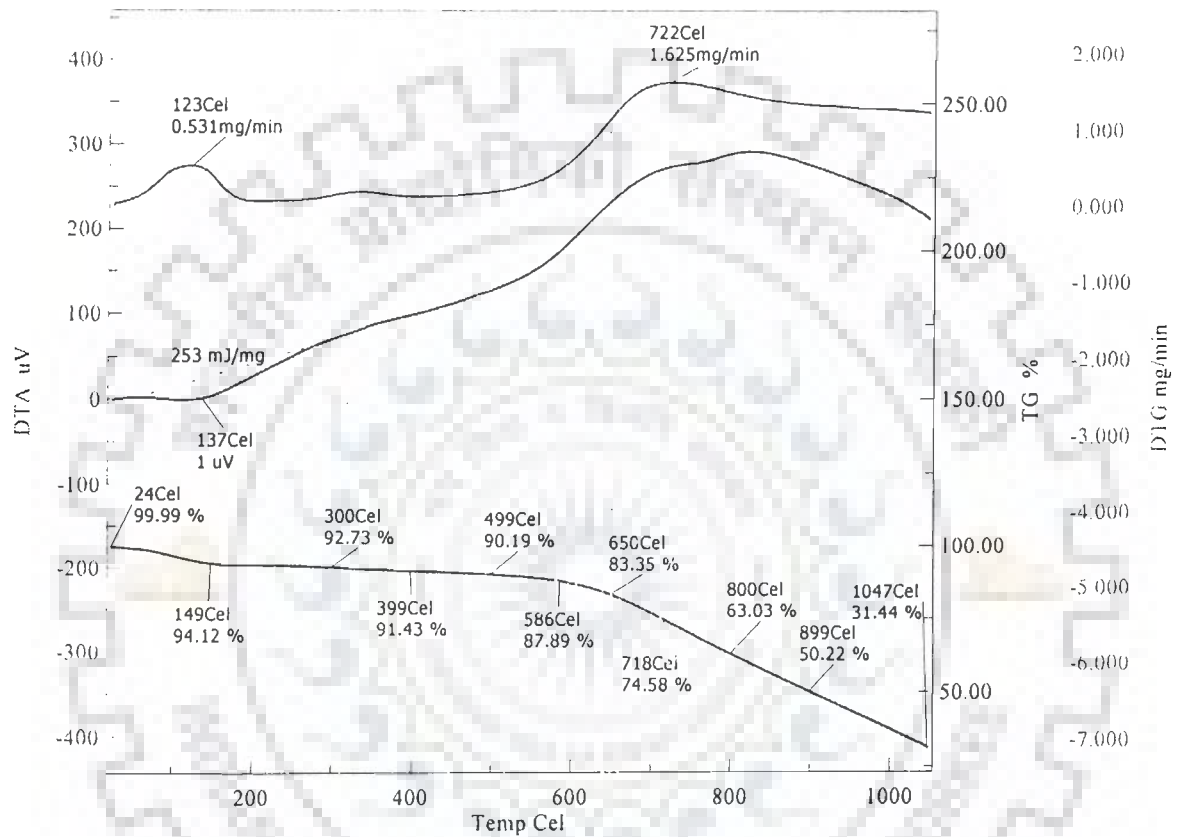**Fig. B-6. Thermogravimetric analysis of GAC - Blank**

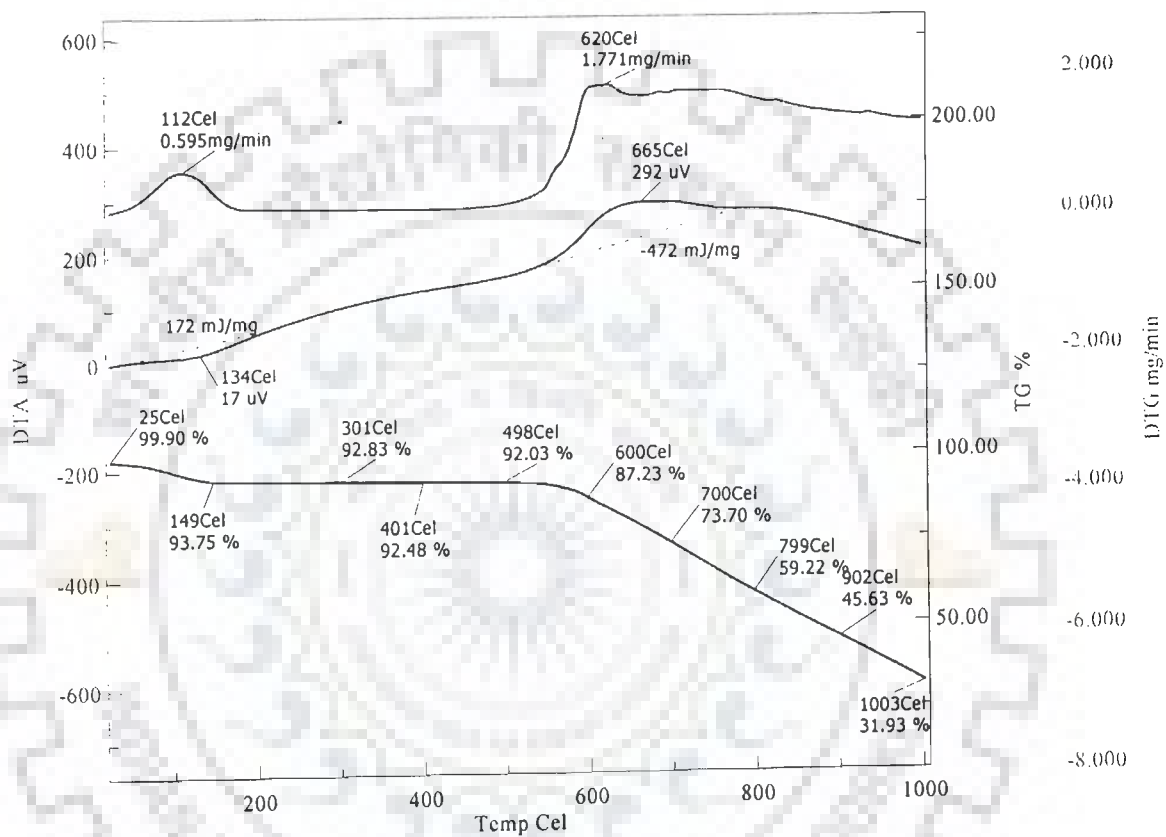**Fig. B-7. Thermogravimetric analysis of GAC loaded with Pyridine**

Fig. B-8. Thermogravimetric analysis of GAC loaded with 2-picoline

CURRICULUM VITAE

NAME IN FULL	:	**DILIP HIRADRAM LATAYE**
FATHER'S NAME	:	SHRI HIRADRAM LATAYE
DATE OF BIRTH	:	22nd OCTOBER 1972
MARITAL STATUS	:	Married
OFFICE ADDRESS	:	Lecturer (Senior Scale) Department of Civil Engineering V.N.I.T., Nagpur - 440 011 (INDIA)
PERMENENT ADDRESS	:	Village/Post: Lohara, Tahsil: Deori Distt. : Gondia PIN : 441 902 [Maharashtra]
TELEPHONES	:	**+91 712 2801371** / +91 712 280 1226
FAX	:	+91 0712 2223230
EMAIL	:	dhlataye@vnitnagpur.ac.in diliplataye@rediffmail.com

EDUCATIONAL QUALIFICATION

DEGREE	YEAR	DIVISION	INSTITUTION/UNIVERSITY
B.E. (Civil)	1996	I	V.N.I.T. (Formerly VRCE) NAGPUR – 440 011 (INDIA)
M.Tech. (Env. Engg.)	1998	I	V.N.I.T. (Formerly VRCE) NAGPUR – 440 011 (INDIA)
Ph.D. (Env. Engg.)	2007		I. I. T., ROORKEE

EXPERIENCE:

1. Lecturer, Deptt. of Civil Engg., V. N. I. T., NAGPUR August, 1998 to   May, 2006
2. Lecturer (Sr. Scale), Deptt. of Civil Engg., V. N. I. T., NAGPUR Since May, 2006